Development of an Efficient Off-grid Pumping System and Evaporation Reduction Strategies to Increase Access to Irrigation for Smallholder Farmers in India

by

Emily Gorbaty

B.S. Engineering: Atmosphere/Energy

Stanford University, 2009

Submitted to the Department of Mechanical Engineering

in partial fulfillment of the requirements for the degree of

Master of Science in Mechanical Engineering

at the

MASSACHUSETTS INSTITUTE OF TECHNOLOGY

September 2013

Author……

Department of Mechanical Engineering

August 20, 2013

Certified by……

Alexander H. Slocum

Neil and Jane Pappalardo Professor of Mechanical Engineering

Thesis Supervisor

Accepted by……...

David E. Hardt

Chair, Committee on Graduate Students

Development of an Efficient Off-grid Pumping System and Evaporation Reduction Strategies to Increase Access to Irrigation for Smallholder Farmers in India

by

Emily Gorbaty

Submitted to the Department of Mechanical Engineering on August 20, 2013,

in partial fulfillment of the requirements for the degree of

Master of Science in Mechanical Engineering

Abstract

Due to the unavailability of electricity, about 85% of groundwater irrigation in eastern India employs fuel-powered surface pumps, which can have system efficiencies as low as 5%. As fuel prices continue to rise, impoverished smallholder farmers cannot afford the operation costs of their systems and, as a result, irrigate less land. This research aimed to develop a more efficient off-grid system that eliminates suction head while continuing to utilize a fuel engine on the surface. Design requirements included increased discharge, increased efficiency, portability, maintainability, availability of replacement parts, and affordability. Flow rates and efficiencies of Indian pumps at varying pressure heads were tested to establish baseline performance and test the hypothesis that removing suction lift reduces operation costs. It was found that eliminating suction head can decrease operation costs up to 44% for the farmers. Fuel-driven system options investigated include flexible shafts and telescoping shafts to transmit power from a surface engine to a submersible pump, fluid machinery such as semi-open hydraulic systems, jet pumps, compressed air motors, and air lifts, and off-grid electricity generation employing a household backup generator or automotive alternator. However, none of these alternatives met all the design requirements. Instead, a hybrid motorized-manual rope pump was prototyped and tested on a well in Ruitola, Jharkhand. Although this system does not meet all the design requirements, it has the added benefit of providing domestic water supply. The prototype discharged an average of 155.4 L/min in motorized mode and 17.2 L/min for men and 13.3 L/min for women in manual mode. The rope pump received positive feedback from the users and thus could be taken forward with several modifications to improve performance. To increase the available water resources, evaporation reduction strategies to limit water loss from farm tanks were explored. The strategies employed waste materials and included covering a water surface with waste PET bottles and floats comprised of PET waste bottles and old saris. While waste bottles proved promising in a preliminary test, data in a larger experiment has thus far proved inconclusive and further testing is needed.

Thesis Supervisor: Alexander H. Slocum
Title: Neil and Jane Pappalardo Professor of Mechanical Engineering

Acknowledgements

I would first like to express my gratitude to my advisor, Professor Alexander Slocum, for providing guidance and support throughout this research. Thank you for challenging me and pushing me when I needed to be pushed (even when I didn't realize it). You turned me into a real engineer! Thank you also for teaching me how to roar like a lion into a hallway full of people.

I would also like to thank Professor Leon Glicksman, who advised me during my first year at MIT, for believing in me and starting me off on my journey to become a mechanical engineer.

I am grateful to Dr. Chintan Vaishnav for his guidance in navigating both India and MIT and for our long fascinating discussions about development in India. He has introduced me to fresh perspectives on India as well as new interdisciplinary research methodologies. I also appreciate Dr. Nevan Hanumara's help in teaching me how to organize and present my research clearly.

The local partner, Professional Assistance for Development Action (PRADAN), was crucial to the success of this research. I am indebted to Achintya Ghosh, from PRADAN's Delhi headquarters, who first introduced me to Jharkhand and led me around the state visiting various communities. He opened my eyes to the agricultural and irrigation challenges communities in eastern India face—and then he helped me attempt to tackle one of those challenges by introducing me to the Ranchi and Gumla offices, which would facilitate my research. Thank you to Ashok Kumar and Satyabrata Acharya for organizing everything and providing all the support I needed during my stay in Jharkhand. Thank you to Bapi Gorai for assisting me with pump testing in Gumla District. Thank you to Samir Kumar for helping me communicate with the fabricator and accompanying me to Ruitola for prototype installation, troubleshooting, and testing. Thank you to Shahanawaz Alam and Ananya for identifying the community and the well for the prototype. I am truly grateful for all the generous help and support these and other members of the PRADAN family provided me.

Thank you to Dr. Indrani Medhi, who put me in touch with Rikin Gandhi, who then introduced me to PRADAN. This project could not have happened without your connections.

Swastik Engineering Works (Kadru Diversion Road, Opp. Hotel Yuvraj Palace, Ranchi) helped with the fabrication of the prototype. I am very grateful to Govind Sharma, the owner whom everyone calls Sharmaji, for organizing his employees to get this prototype built as quickly as possible within my tight time constraints. Sharmaji also provided invaluable insight into what is and what is not possible to manufacture and repair in Jharkhand; he was immensely helpful (and patient!) during the design process. I appreciate the help of Gopal Singh Rathor to procure materials and parts and to show me how to navigate the markets. Thank you to the men who helped with the fabrication process: Birendra Prasad with the lathe and Vimal Prasad Lal and Basudeo Sarkar with welding. Birendra deserves a special thank you for accompanying me to the village to help me install and troubleshoot the rope pump system.

To the men and women of the villages of Telya, Shahitoli, Jamtoli, Menatoli, Lutoambatoli, Toto, Ghaghra, Sivrajpur, Jaldega, Kondekera Dandtoli, and Raidih in Gumla District and Ruitola in Khunti District who took the time to help me with my project, whether to answer interview questions, join a discussion group, assist with testing pumps (especially Rajesh Oraon in Telya), volunteer a well for the prototype (especially Salim and Turlin Munda in Ruitola), and/or simply offer me a glass of chai:

आपने अपने समुदाय में मेरा स्वागत किये, उसका बहुत धन्यवाद। आपके उदारता, समय और धैर्य की मैं बहुत आभारी हूँ और तहे-दिल से उसकी क़द्र करती हूँ। मेरा काम आपके बिना असंभव होता।

Many, many people in India have enlightened me about rural development. I cannot possibly name all of them here, but a few deserve mention for this groundwater irrigation project. Thank you to Dr. Tushaar Shah at the International Water Management Institute (IWMI), Dr. Avinash Kishore at the International Food Policy Research Institute (IFPRI), and Anand Narayan at SELCO Labs.

The evaporation reduction project took place, and is continuing to take place, at Vigyan Ashram in Pabal, Maharashtra. I greatly appreciate the help of Dr. Yogesh Kulkarni, Ranajeet Shanbhag, Mahesh Lade, Devidas Shelar, and Anil in getting the experiment set up and monitoring the data collection of the students. Thank you also to the students who are collecting the data.

The initial pump testing work took place at Iron Dragon Corporation in Pittsfield, New Hampshire. Thank you to Bill Miskoe at Iron Dragon for your help in setting up the experiment and for teaching me about various pipe fittings and mechanical equipment, how to run an engine, and how to troubleshoot pumps. The experience you gave me proved invaluable when I had to test pumps again in India. Thank you also to Deborah Slocum, who, along with Professor Slocum, graciously hosted me during my time in New Hampshire.

This research was funded by the MIT Tata Center for Technology and Design. Thank you to the directors, Professor Charles Fine, Dr. Robert Stoner, and Patricia Reilly, for giving me the opportunity to be a Tata Fellow. Thank you also to Professor John Ochsendorf for not only informing me of the opportunity but also helping me apply and advocating for me.

I could not have gotten through this research without the help and support of all my friends, but one stands out the most. Thank you to Alonso Domínguez for generously helping me every step of the way. Thank you for your patience every time I obnoxiously ran over to your desk, even when you were super busy. Thank you for bouncing around ideas with me, giving me advice, and challenging me to be the best engineer I could be, to really understand fluid mechanics, to go back to the basics every time I confused myself. Thank you for teaching me MATLAB (and helping troubleshoot again and again), the magic of Illustrator to make beautiful plots, and the power of font choice (sorry about the Times New Roman). Thank you for recovering my lost documents—including this thesis—and revealing the deep secrets of the Microsoft Office Suite, even when I decided not to learn your beloved LaTeX. Most of all, thank you for being a supportive friend when I needed one most. This thesis would not be here today without your above-and-beyond assistance, and I will forever be grateful.

Thank you also to Marena Lin for your advice, willingness to brainstorm at all hours, and support in and out of India. Thank you for convincing me of the importance of agriculture and introducing me to the myriad associated issues, for pushing me to dig deeper into India and international development, and most of all, for making me think and rethink. I would also like to thank Suhrid Deshmukh for helping me translate documents in Hindi and Marathi and for feeding me cookies.

Thank you to my family, my mother Dena, my father Mayer, and my brother Ben, for their unwavering love and support not just during my time at MIT, but throughout all of my life. I would not be where I am today without you.

Contents

List of Figures

List of Tables

List of Symbols

A	cross-sectional area of the pipe / shaft	[m^2]
A_0	cross-sectional area of the mandrel wire	[m^2]
A_{land}	area of land irrigated	[m^2]
A_{pipe}	cross-sectional area of the pipe	[m^2]
B	bending stiffness	[Nm^2]
c_{hr}	cost of pump rental per hour	[INR/hr]
c_L	cost of kerosene per liter	[INR/L]
C_w	specific heat of water	[MJ/kgK]
d	diameter of the wire	[m]
D	pipe diameter	[m]
$d_{pulleywheel}$	diameter of the pulley wheel	[m]
d_{sheave}	diameter of the sheave on the engine shaft	[m]
E	elastic modulus of the material / evaporative flux	[Pa] / [mm/day]
e_a	actual vapor pressure	[kPa]
e_s	saturated vapor pressure	[kPa]
f	friction factor	
$f(u)$	function of wind speed	
F_g	force of the water due to gravity	[N]
F_p	force exerted by the pump	[N]
g	gravitational acceleration	[m/s^2]
G	ground heat flux	[MJ/m^2day]
h	Head	[m]
h_i	pitch distance	[m]
$H_{dynamic}$	dynamic head	[m]
H_{static}	static head	[m]
H_{total}	total head	[m]
h_{water}	height of irrigation water	[m]
i	layer number, increasing outwards	
I	area moment of inertia	[m^4]
J	polar moment of inertia	[m^4]
k	stiffness coefficient determined by supports	
K	pressure loss coefficient	
L	length of the pipe	[m]
L	length of pipe / shaft	[m]
L_{shaft}	total length of shaft when extended	[m]
M	bending moment	[Nm]
m	mass	[kg]
n	number of pistons per unit length	[number/m]
N_c	critical speed of the shaft	[rpm]
$n_{sections}$	number of sections the shaft is divided into	
n_{wires_i}	number of wires in the layer	
P	tensile force on the shaft / power output from engine	[N] / [W]

$P_{EngineIn}$	power input into engine	[W]
$P_{PumpOut}$	power output from the pump	[W]
Q	flow rate	[m^3/s]
Q_{fuel}	rate of fuel consumption	[L/s]
Q_{sol}	global horizontal solar radiation	[W/m^2]
r	mean radius of the flexible shaft	[m]
R_c	critical radius of curvature	[m]
Re_D	Reynolds number with diameter as characteristic length	
RF	daily rainfall	[mm]
RH	average relative humidity	[%]
r_i	inner radius of the hollow shaft	[m]
r_{layer_i}	mean radius of the layer	[m]
R_n	net radiation	[MJ/m^2day]
r_o	outer radius of the hollow shaft	[m]
$r_{outermost}$	outer radius of the outermost segment	[m]
r_{pipe}	inner radius of the pipe	[m]
$r_{ropewheel}$	radius of the rope wheel	[m]
r_{solid}	radius of a solid shaft	[m]
R_{wb}	net radiation at wet bulb temperature	[°C]
s	space between layers and between wires in a layer	[m]
T	Torque	[Nm]
t	time required to consume all the kerosene in the engine	[s]
T_a	average dry bulb air temperature	[°C]
T_c	critical torque	[Nm]
T_{cs}	torque at critical speed	[Nm]
T_d	dew point temperature	[°C]
T_e	equilibrium temperature	[°C]
T_w	average water temperature	[°C]
T_{w0}	initial water temperature	[°C]
T_{wb}	wet bulb temperature	[°C]
u	average wind speed	[m/s]
U	volumetric energy density of kerosene	[J/L]
v	velocity of the water	[m/s]
$V_{kerosene}$	volume of kerosene poured into the engine	[L]
V_{layer_i}	volume of the layer	[m^3]
V_p	linear velocity of the rope	[m/s]
V_{shaft}	total volume of the telescoping shaft	[m^3]
V_{total}	total volume of the flexible shaft	[m^3]
W_{eng}	engine power output	[W]
x	gap between piston and pipe wall	[m]
Z	depth of water	[m]
z_{inlet}	height of the inlet of the system	[m]
z_{outlet}	height of the outlet of the system	[m]
α	pitch angle	[rad]
α	Absorptivity	
γ	psychrometric constant	[kPa/°C]

Δ	slope of the saturation vapor pressure-temperature curve	[kPa/°C]
Δ_{wb}	svp-t curve at wet bulb temperature	[°C]
ε	emissivity / effectiveness	
η	Efficiency	
λ	latent heat of vaporization	[MJ/kg]
μ	dynamic viscosity of the fluid	[Pa·s]
ρ	density of the material / fluid	[kg/m^3]
ρ_w	density of water	[kg/m^3]
σ	normal stress / Stefan-Boltzmann constant	[Pa] / [W/m^{2}K^4]
τ	shear stress / time constant	[Pa] / [days]
τ_{allow}	maximum shear stress	[Pa]
τ_{eng}	torque of the engine shaft	[Nm]
$\tau_{pulleywheel}$	torque load on the pulley wheel	[Nm]
$\tau_{ropewheel}$	torque load on the rope wheel	[Nm]
ω_c	critical speed of the shaft	[rad/s]
ω_{eng}	angular velocity of the engine shaft	[rad/s]
$\omega_{pulleywheel}$	angular velocity of the pulley wheel	[rad/s]
$\omega_{ropewheel}$	angular velocity of the rope wheel	[rad/s]

List of Acronyms

APHRODITE	Asian Precipitation – Highly Resolved Observational Data Integration Towards Evaluation of Water Resources
APL	Above Poverty Line
BPL	Below Poverty Line
CGWB	Central Ground Water Board
DEHA	di(2-ethylhexyl) adipate, $C_{22}H_{42}O_4$
DEHP	di(2-ethylhexyl) phthalate, $C_6H_4(C_8H_{17}COO)_2$
GDP	Gross Domestic Product
GOI	Government of India
HDI	Human Development Index
INR	Indian Rupee (currency of India)
ISHRAE	Indian Society of Heating, Refrigerating, and Air-Conditioning Engineers
KKPKP	Kagad Kach Patra Kashtakari Panchayat
MIC	Minor Irrigation Census
MNREGA	Mahatma Gandhi National Rural Employment Guarantee Act
MOA	Ministry of Agriculture
MoWR	Ministry of Water Resources
MRI/JMA	Meteorological Research Institute of Japan Meteorological Agency
MTA	Ministry of Tribal Affairs
MWRRA	Maharashtra Water Resources Regulatory Agency
NGO	Non-governmental organization
NTFP	Non-Timber Forest Produce
OBC	Other Backward Caste
PDS	Public Distribution System
PET	Polyethylene terephthalate
PMC	Pune Municipal Corporation
PRADAN	Professional Assistance for Development Action
RIHN	Research Institute for Humanity and Nature
RKVY	Rashtriya Krishi Vikas Yojana (National Agriculture Development Program)
ROI	Return of Investment
SC	Scheduled Caste
ST	Scheduled Tribe
SWaCH	Solid Waste Collection and Handling Cooperative
TMY	Typical Meteorological Year
TWC	Tribal Welfare Commission
USD	United States Dollar

Chapter 1: Introduction

1.1 Introduction

"India lives in its villages," Mahatma Gandhi once famously declared. Sixty-six years after independence, much of India still lives in its villages. According to the 2011 census, 68.84% of the Indian population, or about 833.1 million people, live in rural areas [1]. The vast majority of the rural population depends on agriculture to survive. Despite employing approximately two-thirds of the Indian population, agriculture accounts for only 21% of the nation's Gross Domestic Product (GDP), according to the World Bank [2]. There is great opportunity to increase agricultural earnings; improved irrigation could play a major role in boosting yields and profits. The poorest farmers live in eastern India, where access to irrigation is most seriously constrained and thus where this research is focused.

Irrigation is critical to the productivity of agriculture, as it allows a farmer to ease his dependency on the rains in case of a late monsoon or drought, grow crops during drier seasons, and cultivate more profitable crops, which tend to be more water-intensive. Unfortunately, many farmers in India cannot afford irrigation. As a result, 55% of all agriculture in India is solely rain-fed, as of 2009 [3]. In some states in eastern India, less than 30% of agricultural land is irrigated; in Jharkhand, only 2.4% of cultivated land is irrigated, as of 2010 [4]. For smallholder farmers[1] in this region, groundwater is the primary source of irrigation, but less than 20% of the groundwater resource is exploited (exploitation up to 65% is considered safe by India's Central Ground Water Board) [5].

In eastern India about 92% of groundwater extraction utilizes diesel- or kerosene-powered surface pumps due to the scarcity of electricity [6]. The Government of India has already begun eliminating fossil fuel subsidies in phases. As the price of fuel rises, smallholder farmers irrigate less of their land or return to only rain-fed cultivation and grow less water-intensive—and less profitable—crops. This decline in irrigation results in significantly lower incomes and migration for alternative employment during the dry seasons [7, 8]. A cheaper means of irrigation would provide farmers with a more stable livelihood and their families with an improved quality of life.

[1] Defined as farmers who own less than two hectares of land.

This research therefore aims to bring down the operation costs of irrigation for smallholder farmers by developing a more efficient pumping system.

1.2 Regional Irrigation Variations in India: Fuel vs. Electric, East vs. Rest

Irrigation in India is generally divided into major and minor irrigation. Minor irrigation refers to irrigation structures that serve areas less than 2000 hectares. This research focuses on minor irrigation because India's poorest farmers utilize minor irrigation schemes. The Ministry of Water Resources (MoWR) divides minor irrigation into five categories: dug wells, shallow tube wells, deep tube wells, surface lift systems, and surface flow systems. Dug wells, shallow tube wells, and deep tube wells all fall under groundwater irrigation. Dug wells are hand-dug wide-diameter open wells. Shallow tube wells are boreholes drilled to depths less than 100 meters. Deep tube wells are boreholes drilled to depths greater than 100 meters. Surface lift systems include perennial and seasonal surface sources such as ponds and manmade tanks, but they are often referred to simply as tanks. Surface flow systems include rivers, streams, and manmade canals and are sometimes only called canals. The growth of cultivated area served by groundwater, canal, and tank structures are given in Figure 1.1. Groundwater irrigation has grown at much faster rates than canal and tank irrigation since the 1970's and now accounts for more than 90% of all minor irrigation structures, according to MoWR's Minor Irrigation Censuses. In fact, India by far consumes more groundwater than any other country in the world [9].

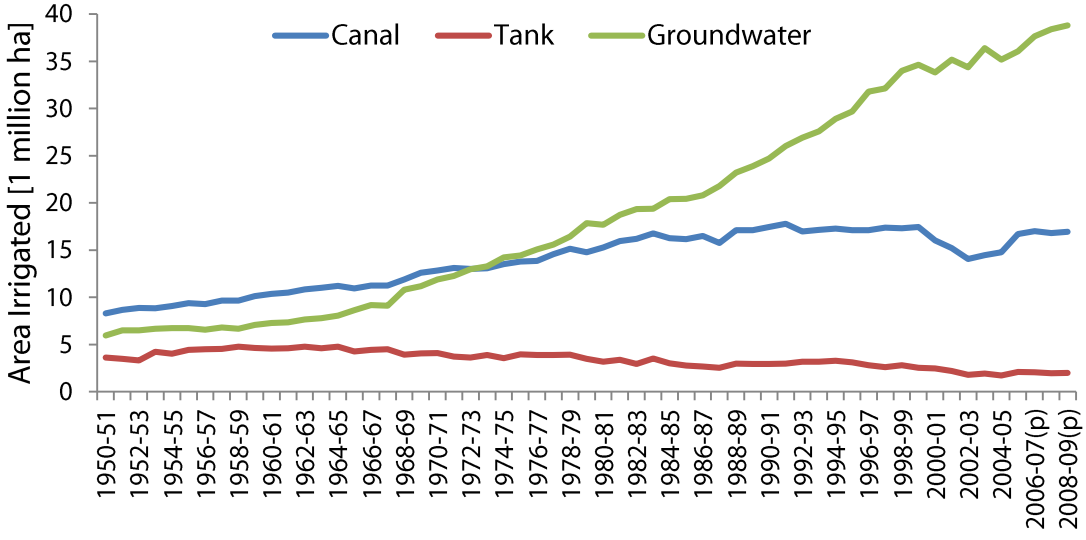

Figure 1.1. Irrigated area by source in India **[4]**.

The majority of this research focused on groundwater irrigation due to its importance among poor communities in eastern India. Measures to reduce evaporative losses from tanks were also explored, as discussed in Chapter 5, because of the necessity to revive tank irrigation as a sustainable alternative or supplement to groundwater. An introduction to tank irrigation will be given in that chapter.

Groundwater resources in India face two opposite problems. In parts of the country that have an extensive electricity grid, water tables have been plummeting. Electricity is often free or extremely cheap for agricultural purposes, so farmers have no incentive to limit the amount of water they pump. However, in eastern India, where electricity is scarce and pumps are run on expensive diesel, groundwater is underutilized—under 40% of annually-renewable groundwater resources are exploited (these resources are replenished with the monsoon rains) [9]. The difference in water levels between the electricity and diesel regimes can be seen in Figure 1.2, which reveals that in eastern India, levels rarely fall deeper than twenty meters, even during the driest month. Climate also benefits eastern India, which sees heavier rainfall than the western deserts. In fact, during monsoon season eastern India often suffers from flooding, which is a result of groundwater reject. Groundwater reject occurs when the ground is so saturated it cannot accommodate any additional water. Increasing groundwater utilization in eastern India has the potential to alleviate water-logging and flooding [5]. While overexploitation of groundwater resources in western India is certainly an important challenge to tackle, this research focuses on increasing groundwater utilization in eastern India.

Eastern India experiences underutilization of groundwater due to several constraints on pumping. According to the Minor Irrigation Census in 2001, 73.3% of groundwater structures in eastern India faced challenges that limited usage. These constraints included inadequate energy access, mechanical breakdown, and low water discharge. The insufficient energy, in the case of eastern India, reflects not an unreliable electricity grid but high variable costs of diesel required to run the pumps. Even if farmers had installed wells, they could not afford the operation costs of fuel to extract water from these wells [9]. By investigating technology options to decrease the operation costs, reduce mechanical breakdowns (or at least make breakdowns easier to repair), and increase water discharge, this research hopes to promote greater exploitation of renewable groundwater resources.

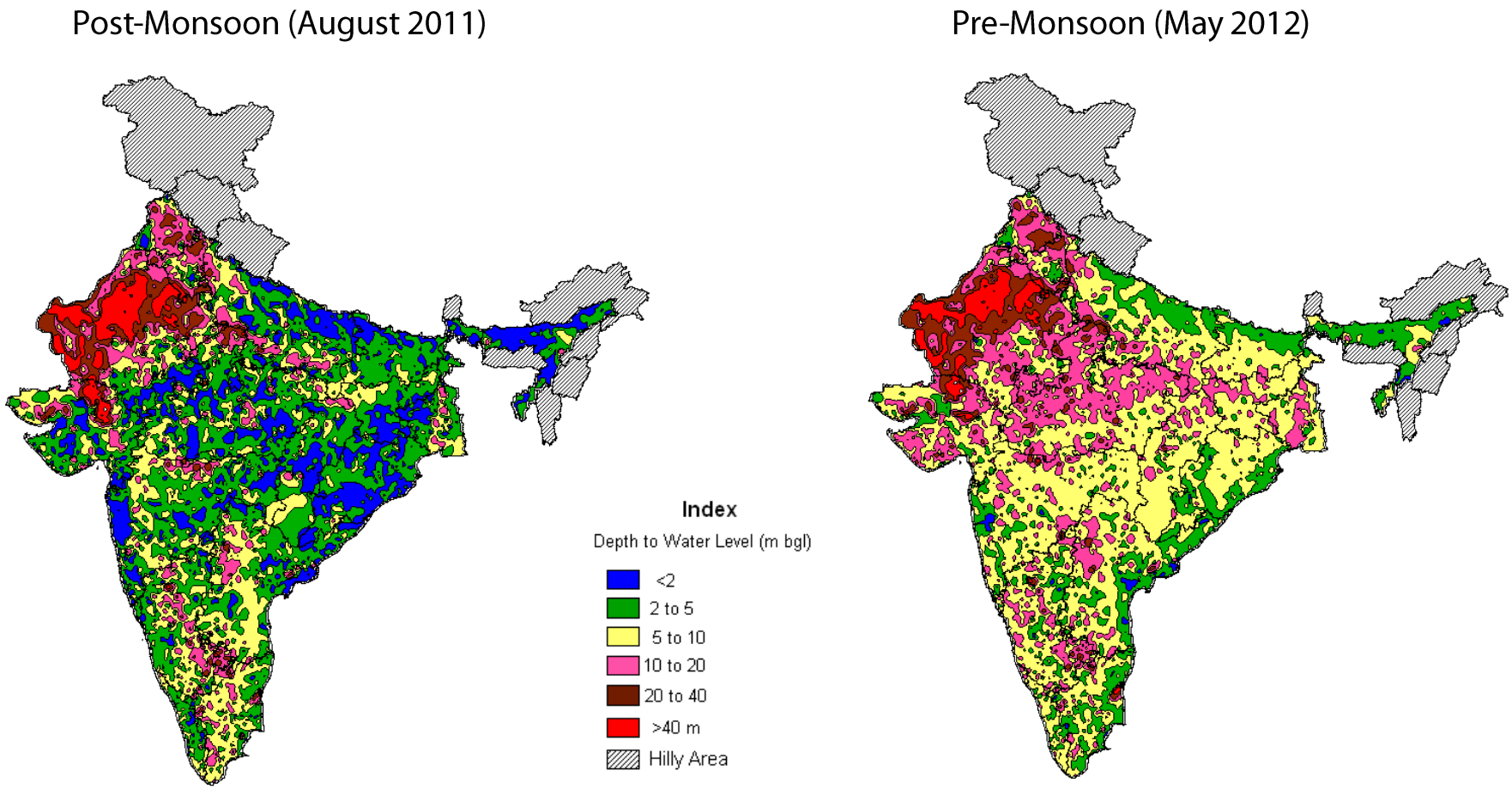

Figure 1.2. Groundwater resources expressed as depth to the water table during the highest and lowest months (August and May, respectively). **[10]**

1.3 Socioeconomic Context: Jharkhand

This research is focused on eastern India and parts of central India. Specifically, it is hoped that this project would benefit agrarian communities in the states of Bihar, Jharkhand, Odisha, Chhattisgarh, West Bengal, and Assam (Figure 1.3). These states have among the lowest Human Development Index (HDI) ratings and highest poverty incidence rates in India, as shown in Table 1.1 and Table 1.2.

The field location for this research is in Gumla district, Jharkhand (see Figure 1.4). Jharkhand's HDI is ranked 24 out of 28 Indian states [11] and its below poverty line (BPL) population is ranked 25 out of 28 [12], thereby making Jharkhand one of the poorest and least-developed states in India. According to the University of Oxford's Multidimensional Poverty Index, which employs indicators that account for living standards, infrastructure, health, and education and was created for the United Nations Development Programme's 2011 Human Development Report, Jharkhand is the second-poorest state in India, after Bihar, with 51% of its population living in severe poverty (53.5% of Bihar's population is severely impoverished) [13].

Table 1.1 2007-2008 Human Development Indices (HDI) for major states in India in descending order. **[11]**

State	HDI	State	HDI
Kerala	**0.790**	Uttarakhand	0.490
Himachal Pradesh	0.652	Andhra Pradesh	0.473
Goa	0.617	Assam	0.444
Punjab	0.605	Rajasthan	0.434
Northeast States (Excluding Assam)	0.573	Uttar Pradesh	0.380
Maharashtra	0.572	Jharkhand	0.376
Tamil Nadu	0.570	Madhya Pradesh	0.375
Haryana	0.552	Bihar	0.367
Jammu and Kashmir	0.529	Odisha	0.362
Gujarat	0.527	Chhattisgarh	0.358
Karnataka	0.519	**India**	**0.467**
West Bengal	0.492		

Table 1.2. The number and percentage of the population of each state that lives below poverty line (BPL) in ascending order. [12]

(No. of People in 100,000)

States	Rural		Urban		Total	
	% of Population	No. of People	% of Population	No. of People	% of Population	No. of People
Goa	11.54	0.6	6.9	0.6	8.7	1.3
Jammu and Kashmir	8.1	7.3	12.8	4.2	9.4	11.5
Himachal Pradesh	9.12	5.6	12.6	0.9	9.5	6.4
Kerala	12	21.6	12.1	18	12	39.6
Sikkim	15.51	0.7	5	0.1	13.1	0.8
Punjab	14.61	25.1	18.1	18.4	15.9	43.5
Meghalaya	15.34	3.5	24.1	1.4	17.1	4.9
Tamil Nadu	21.18	78.3	12.8	43.5	17.1	121.8
Tripura	19.84	5.4	10	0.9	17.4	6.3
Uttarakhand	14.85	10.3	25.2	7.5	18	17.9
Haryana	18.56	30.4	23	19.6	20.1	50
Nagaland	19.32	2.8	25	1.4	20.9	4.1
Mizoram	31.12	1.6	11.5	0.6	21.1	2.3
Andhra Pradesh	22.75	127.9	17.7	48.7	21.1	176.6
Gujarat	26.65	91.6	17.9	44.6	23	136.2
Karnataka	26.14	97.4	19.6	44.9	23.6	142.3
Maharashtra	29.51	179.8	18.3	90.9	24.5	270.8
Rajasthan	26.42	133.8	19	33.2	24.8	167
Arunachal Pradesh	26.16	2.7	24.9	0.8	25.9	3.5
West Bengal	28.79	177.8	22	62.5	26.7	240.3
Madhya Pradesh	41.98	216.9	22.9	44.9	36.7	261.8
Odisha	39.2	135.5	25.9	17.7	37	153.2
Uttar Pradesh	39.36	600.6	31.7	137.3	37.7	737.9
Assam	39.87	105.3	26.1	11.2	37.9	116.4
Jharkhand	41.56	102.2	31.1	24	39.1	126.2
Manipur	47.42	8.8	46.4	3.7	47.1	12.5
Chhattisgarh	56.13	108.3	23.8	13.6	48.7	121.9
Bihar	55.33	498.7	39.4	44.8	53.5	543.5
Total India	**33.8**	**2782.11**	**20.9**	**764.7**	**29.8**	**3546.8**

*The total India figures are greater than the sum of the state figures because they include Union Territories and the Delhi National Capital Region.

Figure 1.3. Map of India. The states of eastern India are in green.

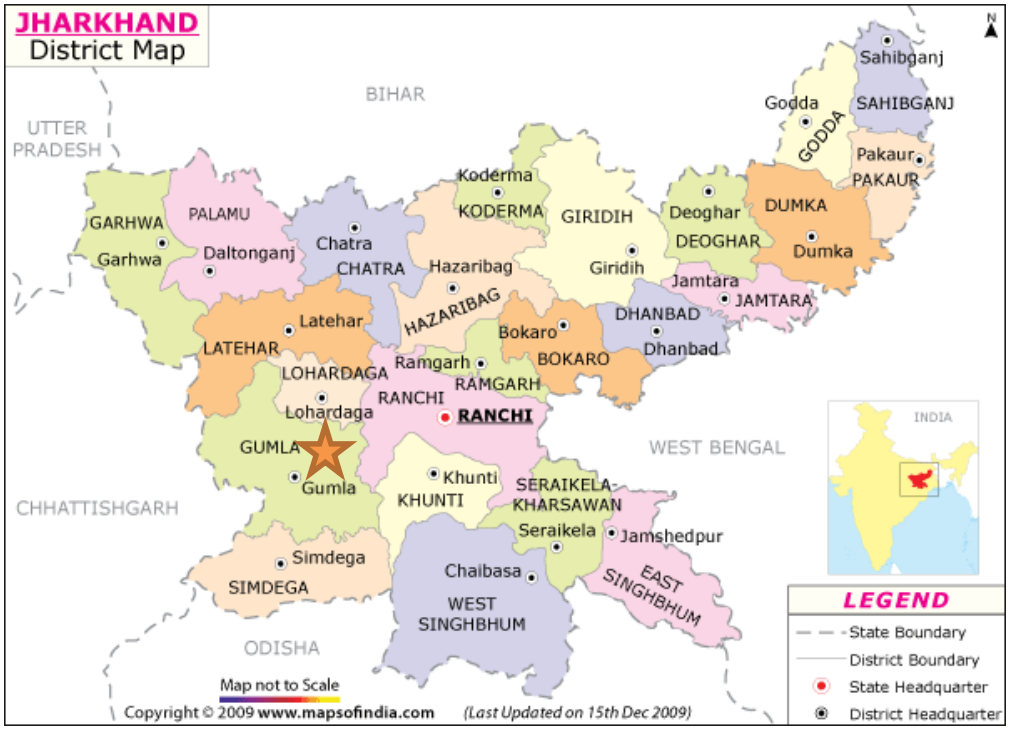

Figure 1.4. Districts of the state of Jharkhand. The field work for this research took place in Gumla District. **[14]**

1.3.1 Economy of Adivasi Communities

Approximately 26.3% of the population of Jharkhand belongs to ethnic groups known as "Scheduled Tribes" (STs) [1]. These groups are also known as *adivasi* (indigenous) or *vanvasi* (forest-dwelling). Article 342 of the Constitution of India defines STs as follows:

> "…an endogamous group with an ethnic identity; who have retained their traditional cultural identity; they have a distinct language or dialect of their own; they are economically backward and live in seclusion, governed by their own social norms and largely having a self-contained economy." [7]

The dominant tribes in Jharkhand are Oraon, Santhal, Munda, Ho, and Saber. Gumla District, the field site for this research, is designated as a "Scheduled Area," meaning that a large proportion of its population is tribal. Gumla's population is 68.36% ST—the highest percentage of any district in Jharkhand—and the largest adivasi group in Gumla is the Oraon [15].

As several policies by the Government of India have promoted assimilation of tribes into mainstream society, many of these adivasi communities are in the midst of a transition from a forest-based lifestyle to a more settled one. Traditionally, the adivasis lived off the forest as hunter-gatherers. Today, each community is in a different state of transition: some are still fully forest-dependent, some have become fully agrarian, settled societies, and others could fit anywhere in-between on the spectrum. Modern tribal livelihoods now fall into three categories: forests, agriculture, and migration. Households may be involved in any combination of the three [7].

The forest economy, which dominates the hilly areas of central and eastern India, involves collecting non-timber forest products (NTFP) such as fungi, roots, tubers, fruits, and nuts and participating in forestry operations. Those engaged in agriculture cultivate either their own land or disputed forest lands. In the eastern hills, the staple crop is rice, more popularly called "paddy" in India, and minor cereals are grown in the central hills. After the monsoon harvest, many migrate to work as laborers in highly productive agricultural areas such as Punjab, in construction in cities, or in mines or factories closer to home [7].

While shifting agriculture is popular among some tribes, in Gumla tribal farmers tend to cultivate the same land year after year. In 1989, the Planning Commission established "Agro-Climatic Zones" to assist with regional development planning; Jharkhand lies in Agro-Climatic Zone VII. As illustrated in Figure 1.5, the land in this zone encompasses three types: upland, midland, and lowland, each with unique irrigation challenges. Groundwater tends to sit deeper in

upland areas, because water travels downhill even underground, so wells must be dug deeper. Additionally, the layer of soil in the uplands is thinner, so hard rock is closer to the surface; digging wells becomes more difficult. Land passes down through the family, and fathers divide each type of land equally among their sons. This system of inheritance results in land holdings that are not contiguous, thereby creating additional challenges for irrigation. Often long hoses are needed to delivery water to plots far from the well, thereby increasing pipe losses and reducing efficiency and flow rates. Due to variations in water availability, soil characteristics, and climate, farmers grow different crops at each of the three levels of land.

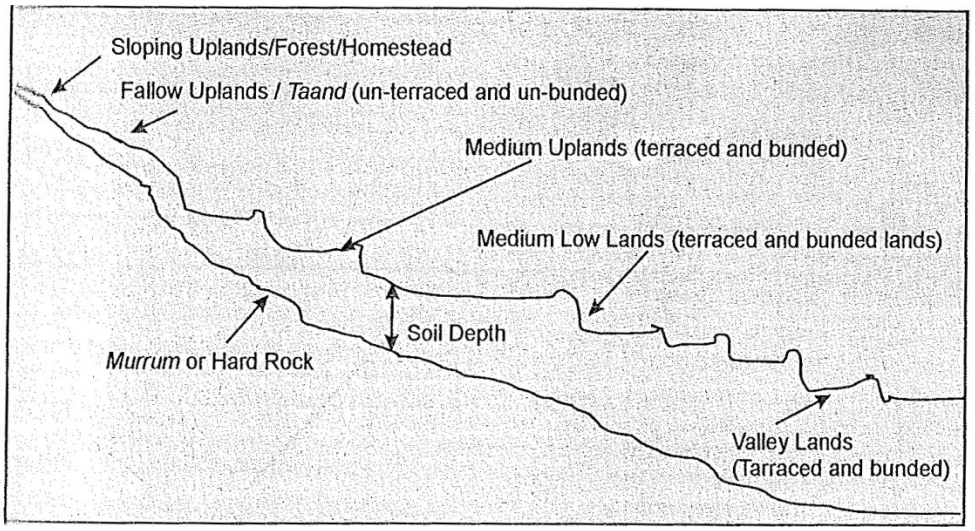

Figure 1.5. Typical terrain in the Agro-Climatic Zone VII of India. **[16]**

1.3.2 Agriculture and Irrigation in Gumla District

Discussions were held in July 2012 with groups of five to twenty farmers in the villages of Shahitoli, Jamtoli, Menatoli, Lutoambatoli, Toto, Ghaghra, Sivrajpur, Jaldega, Kondekera Dandtoli, and Raidih in Gumla District about their crops and irrigation. The *kharif* crop is grown during the monsoon and is planted after approximately ten days of rain (in Jharkhand, this is usually in July) and harvested in October. The *rabi* crop is grown during the winter, sown in November, and the *zaid* crop is grown during the Indian subcontinent's summer, which is April to June. Interestingly, the word "zaid" is related to "zyada," which means "more" in Hindi, as it is a bonus crop season. Traditionally, crops could not be grown at all during the summer due to the severe lack of rain and only recently with the onset of irrigation could small plots of land be utilized. The crops grown at each level during each season among these villages are listed in Table

1.3. A greater variety of crops are grown during *rabi* season because during *kharif* season most land must be dedicated to the cash crop of rice. The lowlands are left fallow during the *zaid* season in order to prepare the land for the *kharif* rice. The vast majority of farmers involved in the group meetings revealed that they do not plant in the uplands and midlands during the *zaid* season because they cannot afford irrigation. Those who do grow crops in the summer use less than 10% of their land due to the high price of irrigation. Additionally, some farmers said that during *rabi* season they utilize only 15 to 50% of their land, others less than that or even none. For example, in the village of Jamtoli, which has 45 households, only five families cultivate their land during *rabi*, and none during *zaid*. The farmers who decide not to grow crops during the drier seasons migrate to mines, factories, and cities to work as manual laborers. The farmers estimated that between 20 and 60% of households send at least one family member to work elsewhere.

The full range of water requirements and irrigation frequencies for each crop during each season as recalled by the groups of farmers in the ten villages are given in Table 1.4. The water variation for each crop may be a result of the differences in soil, microclimatic conditions, and/or the farmers' abilities to pay for irrigation. The farmers did not keep track of water requirements for most crops during *kharif* season because they rely solely on rain. Rice is the only exception, because it serves as their primary source of income. The farmers ensure that their rice is always properly watered and therefore sometimes must irrigate during dry spells, even during the monsoon. For crops grown during both *rabi* and *zaid* seasons, the crops receive more water (either a larger quantity of water each time they are irrigated, more frequent irrigation, or both) during *zaid* season because the water is consumed faster in the heat. It is important to note that the water requirements listed may or may not be the actual water requirements for each crop but are simply the requirements reported by the farmers. It is possible that the farmers push the crops to their survival limits in order to save money; it is unclear how healthy these crops might be. The greater water requirements during *zaid* season lead to higher irrigation costs that most farmers in these villages cannot afford. Therefore, most do not cultivate and lose out on the income of a crop season.

Every farmer said that he irrigates in the late afternoon or early evening, always after 4:00 pm, in order to reduce water loss due to evaporation. The sources of water for this irrigation and the pumps used to extract the water are given in Table 1.5, as reported by the farmers who partook in the discussions. Though there are some surface water irrigation schemes in the area, almost all farmers said that open wells are their primary source of irrigation, if they irrigate at all. Most

farmers explained that they retrieve the water by renting a small 1.5 or 3 hp gasoline-start, kerosene-run pump from a neighbor, even when larger capacity pumps are available, because they are cheaper to rent. The rental pumps are delivered to the well via bicycle. A typical well layout and pump system are given in Figure 1.6. Wells are fairly standardized in Jharkhand because they are mostly installed under government schemes such as the Mahatma Gandhi National Rural Employment Guarantee Act (MNREGA) and Tribal Welfare Commission (TWC) that specify well dimensions.

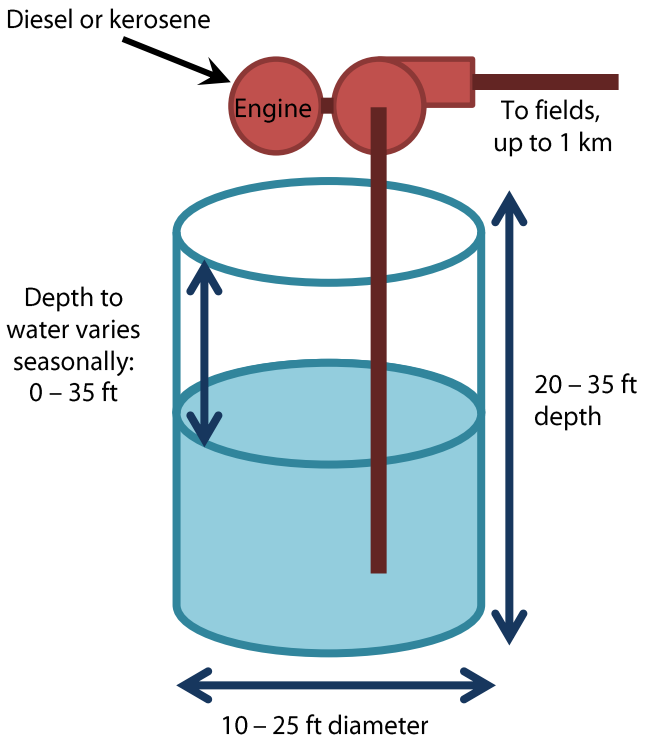

Figure 1.6. Typical well layout with fuel pump in Jharkhand.

Table 1.3. Crops grown in the upland, midland, and lowland fields during each season in ten villages in Gumla.

	***Kharif* / Monsoon crop (July – October)**	***Rabi* / Winter crop (November – March)**	***Zaid* / Summer crop (April – June)**
Upland	Rice (*goda*)*	Cabbage	Pumpkin
	Tomato	Cauliflower	Bitter gourd
	Millet	Potato	Beans
	Groundnut	Onion	Maize
	Cauliflower	Pumpkin	Onion
	Radish	Mustard	Potato
	Black gram	Peas	Tomato
	Green gram	Wheat	Watermelon
	Chili	Chili	
	Okra	Eggplant	
	Pumpkin	Red lentil	
	Maize	Radish	
	Beans	Spinach	
	Almond	Tomato	
Midland	Rice (*lalat*)*	Peas	Pumpkin
		Cabbage	Bitter gourd
		Cauliflower	Bottle gourd
		Potato	Cucumber
		Onion	Okra
		Wheat	Green beans
		Pumpkin	Maize
		Bottle gourd	
		Cucumber	
		Maize	
Lowland	Rice (*kalinga*)*	Onion	
		Potatoes	
		Cauliflower	
		Cabbage	
		Wheat	
		Chickpea	
		Black gram	

*Italicization indicates the varieties of rice in Hindi. Different varieties of rice are grown at each level of land due to the differences in soil, water, and microclimatic conditions.

Table 1.4. Seasonal water requirements and irrigation frequency for crops, according to farmers in Gumla.

Season	Crop	Water Requirement [in]	Irrigation Frequency
Kharif	Rice*	2 – 4	Rain-fed
	Maize	—	Rain-fed
	Millet	—	Rain-fed
	Black gram	—	Rain-fed
	Beans	—	Rain-fed
	Almond	—	Rain-fed
	Groundnut	—	Rain-fed
	Cauliflower	—	Rain-fed
	Okra	—	Rain-fed
	Tomato	—	Rain-fed
	Radish	—	Rain-fed
	Chili	—	Rain-fed
	Pumpkin	—	Rain-fed
Rabi	Cabbage	1 – 1.5	Every 9 – 11 days
	Cauliflower	1 – 1.5	Every 10 – 15 days
	Potato	1 – 1.5	Every 9 – 15 days
	Peas	2	Every 4 – 15 days
	Onion	1	Every 3 – 10 days
	Wheat	1 – 2	Every 6 – 18 days
	Maize	1 – 2	Every 12 – 15 days
	Pumpkin	1	Every 8 – 18 days
	Bottle gourd	1 – 1.5	Every 8 – 18 days
	Cucumber	1.5	Every 8 – 18 days
	Mustard	1	Every 6 – 8 days
	Eggplant	1 – 1.5	Every 9 – 15 days
	Red lentil	2	Every 15 to 30 days
	Radish	1 – 1.5	Every 9 – 15 days
	Spinach	1	Every 9 – 15 days
	Tomato	1.5	Every 3 – 9 days
	Chickpea	2	Every 30 – 45 days
	Chili	1.5	Every 7 days
Zaid	Pumpkin	1.5	Every 6 – 8 days
	Bitter gourd	1.5	Every 6 – 8 days
	Bottle gourd	1.5	Every 6 – 8 days
	Cucumber	1.5	Every 6 – 8 days
	Okra	1.5 – 2	Every 6 – 8 days
	Green beans	1.5 – 2	Every 7 – 9 days
	Beans	1.5 – 2	Every 5 – 7 days
	Maize	1.5	Every 6 – 8 days
	Onion	1 – 1.5	Every 5 – 7 days
	Potato	1 – 1.5	Every 5 – 7 days
	Tomato	2	Every 2 – 5 days
	Watermelon	1.5 – 2	Every 6 – 8 days

*Farmers keep track only of water requirements for rice during *kharif* season, due to its economic importance.

Table 1.5. Water sources (excluding rain) and pumps in villages in Gumla where group discussions took place. Information is given as reported by the farmers**.**

Village [No. of Households]	WATER SOURCES							PUMPS			
	Water Source	No.	Well Depth	Depth to Water (June)	Depth to Water (Sept)	No. Households Served	Funding*	Size [hp]	Fuel**	No.	Owner
Shahitoli (50)	Open well	6	25 – 30 ft (lowland) 30 – 35 ft (upland)	> 20 ft (lowland) > 25 ft (upland)	5 ft (lowland) 10 – 15 ft (upland)	5 per well	TWC, PRADAN	2 5	Diesel Diesel	2 8	Individual Individual
	Stream	2	—			10 per stream		8	Kerosene	5	Community
Jamtoli (45)	Open well	6	20 ft (lowland) 25 ft (upland)	15 – 18 ft (lowland) Dry (upland)	0 ft (lowland) 5 ft (upland)	5 – 10 per well	MNREGA	3	Kerosene	3	Individual
Menatoli (15)	Open well	9	20 – 25 ft (lowland) 25 – 30 ft (upland)	18 – 23 ft (lowland) Dry (upland)	0 – 5 ft (lowland) 5 – 10 ft (upland)	1 – 3 per well	TWC	3	Kerosene	1	Individual (in disuse)
	Pond	1	—	Not specified	Dry	3					
Lutoambatoli (36)	Open well	7	30 ft	25 – 28 ft	5 – 10 ft	3 – 5 per well	TWC, MNREGA	1.5	Kerosene	1	Individual
	Pond	3	—	Not specified	Dry	6 per pond	PRADAN	8	Diesel	1	Community
Sivrajpur (82)	Open well	29	25 – 30 ft (lowland) 40 ft (upland)	20 – 25 ft (lowland) 35 ft – dry (upland)	0 – 5 ft (lowland) 10 ft (upland)	1 – 3 per well	TWC, MNREGA	3 3.5 5 8	Kerosene Kerosene Diesel Diesel	2 9 2 1	Individual Individual Individual Individual
	Canal	1	—	Not specified	Not specified	15	PRADAN	8	Diesel	1	Community
Jaldega (94)	Open well	22	30 ft	25 ft - dry	5 ft	2 – 5 per well	TWC	1.5	Kerosene	3	Individual
	Pond	1	—	Not specified	Not specified	10					
Kondekera Dandtoli (40)	Open well	20	30 ft (lowland) 35 ft (upland)	23 – 27 ft (lowland) 30 – 33 ft (upland)	2 – 7 ft (lowland) 5 – 10 ft (upland)	1 – 3 per well	TWC, MNREGA	1.5 3	Kerosene Kerosene	5 3	Individual Individual

*TWC = Tribal Welfare Commission. MNREGA = Mahatma Gandhi National Rural Employment Guarantee Act. PRADAN = an agricultural NGO.

** Kerosene = gasoline-start, kerosene-run. Significantly more kerosene is consumed than gasoline.

1.4 Groundwater Markets

Groundwater markets in India are informal and lack legal regulation, partially due to nebulous water rights. Though there are variations between regions, generally the market is divided into "water sellers" and "water buyers." Water sellers are those who own means of irrigation, whether that involves an electrified tube well or a mobile diesel pump, and hire out these means [17]. In eastern India, the water sellers overwhelmingly own fuel-powered pumps (though "diesel" is commonly used in literature, kerosene pumps, as discussed below, have been growing in popularity), as approximately 91.9% of all pumps in the region run on fuel, as of the 2001 Minor Irrigation Census [9]. The water buyers either purchase water from the tube wells, which are delivered to their fields via long discharge hoses, or rent fuel pumps on an hourly basis.

The vast majority of pumps are individually-owned [18]. Wells, too, are almost entirely privately owned, even if some government assistance was required in acquiring the funding and resources to dig the wells [9]. Questions over who sells and who buys water remain uncertain, as does the equitable distribution of benefits. The largest group of water sellers as of 1998 was likely farmers who own one to four hectares of land, as they owned approximately 50% of pumps at that time. However, the trend of pump ownership was shifting from the large and very large farmers toward the medium, small, and marginal farmers. Small and marginal farmers are usually water buyers, but ownership of pumps among this group is increasing. Those with especially small plots of land, or unproductive land, see renting out pumps as an opportunity to supplement their income in lieu of profitable crops [17].

Transactions can occur in a variety of ways, depending on location. Water buyers can pay the water sellers by the hour, by the day, or a flat rate for the entire season. Payment can be in the form of cash or crop-sharing (that is, the water buyer will give a certain percentage of his yield to the water seller). The water seller sometimes acquires the fuel and charges the water buyer for it, or else the water buyer purchases the fuel separately and pays only the rental fee to the water seller [18].

In some regions, water sellers operate like an oligopoly. With very few water sellers operating within a given area, they often work together to ensure similar rates. When interviewing farmers, the author discovered that within a village every pump owner charges approximately the same hourly rental rates. Therefore, though small competition does exist, it does not result in lower

costs for the water buyer. As a result of the oligopoly, it is possible that even with reduced fuel costs, operation costs will be kept high by the water sellers.

Where fuel pumps are rented out, they are transported to the well by the pump owner on a bicycle, as shown in Figure 1.7. These fuel pumps must be babysat; a person must stay nearby in order to ensure smooth operation of the pump, refill the fuel tank as necessary, or troubleshoot if something goes wrong. The pump owners, if renting out to a farmer who is inexperienced with engines and pumps, must fulfill this role of operator and stay with the pump during hours of irrigation. Under these circumstances, the pump owner might increase the hourly rental price for his labor. Additionally, in some situations, especially during particularly busy seasons, the pump owners might increase the hourly rental fee in order to discourage water buyers and make up for lost hours of productivity tending to his own farm. During sowing season, for example, the pump owner's time becomes more valuable to him than the income earned from renting out his pump [19].

Figure 1.7. Transporting a pump and associated hoses to a well.

Because rental costs are higher than fuel costs, according to the economics researcher interviewed, advances in efficiency of the pump would not make much difference to the pumping behaviors of farmers. Although the farmers would spend less on fuel using a more efficient system, the time cost would remain high. If farmers want to spend the money saved from reduced fuel consumption on additional pumping hours, the pump owners might raise their hourly rates in response in order to limit the amount of time they must expend on renting out the pumps, especially during busy seasons. Therefore, because a more efficient pump may lead to increased rental costs, greater efficiency does not necessarily reduce total operation costs [19]. In that case, the goal should be to increase the quantity of water farmers can extract per hour so that they can utilize more irrigation per rupee.

To achieve widespread adoption, increased performance must be achieved at a capital cost similar to pumps already on the market. Capital cost reigns supreme over operation costs in financial decision-making among the poor in rural India [20]. The author learned from pump dealers in the market in Ranchi, the capital of Jharkhand, that gasoline-start, kerosene-run pumps ranging from 1.5 hp to 3.5 hp cost between INR 8,500 and INR 25,000 (approximately USD 140 to USD 410). Therefore, the cost of the pump developed in this research should be cost-competitive with this range. (However, achieving such low costs would be difficult in for a prototype.)

1.5 Impacts of Rising Fuel Prices

The Government of India historically has heavily subsidized fossil fuels, but as of January 2013 subsidies are being phased out [21]. The rise in fuel prices puts an energy squeeze on agriculture, as many implements require diesel to run. In parts of India without electricity, this energy squeeze is particularly severe, as they rely on diesel not only for tractors, tillers, and threshers but also for irrigation. Despite the dramatic rise in the cost of agricultural inputs and irrigation, the farm-gate price[2] of crops has not increased similarly (Figure 1.8). Although diesel rates experienced an eight-fold increase between 1990 and 2007, during the same time the nominal price of rice rose by less than 50% [22]. When energy costs rise but profits do not rise with it, meaningful impacts on smallholder agriculture can occur.

[2] Farm-gate price is the price at which a product is sold from the farm (not necessarily on the market). In other words, it is the revenue earned by the farmer.

The effects of this energy squeeze on agriculture are varied. Studies, including those by Shah (2007) [22], Mukherji (2007) [23], and Kumar et al. (2008) [24], have found that higher energy costs reduce irrigation in some cases, while in other cases farmers figure out adaptation strategies. In some areas, the groundwater economies have been shrinking as pump rentals decline. In these regions, the amount of land under irrigation has actually fallen [23]. In other areas, farmers continue pumping but devise innovative practices to increase water productivity and optimize other inputs such as fertilizers [24]. Some farmers switch to less water-intensive crop varieties (which are often less profitable), while others try growing more profitable but high-risk crops such as vegetables. However, these more profitable crops have actually become less profitable as they flood the market and rising fuel costs lead to increased transportation costs. Other farmers completely stop irrigating and return to rain-fed cultivation [23].

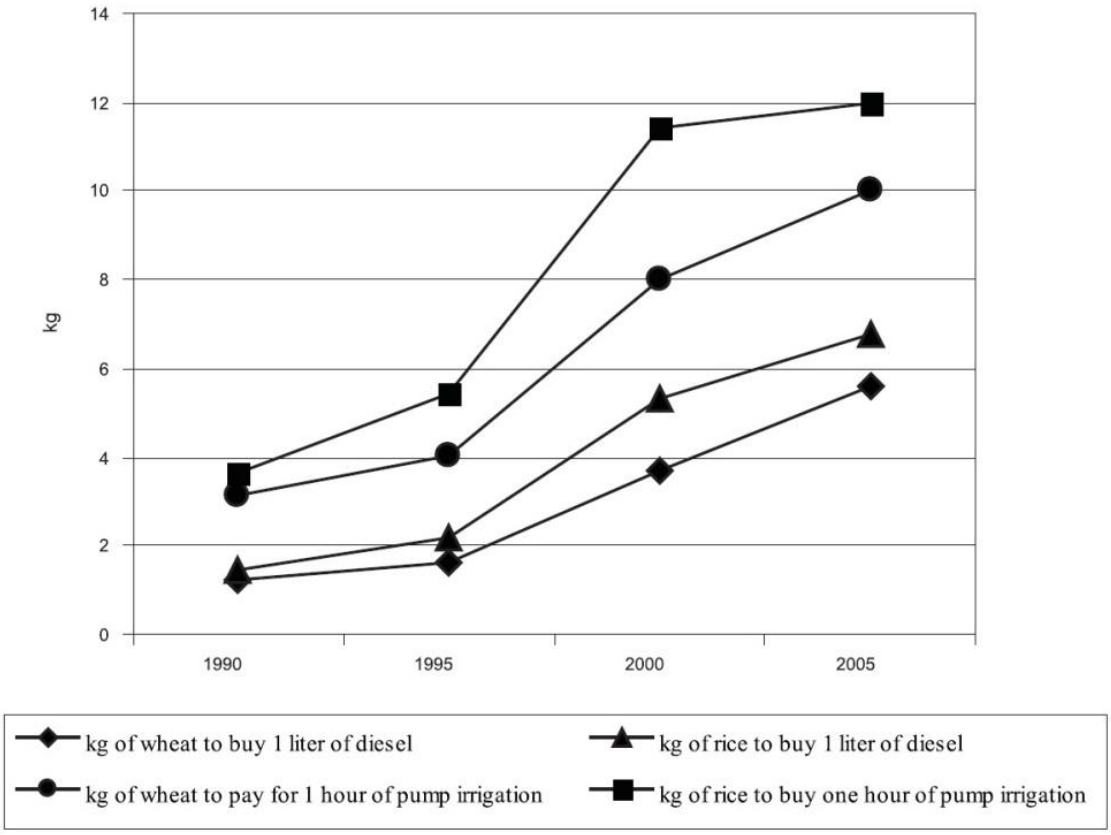

Figure 1.8. Amount of wheat and rice required to purchase irrigation in Deoria, eastern Uttar Pradesh. **[22]**

Some small and marginal farmers abandon farming and migrate for work. Some of these migrants go to Punjab and Haryana, where there is plenty of cheap electric pumping infrastructure, to lease and cultivate land. While these farmers are gone, they lease out their land to either large

or landless farmers. However, many landless farmers are finding farming unaffordable and also migrate for work rather than leasing land. As a result, in some cases, larger landowners face a labor shortage and agricultural productivity in an entire region can decline [22].

Migration has serious implications on the well-being of a family. In many cases where the entire family moves, especially to a state where the family does not have official residency, the family cannot avail of social services, such as education and healthcare. Children must drop out of school and illnesses go untreated. The energy squeeze on irrigation can aggravate these problems by forcing a surge in migration [7].

All of these changes have led to transformations in the role of women. In West Bengal, where a rice boiling industry once thrived, women are finding themselves out of work—and out of a source of income—as *boro* rice cultivation falls (*boro* is a more water-intensive, though profitable, variety of rice). The switch to vegetables from grains requires more in-field labor, so women find themselves spending more time in the field. Additionally, many families who give up on farming move their focus to animal husbandry and dairy. Women are often the ones who must care for the livestock. The energy squeeze, then, increases the burden imposed on women [22].

Interestingly, many farmers have adjusted by switching fuels. Farmers have started pouring kerosene into their diesel pumps, because kerosene is much cheaper than diesel and available at subsidized rates through the Public Distribution System (PDS). PDS kerosene is intended for cooking and lighting, and a household can purchase up to four liters per month. Chinese pumps, which accept kerosene and are cheaper, lighter, and more efficient than Indian pumps, have become very popular in West Bengal. Originally, these pumps were smuggled into India through Bangladesh [23]. They are now legal and assembled in Kolkata. Many Indian-manufactured kerosene pumps have entered the market as well. Thanks to the rapid growth of kerosene pumping and the limited quantity of kerosene available through the PDS (only 4 L allowed per household), the kerosene black market has been thriving. Black market kerosene is sometimes adulterated and can damage the engine over time [22].

1.6 Irrigation Pumping Inefficiency

Pumping systems in India are very inefficient, thereby causing higher operation costs than necessary. System efficiencies—that is, the efficiencies of entire pumping systems inclusive of power source, pump, piping, and pipe fittings—of electric pumping systems have been found to be as low as 13%, while diesel pumping systems can have system efficiencies as low as 5% [5]. Rectification programs across the country, which served both to investigate the pump efficiency issues as well as increase efficiencies of working pumps, have found the following common problems [25, 5, 26]:

- Improper installation
- Check valve or foot valve in need of replacement
- Overheating
- Engine speed needed to be reduced
- Poor or superfluous pipe fittings
- Excessive delivery pipe length
- High suction lift
- Poor condition of foundations causing greater vibration
- Absence of technical services available to farmers

Sikka and Bhatnagar (2006) described studies conducted by the Indian Council of Agricultural Research (ICAR) under the All India Coordinated Research Project (AICRP) on "Optimisation of Ground Water Utilization through Wells and Pumps" that tested the efficiency of pumps before and after rectification measures in Jabalpur, Madhya Pradesh. They found that 95% of pumping systems had efficiencies less than 50%, and more than 35% of pumping systems had efficiencies below 20%. Every pump with efficiency less than 20% faced problems with suction lift, fittings including the foot valve, and/or poor installation. The results of this study are given in Table 1.6. The study found that rectification measures could improve water discharge by 22.9% to 68.6%, with an average of 40.0%, and efficiency by 24.7% to 69.0%, with an average of 41.9% [25]. Unfortunately, the effect of each individual rectification measure on water discharge and efficiency was not identified.

Table 1.6. Discharge and efficiency before and after rectification measures for ten pumps in Jabalpur, 1998. **[25]**

Make	Year*	HP	Discharge, L/s			Efficiency, %			Rectification Measures*			
			Before	After	%	Before	After	%	S	F	L	FT
I	1989	5	6.35	8.15	28.3	21.95	28.01	27.6	-	Y	Y	Y
II	1993	5	7.00	11.80	68.6	24.50	41.4	69.0	1.70	-	Y	Y
III	1991	5	5.50	8.60	56.4	17.14	26.81	56.4	0.40	Y	Y	Y
IV	1996	5	7.00	8.60	22.9	18.20	23.42	28.7	-	Y	Y	Y
V	1992	5	5.00	7.10	42.0	24.21	34.38	42.0	1.20	Y	Y	Y
VI	1996	5	8.00	9.85	23.1	20.30	25.32	24.7	-	-	Y	Y
VII	1987	5	3.60	5.25	45.8	10.54	15.37	45.8	-	Y	Y	Y
VIII	1990	5	4.50	7.30	62.2	8.71	14.23	63.4	0.90	Y	Y	Y
IX	1992	5	6.00	8.65	44.2	16.88	24.34	44.2	1.00	Y	Y	Y
X	1996	7.5	11.50	14.96	30.0	18.40	23.28	26.5	-	Y	Y	Y
Average			6.45	9.03	40.0	18.08	25.66	41.9				

S – Suction head reduced (m); F – Foundation improved; L – Leakage stopped; FT – Excessive fitting removed. *Year of installation

In addition to these problems, pumps are usually oversized for their application. Farmers are ill-informed about how to select an appropriate pump. Until recently, few pumps rated under 5 hp were available on the market, but pumping on a shallow well serving a small farm usually does not require such high power inputs. If a farmer uses a too-large-capacity pump, his pump will not operate near its best efficiency point and fuel consumption will increase. Not only do farmers not know how to select pumps, they also do not know how to maintain or repair pumps. Many pumps receive little or poor maintenance, and local mechanics, though knowledgeable, often do not have access to replacement parts [26].

1.7 Research Goals

This research mostly concentrates on reducing pumping inefficiencies, specifically by tackling the suction head problem, while continuing to employ the fuel engines currently in use. Options utilizing other sources of power were eliminated due to the high costs of these alternatives. Kumar and Kandpal (2007) found that switching to renewable energy technologies for pumping depends on energy resource availability, groundwater availability, affordability, and the willingness of farmers to invest in new technologies. Small and marginal farmers, Kumar and Kandpal discovered, would not meet these criteria and thus would be unlikely to adopt pump

systems employing renewable energy [27]. Purohit (2007) conducted a financial evaluation of various energy alternatives. He concluded that solar photovoltaic pumps would never pay back for themselves without subsidies; for solar pumps to become cost-competitive, diesel rates would have to triple. Even with subsidies, he found that solar pumps would not be a viable option for small and marginal farmers. Wind power would not be reliable due to its intermittency. Treadle pumps are very labor-intensive, offer low-lift (they are suction pumps), and are unpopular with farmers. Purohit learned that a dual-fuel engine running on biogas would be the most attractive and affordable option if and only if there is cheap, plentiful availability of biomass—but in most of India, despite the hype around biomass, there is no such availability. Biomass, such as dung, wood, and agricultural waste, serves many other purposes in rural India, including but not limited to cooking, heating, construction, and fertilizer [28]. The focus of this research, then, is not on the power source but on improving the efficiency of the use of mechanical output from that power source.

Reduction or elimination of suction head was chosen as the primary inefficiency issue to tackle in this research because of its great potential to significantly improve pump performance. Figure 1.9 illustrates the effect of varying suction head on total head and efficiency as a function of flow rate. Under suction conditions, the head capacity and efficiency break away from the rated head and efficiency. These breakaway points indicate the point at which cavitation begins to occur. As suction lift increases, the flow rate at which cavitation begins decreases, and higher head capacity and efficiency cannot be achieved [29].

Cavitation in a centrifugal pump occurs when the pressure of the water at the inlet falls below the vapor pressure of water at that temperature, thereby forming vapor bubbles. The higher the suction head is, the lower the pressure on the inlet side of the impeller must be to pull water up. When the liquid-vapor mixture is suddenly subjected to high pressure on the discharge side of the pump, the bubbles implode and burst holes in the impeller. In addition to significantly decreasing the flow rate and efficiency, the damage caused by cavitation can shorten the lifetime of the impeller and the pump. Even when cavitation does not occur, under suction conditions the presence of bubbles in the fluid can decrease the density of the fluid, thereby resulting in lower flow rates and efficiency [30].

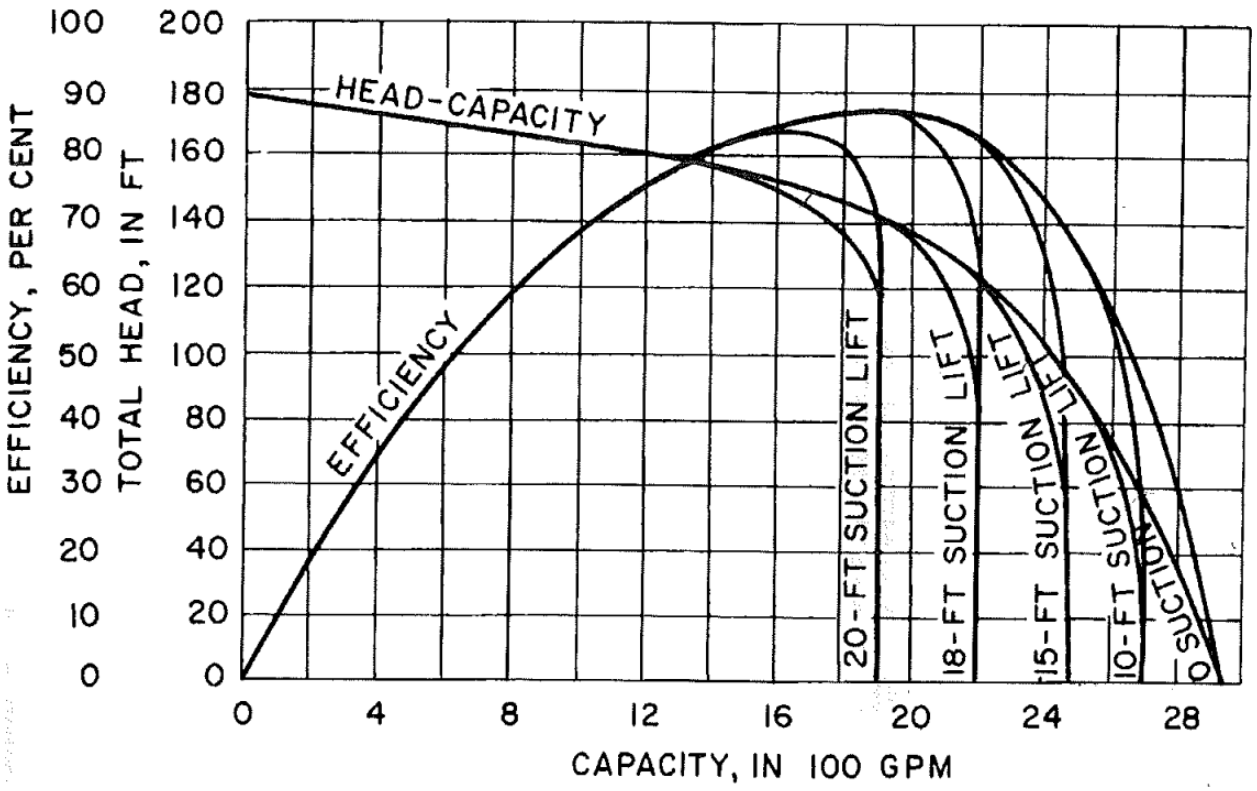

Figure 1.9. Flow rate versus total head and efficiency for an example centrifugal pump operating under varying suction conditions. **[29]**

Eliminating, or at least reducing, suction head should significantly improve pump performance and reduce operation costs. Figure 1.10 illustrates the change in performance of a 1.5 hp pump with and without suction conditions. The operation point of the pump occurs when the system curve, in blue in the figure, intersects with the pump curve, in red. The increase in flow rate when suction head is removed is much greater for shorter distances than for longer distances due to lower pipe losses. However, there are still savings when the field is far from the well. It is estimated that eliminating suction head could decrease operation costs by 10% to 35%, depending on the length of the delivery pipe, due to increased flow rates.

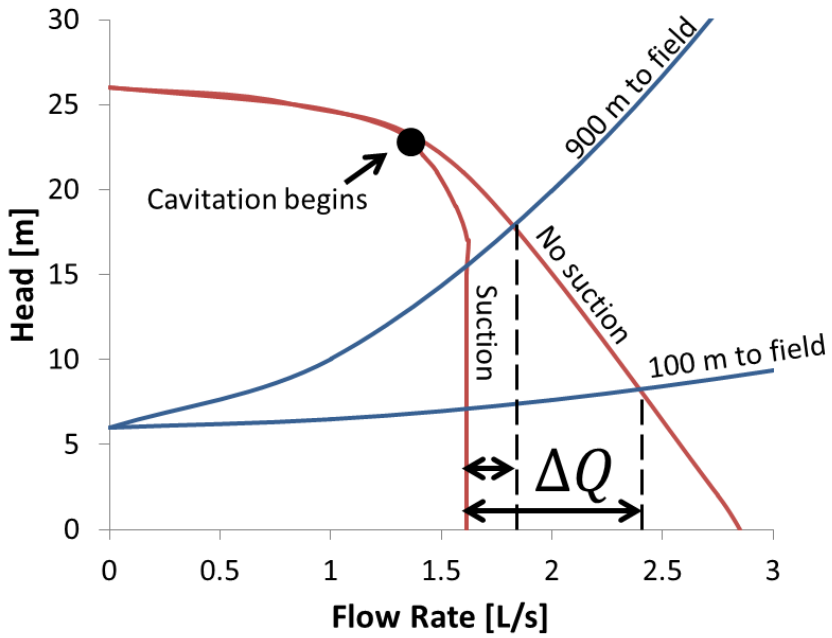

Figure 1.10. Difference in performance of an example 1.5 hp pump with and without suction conditions.

1.7.1 Design Requirements

In order to develop a pumping system that will not only benefit but also actually be utilized by smallholder farmers in eastern India, certain design requirements must be met. As explained above in the discussion about groundwater markets, operation costs include both fuel and rental costs, so both fuel consumption and the hours required to irrigate a plot of land must be reduced. In fact, rental costs can be higher than fuel costs. Therefore, both energy efficiency and flow rates should be increased, with a greater emphasis on water discharge. Baseline fuel consumption and water discharge are established by testing pumps available on the Indian market, as described in Chapter 2. The suction head will be diminished or eliminated in an attempt to improve the efficiency and discharge.

Additionally, because the pumps are transported from well to well on the back of a bicycle, the pump must be portable and at least somewhat lightweight. Current Indian-manufactured 3 hp pumps weigh around 40 kg; the weight of the pumping system developed in this research should not be much greater than this.

Furthermore, as mentioned above, a very common problem that leads to pumps falling into disuse or inefficiency is the lack of maintenance and inability of local mechanics to access

replacement parts. Therefore, the pump must be made easily maintainable and consist of parts that can be readily available in rural India.

Finally, capital cost is a huge hurdle for impoverished smallholder farmers, so the pumping system should be made as affordable as possible. To compete with pumps on the market, the system should cost INR 25,000 or less. In summary, the design requirements to be met include:

- Flow rates greater than current flow rates
- Efficiency improved over varying heads by reducing or eliminating suction lift
- Portable on a bicycle (about 40 kg/about 90 lb)
- Easily maintained and repaired by local mechanics; replacement parts must be readily-accessible
- Affordable capital cost for smallholder farmers (less than INR 25,000)

It is hoped that a pumping system that meets these requirements could reduce the operation costs of groundwater extraction, thereby allowing farmers to irrigate more of their land for additional seasons and increase their income. A higher income from agriculture thanks to improved irrigation would stabilize their livelihood, thereby reducing the need for migration and improving the quality of life for farmers and their families.

1.8 Outline of Thesis

This introductory chapter explained the importance of groundwater irrigation to smallholder farmers and the need for more efficient pumping. Chapter 2 describes testing undertaken to establish the baseline performance of pumps currently on the Indian market as well as to assess the impact of reducing suction head. Chapter 3 explains the various technology options investigated to run a submersible pump with a surface-mounted fuel engine. Chapter 4 discusses the fabrication and testing of a prototype. Chapter 5 assesses strategies to reduce evaporation from farm tanks. Chapter 6 gives the conclusions and ideas for future work.

Chapter 2: Testing Indian Pumps for Baseline Performance

2.1 Objective

In order to assess options for pumping systems that meet the design requirements for small farmers in eastern India, it was necessary to establish the baseline performance and operation costs of the pumping systems the farmers currently employ. The performance factors analyzed included the pump performance curve of flow rate versus head and flow rate versus system efficiency. These flow rates and efficiencies were then translated into operation costs for the farmer in the form of hourly rental and fuel costs at each pressure head, which reflects a well depth from which a farmer might pump water for irrigation. Alternatives to the existing systems, as described in Chapter 4, would be compared to the performance and operation costs of the pumps tested.

In addition to establishing baseline pressure head and efficiency at each flow rate, the pump evaluation would test the hypothesis that lowering the pump closer to the water level decreases operation costs by increasing the flow rate and efficiency at each well depth. By eliminating, or significantly diminishing, suction head, we expect higher flow rates and efficiency due to a reduction in bubbles. Bubbles form when the pressure of the water falls below the vapor pressure of water; when the suction head increases, it lowers the pressure on the inlet side of the pump to pull the water up. The presence of bubbles can result in lower flow rates and efficiency because they decrease the density of the fluid and can cause cavitation at the impeller when they implode under high pressure on the discharge side [30].

2.2 Testing the Pumps in the United States

Initially, four pumps from India were tested in the United States at Bill Miskoe's Iron Dragon Corporation in Pittsfield, New Hampshire, in order to take advantage of the easier availability of resources, such as readily-procured digital flow meters and differential pressure gauges. Unfortunately, we were not able to obtain the desired results due to unforeseen challenges, as described in the following sections.

2.2.1 Acquisition of Pumps

Four pumps were acquired from India. Two of these pumps were Indian-manufactured models, and the two other pumps were Chinese-manufactured. One used and one new version of each pump model was procured. All four pumps are close-coupled to their engines and run primarily on kerosene, with gasoline used to start up the engine. The Indian pumps employ 3 hp Honda GK200 engines. The five-year-old used Indian pump-set utilizes a Mahendra WMK 2020 pump while the new pump-set uses an USHA UNK 2020B pump. Both the four-year old Chinese pump and new Chinese pump were clear copies of the Honda pumps with similar external appearances and labels, but the actual manufacturer is unknown. Photographs of these pumps are given in Figure 2.1 and Figure 2.2. The Indian pumps weighed 80 lb while the Chinese pumps weighed 60 lb. The Indian pump had a larger impeller-to-chamber volumetric fill ratio than the Chinese pump, which had a smaller impeller in a wide chamber (Figure 2.3). The Chinese pumps also have a convenient priming port on top of the casing.

Ashok Kumar at PRADAN purchased the used pumps from farmers and new pumps from the market in Ranchi. He bought the Indian-manufactured pumps from Telya village in Gumla District, Jharkhand, but he had to go to Purulia District in West Bengal to find old Chinese-made pumps. According to PRADAN, Chinese pumps dominate the market in West Bengal but have only recently begun making inroads into Jharkhand. Therefore, finding an aged Chinese pump in Jharkhand was not possible. However, agricultural economists predict that Chinese pumps will soon take over the market in Jharkhand and the other states of eastern India due to their cheaper cost [23, 22, 5]. Bapi Gorai at PRADAN took care of the shipping, and Tashi Wangtak at Eco Tasar Silk Private Limited, a for-profit subsidiary of PRADAN that was originally founded to sell tasar silk products created by PRADAN-trained women's self-help groups, handled the finances.

(a) (b)

Figure 2.1. The Indian-manufactured pumps acquired from Jharkhand. (a) New Honda GK200 engine coupled to an USHA UNK 2020B pump. (b) Used Honda GK200 engine coupled to a Mahendra WMK 2020 pump.

(a) (b)

Figure 2.2. The Chinese-manufactured pumps acquired from West Bengal. (a) New pump. (b) Used pump.

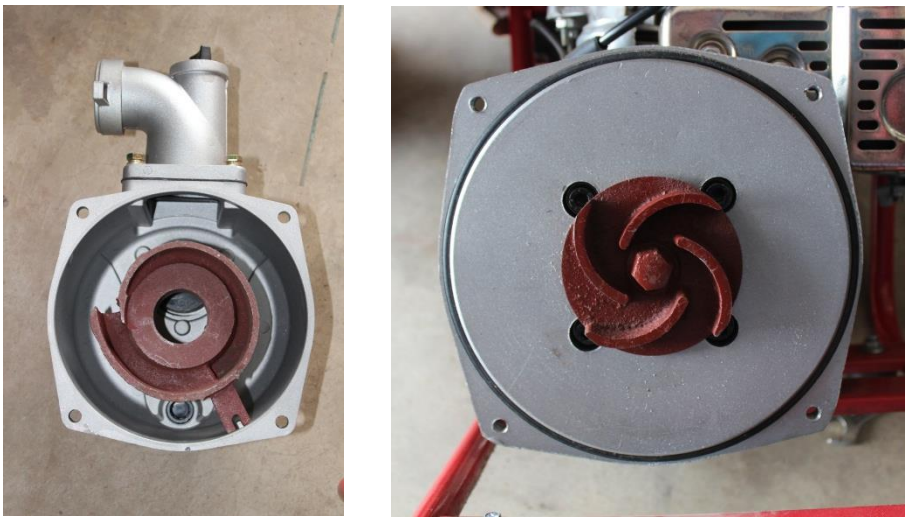

(a)

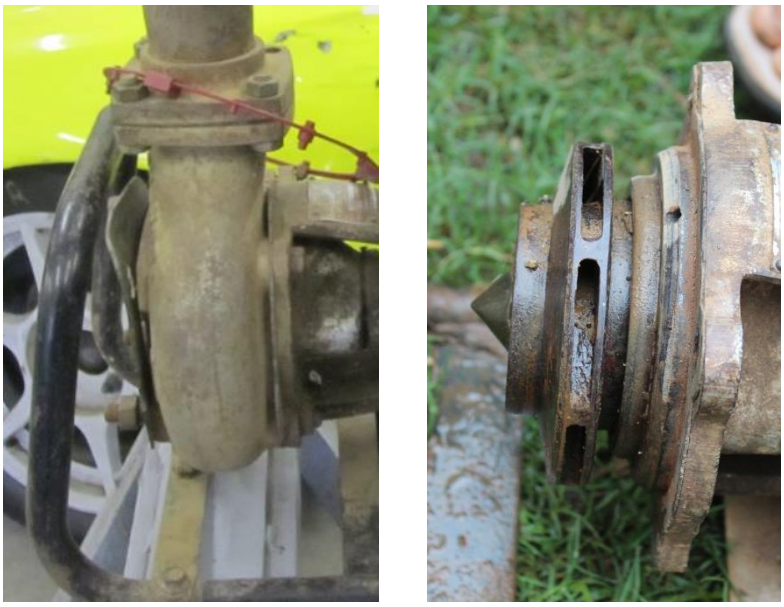

(b)

Figure 2.3. The impeller-to-chamber fill ratio of the Chinese pump (a) is lower than that of the Indian pump (b).

2.2.2 Experimental Set-up

The pump systems were tested in two configurations in order to compare the flow rate versus head and efficiency under suction conditions and simulated submerged conditions as a means to test the hypothesis that performance improves when suction head is reduced. Instead of searching for a well in New England that matches conditions in India, the well was simulated using a bucket lift. To simulate a pump sitting on top of a well, the pump was elevated above the water container in a bucket lift. To simulate a pump submerged in a well, the pump remained on the ground, and the hose was elevated above the water tank and pump. The hose was to be fitted with

a digital flow meter to measure the flow rate and a differential pressure gauge to measure the pressure change across the pump. However, the differential pressure gauge had not yet arrived by the first day of testing. It was decided to go ahead and conduct a practice run anyway in order to figure out how the test might work. We intended to employ the pressure gauge in subsequent testing. Unbeknownst to us at the time, we would not be able to test further, due to difficulties operating the pump.

For the first test, a one-meter tall tank, previously used to store vegetable oil, served as the water source for the pump test. The tank was filled with water from a local well. The pump sat on the ground near the tank, with the water level inside the tank above the pump inlet, thereby creating positive pressure (Figure 2.4). The water exited the outlet hose at the top of an upside-down 55-gallon drum that was strapped to the side of the bucket lift to act as a funnel to return the water back to the tank (Figure 2.5). Two 90-degree elbows were attached to the end of the hose to create a hook to keep the hose in place at the top of the drum. To measure the height that the bucket lift was raised, a tape measure was tied to the top of the bucket, at the same level as the outlet into the drum, and hung down to the ground. This setup is shown in Figure 2.6 and Figure 2.7. However, this setup would not be used again, because at the lower elevations, the drum overflowed and much water was lost, thereby wasting limited well water. For the other tests, a nearby canal was to be used instead so that the water could return to its source. Using a canal, though, would not completely remove suction when simulating submersible conditions, because the water level would not sit above the pump as with the water tank. Therefore, positive pressure at the inlet would be lost. The updated set-up used in later pump testing attempts is given in Figure 2.8.

Figure 2.4. A water tank served as the water source for the pump system, and the water level sat above the inlet of the pump during simulated submerged conditions.

Figure 2.5. A makeshift funnel was created by strapping an oil drum to the back of the bucket lift.

Figure 2.6. The original experimental set-up for the simulated submerged conditions.

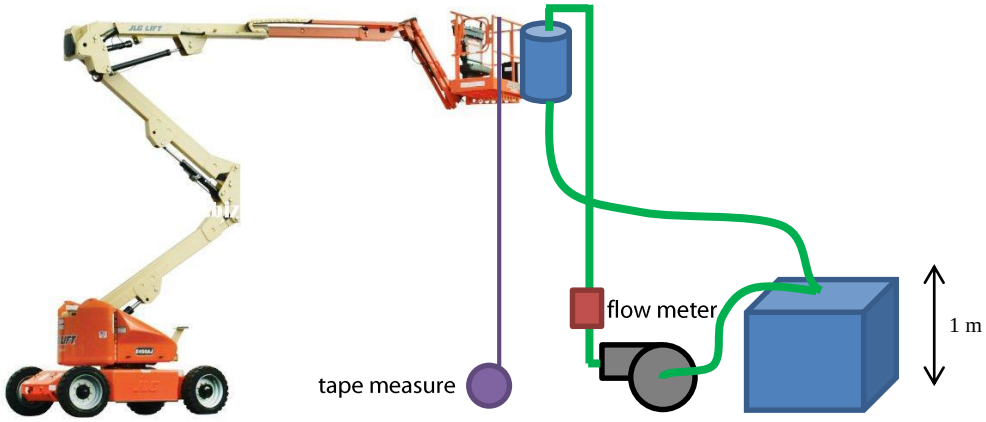

Figure 2.7. Set-up for the first test under simulated submerged conditions. The water level in the tank always sat above the pump, so suction was eliminated. The inlet hose of the pump is connected to the water source through a hole in the top of the tank, and the return hose deposits the water back in the tank through the same hole.

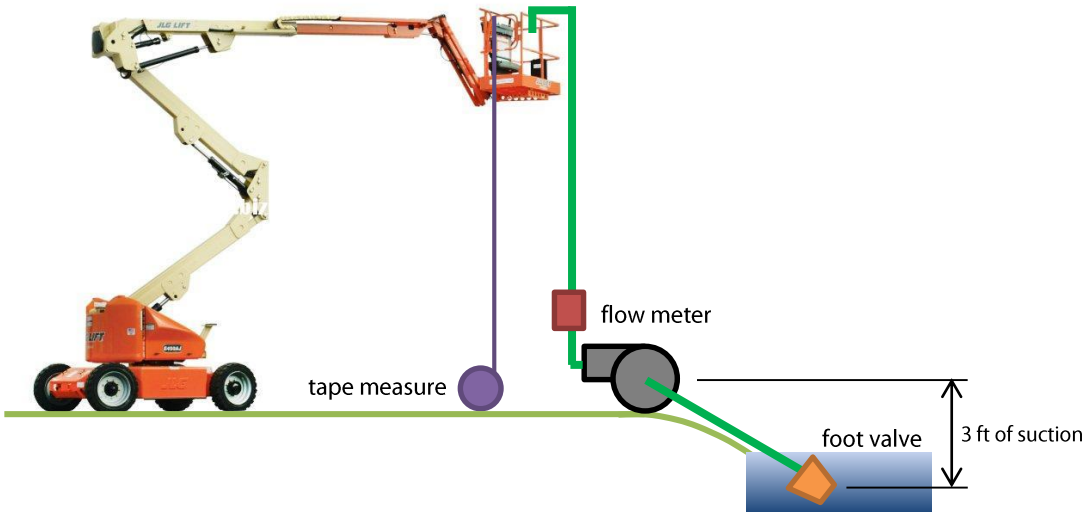

Figure 2.8. Updated set-up for subsequent tests under simulated submerged conditions. Note that suction is not completely eliminated in this set-up but is instead greatly reduced.

2.2.3 Testing Procedure

In order to gather flow rate versus head and efficiency (involving fuel consumption) performance data, the test measured the height, time required to consume 10 mL of kerosene, and flow rate. The test was run at the same hydrostatic head (the same elevation of the bucket lift) three times before the pump was raised further. The following procedure was conducted for the set-up depicted in Figure 2.7:

1. Fill the water tank, and put the suction hose into the tank.
2. Fill the tank labeled “petrol” with gasoline.
3. Pour 10 mL of kerosene into the tank labeled “kerosene.”
4. Start the engine on gasoline, with the dial pointing to “start.” Run the engine on gasoline until the engine is warm and the system is primed.
5. Switch to kerosene by moving the dial on the front of the engine from “start” to “run.”
6. Run the pump until it stops. Read the water meter while the pump is running and record the flow rate. Using a stopwatch, measure the time required to empty the tank and record the value in seconds.
7. Open the carburetor valve to bleed out excess kerosene.
8. Repeat steps 3 to 7 two more times.
9. Raise the bucket lift by five feet.

10. Repeat steps 3 to 9 until the pump has been tested from 5 to 25 feet of static head under both conditions.

All values were recorded in the test matrix shown in Table 2.1. However, during the initial practice run, the pressure difference across the pump was not recorded, due to the absence of the differential pressure gauge.

Table 2.1. Test matrix for recording data.

Pump	Height of bucket lift (ft)	Flow rate (gal/min)	Pressure difference (psi)*	Time to consume 10mL kerosene (s)
Indian – new	5			
	5			
	5			
	10			
	//	//	//	//
	30			

// indicates additional rows in between what is displayed.

*Pressure difference could not be measured because the differential pressure gauge had not arrived in time for the first series of tests.

2.2.4 Troubleshooting

We experienced much difficulty in running the pumps, and ultimately, we never successfully operated the pumps under suction conditions. Because we decided to switch from a well-fed water tank to a canal in order to save water, even simulated submerged conditions still involved some suction. This section describes the troubleshooting we attempted. The data from the first tests under simulated submerged conditions using the water tank (Figure 2.7) are given below in Section 2.2.5.

The first pump we tried to run was the new Indian pump, and the problem we repeatedly attempted to address was leaking. Water was leaking from both the suction and discharge sides of the pump. On the suction side, a gummy thread sealant had been used to cover the entire fitting connection, and holes were discovered in this sealant. However, it seemed odd that such sealant was necessary in the first place. Upon investigation, it was found that the threads of the square flange and the barb fitting did not match. The flange had straight threads while the barb fitting had tapered threads, and someone had tried to correct this poor fit with sealant. We attempted to improve the seal by removing the gummy sealant and replacing it with a lot of Teflon tape. On the

discharge side, both the threaded hole in the flange and the discharge fitting were straight rather than tapered, so there was no jamb. This issue was resolved by wrapping Teflon tape in varying thicknesses along the fitting in order to create a taper.

Even after eliminating these sources of leakage, the new Indian pump still could not pump. The specifications of the pump implied that it was "self-priming" but did not provide a definition of what that entailed with regards to starting the pump. At first this term was assumed to mean that no priming at all was necessary, so the pump was run dry. Even after running the engine for ten minutes, the pump still could not suck water. After consulting user manuals for different pumps, it was learned that the term "self-priming" is a bit misleading and means that the pump is capable of beating out some air bubbles that might be stuck inside the casing—but that the pump must still be filled with water first. Moving forward, we tried pouring water into the casing through the discharge side.

When water was poured into the pump, a huge leak at the shaft coupling was found. The shaft seal did not successfully seal the pump case. This leak was addressed by tightening the screws around the shaft seal. Once this leak was eliminated, more leaks were discovered in the connection on the suction side. Though the clamp securing the hose onto the pump's inlet barb held tight, small bubbles were seen escaping from the connection, thereby indicating that air rushed in and broke the suction. The clamp was moved closer to the end of the barb touching the pump and further tightened. The pump could now operate when its case was filled through the discharge side in the set-up with the water tank that eliminated suction head, but still struggled under suction conditions.

The next pump we tried to test was the new Chinese pump. The inlet and outlet of the Chinese pump had a nominal three inch/eighty millimeter diameter, according to its nameplate. However, the nominal three inch hose was too large by about 1.5 millimeter for the inlet barb that came with the pump. Four hose clamps, rather than only one, were utilized in an attempt to secure the hose on the barb. Despite this effort, the hose still rattled around quite a bit and would have been unable to hold a tight seal. Instead, the barb was built up to a larger diameter. First, a sheet of neoprene was glued to the barb with epoxy, but this resulted in too much added material and the barb became too wide to fit inside the hose. The neoprene was then removed and several layers of electrical tape were wrapped around the barb until it was large enough to fit tightly in the hose.

The plastic union fitting intended to connect the barb to the pump outlet arrived from India broken in two pieces. We attempted to hold the two pieces together with a clamp, but this did not work. A new fitting could not be purchased because the threading was not National Pipe Thread (NPT) or another standard found in the United States. Therefore, the fitting from the old Chinese pump's inlet was moved to the new pump's outlet. However, this fitting too broke while attaching to the inlet, so it was taped together and clamped.

The old Honda pump arrived from India without an inlet flange. The reason for the flange absence was discovered later in India: the flange and its barb are stored attached to the suction pipe and foot valve. Indian farmers screw the entire set-up onto the pump when they need to irrigate their fields and unscrew the entire set-up when they finish. By keeping the set-up together, they do not need to troubleshoot for air leakage every time they start the pump. The new pump's flange did not fit the old pump and therefore could not simply be transferred. A new flange had to be constructed.

A standard heavy-duty 2 ½" companion flange was purchased from a local hardware store in Pittsfield and modified to fit the pump. The diameter between bolts of the old pump's inlet flange and the diameter of each bolt were measured, and holes at the correct diameters were drilled into the purchased companion flange. A 2 ½" to 2" reducing bushing was inserted into the flange to accommodate the 2" connections and hose. The flange was quite large and could not fit inside the pump's frame, so some material was cut off using a bandsaw. In addition to the flange, a new gasket had to be created, as the old gasket was quite worn out. The shape of the old gasket was traced onto neoprene and cut out. The holes for the bolts were punched out. When the new flange and gasket were bolted in, it was found that the bolts were not long enough to accommodate the new flange, which was much thicker than the old flange must have been. The nuts could not fully screw onto the threaded bolts.

After attaching the new flange to the old pump, we attempted to operate the pump under suction conditions but faced heavy leaking. A stud was missing on the back flange (the flange facing the engine) so water shot out the back of the pump case. When a new bolt was inserted, the gasket blocked entry into the bolt hole, as it must not have been aligned properly. A new back gasket was built from a sheet of neoprene to match the bolt holes and a new bolt installed. Leaking also occurred at the front gasket between the flange and pump case, probably because the nuts could not properly fit on the short bolts, as explained earlier. These short bolts were replaced with

longer bolts. Water leaked at the shaft seal as well, and again the screws were tightened, with limited success. After addressing the leakage problems, we tried to test the pump. However, the pump's engine would fail as soon as it experienced any load, so the pump system could not be tested. Although the used engine could not maintain mechanical power generation, the used pump was not transferred to the new engine for testing due to time constraints.

Despite our best efforts at troubleshooting, none of the pumps could operate under suction conditions, even when we could not find leaks, primed the pump, or closed a valve at the discharge to build up pressure. Because even the simulated submerged conditions in the set-up drawing water from a canal required negative pressure at the inlet (Figure 2.8 shows the three feet of suction head), we could not successfully operate the pumps under the "submerged" conditions either.

2.2.5 Results

Because the acquired pumps could not work as expected, we only obtained results for the new Honda pump under simulated submerged conditions in the original set-up with the water tank that provided positive pressure at the inlet. In the absence of the differential pressure gauge, only static head (the difference in elevation between the inlet and outlet of the pump) was measured. Therefore, in order to find the pump performance curve (that is, flow rate versus total head), the dynamic head had to be approximated with a calculation. This calculation is given by [30]

$$H_{dynamic} = \frac{v^2}{2g}\left(\sum \frac{fL}{D} + \sum K\right) \qquad \text{(Eq. 2.1)}$$

where

v	=	velocity of the water	[m/s]
g	=	gravitational acceleration	[m/s^2]
L	=	pipe length	[m]
D	=	pipe diameter	[m]
f	=	friction factor	
K	=	pressure loss coefficient	

The gravitation acceleration is 9 m/s^2 and the friction factor f for turbulent flow in a smooth-walled pipe is [30]

$$f = \left[1.8 \log\left(\frac{\mathrm{Re_D}}{6.9}\right)\right]^{-2} \quad \text{(Eq. 2.2)}$$

where

$$\mathrm{Re_D} = \frac{\rho v D}{\mu} \quad \text{(Eq. 2.3)}$$

where

$\mathrm{Re_D}$	=	Reynolds number with diameter as characteristic length	
ρ	=	density of the fluid	[kg/m^3]
μ	=	dynamic viscosity of the fluid	[Pa·s]

According to the National Institute of Standard and Technology (NIST)'s Thermophysical Properties of Fluid Systems database, at 20 °C the density of water is 998.21 kg/m^3 and the dynamic viscosity is 0.0010014 Pa·s [31]. For these calculations, the density and dynamic viscosity were rounded to 1000 kg/m^3 and 0.001 Pa·s, respectively.

Because the velocity *v* is not known but the flow rate *Q* [m/s^3] was measured using a digital flow meter, the flow rate $Q = vA$, where A is the cross-sectional area of the hose, must be substituted into this equation. Substituting Q and the equation for *f*, the final calculation for dynamic head is

$$H_{dynamic} = \frac{\left(\frac{4Q}{\pi D^2}\right)^2}{2g}\left\{\left[1.8 \log\left(\frac{4\rho Q}{6.9\pi\mu D}\right)\right]^{-2}\left(\frac{L}{D}\right) + \sum K\right\} \quad \text{(Eq. 2.4)}$$

The hose diameter was 2 inches (0.05 m) and the length of hose was 30.83 feet (9.4 m). The sum of pressure loss coefficients, also called K-factors, due to hose fittings is given in Table 2.2.

The static head is given by

$$H_{static} = z_{outlet} - z_{inlet} \quad \text{(Eq. 2.5)}$$

where

z_{outlet} = height of the outlet of the system [m]

z_{inlet} = height of the inlet of the system [m]

z_{outlet} was measured by the tape measure tied to and hanging from the bucket lift. The uncertainty for z_{outlet} is ±5 mm. The water level in the tank fluctuated as the rates of water leaving the tank and re-entering the tank varied and were not equal to each other. Therefore it was assumed that the water level in the tank, z_{inlet}, was at half the height (0.5 m) of the tank, with an uncertainty of half the height (± 0.5 m). The total head is calculated as

$$H_{total} = H_{dynamic} + H_{static} \quad \text{(Eq. 2.6)}$$

The flow rate was measured with a digital flow meter. This flow meter tended to stabilize for a few seconds, then jump to a new value and stabilize for a few seconds, and so on. Each time the meter stabilized, the value was recorded. Those flow rate values were then averaged, and the standard deviation of those values was used as the uncertainty. The averages were used as the *Q* value in equation 2.4 to approximate the dynamic head. The total head versus flow rate results of the practice run are given in Figure 2.9.

Table 2.2. Pressure loss coefficients of the test system. **[32]**

Element	**Quantity**	**K-factor**	**Subtotal K-factor**
Entrance	1	1	1
Barb	6	0.2	1.2
Union	2	0.08	0.16
90° Elbow	2	0.57	1.14
Flow meter	1	7	7
Exit	1	1	1
TOTAL			**11.5**

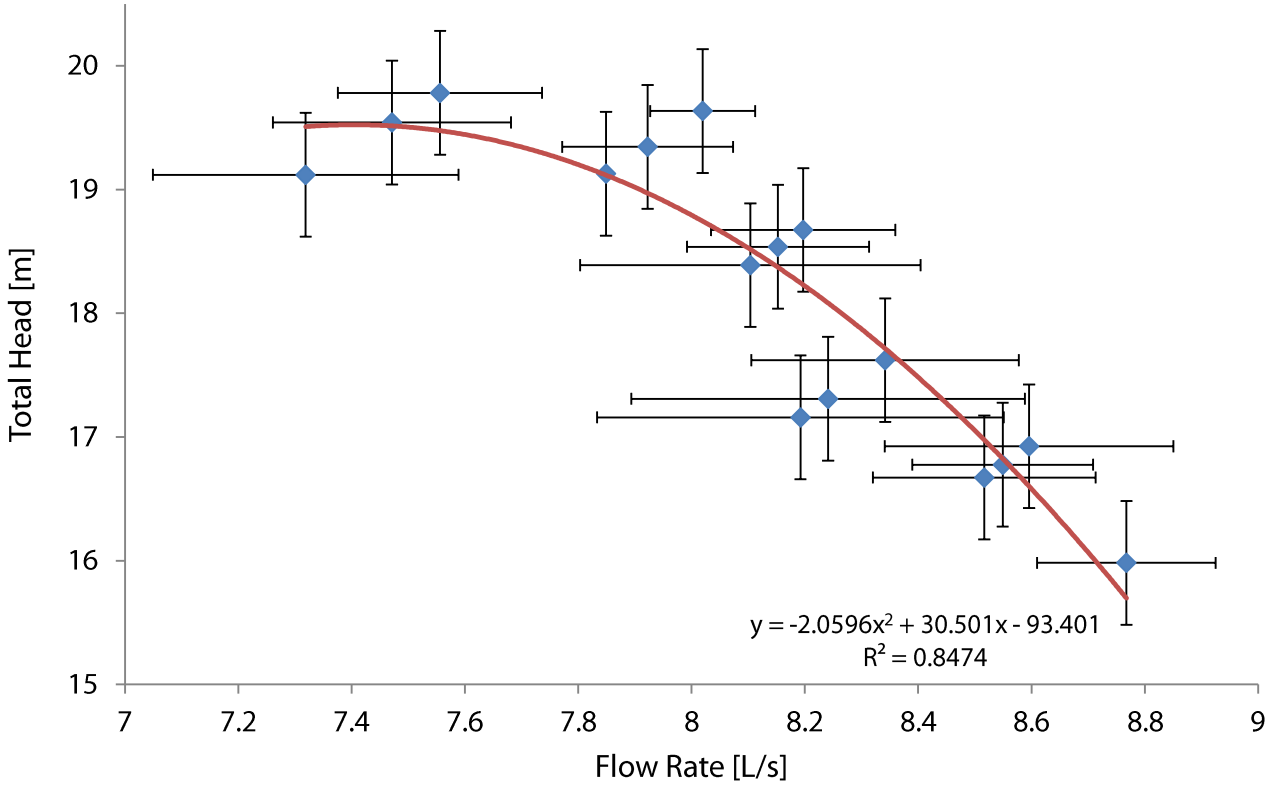

Figure 2.9. Total head versus flow rate results for the new Indian pump under "submerged" conditions. $R^2 = 0.85$ for the best-fit second-order polynomial

The efficiency of the pump could not be isolated from the efficiency of the engine, as the shaft seal concealed the shaft and blocked any measurement of angular velocity or torque. Additionally, farmers in India care about fuel consumption (fuel is an important cost) and thus are more concerned with the coupled engine-pump efficiency. This engine-pump efficiency is given by

$$\eta = \frac{P_{PumpOut}}{P_{EngineIn}} \qquad \text{(Eq. 2.7)}$$

where

η	=	efficiency	
$P_{PumpOut}$	=	power output from the pump	[W]
$P_{EngineIn}$	=	power input into engine	[W]

Fuel consumption of the system was measured by pouring a known quantity of kerosene, 10 mL, into the engine and recording the amount of time until the engine shut off. The kerosene

was measured in a graduated cylinder with gradations of 1 mL, so the uncertainty is ±0.5 mL. The time was measured using a stop watch, with an uncertainty of two seconds. Fuel consumption was converted to power consumption using the following equation:

$$P_{input} = \frac{V_{kerosene} U}{t} \quad \text{(Eq. 2.8)}$$

where

$V_{kerosene}$	=	volume of kerosene poured into the engine	[L]
U	=	volumetric energy density of kerosene	[J/L]
t	=	time required to consume all the kerosene in the engine	[s]

Ten milliliters of kerosene were consumed by the engine, and the volumetric energy density of kerosene is approximated at 33.8 MJ/L, according to the Intergovernmental Panel on Climate Change (IPCC) [33]. The power output by the pump was calculated using the measured flow rate and total head, as

$$P_{PumpOutput} = \rho g H_{total} Q \quad \text{(Eq. 2.9)}$$

Therefore the engine-pump efficiency is

$$\eta = \frac{p g H_{total} Q t}{V_{kerosene} U} \quad \text{(Eq. 2.10)}$$

The efficiency results are given in Figure 2.10. The uncertainty carries over from the uncertainties in flow rate, head, and fuel consumption.

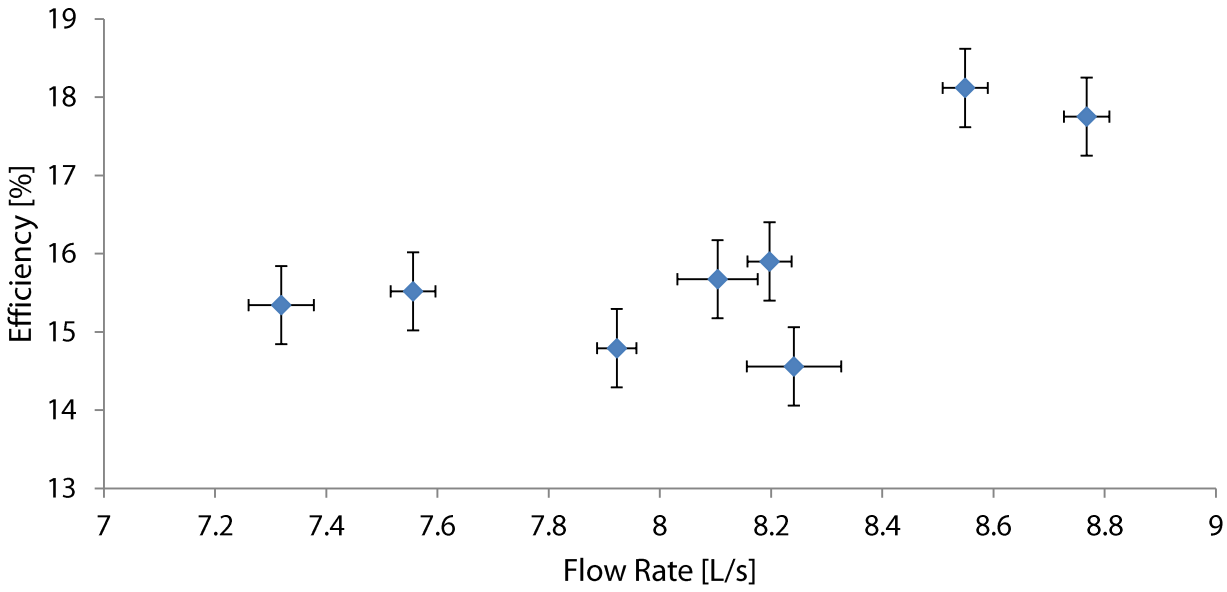

Figure 2.10. Flow rate versus efficiency results for the new Indian pump under "submerged" conditions.

Fuel consumption and pump performance were translated into operation costs for the farmers. Farmers pay per hour to rent the pump and per liter of kerosene to run the pumps. The rental charge varies very widely from village to village, and the price of kerosene varies from INR 18/L through the subsidized Public Distribution System to INR 30/L through the black market (the legal market rate is INR 25/L). Costs to fill one acre of land with two inches of water (which is the amount of water farmers, when interviewed, claimed they use to irrigate) were calculated. The time in hours required for this unit of irrigation is

$$t_{irrig} = \frac{A_{land} h_{water}}{3600 Q} \qquad \text{(Eq. 2.11)}$$

where

A_{land}	=	area of land irrigated	[m^2]
h_{water}	=	height of irrigation water	[m]
Q	=	flow rate	[m^3/s]

and 3600 represents the number of seconds per hour. The assumed land area is one acre (4047 m^2) and the assumed height of irrigation water is two inches (0.05 m). The rental costs are

$$C_{rent} = c_{hr} t_{irrig} \quad \text{(Eq. 2.12)}$$

where

c_{hr} = cost of pump rental per hour [INR/hr]

The fuel costs are

$$C_{fuel} = 3600 c_L Q_{fuel} t_{irrig} \quad \text{(Eq. 2.13)}$$

where

c_L = cost of kerosene per liter [INR/L]

Q_{fuel} = rate of fuel consumption [L/s]

The operation cost results are given in Figure 2.11. As in the efficiency results, the uncertainty carries over from the uncertainties in flow rate, head, and fuel consumption. The vertical error bars also account for the hugely varying hourly rental costs, which dwarf uncertainties in calculations. Those error bars do not represent the entire spectrum of possibilities an individual farmer could see (his local rental service would charge at one point along that spectrum) but rather reflect the spectrum of hourly rental charge possibilities across Gumla District, Jharkhand. These results reveal that rental costs—in other words, the time required to irrigate—are actually a larger component of operation costs than the cost of fuel consumed.

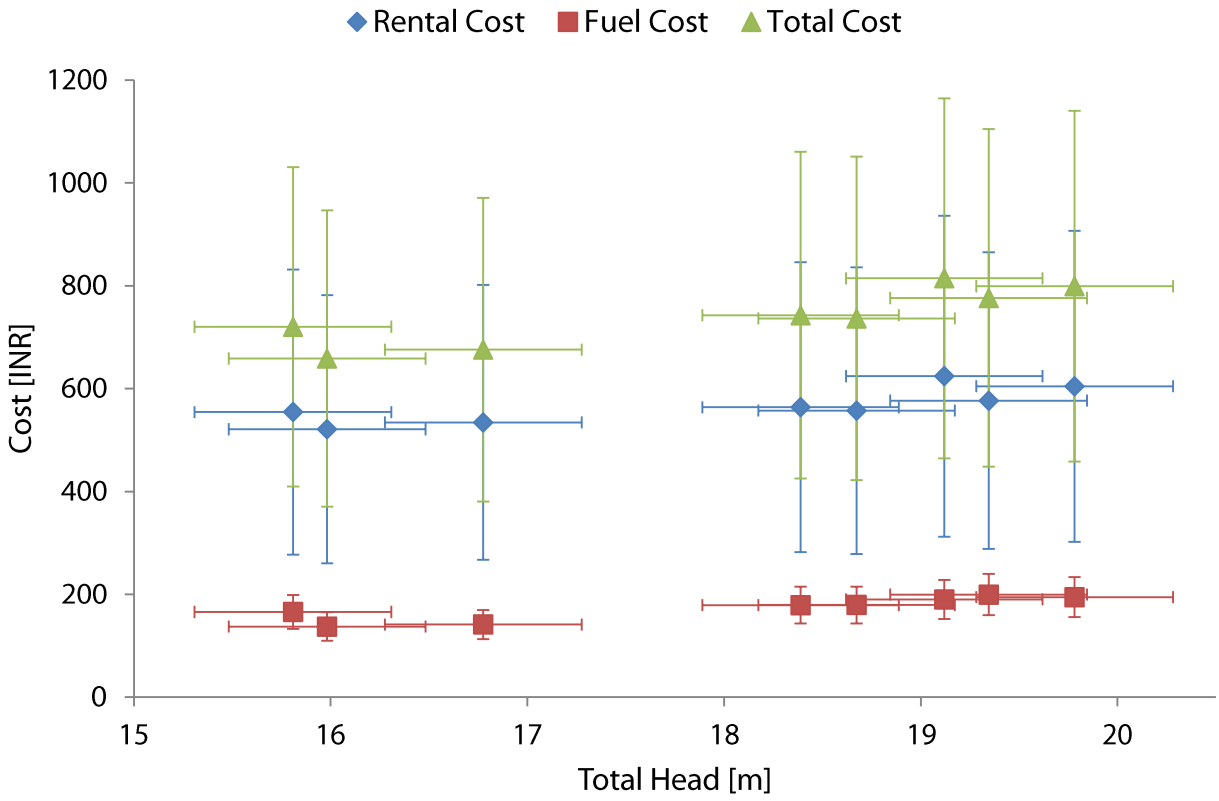

Figure 2.11. Operation costs to irrigate one acre of land with two inches of water with the new Indian pump under "submerged" conditions.

The first test worked well, but some changes were required for subsequent tests. To eliminate much uncertainty, a differential pressure gauge would be used to measure, rather than estimate through calculations, the actual total head experienced by the pump. Additionally, it was discovered that the funnel was not effective at siphoning all the water back to the tank, and a huge amount of water was lost when the drum overflowed. This water comes from a well that Iron Dragon Corporation believed to be deplete-able. Instead, a perennial surface source such as a canal would be used to supply water to the system for subsequent tests. Using a surface source also eliminated the uncertainty associated with the fluctuating water levels in the tank, because the canal water level would not change. By placing the pump system adjacent to the surface source, the water would naturally return to its source as it exits the system. However, because using a surface source does not eliminate suction head and we could not figure out how to successfully operate the pumps under suction conditions, we were unable to acquire further data for the pumps tested in the United States. We would finally be able to obtain pump performance data by testing

the pumps with Indian farmers, who knew how to troubleshoot and properly seal the leaks with strips of rubber, as discussed below in Section 2.3.4.

2.3 Testing the Pumps in India

Because the pumps could not be successfully tested in the United States, similar pumps were tested in rural India. The pumps shipped to the United States may have been damaged in intercontinental transit. Additionally, perhaps we were not operating the pumps correctly, and in India farmers would be available to demonstrate how they run the pumps and to help with troubleshooting. The pumps were not purchased but rented for the day of testing.

2.3.1 Identification of Pumps to Test

Ashok Kumar, the person who procured the first set of pumps, returned to Telya, the village where he bought the pumps, to engage the farmers there for further testing, because these farmers were familiar with the project and previously expressed willingness to help. Rajesh, the farmer who sold his used Honda pump to Ashok, found other farmers in his community who owned pumps and who volunteered to have them tested. The pump sets tested were a twelve-year-old three-horsepower Honda GK200 engine close-coupled to a Mahendra WMK2020 pump and a five-year-old Honda GK200 close-coupled to an USHA UNK 2020B pump. Both pumps had nominal two-inch/fifty-millimeter inlets and outlets.

2.3.2 Experimental Set-up

The water level in the wells would not vary during the short duration of testing, so changing well conditions had to be simulated. To simulate a pump sitting on top of a well, the pump was elevated above the water source. To simulate a pump submerged in a well, the pump was positioned as close as possible to the water source, and the discharge hose was elevated. Even close to the water source, however, the pump must generate negative pressure at the inlet, because the inlet sits a few inches above the stream. Access to a bucket lift to simulate different well depths was not possible. Luckily, Jharkhand is a hilly state with many streams. Therefore, in order to vary the static head, the pump or hose was carried uphill from a stream, and, in one case, an irrigation tank. Fortunately, the accuracy of the static head was not very important because a differential pressure gauge was used to measure the total head (the total head is equal to the static head plus

dynamic head). The differential pressure gauge was attached to the hoses via tees at the inlet and outlet of the pump. The flow meter was connected to the outlet hose. Figure 2.14 shows the set-up of the instrumentation in the pump system. The set-up for a pump under suction conditions is shown in Figure 2.12 and under simulated "submerged" conditions in Figure 2.13.

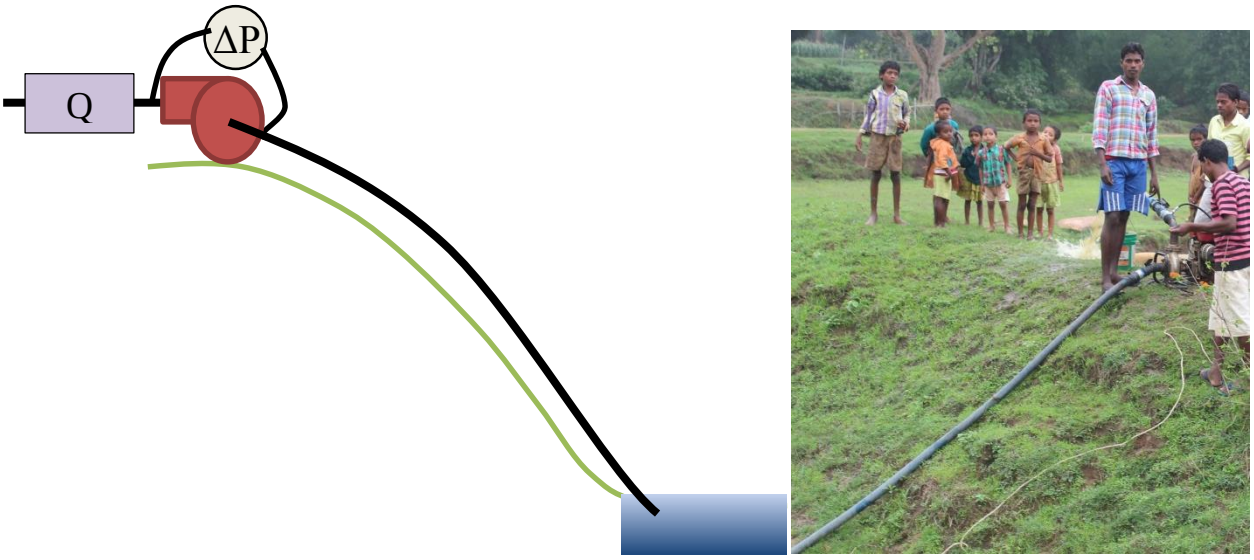

(a) (b)

Figure 2.12. Test set-up for a pump operating under suction conditions. (a) Schematic. (b) Photograph.

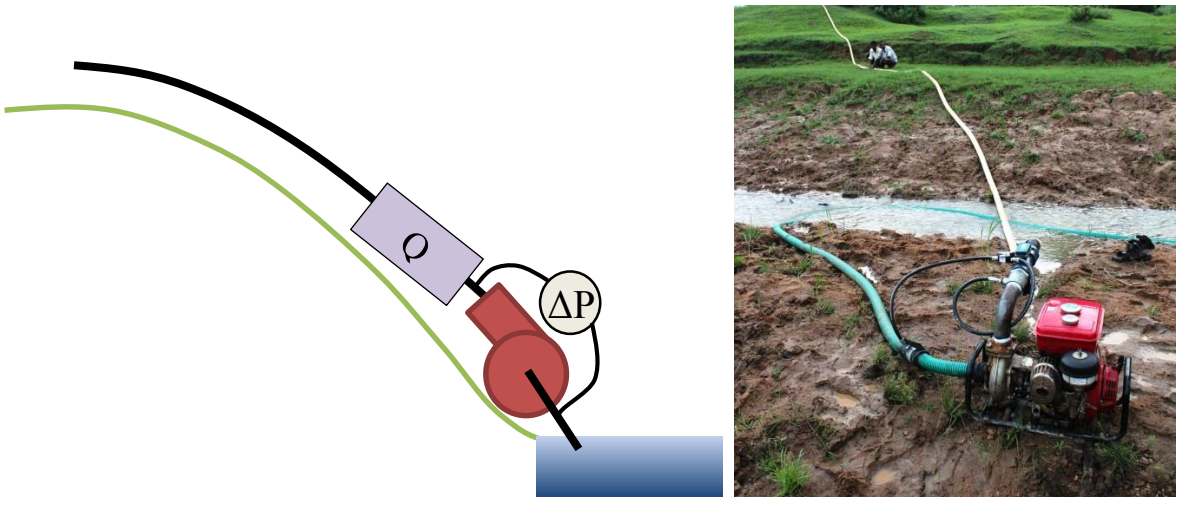

(a) (b)

Figure 2.13. Test set-up for a pump operating under "submerged" conditions. (a) Schematic. (b) Photograph.

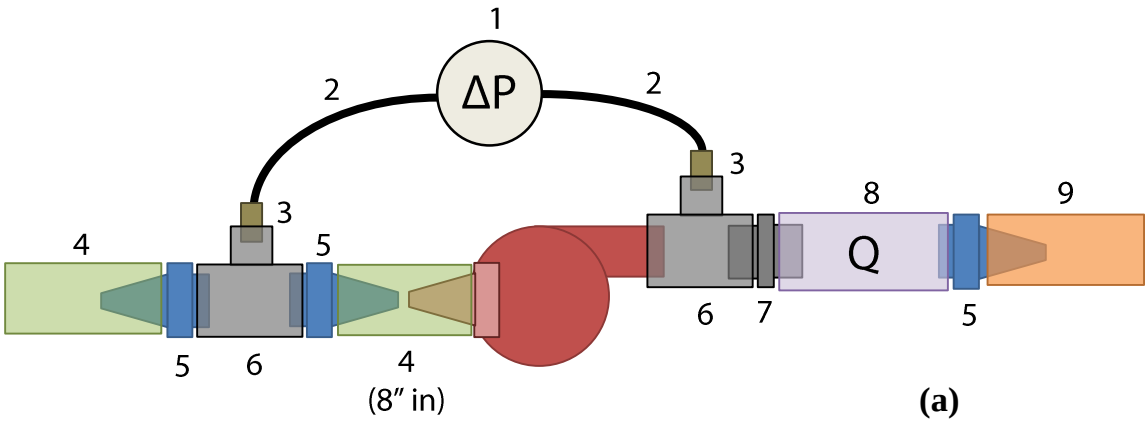

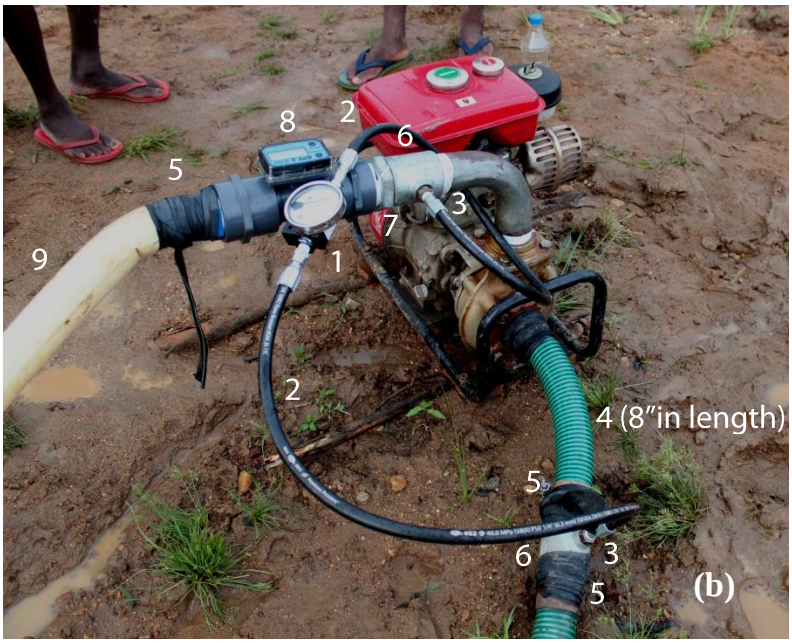

1. Differential pressure gauge
2. ¼″ hydraulic hose with male connections
3. Male ½″ to female ¼″ reducer
4. 2″ suction hose
5. 2″ barb
6. 2″ x ½″ x 2″ tee
7. 2″ male to male adapter
8. Digital flow meter
9. 2″ delivery hose

Figure 2.14. Set-up of the pump outfitted with pressure and flow rate instrumentation. (a) Schematic. (b) Photograph. The change in pressure between the pump inlet and the pressure gauge due to the barbs and eight-inch piece of hose are negligible compared to the overall system change in pressure.

2.3.3 Test Procedure

The experimental procedure for the pumps tested in India was very similar to the procedure for the pumps attempted to be tested in the United States. The time required to consume a known quantity (20 mL) of kerosene, differential pressure, and flow rate were measured in order to establish the flow rate versus head and efficiency performance for the pumps. The test was run at the same head (the same elevation above the water source) three times before the pump or hose was raised further. The following procedure was executed:

1. Place the pump next to a surface water source, such as a stream or irrigation tank. Put the suction hose, with a foot valve, into the water.
2. Fill the tank labeled “petrol” with gasoline.
3. Pour 20 mL of kerosene into the tank labeled “kerosene.”
4. Start the engine on gasoline. Run the engine on gasoline until the engine is warm and the system is primed.
5. Restart the engine using kerosene and hit “start” on the stopwatch.
6. Run the pump until it stops. Read the water meter and differential pressure gauge and record the flow rate and differential pressure while the pump is running. Hit “stop” on the stopwatch when the engine cuts out. Record the value in seconds.
7. Open the carburetor valve to bleed out excess kerosene.
8. Repeat steps 3 to 7 two more times.
9. Climb uphill approximately one meter, carrying the pump (to test suction conditions as in Figure 2.12). For “submerged” conditions, move the outlet hose uphill while keeping the pump and inlet hose near the water (Figure 2.13).
10. Repeat steps 3 to 9 until the pump has been tested from 0 to 7 meters of static head under both conditions.

All values were recorded in the test matrix, as shown in Table 2.3.

Table 2.3. Test matrix for recording data.

Pump	Flow rate (gal/min)	Pressure difference (psi)	Time to consume 20 mL kerosene (s)
	//	//	//

// indicates additional rows in between what is displayed.

2.3.4 Operation of the Pump and Troubleshooting

Not nearly as much troubleshooting was required with the pumps tested in India as the pumps tested in the United States. The farmers did not trust the Teflon tape around the pipe threads to prevent leakage and insisted that each hose fitting be covered with a strip of rubber cut from a

used bicycle tire (Figure 2.15). The farmers' idea of using bicycle tire rubber worked brilliantly, and the pumps were able to operate under suction conditions without a problem, despite heavy leaking at the shaft seal.

Figure 2.15. Wrapping rubber from used bicycle tires around the pipe fittings to eliminate leakage.

Indian farmers primed the pump casing before operation by pouring water through the discharge outlet before attaching the delivery pipe. They retrieved the water for priming from the well by lowering and raising the bucket with the assistance of a large counterweighted lever. They guided the water into the discharge outlet (or in this case, through the fittings that had been connected to the outlet) using their hands. This process is depicted in Figure 2.16.

Additionally, it turned out that in the United States the pumps had been run differently than they generally are in India. At Iron Dragon Corporation, we had tried turning on the engine with gasoline for a few seconds and then moving the dial from "start" to "run" to switch to kerosene without turning off the engine. However, the Indian farmers followed a different procedure. They let the engine run for a longer period of time on gasoline, and then turned off the engine. With the engine off, they moved the dial to "run" and then pulled the recoil starter to restart the engine while it was still hot, this time on kerosene. (We had tried this method once in New Hampshire but it did not work, possibly because we had not run the engine for a long enough period of time to fully warm up.)

Figure 2.16. Retrieving water from the well using a counterweighted lever and priming the pump by hand.

Sometimes, while flow rate measurements were being recorded, the flow meter display would suddenly fall to zero, even though the flow had not stopped. It turned out that silt or debris in the water had caught onto one or more of the flow meter's turbine blades and prevented the turbine from continuing the turn (Figure 2.17). Each time this happened, the flow meter had to be removed from the pump set-up and a long thin twig was used to dislodge the bit of mud between the turbine blade and the wall of the flow meter.

Figure 2.17. The turbine inside the flow meter sometimes got stuck when silt in the water prevented it from turning.

The delivery hoses used by the farmers are very flimsy; they are purposefully thin-walled and foldable for easy storage. However, the flimsiness sometimes resulted in high water pressure sprouting holes in the hose, as in Figure 2.18. The hose would either be replaced by another hose or the hole would be patched with rubber and held together by hand.

Figure 2.18. Holes in the delivery hose were a common problem.

2.3.5 Results

Flow rates, differential pressure, and fuel consumption measurements were taken in order to compare the performance of the pumps under suction and simulated submerged conditions as well as to assess the decline in performance over time. We expected to see a decrease in flow rate and efficiency at higher heads under suction conditions due to the presence of bubbles that could implode at the impeller as cavitation and/or reduce the density of the fluid moving through the pump.

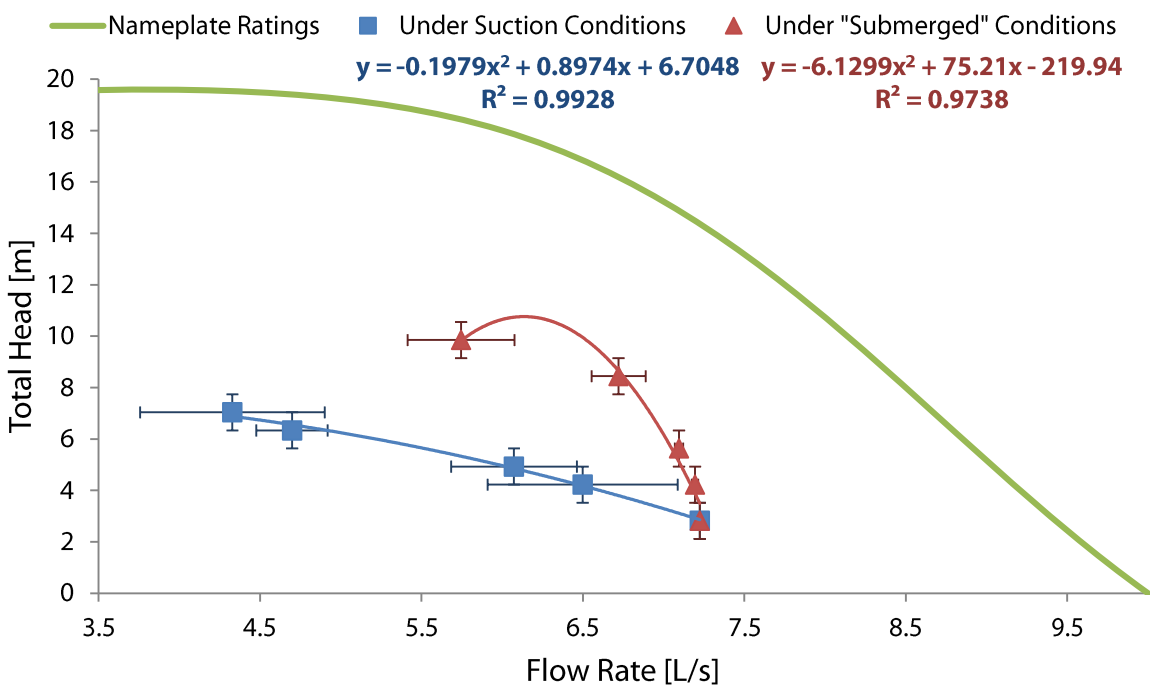

Figure 2.19. Flow rate versus total head performance for the twelve-year-old Honda GK200 engine coupled to a Mahendra WMK 2020 pump.

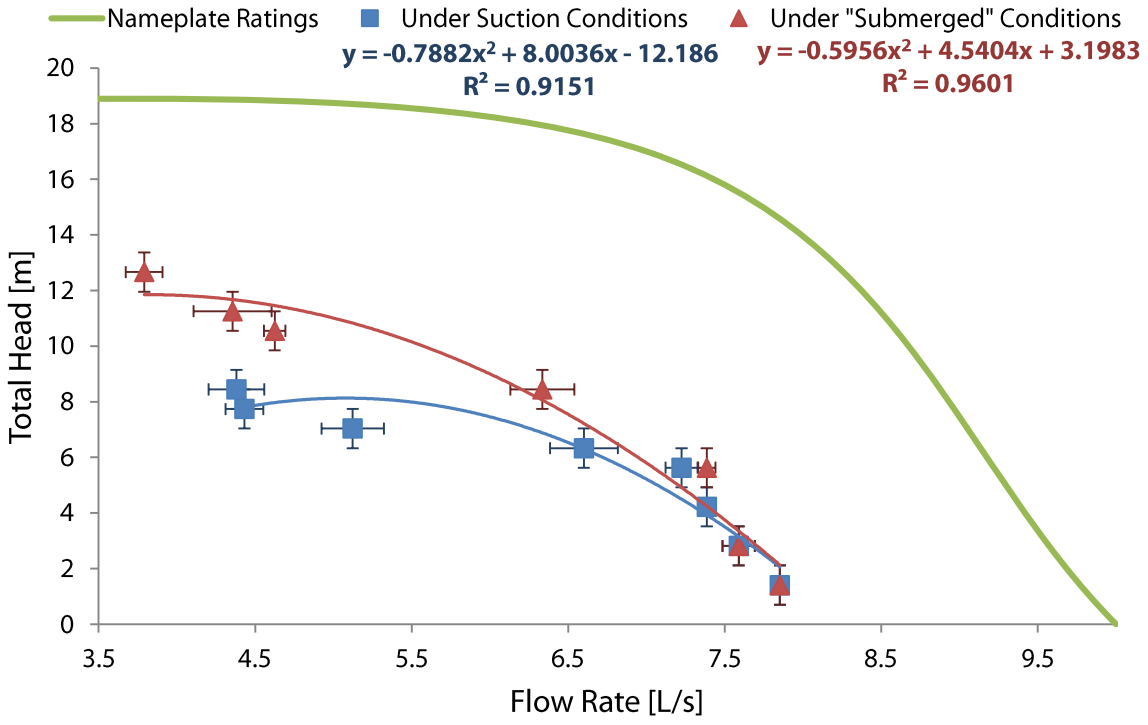

Figure 2.20. Flow rate versus total head performance for the five-year-old Honda GK200 engine coupled to an USHA UNK 2020B pump.

The flow rate versus total head results for the twelve-year-old three-horsepower Honda GK200 engine coupled to a Mahendra WMK 2020 pump are given in Figure 2.19, while the results for the five-year-old Honda GK200 engine and USHA UNK 2020B pump are shown in Figure 2.20. The dynamic head calculations required for the pumps tested in the United States were not necessary, as a differential pressure gauge was employed to measure the total change in pressure experienced by the pump. The curves representing the nameplate ratings were derived by fitting a second-order polynomial to three points given by the nameplate affixed to the pump: maximum head, maximum flow rate, and the best efficient point. The data points and error bars represent the averages and standard deviations in measurements, respectively, at each elevation. As anticipated, the pumps were able to produce a higher flow rate when under simulated submerged conditions compared to suction conditions, and the difference in flow rate performance between pulling and pushing water increased with head. Both pump systems far underperformed compared to their nameplate ratings, possibly due to cavitation at the impeller and clogging between the impeller disks due to debris and organisms in the water. (Organisms such as small shellfish and crabs were actually found.) The five-year-old pump outperformed the twelve-year-old pump, probably because of wear and tear over time.

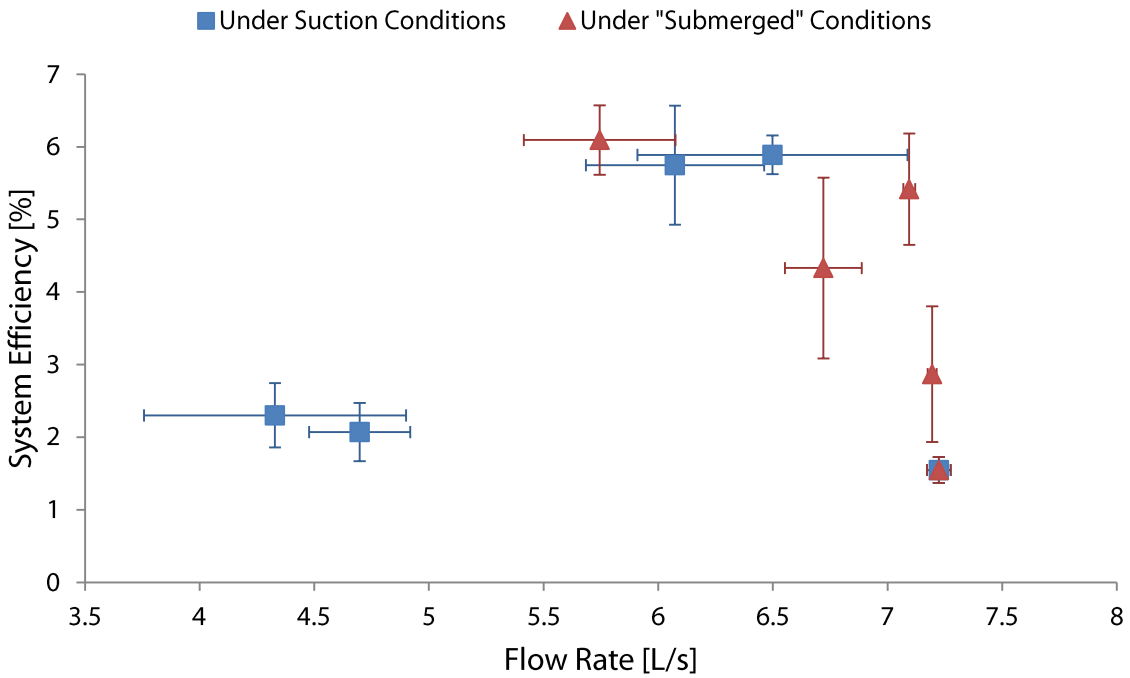

Figure 2.21. Flow rate versus system efficiency for the twelve-year-old Honda GK200 engine coupled to a Mahendra WMK 2020 pump.

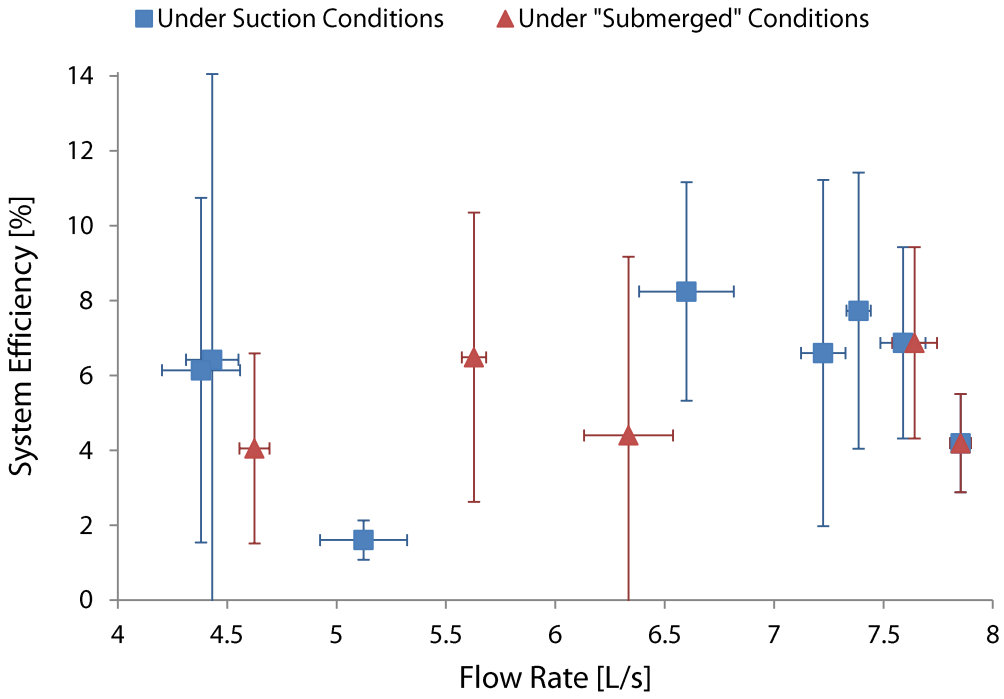

Figure 2.22. Flow rate versus system efficiency for the five-year-old Honda GK200 engine coupled to an USHA UNK 2020B pump.

These results were translated into operation costs to irrigate one acre of land with two inches of water using equations 2.11, 2.12, and 2.13, as for the pump tested in the United States (note that farmers normally irrigate far less than one acre at a time). As described in Section 2.2.5, the error bars account for both uncertainty propagation from experimental data as well as the very wide range of rental rates in Jharkhand. The results, shown in Figure 2.23, reveal that farmers could reduce operation costs by switching to a submersible pump—which is not an option for farmers who lack access to electricity—or by lowering their pump closer to the water level. Many farmers already do this when the water level falls below what can be brought to the surface by suction (when the water table falls below seven meters in depth). Some farmers hoist their pumps down into the well using rope, while others dig a trench to the bottom of the well and drill a hole through the well's wall for the hose. Farmers could save money on irrigation if they repeated these procedures when the water level has not fallen beyond the reach of suction.

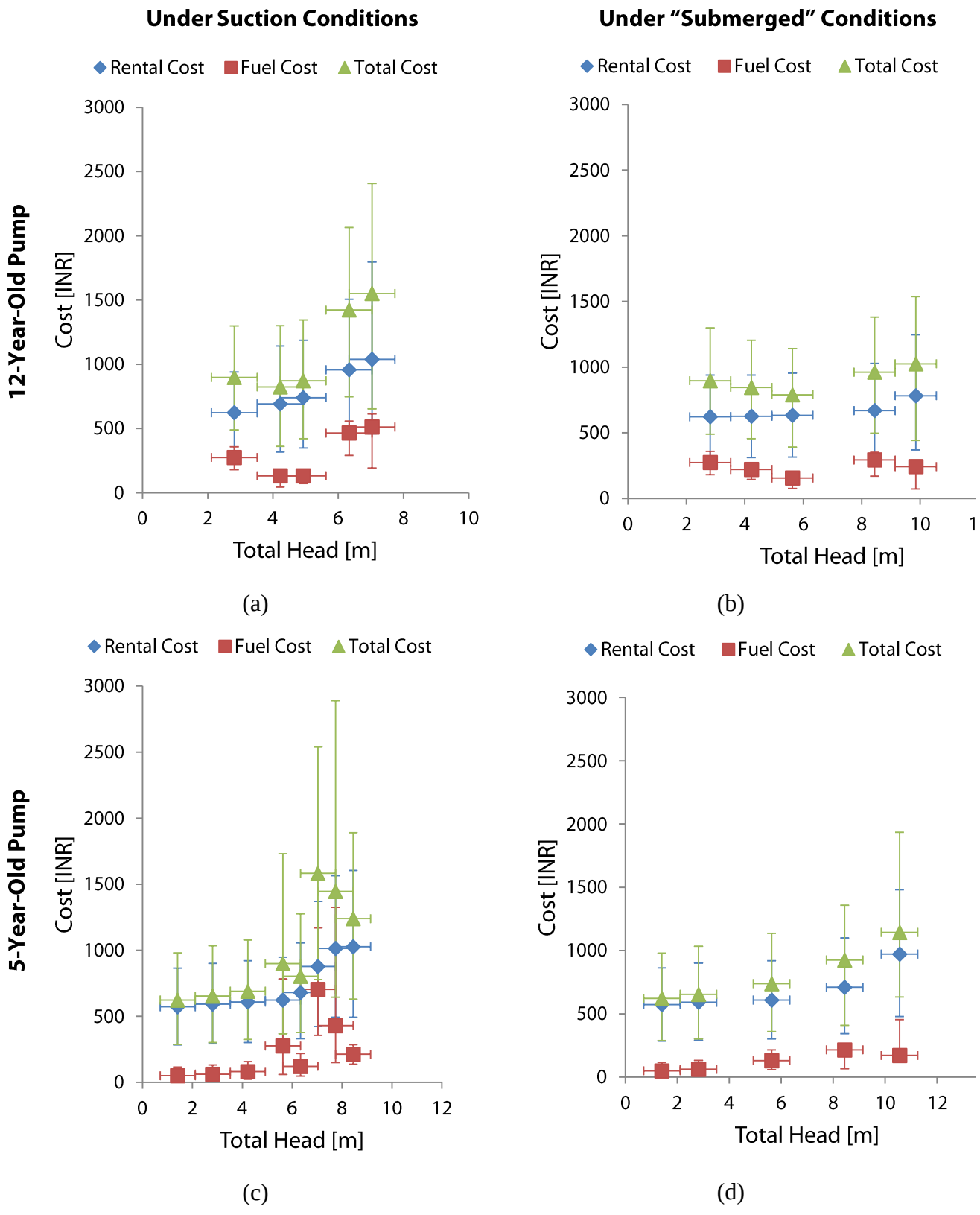

Figure 2.23. Operation costs to the farmer, broken down into fuel and rental costs. (a) Twelve-year-old pump under suction conditions. (b) Twelve-year-old pump under simulated submerged conditions. (c) Five-year-old pump under suction conditions. (d) Five-year-old pump under simulated submerged conditions.

2.4 Chapter Conclusion and Future Work

Although many difficulties were faced while attempting to test the pumps in the United States, testing the pumps with the help of the farmers in India proved fruitful. In the future, it is recommended to test technologies with the people who have experience operating the technologies. As evidenced by this experience, those users often have some tricks up their sleeves to get their machines working that we might not be aware of when trying to operate the technologies out of context.

We discovered that the hourly rental costs outweighed fuel costs. Rent accounted for 69 to 92% of the total operation costs for the five-year-old Honda pump and 67 to 85% for the twelve-year-old pump. Therefore, the time required to irrigate a field, or higher flow rates that can increase the amount of water extracted in a given amount of time, is the farmer's greatest concern. Although fuel consumption measured inconsistently, farmers save money by reducing irrigation time as a result of higher flow rates at a diminished suction head. Despite the variations in fuel consumption, it was found that the proportion of total costs resulting from rent decreased with rising head, so fuel consumption becomes more important at higher heads.

We also verified our hypothesis that lowering the pump closer to the water level decreases operation costs. We found that almost eliminating suction lift lowered total operation costs by 17 to 25% for the five-year-old pump and up to 44% for the twelve-year-old pump, compared to the prediction that removing suction head could decrease costs by up to 35%. As expected, greater savings were accomplished at higher heads. These total savings resulted from up to 31% savings in rent and up to 52% savings in fuel for the five-year-old pump and up to 34% savings in rent and up to 67% savings in fuel for the twelve-year-old pump. Removing suction head thus had a greater impact on energy efficiency than on water discharge.

Further research is necessary to see if an improved shaft seal would impact efficiency and flow rate at each head. Leaking at the shaft seal was quite heavy, and it is likely that some air could enter the fluid and decrease its density, thereby reducing efficiency and flow rate. Furthermore, more investigation into impeller design is necessary. The impeller disks could be placed farther apart in order to reduce clogging. Also, although ultimately no data could be collected about the Chinese pumps during this study, the huge difference in impeller-to-chamber fill ratio between the Chinese and Indian pumps is curious. The effect of fill ratio on efficiency should be explored. In

addition to physically lowering existing pumps closer to the water level, changes to pump design could reduce operation costs and thus should be examined.

Chapter 3: Pump System Options

3.1 Introduction

The goal of this research was to devise an efficient off-grid irrigation solution that would employ a fuel-powered engine on the surface to drive a submersible pump in the well. Such a system would eliminate suction head and thus cavitation, thereby increasing both efficiency and lifetime of the pump and decreasing operation costs. The options investigated to accomplish this aim include extended torque transmission, fluid machinery, and off-grid electricity generation. The extended torque transmission alternatives incorporated flexible shafts, nested telescoping shafts, and segmented telescoping shafts. The fluid machinery study explored semi-open hydraulic systems, jet pumps, compressed air motors, and air-lifts. Electricity generation involved small diesel generators and automotive alternators coupled to the small gasoline-start, kerosene-run engines already in use. Each option was assessed according to metrics including efficiency, maintainability, and portability, as determined by the design requirements described in Chapter 2.

3.2 Extended Torque Transmission

3.2.1 Flexible Shafts

A flexible shaft allows for torque transmission in bent configurations around odd geometries without the use of extra parts such as universal joints or gearboxes, thereby accommodating misalignment between a motor and its driven device and limited space constraints (Figure 3.1). A typical flexible shaft has a torsional-to-flexural stiffness ratio of 50:1, while a typical solid steel shaft has a 0.8:1 ratio [34].

A shaft with such flexibility could be rolled up onto a spool for storage. It was hoped that a flexible shaft could transmit torque from an engine on the surface to the submersible pump while still providing portability. If the flexible shaft could have a small enough radius of curvature, the spool storing the shaft could be transported from well to well on a bicycle, and farmers could lower and raise the shaft and pump using a hand crank.

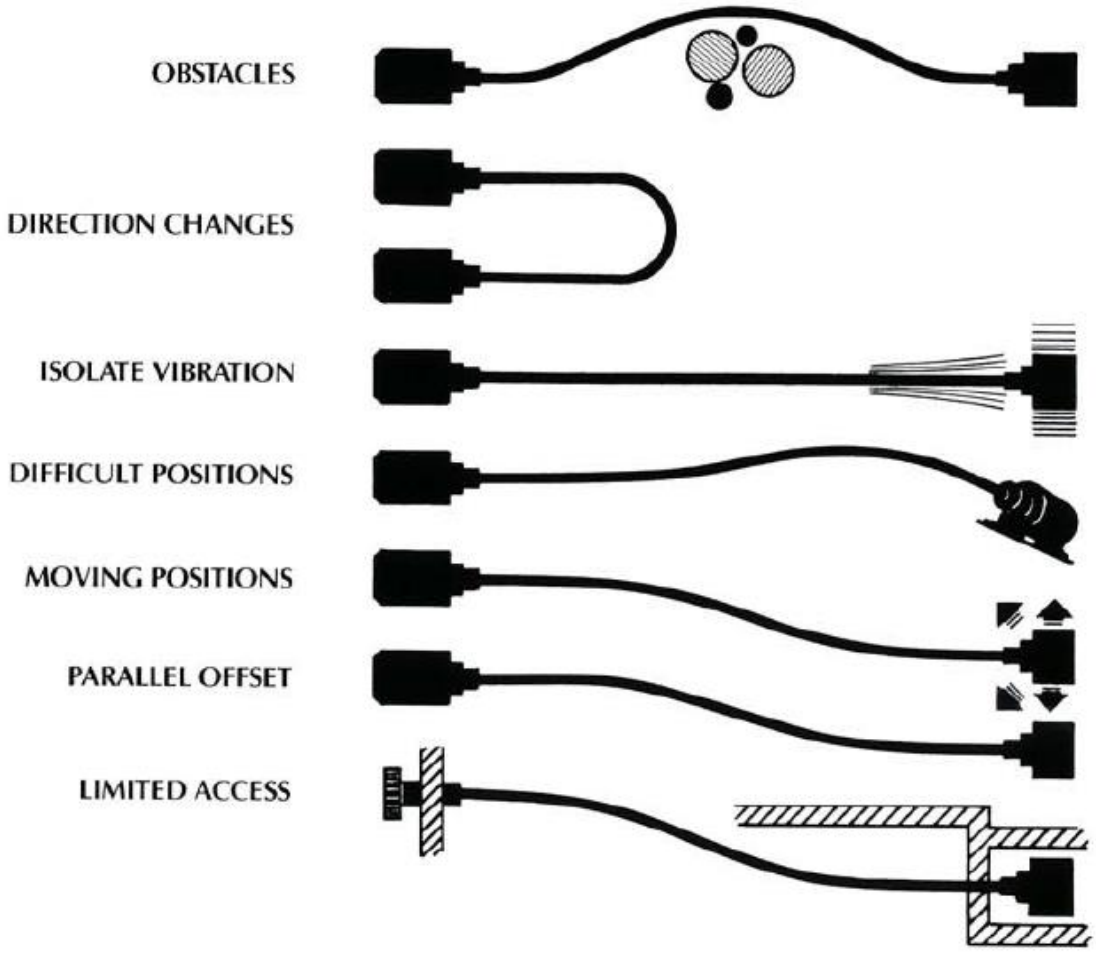

Figure 3.1. Typical uses and configurations of flexible shafts. **[35]**

3.2.1.1 Prior Art

Not many researchers have published articles on flexible shafts. Adam Black, III characterized the behavior and geometry of flexible shafts in his Ph.D. dissertation *On the Mechanics of Flexible Shafts* (1988) [36]. Black's model will be discussed in detail below in Section 3.2.1.2. Jay A. Muelhofer utilizes this model in his Master's thesis *Flexible Shaft Drilling for Cased Well Exploration* (1994) [34] on a flexible shaft design for drilling oil wells.

Based on his dissertation research, Black designed and patented a flexible shaft that combines the attributes of a rotary cable and push-pull cable in order to transmit torque, compression force, and tension force (US patent 7,089,724, 2006). In his patent, he explains that a rotary flexible shaft typically is made of a core, or mandrel, wire, surrounded by layers of wires wound in alternating directions, as shown in Figure 3.2. Typically, the number of wires increases

with each layer outwards, and the pitch angles vary from thirty to fifty-five degrees. The failure mode of these shafts involves helixing or unwinding, usually due to compressive forces or a high torque load [37]. The earliest flexible shaft employing a related wire configuration dates back to 1896 (US patent 571,869 [38]), and several other patents have utilized similar designs (US patents 1,952,301 [39], 2,401,100 [40], 3,791,898 [41], 4,112,708 [42], 5,288,270 [43], 6,881,150 [44] among others).

In order to limit the possibility of helixing, shafts are generally supported by a conduit, which acts as a uniform bearing surface. The conduit also serves to protect the flexible shaft from wear and tear due to environmental conditions [34].

When selecting a flexible shaft, the company Elliott Manufacturing recommends considering the torque load, operating speed, direction of rotation, minimum radius of curvature during operation, and torsional deflection. Generally, for flexible shafts higher rpm and lower torque is advised in order to minimize the possibility of helixing. Three types of shaft cores, which meet different direction of rotation requirements, are commercially available: power drive, remote control, and non-ravel. Power drive cores are designed to operate in a single direction, and operation in the opposite direction results in a 30% or more reduction in torque transmission. These cores have fewer layers made of wider-diameter wires. Remote control, or bidirectional, cores can be in used in both directions but must be operated at low speeds (less than 100 rpm) and generally comprise more layers and wires. Non-ravel, or assembled, cores operate unidirectionally like power drive cores but allow for extreme flexibility (smaller radii of curvature) and higher speeds [35].

Pacelli et al. (US patent 2007/0093840) designed a flexible shaft employing a different concept. Rather than wrapping wires in alternating directions around a mandrel wire, Pacelli et al. linked shaft segments to each other via at least one flexible member or wire (Figure 3.3). The segments can shift along the member(s), thereby permitting the shaft to bend. The authors suggest that this design would be best utilized for medical devices or to guide a tool along a curvilinear path [45]. Although Pacelli et al.'s flexible shaft is capable of transmitting rotary motion, this design was not further explored for pump applications, because this less common technology would be difficult to repair or replace in India.

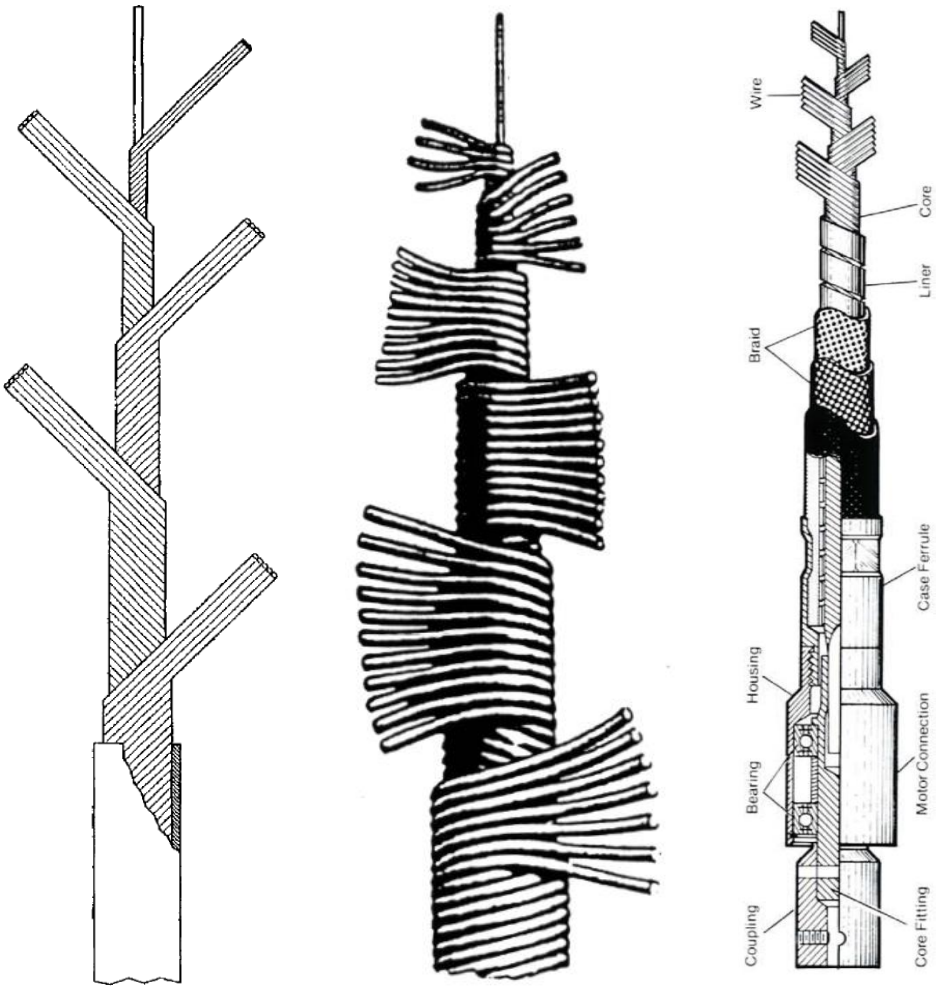

Figure 3.2. Flexible shaft construction. **[37, 34, 35]**

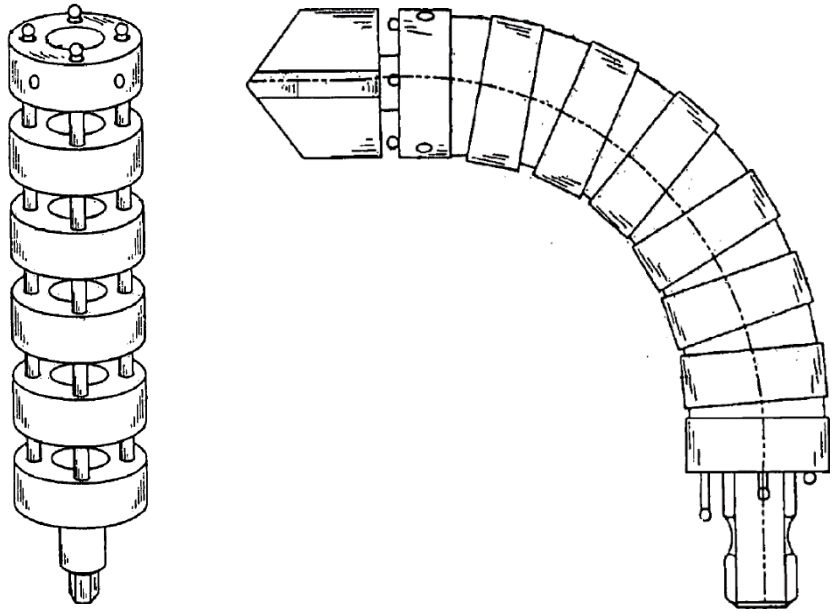

Figure 3.3. Segmented flexible shaft. **[45]**

3.2.1.2 Model of Flexible Shafts

The model used to assess the feasibility of the flexible shaft to transmit torque from an engine mounted on the surface to a pump submerged down in a well was adapted from Adam Black, III's Ph.D. dissertation *On the Mechanics of Flexible Shafts* (1988) [36]. Black devised and verified with experimental data a set of equations that characterizes the performance of a flexible shaft based on its geometry. These equations have been reorganized to output the geometry that results in the performance requirements. The type of shaft analyzed was the one comprised of layers of wires wound in alternating directions, described earlier in 3.2.1.1 Prior Art and shown in Figure 3.2. A representative cross-section of the wires and spaces are given in Figure 3.4. Each wire can be thought of as analogous to open-coiled helical springs that deform in the axial plane when bent, as explained by Timoshenko (1956) [36].

A set of assumptions were required to simplify Black's model, since his equations build up to shaft performance wire layer-by-wire layer. The following assumptions were made:

- All wires, including the mandrel, are of equal diameter.
- All pitch angles are equal.
- All spaces between layers and between wires within a layer are of equal distance.
- There are no axial (tensile or compressive) forces acting on the shaft.
- The material of the shaft is steel with an elastic modulus of 210 GPa [46].

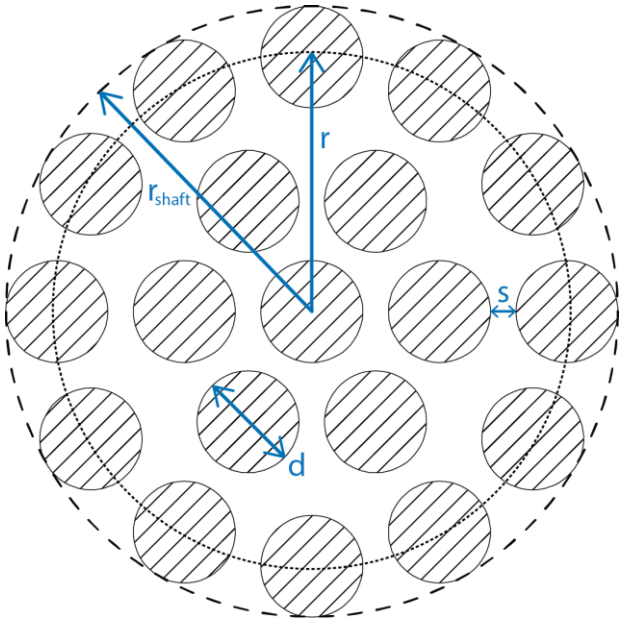

Figure 3.4. Not-to-scale cross-section of an example flexible shaft. r_{shaft} is the shaft radius, r is the mean radius to the outermost wire, d is the diameter of a wire, and s is spacing between layers and between wires within a layer.

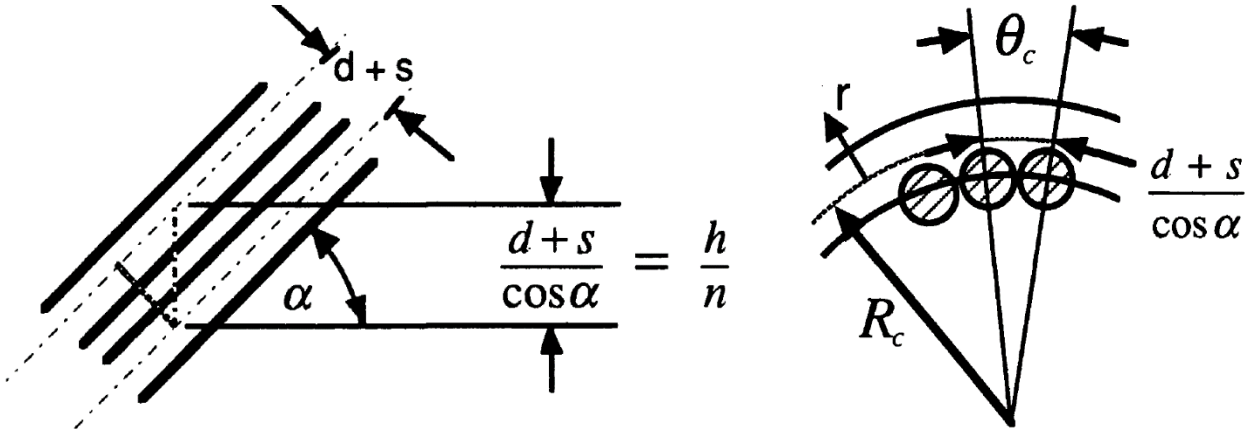

Figure 3.5. Wire spacing geometry at the critical radius of curvature. **[34]**

The maximum torque that a shaft can experience without failure is known as the "critical torque," T_c. In order to prevent torsional instability, which leads to helixing, the torque load on the shaft must be less than the critical torque. According to Black [36], linear torsional stability theory says that the critical torque for an elastic rod is

$$T_c = 2\left(\frac{B^2\pi^2}{L^2} + BP\right)^{\frac{1}{2}} \qquad \text{(Eq. 3.1)}$$

where

T_c	=	critical torque	[Nm]
B	=	bending stiffness	[Nm^2]
L	=	length of shaft	[m]
P	=	tensile force on the shaft	[N]

Equation 3.1 suggests that increasing the bending stiffness or the tensile force would allow the flexible shaft to transmit higher torque before becoming unstable and helixing, while increasing the shaft length would decrease the torque capacity. For simplification, it was assumed that there are no axial forces, or $P = 0$. Muelhoefer found that while the equation worked for tensile forces, it broke down for compressive forces (which he defined as a negative value for P). He also assumed that no axial forces were present when applying Black's model to drilling [34]. Without axial forces, the critical torque simplifies to

$$T_c = \frac{2B\pi}{L} \quad \text{(Eq. 3.2)}$$

Black found that the effective bending stiffness *B* of a flexible shaft could be approximated as [36]

$$B = A_0 E r^2 \quad \text{(Eq. 3.3)}$$

where

A_0	=	cross-sectional area of the mandrel wire	[m^2]
E	=	elastic modulus of the material	[Pa]
r	=	mean radius of the flexible shaft	[m]

Note that *r* does not include the full diameter of the outermost wire. The "mean radius" indicates the radius of the shaft from the center of the mandrel to the center of the outermost wire, as in Figure 3.4. The cross-sectional area of the mandrel wire is defined as

$$A_0 = \pi r_{central}^2 \quad \text{(Eq. 3.4)}$$

where

$r_{central}$	=	the radius of the mandrel wire	[m]

Substituting equation 3.4 into equation 3.3 and equation 3.3 into equation 3.2 and algebraically reorganizing, the radius of the shaft from the center of the mandrel to the center of the outermost wire layer can be found at a specified torque capacity as

$$r = \sqrt{\frac{T_c L}{2\pi^2 r_{central}^2 E}} \quad \text{(Eq. 3.5)}$$

The total radius of the flexible shaft is then

$$r_{shaft} = r + \frac{d}{2} \quad \text{(Eq. 3.6)}$$

where

d = diameter of the wire [m]

The number of layers in a flexible shaft is thus

$$n_{layers} = \frac{r_{shaft} - r_{central}}{d + s} \quad \text{(Eq. 3.7)}$$

where

s = space between layers and between wires in a layer [m]

Since the number of layers must be a whole number, the result of equation 3.7 was rounded up to the next integer. The radius of each layer is

$$r_{layer_i} = r_{central} + s + \frac{d}{2} + (i - 1)(d + s) \quad \text{(Eq. 3.8)}$$

where

i = layer number, increasing outwards

r_{layer_i} = mean radius of the layer [m]

The number of wires in each layer is determined by

$$n_{wires_i} = \frac{2\pi r_{layer_i} \sin \alpha}{d + s} \quad \text{(Eq. 3.9)}$$

where

n_{wires_i} = number of wires in the layer

α = pitch angle [rad]

The pitch distance—that is, the axial distance of a single coil—is calculated as

$$h_i = \frac{n_{wires_i}(d + s)}{\cos \alpha} \quad \text{(Eq. 3.10)}$$

where

h_i = pitch distance [m]

The volume of each layer, reflecting the geometry of a spring, is

$$V_{layer_i} = \frac{2\pi^2 L r_{layer_i} n_{wires_i}}{h_i}\left(\frac{d}{2}\right)^2 \quad \text{(Eq. 3.11)}$$

where

V_{layer_i} = volume of the layer [m^3]

The total volume of the flexible shaft is the sum of the volumes of each layer.

$$V_{total} = \sum_{i=1}^{n_{layers}} V_{layer_i} \quad \text{(Eq. 3.12)}$$

where

V_{total} = total volume of the flexible shaft [m^3]

The critical radius of curvature is the maximum bend a flexible shaft can tolerate and occurs when all the wires on the inside of the bend have come into contact (when the spaces between the wires on the inside have been eliminated). Upon analyzing the geometry of the wires and spacing (Figure 3.5), Black finds the critical radius of curvature to be [36]

$$R_c = r\left(\frac{d+s}{s}\right) \quad \text{(Eq. 3.13)}$$

where

R_c = critical radius of curvature [m]

This model was run in MATLAB with ranges of torque, shaft length, wire diameter, spacing between wires and between layers, and pitch angles as inputs. Torque was varied from 0 to 20 Nm, because the torque of small engines in India vary from about 2 to 15 Nm. Length was varied from 0 to 30 m, because depths of an open well typically do not extend beyond that. Wire

diameter was varied from 0.1 mm to 1 cm, spacing was varied from 5 μm to 15 μm, and pitch angles were varied from $\pi/6$ to $\pi/3$ rad, because Black in his dissertation suggested that these would be reasonable values for flexible shaft geometry. The outputs of the model included radii of each layer, the shaft, and of curvature, the numbers of layers and wires per layer, the pitch distances, the volume of each layer, and the total volume.

3.2.1.3 Results and Discussion

Though Black's model is likely in use at his company S.S. White Technologies, publicly-available design tables for flexible shafts could not be found. Therefore, the outputs from the model were utilized to create a series of design charts that could be used to determine the geometry of a flexible shaft to meet torque and configuration requirements (with the above-mentioned assumptions for simplification). These plots also reveal the impact of geometric features on torque capacity and radius of curvature.

The results for critical torque versus the radius of curvature and shaft radius are given in Figure 3.6, which reveals that the radius of curvature and shaft radius increase with critical torque and shaft length. (In this case, shaft radius is actually *r*, the mean radius to the outermost wire layer drawn in Figure 3.4. The variable *r* rather than r_{shaft} was plotted in order to fit more information into the chart; *r* and R_c have a linear relationship, as described in equation 3.13, while r_{shaft} *and* R_c do not.) In other words, greater torque capacities and shaft lengths require larger radii of curvature and the shaft. As shown in Figure 3.7, changes in the wire diameter have little influence on the radius of curvature. However, wire diameter does impact the shaft radius. When the wire diameter increases, the shaft radius decreases Figure 3.9(a)) because the number of layers required decreases as wire diameter increases (Figure 3.9(c)). Figure 3.9(b) demonstrates that the radius of the shaft increases with shaft length. As shown in Figure 3.9(d), larger spacing between wires allows for tighter turns, or smaller radii of curvature, because the shaft can only bend until the spaces completely close and the wires all touch. The total volume of the shaft increases as critical torque increases, as shown in Figure 3.8.

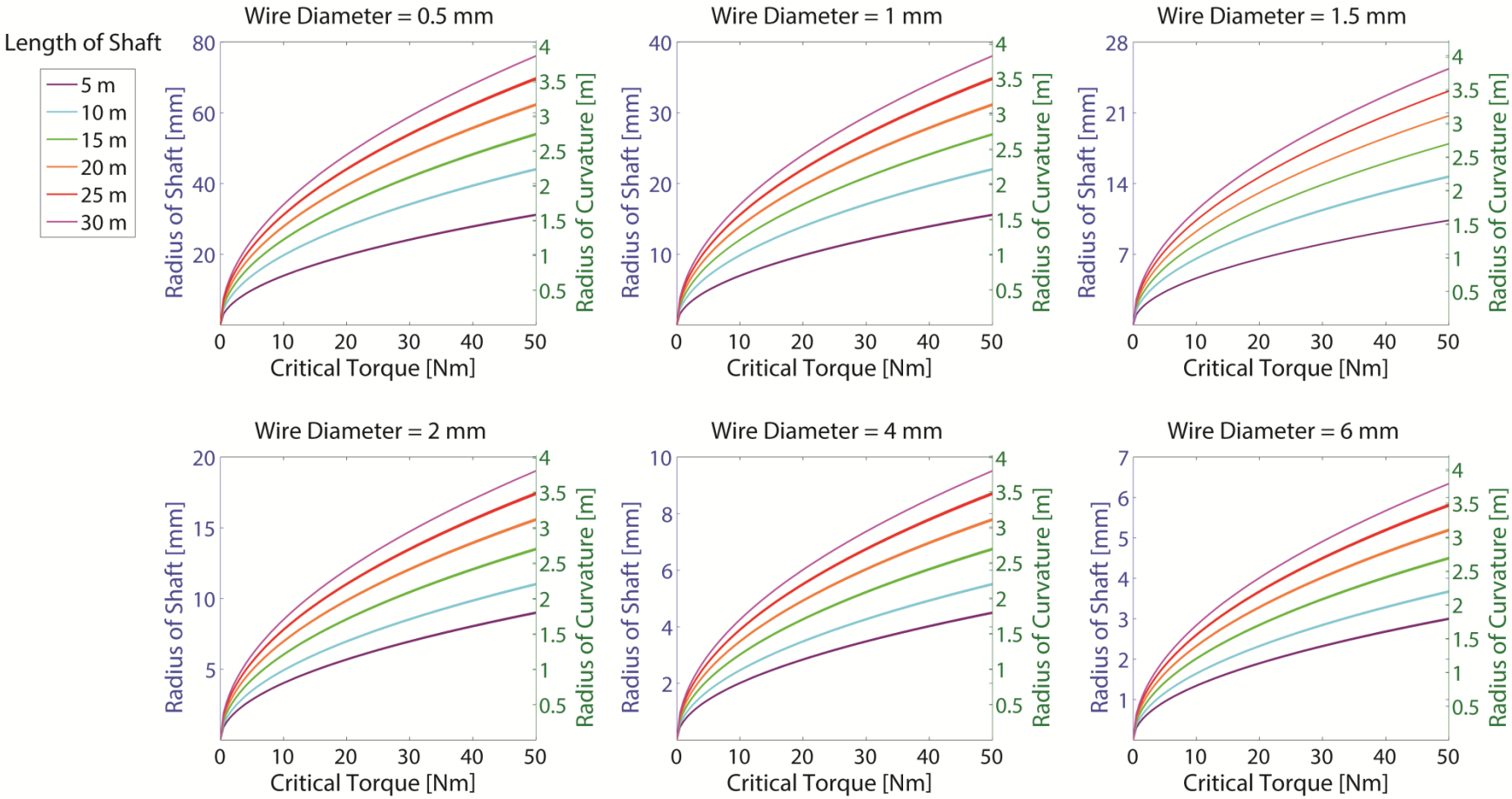

Figure 3.6. Critical torque versus the radius of the flexible shaft and the critical radius of curvature. Note that the shaft radius is actually the mean radius to the outermost wire layer (*r* in Figure 3.4). Each plot represents a different wire diameter input, and each curve indicates a different shaft length input.

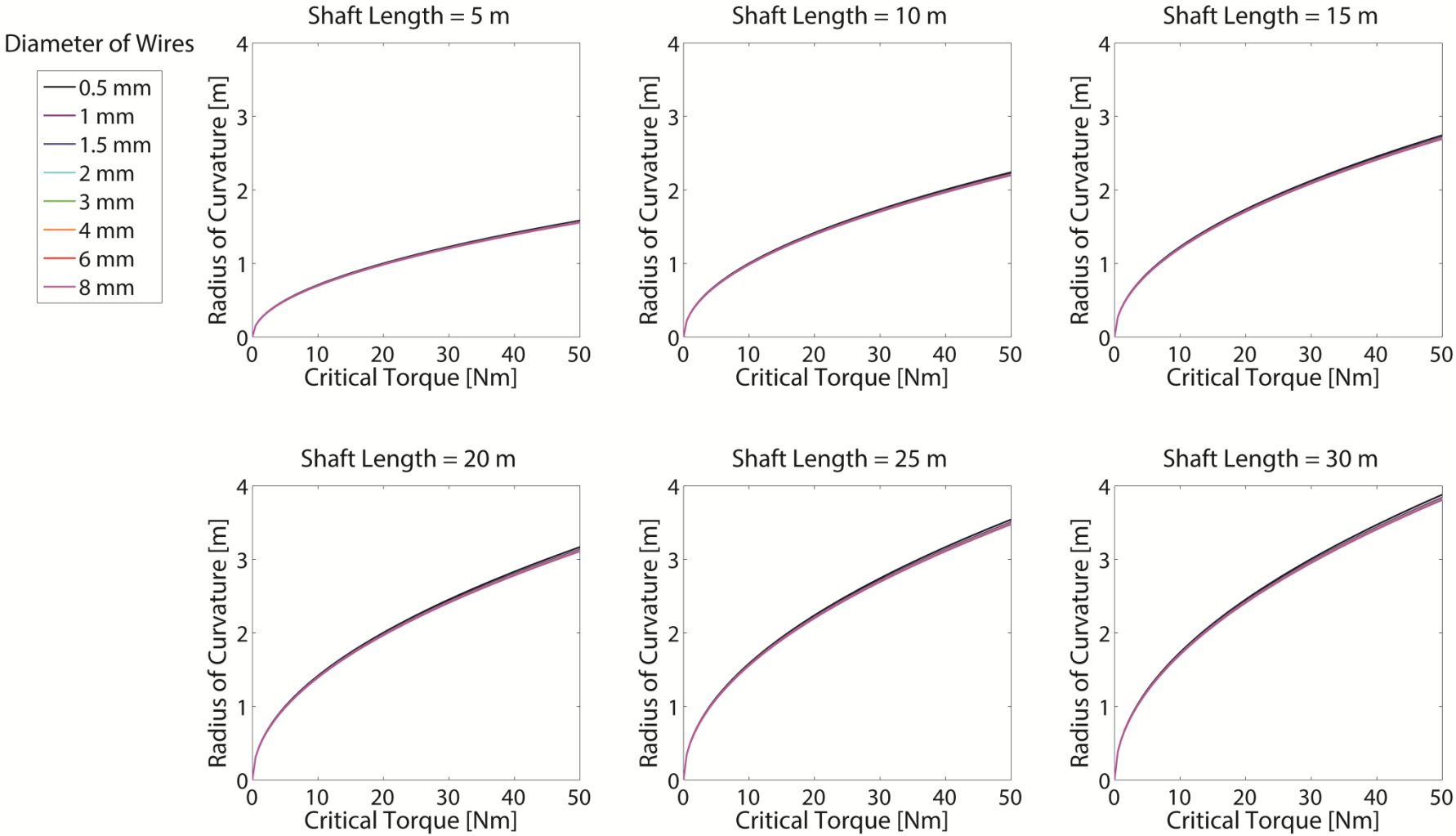

Figure 3.7. Critical torque versus radius of curvature. Each plot represents a different shaft length input and each curve indicates a different wire diameter input.

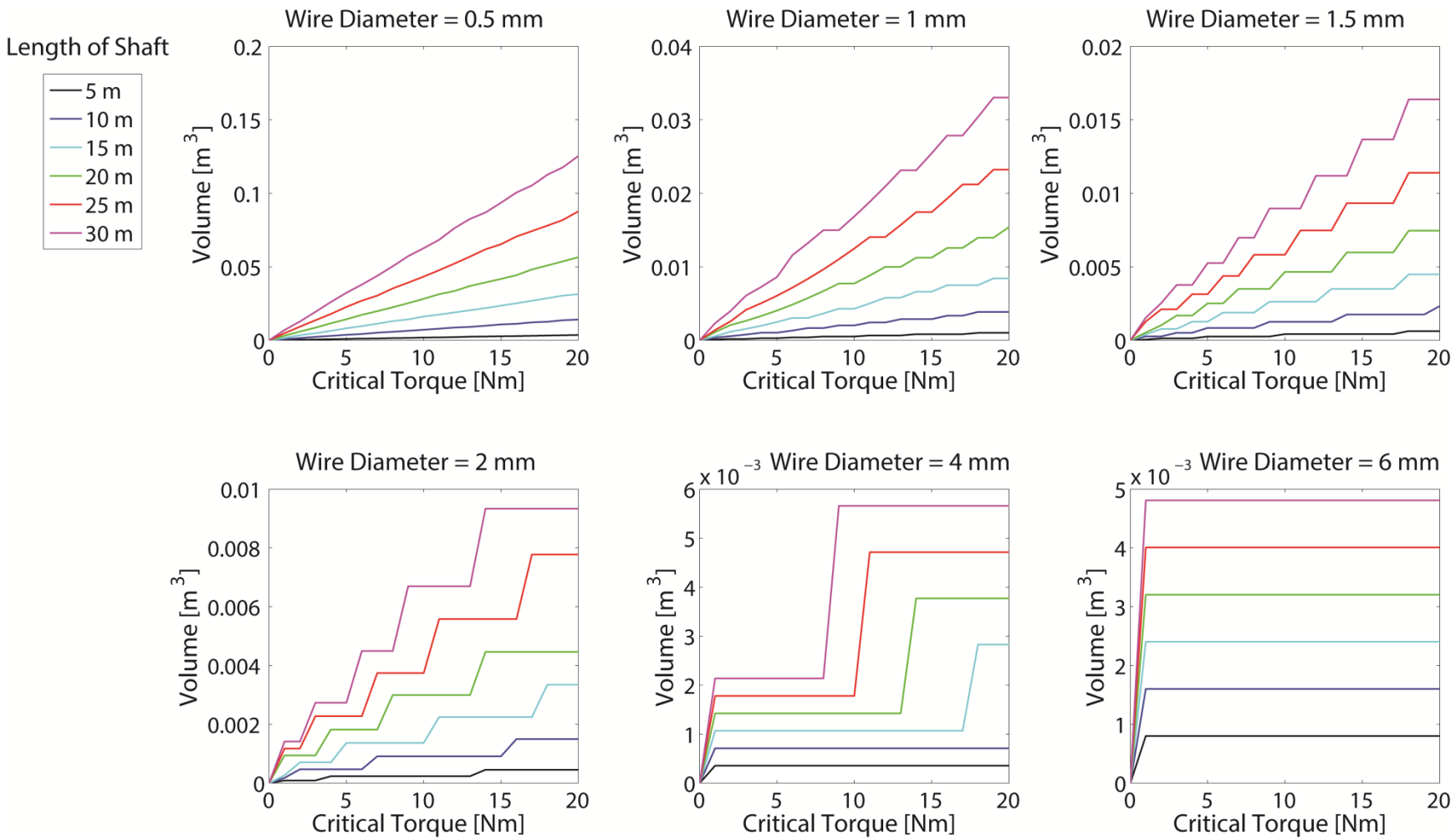

Figure 3.8. Critical torque versus volume of shaft. Each plot represents a different wire diameter input and each curve indicates a different shaft length. The curves are jagged because the number of layers and number of wires in each layer were rounded to the nearest larger integer.

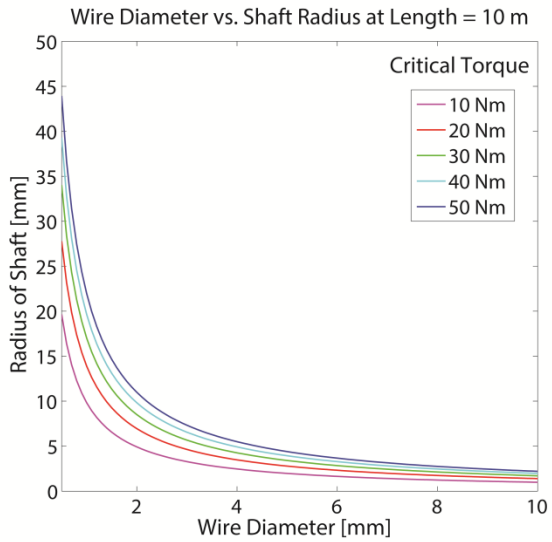

(a)

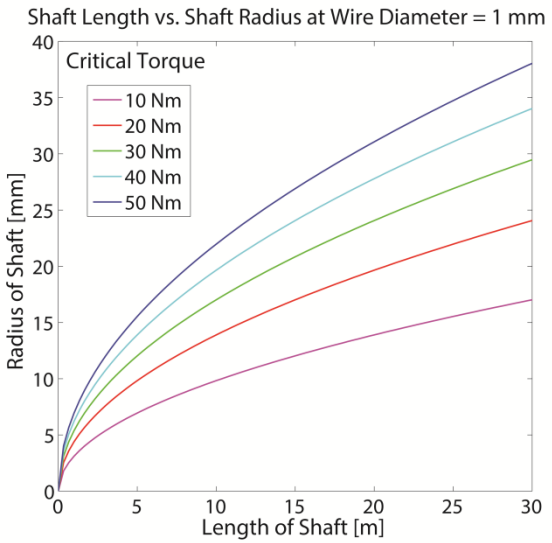

(b)

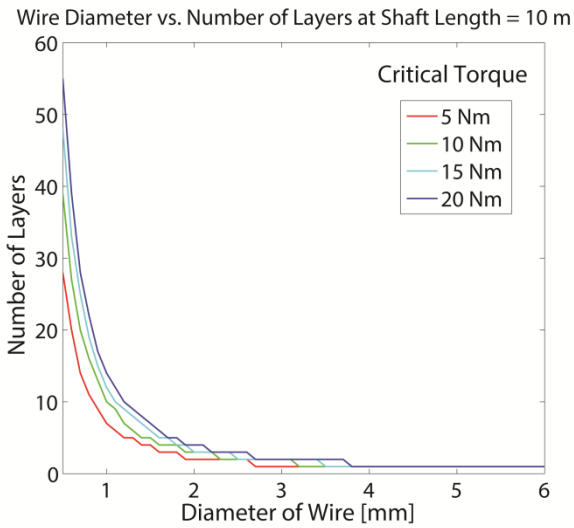

(c)

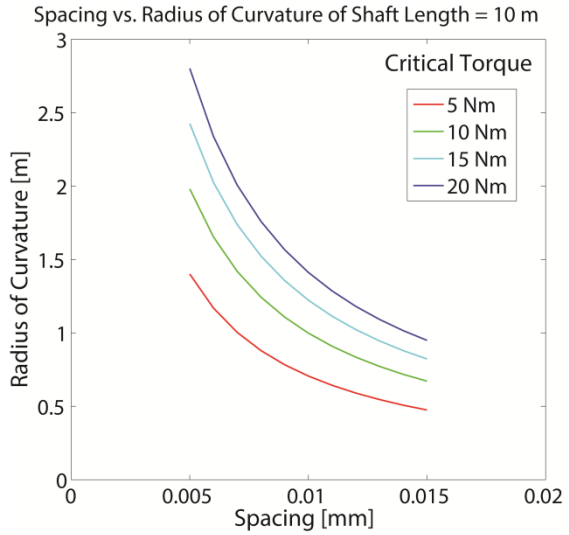

(d)

Figure 3.9. (a) Wire diameter versus shaft radius at 10 m length. (b) Shaft length versus shaft radius with 1 mm wire diameter. (c) Wire diameter versus number of layers at 10 m shaft length. (d) Spacing versus radius of curvature at 10 m shaft length.

One of the most popular brands for small engines in eastern India is Honda, whose engines with capacities under 5 hp start on gasoline and run on kerosene. The maximum torque output for the 1.5 hp model, Honda GK100, is 3.9 Nm. The 3 hp model, GK200, can achieve up to 7.9 Nm of torque. The maximum torque for the 4 hp model, GK300, is 12.4 Nm [47]. Assuming that these models would be used for the pumping system on a well 10 m in depth (10 m is the typical depth of an upland hand-dug open well [16]) and that the efficiency of torque transmission is 100%, the smallest radius of curvature could be approximately 0.63 m for the 1.5 hp engine, 0.89 m for the 3 hp engine, and 1.1 m for the 4 hp engine. For portability purposes, it had been envisioned that the flexible shaft could be rolled up onto a spool and put on the back of a bicycle, as pumps are currently transported from well to well on bicycles. However, these radii of curvature require spools 1.26 m, 1.78 m, and 2.2 m in diameter; these spools would be too large to be portable (for perspective, the average Indian adult male stands at 1.65 m tall [48]). Additionally, the flexible shaft would weigh approximately 24 kg for the 1.5 hp engine, 46.5 kg for the 3 hp engine, and 71.5 kg for the 4 hp engine.

In addition to not meeting the portability requirement, the flexible shaft would be complex and expensive to manufacture. The large volume required would involve high material costs. Repairing flexible shafts would likely be difficult for village mechanics, and replacement parts might be difficult to find in rural India and expensive to purchase. Furthermore, flexible shaft couplings are difficult to seal, which would be problematic when employed in a pumping application. For these reasons, we decided not to move forward with the flexible shaft.

3.2.2 Telescoping Shafts

Because the flexible shaft concept did not meet the portability, maintainability, and cost requirements, telescoping shafts with a right-angle gear box were investigated as another option for extended torque transmission. The telescoping shaft could either be nested, as in Figure 3.10(a), or segmented, as in Figure 3.10(b). The nested shaft could collapse into itself, and the segmented shaft could either fold like tent poles or consist of separate parts that must be reconstructed each time it is used.

The advantages of the nested shaft are that it would be lighter than the segmented shaft, more portable, and easier to assemble on site. However, if one piece breaks, the entire unit would not be usable. Alternatively, a segmented shaft, possibly held together with pins, could still be

used if a piece breaks. The advantage of the segmented shaft, though it could be more cumbersome and time-consuming to assemble, is that it would be comprised of identical parts. With identical parts, the shaft could be easily repaired (a user could borrow a piece from his neighbor in the short term, and many identical parts could be mass-produced and made readily available in the market). The nested telescoping shaft, on the other hand, could perhaps get clogged and replacing parts would be more difficult, as each piece is of a different radius and the entire assembly would require deconstruction to repair.

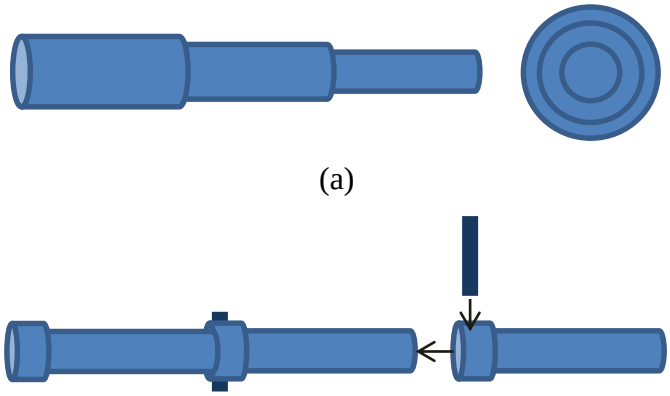

(a)

(b)

Figure 3.10. Telescoping shaft options. (a) Nested. (b) Segmented.

3.2.2.1 Prior Art

Telescoping shafts are more widely used than flexible shafts. A common application is agricultural machinery, particularly for the power take-off (PTO) of a tractor, so it was hoped mechanics in rural India would be familiar with the technology of telescoping shafts. Many patents share similar design features such as splining, teeth, or axially-oriented linear ball bearings to transfer torque between shaft segments (e.g. United States patents 4,103,514 [49]; 6,241,616 [50]; 7,238,113 [51]; and 5,697,850 [52]). An example of a splined telescoping shaft is given in Figure 3.11. In order to Figure out the geometry of the telescoping shafts to meet torque capacity requirements, for the MATLAB modeling it was assumed that each shaft segment had no splines and is a smooth cylinder.

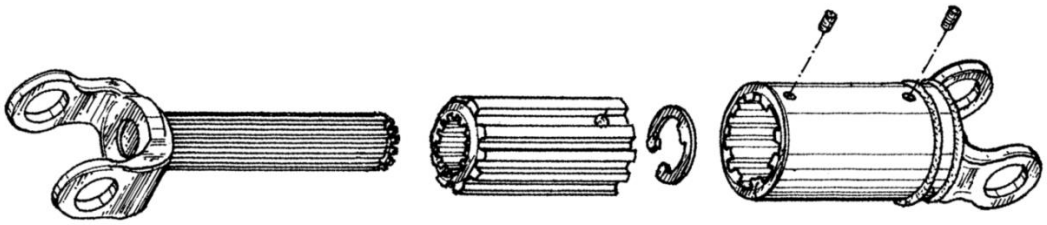

Figure 3.11. An example of a splined telescoping shaft. **[50]**

3.2.2.2 Nested Telescoping Shaft

3.2.2.2.1 Model

The nested telescoping shaft was modeled as a series of concentric hollow rigid shafts. The inner radius of a section was set equal to the outer radius of the previous section, moving in the outward direction. The following assumptions were made:

- Each section is of equal length.
- The material is A-36 steel with an elastic modulus of 210 GPa, maximum shear stress of 100 MPa [53], and a density of 7800 kg/m^3 [54].
- There is no bending moment (M = 0).

The inner and outer radii of the various telescoping shaft segments were determined using the material properties of steel and the forces acting on the shaft. The maximum shear stress a shaft can withstand is related to the shear and normal stresses as

$$\tau_{allow} = \sqrt{\left(\frac{\sigma}{2}\right)^2 + \tau^2} \qquad \text{(Eq. 3.14)}$$

where

τ_{allow}	=	maximum shear stress	[Pa]
σ	=	normal stress	[Pa]
τ	=	shear stress	[Pa]

Normal stress for a hollow shaft can be calculated from the bending moment and area moment of inertia as

$$\sigma = \frac{M r_o}{I} \qquad \text{(Eq. 3.15)}$$

where

M	=	bending moment	[Nm]
r_o	=	outer radius of the hollow shaft	[m]
I	=	area moment of inertia	[m^4]

Likewise, shear stress for a hollow shaft can be calculated from the torque and polar moment of inertia as

$$\tau = \frac{Tr_o}{J} \quad \text{(Eq. 3.16)}$$

where

T	=	torque	[Nm]
J	=	polar moment of inertia	[m^4]

The area moment of inertia for a hollow shaft is

$$I = \frac{\pi(r_o^4 - r_i^4)}{4} \quad \text{(Eq. 3.17)}$$

where

r_i	=	inner radius of the hollow shaft	[m]

The polar moment of inertia for a hollow shaft is

$$J = \frac{\pi(r_o^4 - r_i^4)}{2} \quad \text{(Eq. 3.18)}$$

Substituting equations 3.15, 3.16, 3.17, and 3.18 into 3.14 gives

$$\tau_{allow} = \frac{2r_o}{\pi(r_o^4 - r_i^4)}\sqrt{M^2 + T^2} \quad \text{(Eq. 3.19)}$$

Inputting a range of torques and moments allows MATLAB to solve equation 3.19 for r_o for each shaft segment, assuming that r_i is equal to the r_o of the previous segment. The innermost segment's radius is determined by treating that segment as a solid shaft and finding the outer radius. The area moment of inertia and polar moment of inertia for a solid shaft are, respectively,

$$I = \frac{\pi r_{solid}^4}{4} \quad \text{(Eq. 3.20)}$$

and

$$J = \frac{\pi r_{solid}^4}{2} \quad \text{(Eq. 3.21)}$$

where

r_{solid} = radius of a solid shaft [m]

Substituting equations 3.20 and 3.21 into 3.14 and rearranging the variables allows one to find the radius of the innermost segment, which can be used as the inner radius in the following segment:

$$r_{solid} = \left(\frac{2}{\pi \tau_{allow}} \sqrt{M^2 + T^2}\right)^{\frac{1}{3}} \quad \text{(Eq. 3.22)}$$

Because each segment has the same length and the inner radius of one segment is equal to the outer radius of the previous segment, the volume is equal to the volume of a cylinder with the radius of the outermost segment and the height of a single segment. The shaft's volume is

$$V_{shaft} = \frac{\pi r_{outermost}^2 L_{shaft}}{n_{sections}} \quad \text{(Eq. 3.23)}$$

where

V_{shaft}	=	total volume of the telescoping shaft	[m^3]
$r_{outermost}$	=	outer radius of the outermost segment	[m]
L_{shaft}	=	total length of shaft when extended	[m]
$n_{sections}$	=	number of sections the shaft is divided into	

This model was run in MATLAB with a range of torques, moments, and shaft lengths as inputs. Torque and moment was varied from 0 to 50 Nm and shaft length from 0 to 30 m. The outputs were inner and outer radii of each segment and total shaft volume.

3.2.2.2.2 Results and Discussion

The results of the model described in the previous section are given in Figure 3.12 and Figure 3.13. Figure 3.12 shows the outer radius of each segment; the inner radius of each segment can be considered the same as the outer radius of the previous segment. These radii are independent of shaft or segment length. The segments become thinner farther from the center. Most of the load is carried by the outer part of the shaft, so a shaft with a larger radius can handle a higher load. Thus, when a load is kept constant but applied to a hollow shaft with a larger radius, the shaft can be made thinner. Figure 3.13 reveals that as the number of segments for a given shaft length is increased, the total volume and mass decrease. Volume and mass decrease with the increased number of segments because the length of each section decreases—so the shaft, when collapsed, becomes short and wide rather than long and thin.

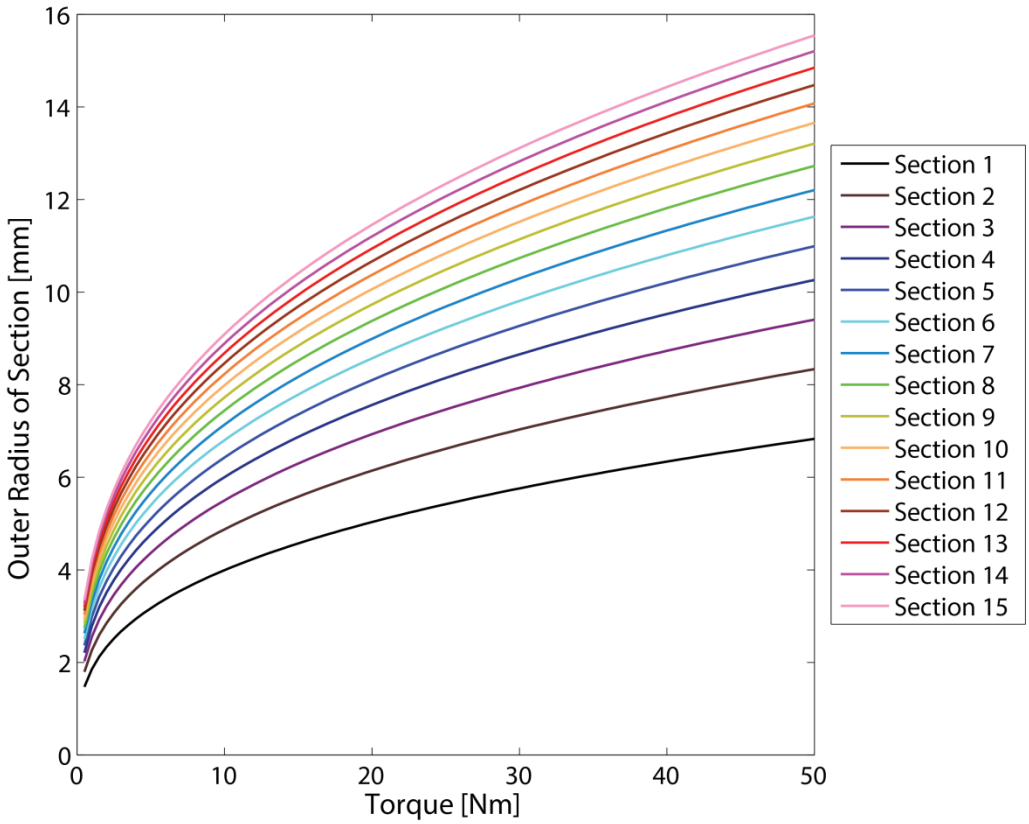

Figure 3.12. Outer radius of each segment, counting from inward to outward.

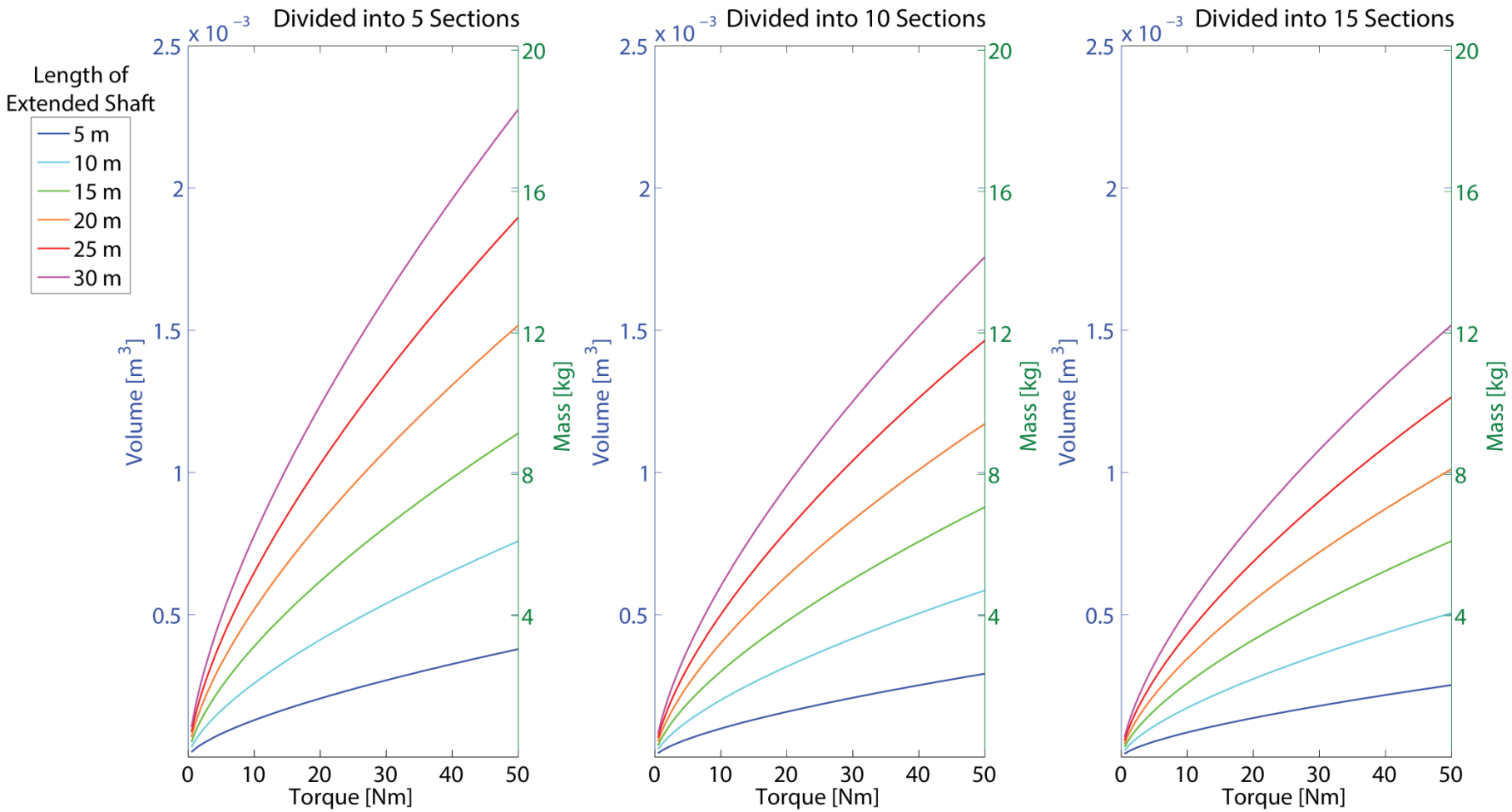

Figure 3.13. Volume and mass of a nested telescoping shaft when divided into 5, 10, and 15 sections.

3.2.2.3 Segmented Telescoping Shaft

3.2.2.3.1 Model

The segmented telescoping shaft was modeled like a rigid shaft. The segmented telescoping shaft, when assembled, would behave like a single long shaft and thus was treated as such. The divisions of the shaft were not relevant for determining the shaft radius. The shaft radii were determined in a manner similar to the nested telescoping shaft segments. For solid shafts, equation 3.22 was utilized, while for hollow shafts, equation 3.19 was solved for the outer radius with a range of inner radii as inputs (1 to 3 cm).

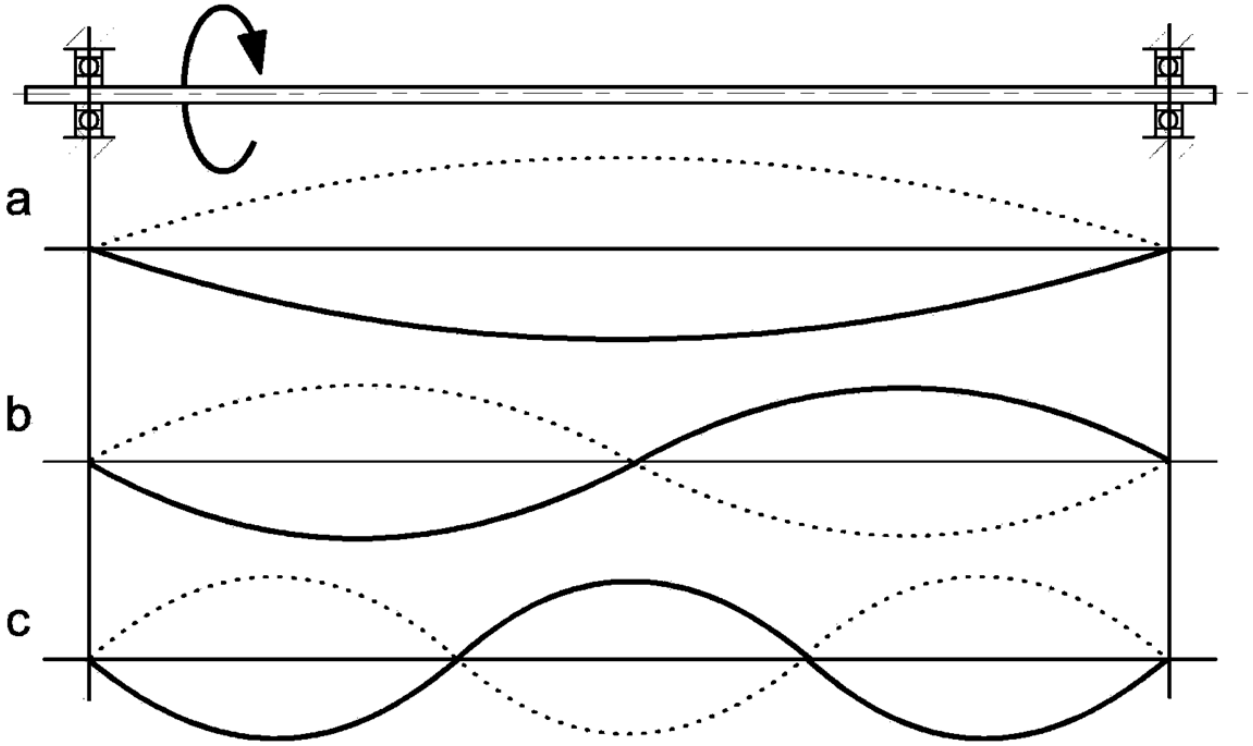

Figure 3.14. Shape of the shaft rotating with shaft whip. (a) First mode of oscillation. (b) Second mode of oscillation. (c) Third mode of oscillation. The first (lowest) critical speed induces the first mode of oscillation of shaft whip, and each subsequent critical speed induces the next mode of oscillation. **[55]**

Shaft whip can be a problem when a shaft is rotating at a high rpm. Shaft whip (Figure 3.14) arises when the frequency of rotation is equal to the shaft's bending natural frequency. The critical speed of a shaft is the speed at which shaft whip will begin to occur and indicates the maximum speed at which a shaft should spin. In the context of a thirty-foot-deep open well, shaft whip could become extreme and pose a serious threat to the safety of well users. A gear box would be required to reduce the speed of the shaft at the engine, which is rated quite high (3000 to 4200

rpm for the Honda GK100, for example), to below the critical speed in order to prevent shaft whip. Another gear box could be used at the pump to increase the speed for the impeller. The critical speed of a shaft is [56]

$$\omega_c = k^2 \sqrt{\frac{EI}{A\rho L_{shaft}^4}} \qquad \text{(Eq. 3.24)}$$

where

ω_c	=	critical speed of the shaft	[rad/s]
k	=	stiffness coefficient determined by supports	
A	=	cross-sectional area of the shaft	[m^2]
ρ	=	density of the material	[kg/m^3]

For a simply-supported shaft, k = 3.142 for the first mode of oscillation (Figure 3.14(a)). To convert the units of critical speed from radians per second to rpm, the following equation can be used.

$$N_c = \frac{60\omega_c}{2\pi} \qquad \text{(Eq. 3.25)}$$

where

N_c	=	critical speed of the shaft	[rpm]

Substituting the cross-sectional area of the shaft ($A = \pi r^2$), the definition of density ($\rho = \frac{m}{V}$, where m = mass [kg] and V = volume [m^3]), and the volume of the shaft ($A = \pi r^2 L$) into equation 3.24 and then substituting the resulting equation into 3.25, the critical speed in rpm can be found.

$$N_c = \frac{60k^2}{2\pi L^2} \sqrt{\frac{EIL}{m}} \qquad \text{(Eq. 3.26)}$$

Transforming the speed of the shaft from the rpm of the engine to equal the critical speed will change the torque. Assuming the gear box operates at 100% efficiency and the engine outputs constant power, the torque of the shaft at critical speed is

$$T_{cs} = \frac{P}{\omega_c} = \frac{60P}{2\pi N_c} \quad \text{(Eq. 3.27)}$$

where

T_{cs}	=	torque at critical speed	[Nm]
P	=	power output from engine	[W]

If the torque of the shaft changes, then so does the radius of the shaft required to handle the torque load. The torque at critical speed should be input into equation 3.22 for a solid shaft and 3.19 for a hollow shaft to find the radius of the shaft at critical speed.

With ranges of engine power and shaft length as inputs, this model was iterated until the radius of the shaft resulted in an rpm equal to the critical speed. Engine power was varied from 0.5 to 4 hp and shaft length from 1 to 20 m.

3.2.2.3.2 Results and Discussion

The results from iterating the model are shown in Figure 3.15. As seen in the plots, the critical speed increases with the length of the shaft. When the shaft is slowed from the engine's speed (for small engines in India, typically around 3000 to 3600 rpm) to the critical speed via a gear box, that shaft must have a higher torque load capacity. The radius required for a larger capacity must also increase. A larger radius means a larger volume and weight. A 1.5 hp engine running a pump system in a 10 m deep well requires a weight of 49.4 kg (solid shaft), 26.3 kg (with a 2 cm inner diameter), or 8.5 kg (with a 4 cm inner diameter). A 10 m deep system employing a 3 hp engine needs a shaft of 69.8 kg (solid shaft), 44.5 kg (with a 2 cm inner diameter), or 16.6 kg (with a 4 cm inner diameter). These weights do not include the two gear boxes required to first step down the speed and then to step the speed back up.

At these weights, the pump systems would have high material costs and be too heavy to be portable on a bicycle. The nested telescoping shafts would face the same shaft whip issues, so Figure 3.12 and Figure 3.13 are not actually accurate. However, because the segmented shaft proved so heavy and the nested shaft would be similarly heavy, the telescoping shaft options were eliminated and it was decided not to correct the nested shaft model to account for shaft whip.

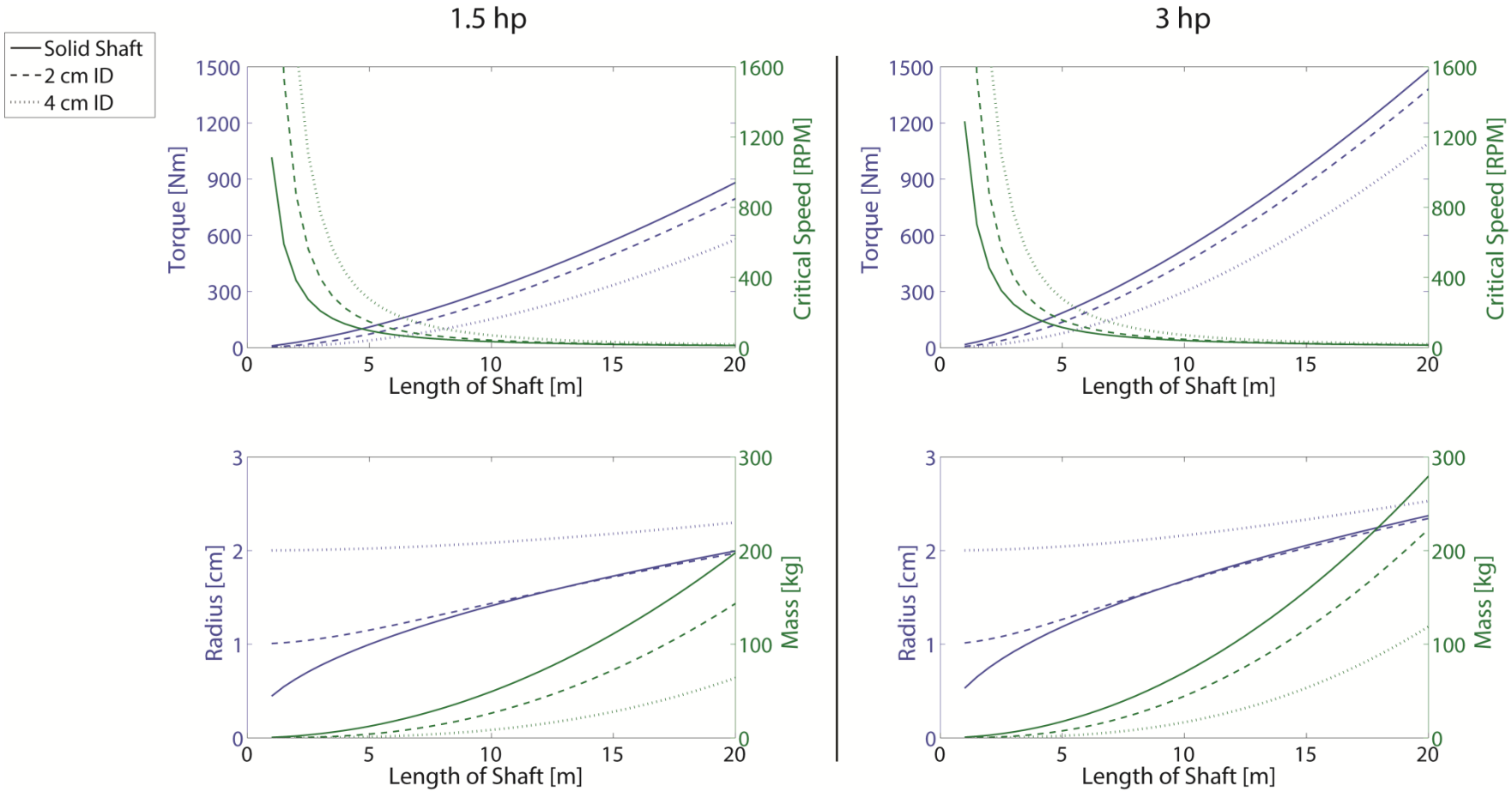

Figure 3.15. Length of shaft versus torque, critical speed, radius, and mass for a shaft connected to a 1.5 hp and 3 hp engine and taking shaft whip into account.

3.2 Fluid Machinery

After the idea of using extended shafts to transit torque from an engine mounted on the surface to a pump down in the well failed to meet all the design requirements, fluid machinery was explored as an alternative. The following fluid machinery options would transfer energy from one fluid to another. A semi-open hydraulic system, jet pump, compressed air motor, and air lift were considered.

3.2.1 Semi-open hydraulic system

A semi-open hydraulic system would pump water at a high pressure and low flow from the surface down to the bottom of the well, where a hydraulic motor would drive a pump to push water back up to the surface (Figure 3.16). The water supply for the system would be provided by a simple bucket, which due to the low volume required for the hydraulic hoses would be enough to get the system started. Part of the return supply would feed back into the bucket to keep the system going. An advantage of this system is that hydraulic hoses are widely available in small towns in India for motorcycle brake lines and tractor hydraulics. Furthermore, hydraulic hoses would be more portable than a flexible or telescoping shaft due to their lighter weight and greater flexibility.

Upon investigation, it was discovered that a semi-open hydraulic system would be inefficient, as energy is converted through four different mechanisms: the initial diesel or kerosene engine converts fuel to mechanical energy at approximately 30% efficiency [57]; a typical hydraulic pump turns this mechanical energy into fluid energy at 90% efficiency [58]; a hydraulic motor converts the fluid energy into mechanical energy at about 65% to 80% efficiency [59]; and finally, the typical pump in India operates at approximately 60% efficiency [60, 61, 62]. At these common efficiencies, the total system would have an energy conversion efficiency of about 10.5% to 14% (excluding pipe losses). In other words, to drive the same pump normally run by a 3 hp engine in the existing system, an engine that could output 5.1 hp would be required in the semi-open hydraulic system. A larger engine means higher capital costs and reduced portability. This quick calculation also assumes that the hydraulic pump can output the exact pressure and flow rate necessary to run the hydraulic motor. When looking up existing products on the market, the author found that a larger capacity pump would be needed to meet the motor's requirements (for example, a 5.25 hp hydraulic pump would be required to run a 3.5 hp hydraulic motor with the rated 1000

psi and 9 gpm; such a pump, with 90% efficiency, would require an engine that could produce 5.83 hp).

In addition to the efficiency problems, the system would be expensive. The hydraulic motor would cost around USD 400 [63] and the hydraulic pump about USD 250 [58]. Hydraulic hoses cost approximately USD 3.50 per foot [64]; for a thirty-foot-deep well, $105 worth of hose would be required. These items would probably cost a little less in India than in the United States, but they would still be more expensive than other pumping systems. These costs, in addition to the cost of the kerosene engine and submersible pump to be coupled to the hydraulic motor, are unaffordable for smallholder farmers. Therefore, this option was eliminated.

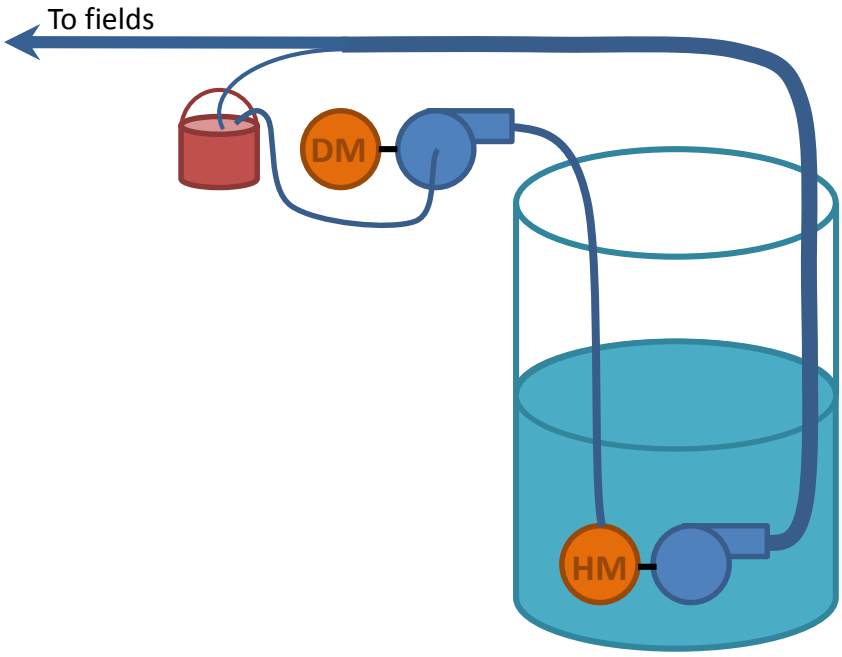

Figure 3.16. Semi-open hydraulic system. "DM" stands for diesel motor, "HM" for hydraulic motor.

3.2.2 Jet Pump

Jet pumps, also called eductors or ejectors, transfer energy from a primary motive fluid to a secondary fluid. The fluids could be gas or liquid. The fluid entering the nozzle of the jet pump creates a pressure difference that entrains the secondary fluid. On a well, a centrifugal pump would push water down and through the jet pump, which would pull in more water as it returns upwards. The total flow would enter the inlet of the centrifugal pump, and the cycle would continue as some of the discharge is redirected back down to the jet pump (Figure 3.17). The advantage of a jet pump is that it would only add one additional piece to the current system. That one piece would

have no moving parts (and thus is simpler, more reliable, and less likely to break) and could be cheaply manufactured using injection molding [65].

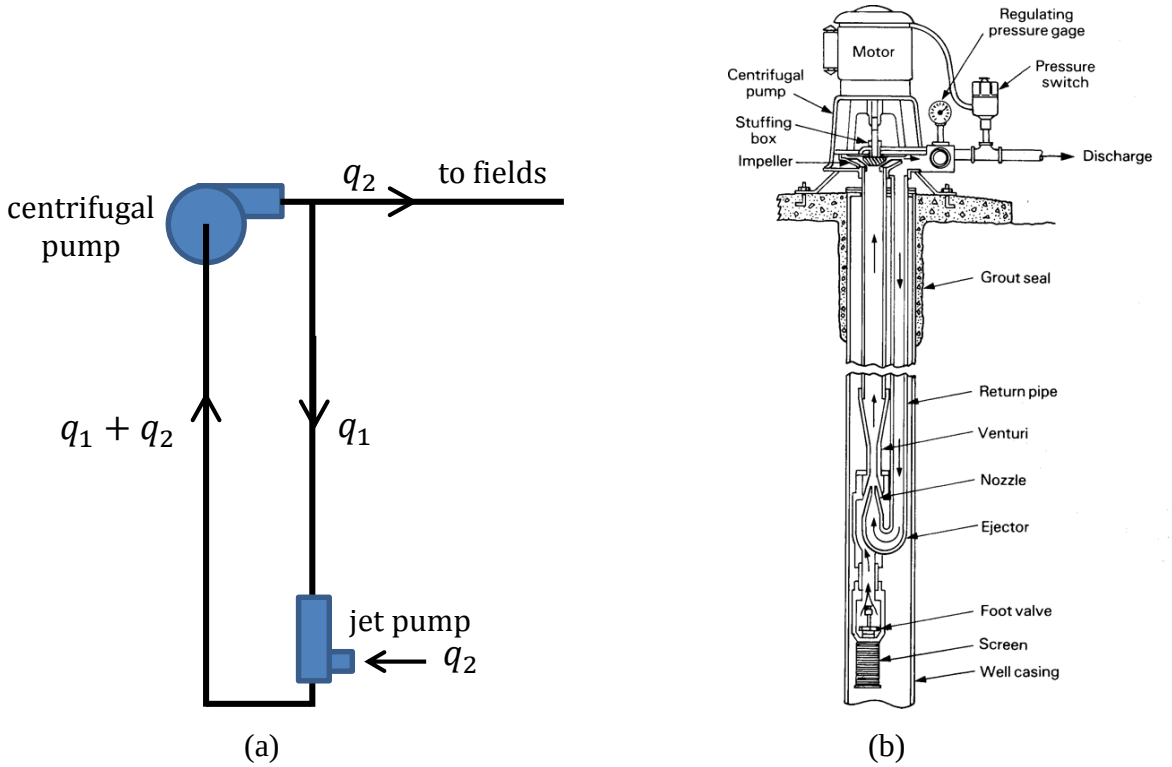

Figure 3.17. Jet pump system. (a) Flow schematic. **[65]** (b) Drawing of system on a well. **[66]**

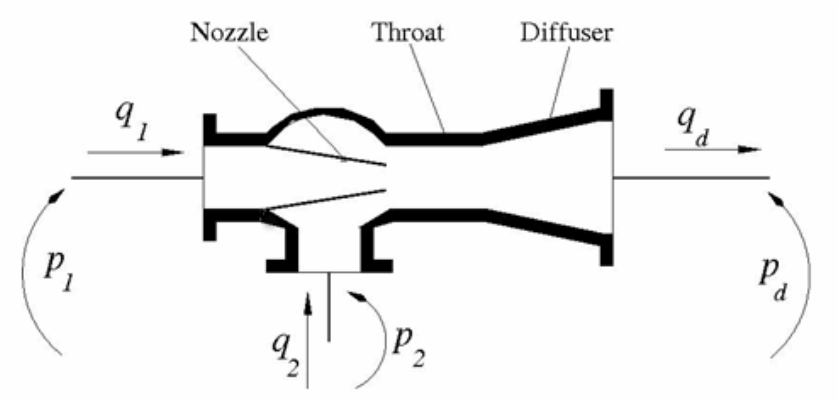

Figure 3.18. Diagram of a jet pump. **[65]**

Jet pump systems, however, are not efficient. The jet pump component itself has a maximum efficiency of approximately 30%. A typical jet pump has an operational *q2*/*q1* (secondary flow rate entrained/primary flow rate entering, as in Figure 3.18) of 0.676 [65]. This

flow ratio means that more primary fluid is needed to push through the pump than secondary fluid obtained from the well. Though the jet pump system does boost suction capabilities of a surface pump, little additional flow rate is gained. The small benefit does not outweigh the loss in portability and extra costs.

3.2.3 Compressed Air Motor

The compressed air motor system would work similarly to the semi-open hydraulic system. Instead of using water to lift water, air is used to lift water. Air is compressed on the surface and pushed down the well to run an air motor that drives a submersible pump. However, this idea was quickly eliminated because it requires multiple times the rated energy of the motor to compress the amount of air needed to run the pump. For example, a 0.9 hp air motor requires 30 cubic feet per minute to run [67]; an air compressor that can deliver 30 cubic feet per minute of air requires a 13 to 18 hp gasoline engine or 5 to 10 hp electric motor [68]. Additionally, prices for an air compressor of this size start around USD 2,500, while the air motor costs between USD 200 and 400. These pieces of equipment would be unaffordable for smallholder farmers.

3.2.3 Air Lift

An air lift, or gas lift, is commonly used to extract oil from wells. The concept is simple: inject air bubbles at the bottom of a rising main to reduce the density of the fluid within the rising main so that the air-water mixture rises to the surface, as shown in Figure 3.19. Because the density of the air-water mixture becomes approximately half the density of water, the fluid rises to approximately twice the distance of the immersed portion of the rising main. If, for instance, the water lies five meters below the surface of the well, the rising main must be at least ten meters long in order to bring water to the surface. Consequently, the well must be dug twice as deep as the lowest possible water level in order to accommodate pumping at all times of the year. During the dry season, when the water falls close to the bottom of the existing well, an air lift would not be able to pump water. The wells would have to be made deeper, which requires both high labor and monetary costs. Furthermore, like the air motor, compressed air would be required. As explained earlier, air compressors are inefficient and expensive. Though the air lift system is attractive due to its simplicity, this system has other disadvantages, including low lift, weak

suction, and unstable, difficult-to-control flow rates [66]. Therefore, the air lift option was eliminated.

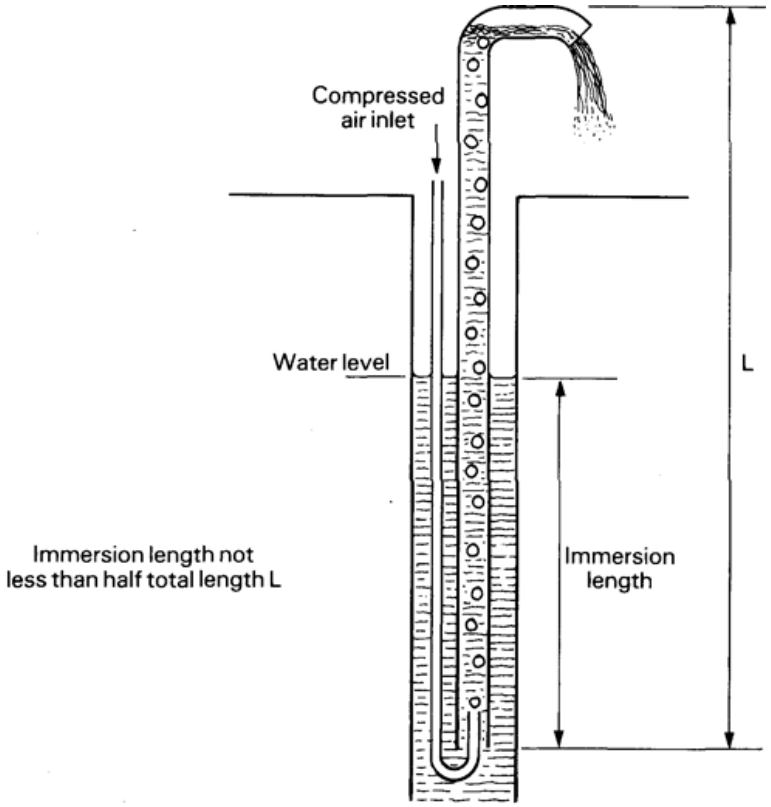

Figure 3.19. Air lift system. **[66]**

3.3 Electricity Generation for Electric Submersible Pump

Mechanically driving a submerged pump either with extended torque transmission or fluid machinery proved infeasible, so we considered devising an off-grid system to power an electric submersible pump entirely using off-the-shelf parts. Electric submersible pumps are widely available throughout India at lower costs than diesel pumps. Electric pumps weigh significantly less than their fuel-powered counterparts, so they easily meet the portability requirements. Additionally, electric cables are much smaller and lighter than shafts or hoses. The challenge, then, was to come up with a cost-effective portable electricity generation solution.

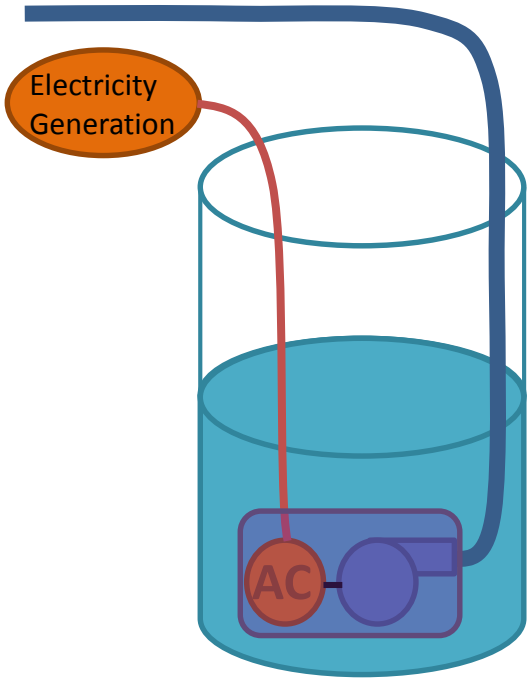

Figure 3.20. Off-grid electric pumping system. "AC" stands for alternating current motor.

Solar panels were quickly ruled out for a number of reasons. The panels would be too large to be portable between wells. Additionally, interviews with farmers revealed that they prefer to irrigate in the late afternoon and early evening in order to prevent water loss due to evaporation. Such timing does not correspond with a solar panel's maximum energy output, which peaks around noon. Expensive batteries would be required to allow farmers to irrigate at the times they prefer. In fact, even with the huge subsidies granted under the Jawaharlal Nehru National Solar Mission (JNNSM), a solar system would be extremely expensive for a smallholder farmer [69]. Furthermore, free electricity for agriculture has led to the rapid depletion of groundwater resources in western India. Imposing a cost on irrigation—such as the cost of diesel—checks the amount of water one would pump. Solar panels would provide energy at no cost to the user, so the farmer would have no incentive to limit his water consumption.

Two other electricity generation options were explored: (a) a small generator running a pump with an AC motor and (b) an engine driving an automotive alternator, which feeds DC current through an inverter to run an AC pump. Anecdotal evidence reveals that farmers use generators to run electric submersible pumps in Gujarat and Madhya Pradesh, but data about performance or prevalence is unavailable [19].

3.3.1 Electric Submersible Pumps

Electric pumps are more efficient than fuel-powered pumps and can produce higher flow rates at lower energy inputs (or, depending on the shape and orientation of the impeller(s), higher heads) [60]. A popular electric open-well model, the 1 hp Kirloskar KOSM-116 available in both single-phase and three-phase AC, is compared to a popular gasoline-start, kerosene-run model, the 1.5 hp Honda WBK15 in Figure 3.21. Although the electric pump is rated at 67% of the power of the kerosene pump, it can attain significantly higher flow rates, which is preferable to farmers, who must pay hourly rental fees as discussed in Chapter 3 and can afford limited pump time. The lower head capacity of the electric pump is not a disadvantage because most wells in Jharkhand in use by farmers are approximately 10 m in depth and would not exceed 15 m.

(Note that borehole pumps—which, in the experience of the author, most people assume the term "submersible pumps" refers to—tend to have the opposite performance of an open-well pump: very high heads with low flow rates rather than high flow rates at low heads [60]. Borehole wells are rare among smallholder farmers in Jharkhand because the hard rock substrate would require expensive drilling equipment [16]. Borehole pumps could still be used in an open well, but they would not be as beneficial, as they produce low flow rates. Likewise, pumps with DC motors are mostly intended to be hooked up to solar panels in a borehole well and produce significantly lower flow rates than their AC counterparts [70].)

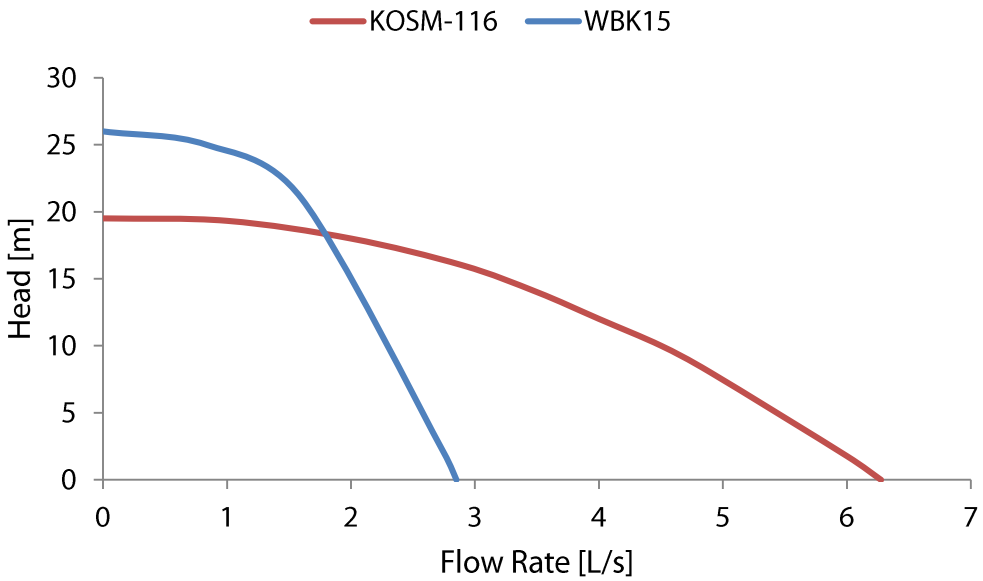

Figure 3.21. The 1-hp Kirloskar KOSM-116 open-well submersible pump compared to the 1.5-hp Honda WBK15 surface pump. **[60, 71]**

3.3.2 Motor Load

In order to size the electricity generator, the electricity requirements—namely, the motor load—must be determined. A motor's rating is not representative of its maximum power requirements. Upon startup, a motor draws significantly higher current than during continuous operation. The initial electric excitement of the electromagnetic rotor results in a back electromotive force (emf) that increases the torque required to turn the rotor. In order to overcome this force and get the motor running, the motor must draw much higher current, called the inrush current [72]. If a motor is to be powered by a generator, it is generally recommended to size the generator capacity two to three times the rated motor capacity in order to handle this inrush current, according to generator retailers in the Ranchi market. However, this measure may be conservative, and it may be possible to push the limits of the system. In order to minimize energy losses and utilize as much available energy as possible, the chosen motor's performance would have to be tested before selecting a generator.

To reduce the maximum electricity requirements, the startup current could be controlled with an inrush current limiting thermistor placed between the AC supply and the motor, as in Figure 3.22. The negative temperature coefficient (NTC) thermistors provide resistance on startup in order to limit the current, thereby allowing a soft start and protecting the equipment. Once the thermistor gets hot, its resistance decreases until it is close to zero, so that energy is not lost during continuous operation. An example of thermistor behavior is given in Figure 3.23. An NTC thermistor can significantly reduce the startup current but increases the time required for the motor to bring down its current load to the continuous rated load [73]. By varying the starting resistance of the thermistors using a resistance decade box, the minimum current required to overcome the high torque load caused by the back emf (in other words, to start the motor) could be found.

The size of the motor, thermistor resistance, and electricity generator would all have to be matched after electricity demands are determined. For example, tests to determine the maximum current load with an NTC thermistor could be run on a variety of pumps plugged into the grid. To use a small 1.5 hp engine plus alternator or 1 kW generator, pumps rated at 1 hp, 0.75 hp, and 0.5 hp should be tested, and the largest pump whose electricity requirements could be met by small generation system selected.

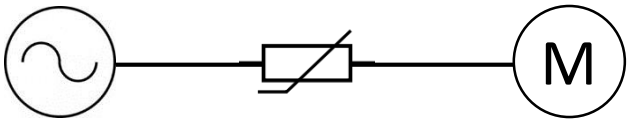

Figure 3.22. Circuit with an AC supply, thermistor, and motor.

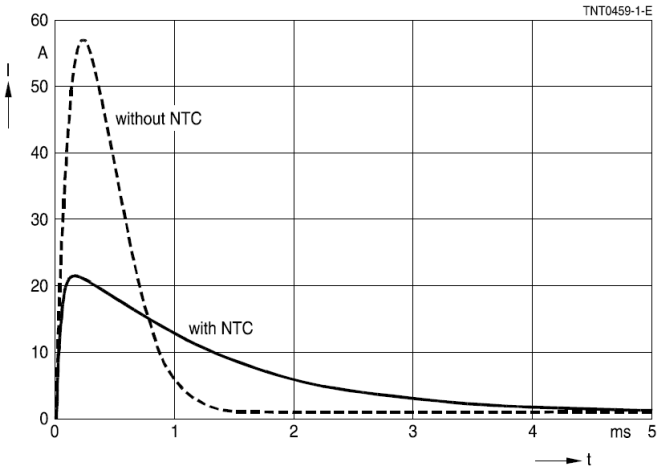

Figure 3.23. Comparison of the current of a motor with and without an NTC thermistor. **[73]**

3.3.2 Electricity Generation Options

3.3.2.1 Household Back-up Generators

Generators are commonly used in businesses and sometimes households to provide backup electricity during power outages. Honda is one of the most popular brands for small generators and manufactures models that run on kerosene and range from 350 W to 2.1 kW. These generators weigh between 21.5 kg (350 W model) and 102 kg (2.1 kW model) and produce 210 V AC electricity [74]. The system, illustrated in Figure 3.24, is much simpler than a system employing an automotive alternator (discussed in the next section, Section 3.3.2.2 Automotive Alternators), but it is heavier—limiting the system's portability—and more expensive. A generator could cost up to INR 60,000, while an engine with an automotive alternator might cost around INR 15,000, according to a machine retailer in the Ranchi market. This option was thus eliminated due to the high costs and heavy weight.

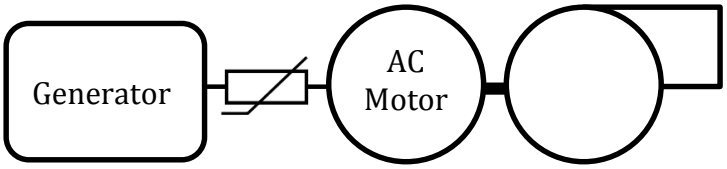

Figure 3.24. Layout of the potential generator-powered prototype.

3.3.2.2 Automotive Alternators

The advantages of using an automotive alternator over a household back-up generator are that they are significantly lighter and already very commonly in use. The much lighter weight (approximately 6 kg [75] versus 75 kg [74] for a household back-up generator) makes this option more portable. Additionally, because every vehicle found in rural India—motorcycles, tractors, and trucks—use alternators, it is likely that local mechanics would know how to repair alternators in need of maintenance and find replacement alternators when necessary.

Automotive alternators, unlike the common household backup generators, do not employ permanent magnet rotors. Instead, they utilize electromagnetic rotors. While electromagnets are more lightweight than permanent magnets, they must be electrically excited in order to induce a magnetic field. Excitation requires a source of electricity, such as a battery, so an automotive alternator, even if spun by a motor, cannot cold-start electricity generation. Alternators output 12 V DC electricity, because they are generally used to charge a battery that runs the electronics of a vehicle. Many alternators utilize this same battery for initial excitation, but some alternators can store residual electricity in their voltage regulators [76].

A small engine size, such as the 1.5 hp Honda GK100, would be employed to run the alternator due to the greater availability of smaller capacity alternators in rural India (choosing a larger engine size would result in greater energy losses through a smaller alternator) and the lighter weight necessary for portability. Due to the poor quality of electricity and the widespread proliferation of open wells, several low-power single-phase AC openwell submersible pumps are available on the Indian market (such as the Kirloskar KOSM-116, discussed above in Section 3.3.1). The availability of single-phase pumps is convenient because the weight and cost of single-phase AC components is significantly less than that of three-phase AC components. DC pumps, as mentioned earlier, greatly underperform compared to AC pumps.

The alternator would have to be close-coupled to the engine, because maintaining tension in a serpentine belt over time may be difficult in the rough conditions to which the system may be subjected when being lugged from well to well in rural India. Furthermore, the belt and pulley would add moving parts that would increase complexity of the system. A clamp-on shaft coupling would be required to attach the alternator shaft to the engine shaft. Because the continuous duty point of the Honda GK100 engine runs at 3600 rpm, a popular Delco 12SI alternator rated at 78 A would produce about 70 A, as shown in Figure 3.25. (The actual speed of the engine shaft would depend on the torque load, but since torque load data is unavailable for alternators—it is generally not included in mechanical specifications—it is assumed that the engine would operate at its continuous duty point.) This speed can be increased without belts and pulleys with a gearbox, but gearboxes in India are very expensive and the small gain in current output would not be worth the cost.

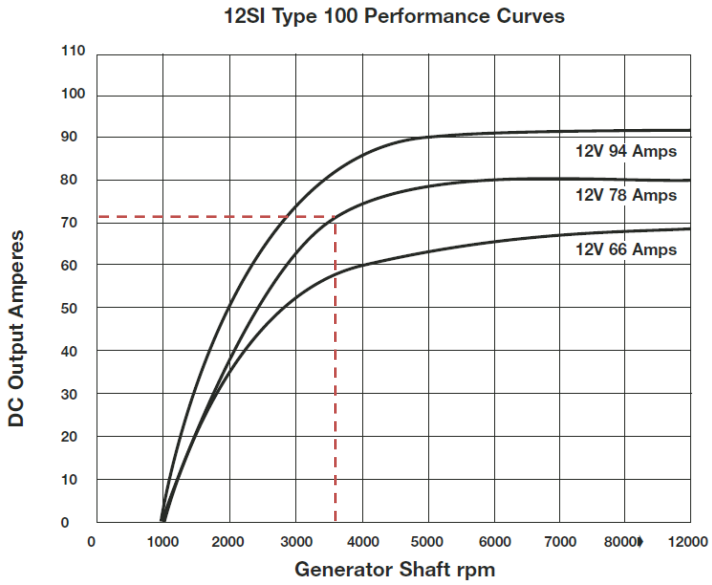

Figure 3.25. Performance of Delco Remy 12SI alternator series. The 78A alternator would be driven at 3600 rpm. **[75]**

Actually, the alternator's stator windings, with three stator leads that connect to three wires, generate three-phase AC current when the excited electromagnetic rotor spins. This AC current is then directed through a rectifier that converts the AC into DC, and the voltage regulator ensures that the DC exits the unit at 12 V (see Figure 3.26 for the circuit diagram). The three wires could bypass the rectifier and regulator, or the rectifier and regulator could be removed from the unit, in order to output three phase AC power [77]. However, the rotors of small alternators such as the

Delco Remy 10SI and 12SI series are equipped with fourteen poles [75]. With fourteen poles, 514.3 rpm is required to generate the 60 Hz of frequency necessary to run the motor, according to the equation $N = 120f/P$, where N = rpm, f = frequency, and P = number of poles. The alternator cannot generate electricity below 1000 rpm [75]. Therefore, running the pump motor with three-phase AC directly from the alternator would not work, and instead the 12 V DC output from the rectifier and regulator would have to suffice.

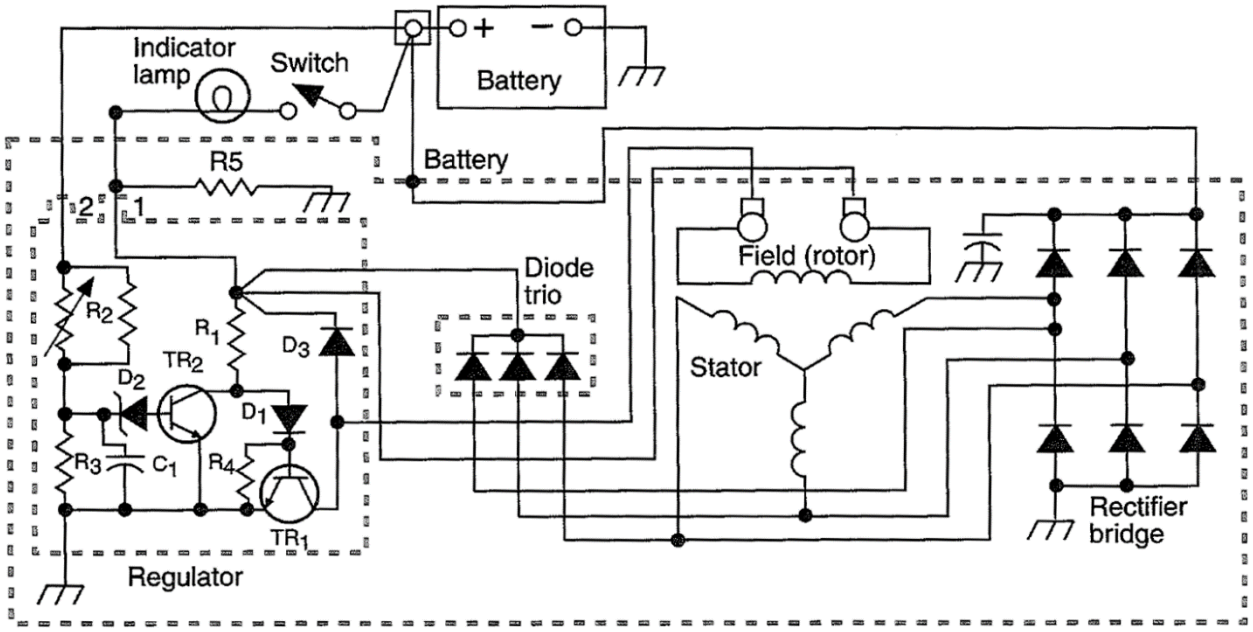

Figure 3.26. Circuit diagram for an automotive alternator. **[77]**

To drive the system using the alternator's DC output, an inverter would be necessary to convert the 12 V DC current into single-phase AC. Solar panels and wind turbines, which generate DC electricity, must employ high-quality inverters, especially if the systems are grid-tied. These inverters typically produce a pure sine wave, can handle voltage fluctuations, and have efficiencies above 95%. However, these inverters are quite large and expensive. At about 40 lb and over USD 1000 [78], they are neither portable nor affordable options for smallholder farmers. Instead, the type of small inverter drivers plug into the cigarette lighters of their cars to charge electronics on-the-go might be a feasible alternative. These inverters are much cheaper, at under $100, and smaller, at about five pounds. However, they produce a modified square wave and experience a lower efficiency at 80 to 85% [79, 80, 81].

A motor running on a modified square wave, rather than a pure sine wave, will consume energy less efficiently and often becomes hotter, thereby reducing the lifetime of the motor if frequently run on a modified square wave [82, 83]. However, the performance of a motor run on a modified square wave could vary widely and depends on the specific components in use. A prototype employing a car inverter would have to be built and tested to determine the impact of the modified square wave on motor performance. The huge savings in costs and weight of the car inverter might still outweigh the reduction in motor efficiency compared to a system with a pure sine wave inverter.

A potential prototype design is depicted in Figure 3.27. The prototype would consist of a 1.5 hp Honda GK100 engine, a 78 A Delco 12SI series alternator (Figure 3.25), a DC-to-AC car inverter, an NTC thermistor, and a single-phase motor connected to an openwell submersible pump. The alternator requires a battery to excite the electromagnet, and this battery would have to be recharged by a small amount of current directed away before the inverter. A resistor along that path would limit the charging current and ensure most current continues on toward the pump's motor. The size of the motor and initial resistance rating of the NTC thermistor would have to be matched to the power supply after conducting some tests to determine the maximum current load with inrush limiters of each pump option, as described in Section 3.3.2 Motor Load.

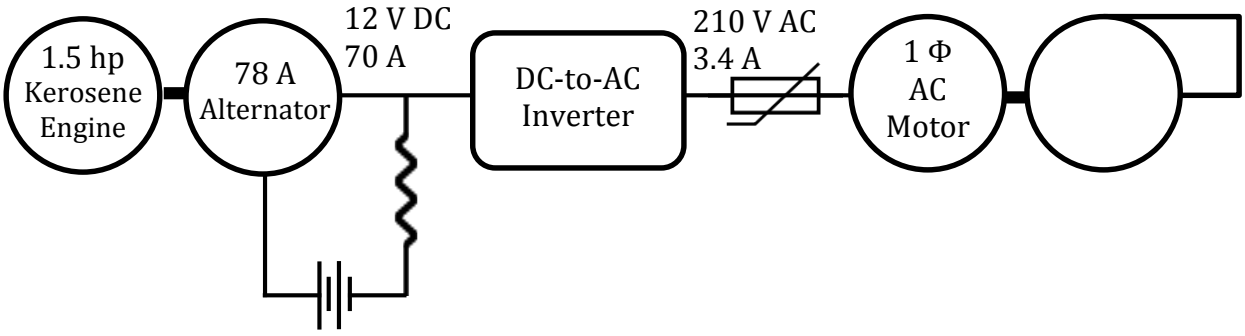

Figure 3.27. Layout of prototype components.

Although it had been planned to build and test this prototype, ultimately it was decided to abandon this system. PRADAN, a non-governmental organization with thirty years of experience working with farmers in rural India, said that the farmers would not be willing to spend the additional money on the extra components such as an alternator and inverter when they have an engine and centrifugal pump. It turns out that farmers already lower their pumps when the water

level falls below the reach of suction capabilities. The primary benefit of the electric system is to eliminate suction head, but the farmers have figured out how to do this without incurring additional capital costs. Therefore, it was decided not to move forward with this system.

3.4 Chapter Conclusions

Many technology options, including flexible shafts, telescoping shafts, fluid machinery such as hydraulics, jet pumps, air motors, and air lifts, and electricity generation, were investigated to run a submersible centrifugal pump with a surface-mounted fuel-powered engine. The results are summarized in Table 3.1. Although some of these alternatives would perform better than the existing system and produce higher flow rates, which farmers desire to cut down hourly rental costs, these technologies faced other challenges. Many of these technologies ended up being too heavy to be portable to be carried from well to well on a bicycle, would be difficult to maintain or replace in rural India, and/or required expensive parts.

Ultimately, none of the options explored in this chapter would be utilized, as they did not meet all the design requirements. The goal of the work in this chapter had been to modify the existing centrifugal pump system, but until the author actually returned to India, trying a completely different type of system had not yet been seriously considered. As discussed in the next chapter, a kind of irrigation technology that does not employ a centrifugal pump would be prototyped and tested.

Table 3.1. Results of investigation into pump system options.

Option	Energy Efficiency / Flow Rates	Portability	Maintainability and Part Replaceability	Conclusion
Flexible shaft	Higher / Higher	Large spool required	Sealing is difficult due to the gaps between wires; replacement parts not readily available	Too large radius of curvature to be stored or transported on a reasonably-sized spool
Telescoping shaft, nested	Higher / Higher	Heavy	Could get clogged; if one piece breaks, entire system rendered useless	Too difficult to repair and too heavy
Telescoping shaft, segmented	Higher / Higher	Heavy	Identical easily-replaceable components	Too time-consuming to reassemble at each well and too heavy
Semi-open hydraulic system	Lower / Higher	Many components	Hydraulic components available for motorcycles and agricultural equipment	Too expensive and inefficient
Jet pump	Lower / Higher	Double the hose length required; extra component	Ejector has no moving parts so less likely to break	Too inefficient
Compressed air motor	Lower / Higher	Heavy	Local mechanics are familiar with air compressors	Too inefficient and expensive
Air lift	Lower / Lower	Rising main is usually installed, so not portable	Local mechanics are familiar with air compressors	Too inefficient and expensive
Generator + electric pump	Lower / Higher	Heavy	Local mechanics are familiar with generators	Too heavy and expensive
Automotive alternator + electric pump	Lower / Higher	Best power/weight ratio (26.4 – 42 W/kg)	Local mechanics are familiar with alternators	Too expensive

Chapter 4: Designing and Prototyping a Hybrid Motorized-Manual Rope Pump

4.1 Introduction

After some discussions with PRADAN, the NGO supporting this research in Jharkhand, it was decided to pursue a hybrid manual and engine-driven version of the rope pump, which is usually only human-powered. The other options explored, as described in previous chapters, did not meet the design requirements described in Chapter 2 for various reasons; the other options were not adequately portable, efficient, maintainable, or affordable, or a combination of any of these. While the rope pump is not a portable pumping system, it meets the other requirements, could be made semi-portable, and offers other advantages, such as easy maintenance and the flexibility to be used for both domestic and agricultural purposes.

The concept of a rope pump, as shown in Figure 4.1, is simple: a rope pulls pistons, or washers, through a pipe, lifting packets of water between the pistons. The rope pump is essentially a positive displacement pump. The rope can be moved with a wheel equipped with a hand crank above the well. The efficiency will be governed by the fit of the piston inside the pipe. If the seal is too tight, friction reduces efficiency. If the gap is too large, leakage reduces efficiency. Ultimately, a study is needed to determine the best type of piston to maximize efficiency.

PRADAN was inspired by the International Development Enterprises – India (IDE-India)'s work with manual rope pumps in the state of Odisha. IDE-India has installed manual rope pumps for irrigation, but in practice the pumps have been more widely used for drinking water and other domestic water purposes. The rope pumps have been popular with women because they are more reliable and easier to repair than the much more common reciprocating piston hand pumps, such as the India Mark II (Figure 4.2), and are less labor-intensive to use than lowering and raising a bucket. However, farmers have not taken to using these pumps for irrigation. PRADAN emphasized that manual irrigation pumps of all types have largely been a failure in India (though they have been moderately successful in some other countries). To irrigate even a small plot of land requires a large volume of water, and manually pumping that amount of water requires a

sustained effort that can be exhausting and take time away from other activities. PRADAN has witnessed that smallholder farmers in India would rather not irrigate at all or spend more money using a fuel-powered pump than expend time and energy on running a manual pump.

PRADAN identified that the rope pump has great potential for irrigation if mechanized, due to its low cost, easy maintenance, and readily-available replacement parts. In fact, PRADAN has seen farmers in West Bengal, frustrated with the manual version of the rope pump, try to add an engine to the system—but simply attaching an engine to a system designed to be operated by hand is not well-engineered, efficient, or safe. In the new system, the engine would ideally be removable, as theft is a problem in many villages and farmer lock up their machines when not in use. In order to allow for both domestic water use, which neither requires high volumes of water nor commands the willingness of families to spend money on fuel, and irrigation, the author decided to design a rope pump to be used both with an engine and a hand crank.

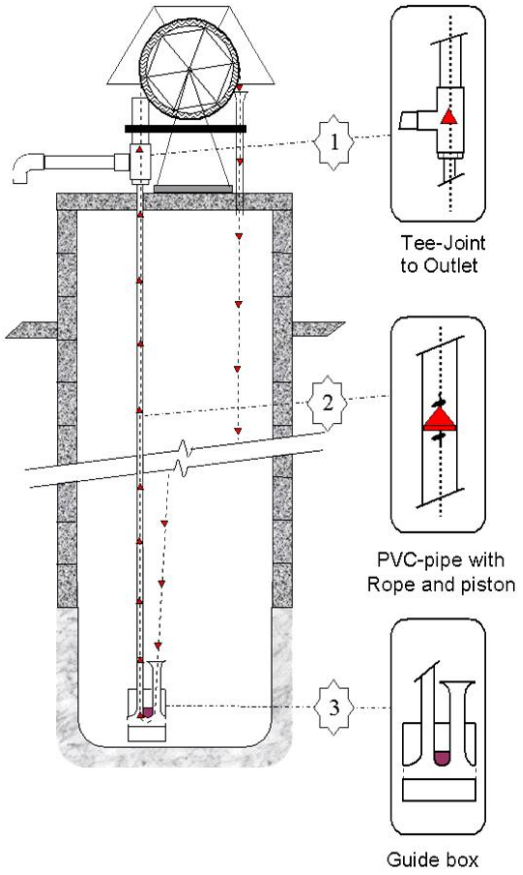

Figure 4.1. A typical rope pump system on a hand-dug open well. **[84]**

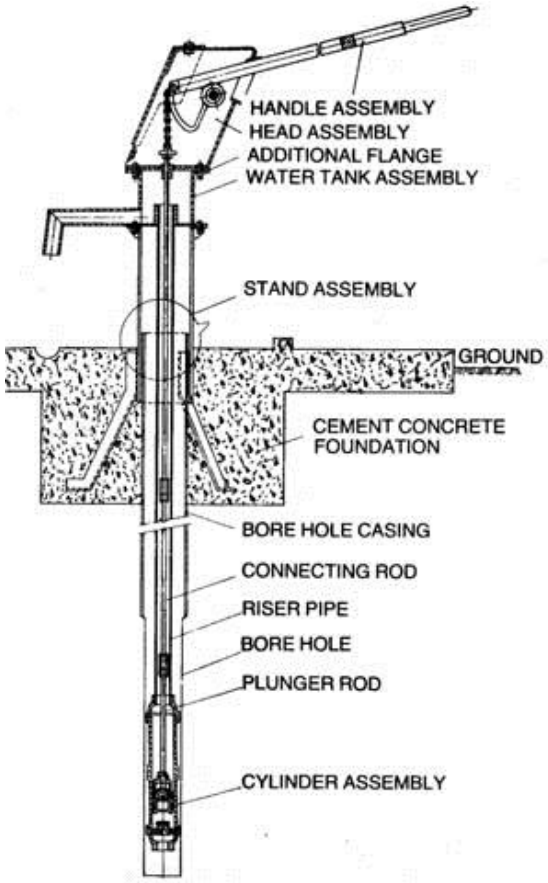

Figure 4.2. The India Mark II, a reciprocating piston pump, is the most popular hand pump in the world. **[85]**

4.2 Evolution of the Rope Pump

The concept of the rope pump, historically known as a chain pump, originated thousands of years ago. The first evidence of the pump has been found in a Babylonian relief from around 700 BC. The relief illustrates a chain of pots ascending full of water and descending empty. If the famous Hanging Gardens of Babylon did indeed exist, it is believed that they may have been irrigated by chain pumps and/or Archimedes' screw pumps. Remains of ancient bilge pumps employing the chain-of-pots concept have been discovered in the ruins of ships commissioned by Roman emperor Caligula in Lake Nemi from 44 to 54 AD. Greek historian Philo of Byzantium and Roman historian Vitruvius wrote of such pumps earlier, in the third century BC and around 30 BC, respectively [86].

A different type of chain pump was developed in China as early as the first century AD. Known as a *long gu che* ("dragon spine machine") or *fan che* ("turnover wheels"), the pedal- or bullock-powered pump utilized square pallets to move water through a slanted flume (Figure 4.3a and b). The Chinese also invented hydropower chain pumps by employing a water wheel to drive

the chain (Figure 4.3c). These pumps drew water from surface sources such as rivers, ponds, and man-made moats to irrigate agricultural fields, provide urban water supply, and water the gardens of palaces [86].

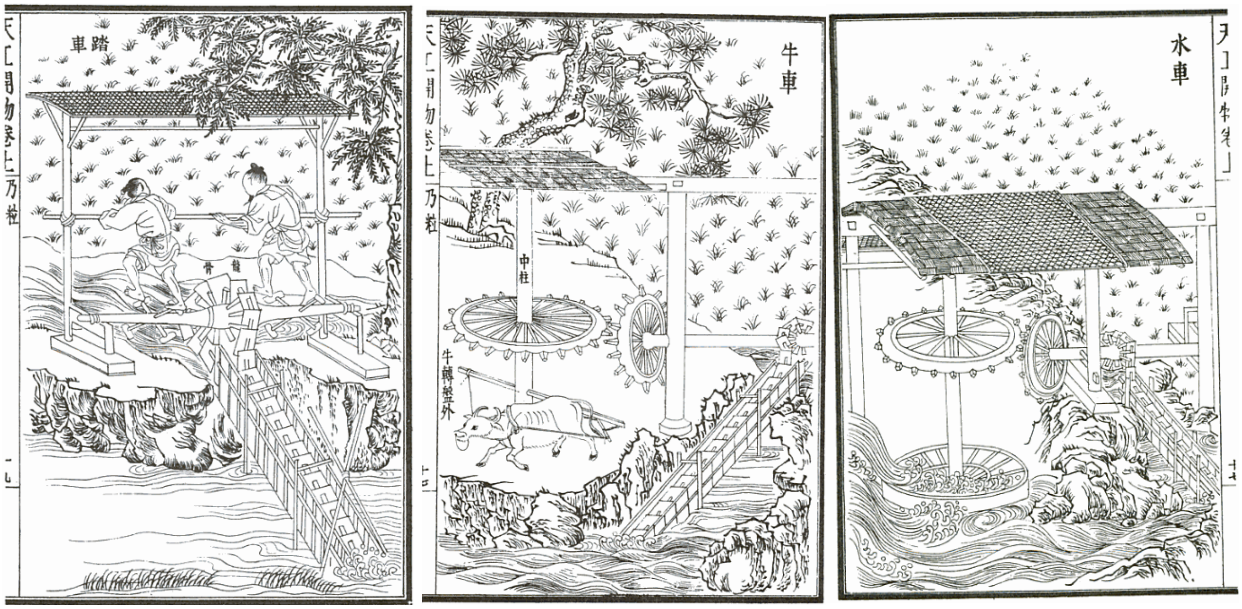

(a) (b) (c)

Figure 4.3. Chinese square pallet chain pumps, as illustrated in Song Yingxing's *Thien Kung Khai Wu* (1637). (a) Pedal-powered dragon spine pump. (b) Ox-pulled dragon spine pump. (c) Hydraulic-powered dragon spine pump. **[86]**

During the Islamic Golden Age (eighth to thirteenth century), engineers designed the *saqiya*, a complex man- or animal-powered chain-of-pots pump that employed gears and a mechanical flywheel. Across the Middle East, camels were utilized to run the *saqiya*. A two-stage pump was built at Joseph's Well in Cairo, pulling water from a depth of 297 feet, to supply water to the Saladin Citadel in the twelfth century AD (Figure 4.4a). In the same century, Muslim inventor Al-Jazari worked on increasing the efficiency of the *saqiya*, constructed a chain pump driven by a water wheel, and described a series of water-lifting machines in use in the medieval Islamic world in a detailed manuscript (one of these is shown in Figure 4.4b). A pump similar to Al-Jazari's inventions was in use for many centuries in Damascus from the thirteenth century onwards [86].

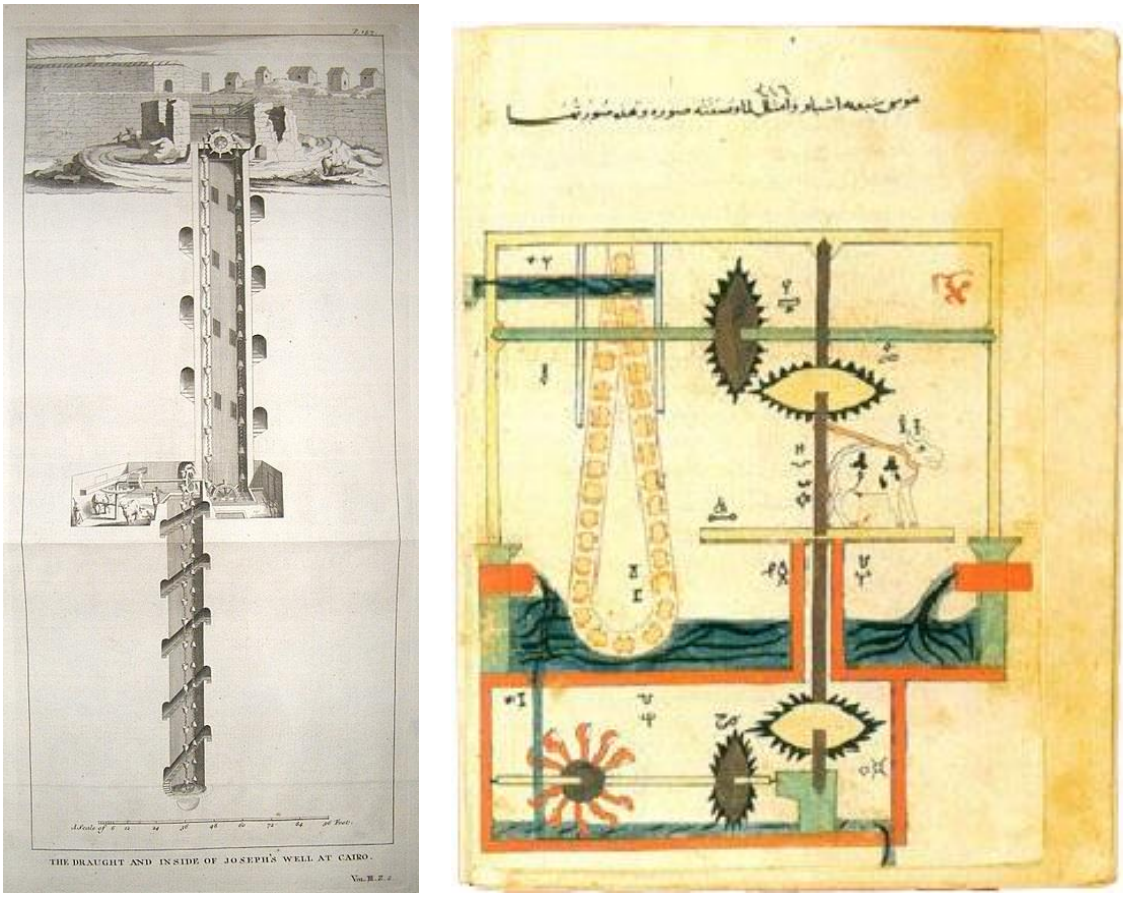

(a) (b)

Figure 4.4. Islamic *saqiya* pumps. (a) Two-stage chain pump at Joseph's Well in Cairo. (b) Al-Jazari's *saqiya* chain pump. **[86]**

During the Renaissance in the fifteen and sixteenth centuries, Italian scientists, including Leonardo da Vinci, described variations of the chain pumps in their manuscripts. Georgius Agricola, a German mineralogist, and Agostino Ramelli, an Italian engineer, explained that the Central European mining industry at the time utilized horse-driven rope pumps that used wooden blocks for pistons. In the eighteenth century, the British Navy employed manual chain pumps as bilge pumps in warships. Rope pumps largely fell into disuse with the rise of the steam engine [87].

The rope pump would be revived after Mao Zedong and the Chinese Communist Party (CCP) rose to power in China. Mao's vision of a modern China involved a transition from an agricultural to an industrial economy. To accomplish this goal, he instituted the Great Leap Forward campaign, which abolished private land ownership, collectivized agriculture, and forced unskilled farmers to work in steel production rather than focus on farming. The failed agricultural

policies of the Great Leap Forward from 1958 to 1961 led to the Great Chinese Famine, during which between 20 and 40 million people starved to death. As part of the relief and recovery efforts, the CCP re-invested in agriculture and agricultural technology. The "liberation pump," an animal-powered chain-and-washer pump illustrated in Figure 4.5, was promoted to "liberate" the agrarian proletariat from drought and hunger (such rhetoric was much in line with the CCP's propaganda). Between two and three million liberation pumps were installed during the 1960's, and many of these still remain in use throughout rural China today. Liberation pumps have since become popular in neighboring Indochinese countries such as Vietnam and Thailand as well [66].

In the 1970's, R. Van Tijen, an engineer at Demotech, a company in the Netherlands, modernized the hand-powered version of the rope pump using new materials such as PVC and polyethylene. Demotech installed their first rope pump in Burkina Faso in 1976. Demotech's rope pump is not patented but is an open source technology that can be built, distributed, or modified by anyone [88]. The pump rose to prominence as part of the relief efforts after Hurricane Mitch in Nicaragua and El Salvador in 1988 as a means to restore water supply. A private company called Bombas de Mecate SA was founded for the purpose of disseminating these pumps throughout Nicaragua [87]. As of 2010, Nicaragua had more hand-powered rope pumps than any other country in the world, with about 70,000 [89]. Bombas de Mecate SA also manufactures an engine-powered rope pump, the Bomegas, but it is significantly less popular than their hand pump. The 1 hp Bomegas models can pump 40 – 50 L/min at 10 m depth [90]. The Practica Foundation has also developed a motorized rope pump, which can produce a flow rate of 120 L/min with a 2 hp engine at 10 m [91]. Maya Pedal, a Guatemalan NGO, manufactures bicycle-powered rope pumps, which they call Bicibombas [92]. PumpAid, a United Kingdom-based NGO, installs manual rope pumps, named Elephant Pumps for their appearance, throughout Zimbabwe, Malawi, and Liberia. In 2010, approximately four million people worldwide were using 100,000 rope pumps [89]. An example of the modern-day hand-cranked rope pump is depicted in Figure 4.6.

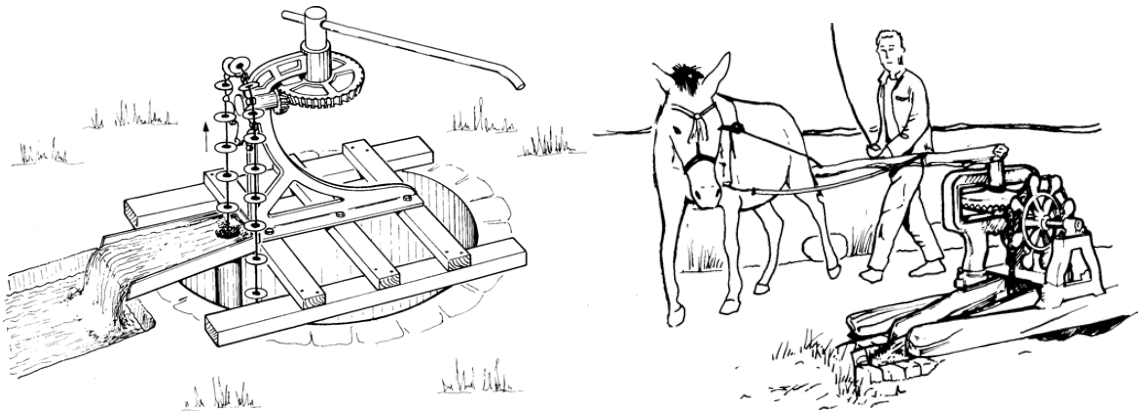

(a) (b)

Figure 4.5. Chinese liberation pump. (a) Isometric view. (b) In use, driven by a donkey. **[66]**

Figure 4.6. Manual rope pump in use in Mozambique. **[93]**

While rope pump technology is ancient and still in use worldwide, the author could not find a version of the pump designed to be powered by multiple mechanisms. The innovation presented in this research is to create a rope pump that can be run in two modes, both by an engine and by hand.

4.3 Model of a Rope Pump

In order to determine the dimensions of each component of the rope pump system, the system was modeled in MATLAB before fabrication. For this model, it was assumed that the volume and weight of the pistons and rope are negligible compared to the volume and weight of the water being lifted. It was also assumed that the PVC pipe maintains a constant inner diameter, even though in reality there are slight variations as a result of the manufacturing process. The system analyzed is depicted in Figure 4.7.

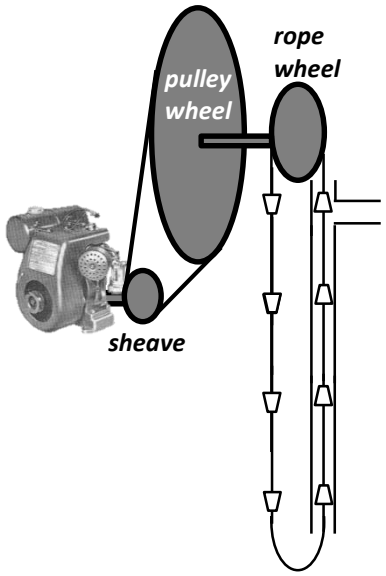

Figure 4.7. A simplified, not-to-scale illustration of the motorized rope pump system.

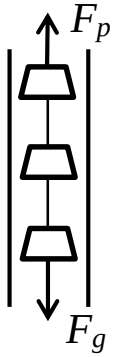

Figure 4.8. Force balance of the rope pump

A force balance on the rope pump is given in Figure 4.8. In order for the pump to lift the water at constant speed, the force exerted by the pump must be equal to the weight of the water.

$$F_p = F_g \quad \text{(Eq 5.1)}$$

where

F_p	=	force exerted by the pump	[N]
F_g	=	force of the water due to gravity	[N]

The weight of the water the pump must lift is

$$F_g = \rho g h A_{pipe} \quad \text{(Eq 5.2)}$$

where

ρ	=	density of water	[kg/m^3]
h	=	head	[m]
A_{pipe}	=	cross-sectional area of the pipe	[m^2]

The density of water is assumed to be 1000 kg/m^3. The area of the pipe is

$$A_{pipe} = \pi \mathrm{r}_{\mathrm{pipe}}^2 \quad \text{(Eq 5.3)}$$

where

r_{pipe}	=	inner radius of the pipe	[m]

The torque load on the rope wheel due to the weight of water at constant angular velocity is

$$\tau_{ropewheel} = F_p r_{ropewheel} \quad \text{(Eq 5.4)}$$

where

$\tau_{ropewheel}$	=	torque load on the rope wheel	[Nm]
$r_{ropewheel}$	=	radius of the rope wheel	[m]

Because the rope wheel sits on the same axle as the pulley wheel, the angular velocity and torque of the pulley wheel are equal to the angular velocity and torque of the rope wheel:

$$\tau_{ropewheel} = \tau_{pulleywheel} \quad \text{(Eq 5.5)}$$

where

$\tau_{pulleywheel}$ = torque load on the pulley wheel [Nm]

$$\omega_{ropewheel} = \omega_{pulleywheel} \quad \text{(Eq 5.6)}$$

where

$\omega_{ropewheel}$ = angular velocity of the rope wheel [rad/s]

$\omega_{pulleywheel}$ = angular velocity of the pulley wheel [rad/s]

Because the pulley wheel is connected to the engine via a v-belt (Figure 4.7), the linear velocity of the pulley wheel must be the same as the linear velocity of the sheave on the engine's shaft. Therefore, the angular velocities of the pulley wheel and sheave are inversely proportional to their respective diameters. Thus

$$\omega_{pulleywheel} = \frac{\omega_{eng} d_{sheave}}{d_{pulleywheel}} \quad \text{(Eq 5.7)}$$

where

ω_{eng} = angular velocity of the engine shaft [rad/s]

d_{sheave} = diameter of the sheave on the engine shaft [m]

$d_{pulleywheel}$ = diameter of the pulley wheel [m]

Since power is a product of the angular velocity and torque and the angular velocities are inversely proportional to their diameters, the torques of the pulley wheel and sheave on the engine shaft must be proportional to their diameters.

$$\tau_{pulleywheel} = \frac{\tau_{eng} d_{pulleywheel}}{d_{sheave}} \quad \text{(Eq 5.8)}$$

where

τ_{eng} = torque of the engine shaft [Nm]

The linear velocity of the outer edge of the rope wheel, and therefore of the rope, is

$$V_p = \omega_{ropewheel} r_{ropewheel} \quad \text{(Eq 5.9)}$$

where

V_p	=	linear velocity of the rope	[m/s]

The critical velocity V_c is the minimum velocity of the rope required for the pump to be able to lift the water. In order for the pump to successfully operate, the condition of $V_p \geq V_c$ must be met. This critical velocity was determined by Smulders and Rijs (2006) by analyzing the gap leakage between the piston and the pipe wall, as shown in Figure 4.9 [87].

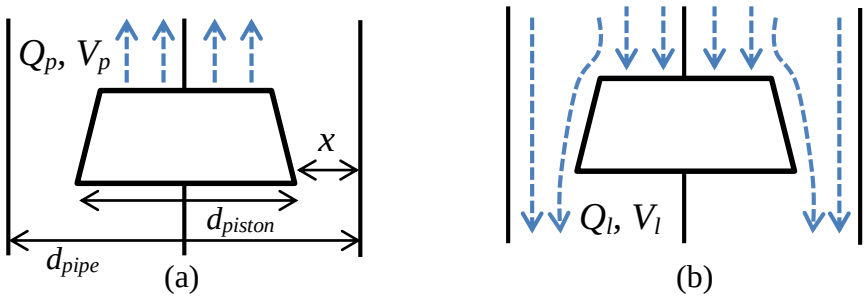

Figure 4.9. Streamlines representing the movement of water inside the pipe from the reference frames of (a) the outside world and (b) the rope and piston. x is the gap width, Q and V_p are the flow rate and velocity, respectively, of the water pushed up by the piston, and Q_l and V_l are the flow rate and velocity of the leakage between the piston and the pipe wall. The drawing is not to scale, and the gap is exaggerated.

The critical velocity as derived by Smulders and Rijs (2006) is [87]

$$V_c = \frac{4x}{d_{pipe}} \sqrt{\frac{2gh}{Ln}} \quad \text{(Eq 5.10)}$$

where

x	=	gap between piston and pipe wall	[m]
L	=	length of the pipe	[m]
n	=	number of pistons per unit length	[number/m]

The actual flow rate Q_p [m^3/s] is thus the ideal flow rate minus the leakage flow rate, and can be defined as

$$Q_p = \pi r_{pipe}^2 (V_p - V_c) \quad \text{(Eq 5.11)}$$

The pump's power output W_{out} [W] is calculated as

$$W_{out} = \rho g h Q_p \quad \text{(Eq 5.12)}$$

Efficiency η is defined as

$$\eta = \frac{W_{out}}{W_{eng}} \quad \text{(Eq 5.13)}$$

where

W_{eng} = engine power output [W]

The Vijay Villiers C12 engine was selected for the prototype because it is the most commonly-used engine in rural Jharkhand, according to PRADAN and local engine retailers. The engine was assumed to always perform at the same operation point of 1.1 kW at 3000 rpm and 3.5 Nm torque. While this assumption is likely not true, as normal engine behavior responds to the load on the engine, this assumption had to be applied due to lack of information. Specifications available for the most popular engines in Jharkhand include only this one operation point. When interviewed, engine retailers as well as manufacturers could not provide any further specifications; they could not provide performance curves or even a range of operating speeds. The maximum torque load the engine can handle is thus unknown. The system was designed for the maximum torque load—that is, at the deepest head—to be equal to the torque at the single operation point. As a result, the rope pump experiences inefficiency at lower heads, as available torque remains unutilized and the maximum speed is assumed to be the speed at the single point.

The pump had to be designed using standard Indian pipe and pulley wheel sizes. In some countries, the pistons on manual rope pumps are made using injection-molded polypropylene or polyethylene [94]. However, in order to reduce fabrication costs and time, it was decided to make the pistons out of solid nylon on a lathe. These stoppers, at 31 mm, fit nicely into a nominal 1 ¼" PVC pipe, the inner diameter of which measured at 32.5 mm, for a gap distance of 0.75 mm on each side of the stopper, as shown in Figure 4.10.

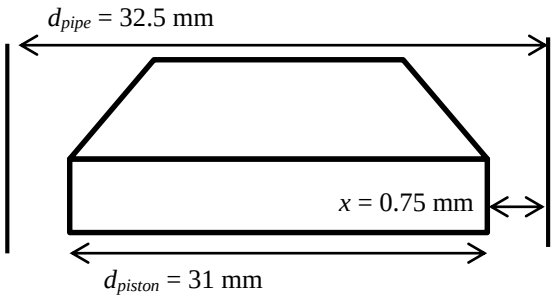

Figure 4.10. Dimensions of piston inside the PVC pipe.

Using pipe radius r_{pipe} = 32.5 mm, maximum head h = 10 m, and available engine torque τ_{eng} = 3.5 Nm (again, it was assumed this torque was not variable) in the above set of equations, it was determined that the best standard diameters for the engine shaft's sheave, the pulley wheel, and the rope wheel are 2.5 inches, 24 inches, and 8 inches, respectively ("best" here indicates the highest flow rate). The resulting flow rate and efficiency at each head for a varying number of pistons per meter are given in Figure 4.11 and Figure 4.12. Originally, the prototype employed two pistons per meter (tied onto the rope at intervals of 0.5 m), because two pistons per meter provided the greatest jump in flow rate without too much added material cost (though there is very little difference in energy efficiency). However, as discussed later in Section 4.6 Troubleshooting, the prototype had to be changed to accommodate five pistons per meter (intervals of 0.2 m) so that a piston could always be grabbed by the small pulley, thereby reducing slippage. As can be seen in Figure 4.13, the rope pump should give a higher flow rate than both the actual performance and rated performance of the currently-used centrifugal pumps tested in the field (as described in Chapter 3)—and at half the input power. In this model, the rope pump is assumed to be coupled to a 1.5 hp Vijay Villiers C12 engine, which ultimately was employed in the prototype, while the centrifugal pumps tested earlier were driven by 3 hp Honda GK200 engines. Because farmers must essentially babysit the pump while it runs to ensure smooth operation, they care about the amount of time it takes to fill their fields. With higher flow rates, the rope pump should reduce the time spent irrigating and allow the farmers to use that time to accomplish other tasks.

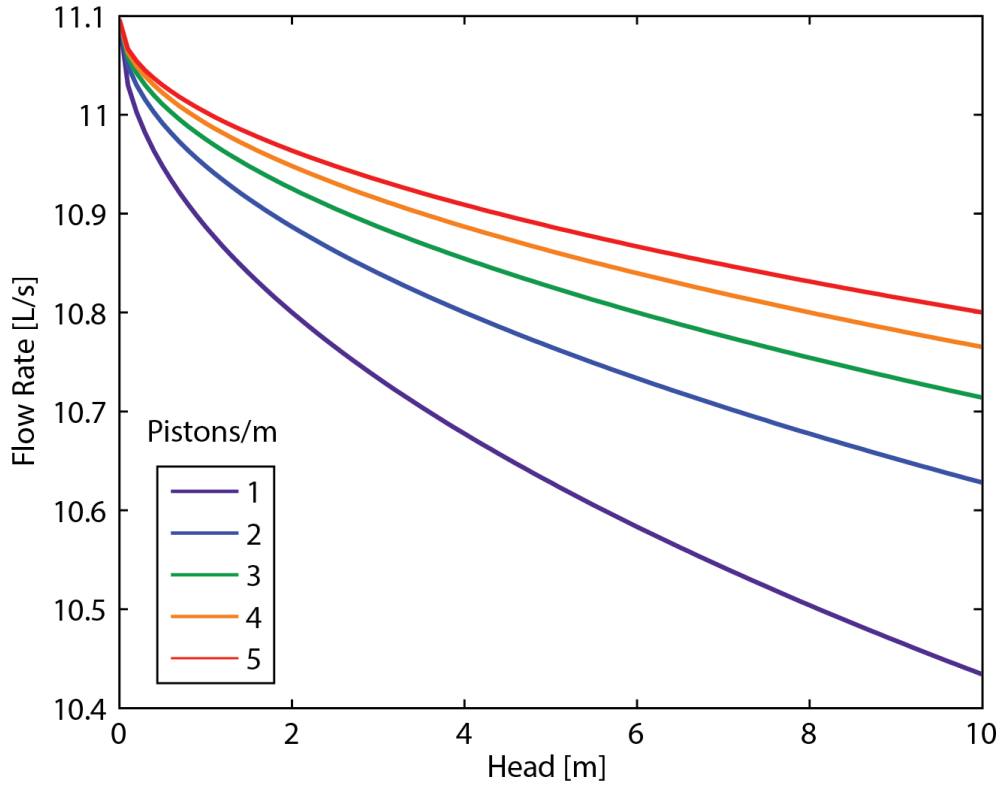

Figure 4.11. Expected flow rate of the rope pump as a function of head at different piston intervals.

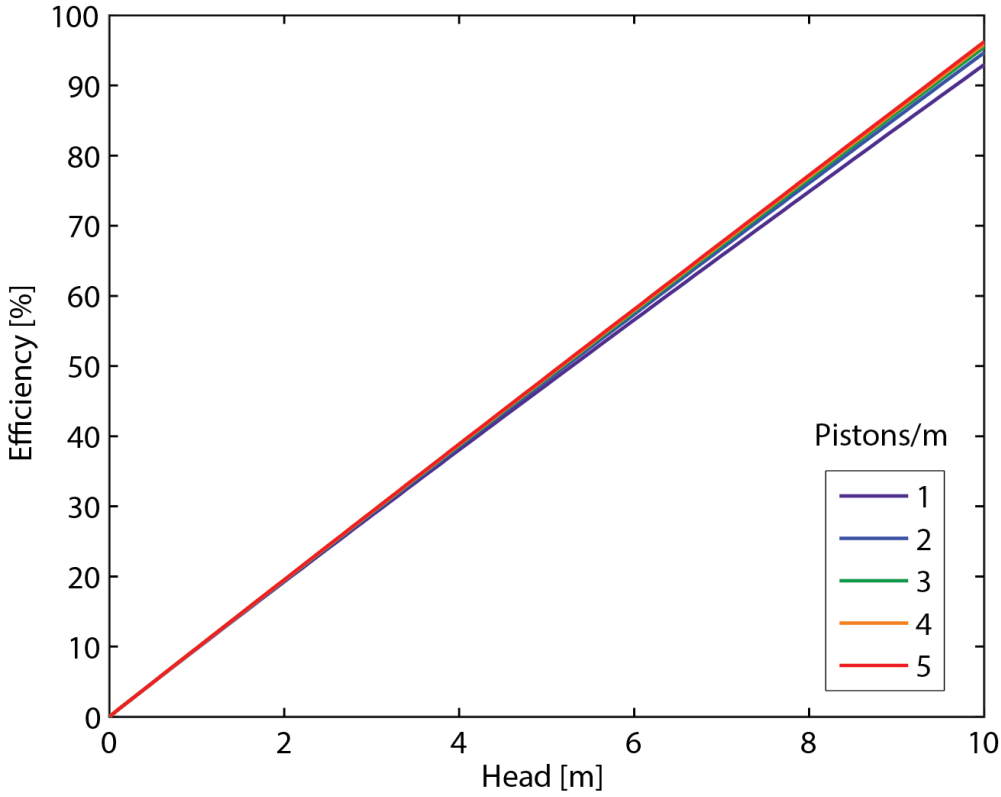

Figure 4.12. Expected efficiency of the rope pump as a function of head at different piston intervals. Efficiency decreases as head decreases due to unutilized torque under the assumption of invariable engine performance.

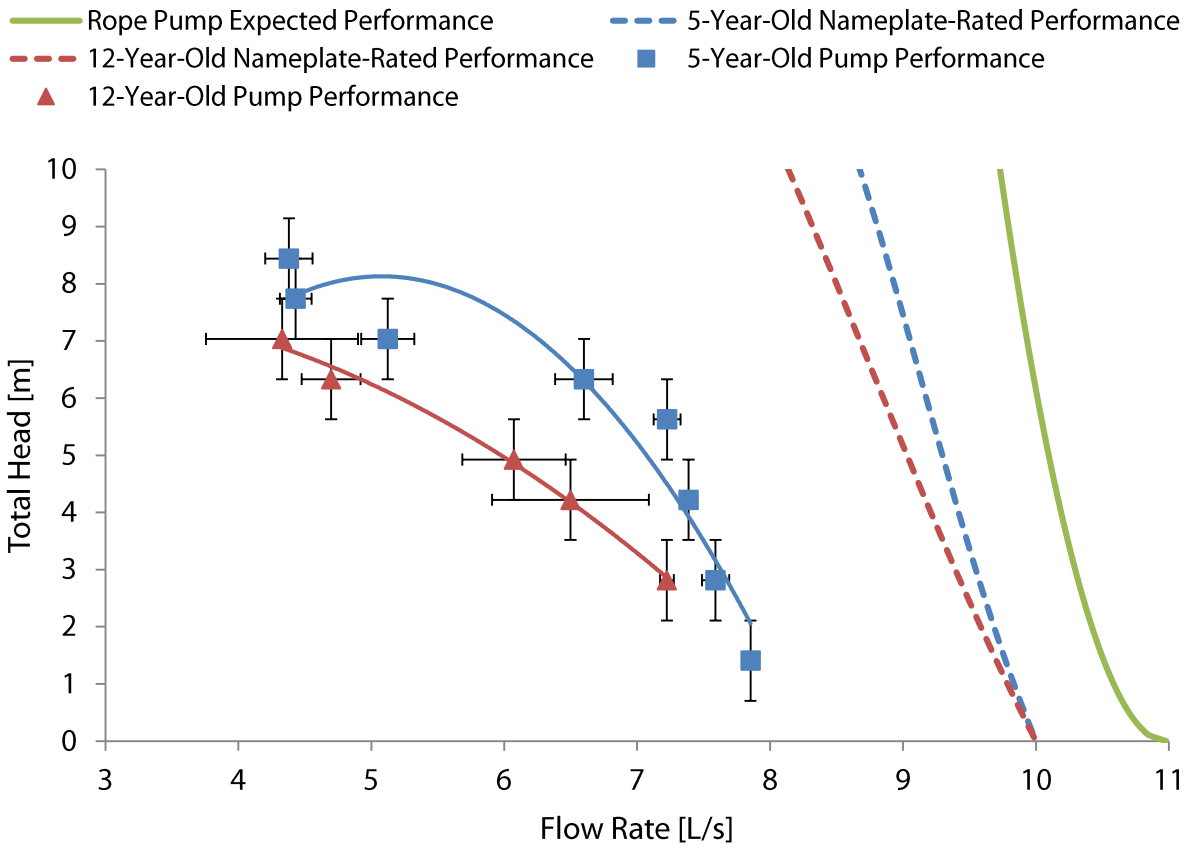

Figure 4.13. Comparison of expected rope pump performance with 2 pistons/meter to the rated and actual performance of Honda engine-driven pumps tested in the field (see Chapter 3 for testing details).

4.4 Fabrication of the Prototype

The help of Govind Sharma (respectfully known as Sharmaji) and his team at Swastik Engineering Works in Ranchi was enlisted for fabrication. The materials and some readymade parts were purchased in the markets of Ranchi. Remaining parts were built and assembly completed in Sharmaji's workshop. Birendra Prasad, Vimal Prasad Lal, and Basudeo Sarkar contributed excellent welding and lathing, while Gopal Singh Rathor assisted greatly in the acquisition of materials and parts.

The design process was perhaps a bit unconventional. Given the time constraints, the author did not have time to 3-D model the system in a CAD program. Instead, hand drawings were brought to the workshop, where Sharmaji and his employees quickly conducted a design review that brought to light what is and is not possible in Ranchi, a minor Indian city without the resources of Delhi or Kolkata or cities in the United States. Many changes to the original design were made, as some components, part sizes, materials, and fabrication facilities were unavailable. For example,

the initial requested pulley sizes and pipe fittings, which can be easily ordered online in the United States, were not sold on the Ranchi market. Manufacturing processes such as custom injection molding would have been difficult to find in the city. Some parts and materials could be specially-ordered from Kolkata, but it was decided, for the sake of time and later repair-ability, to use only what was available in Jharkhand. Some hand drawings from the design process with Sharmaji and his team are given in Figure 4.15. The final system is depicted and its components labeled in Figure 4.14. The number of each component in Figure 4.14 corresponds with the number of the subsection that discusses the fabrication of that component. Figure 4.16 provides a 3-D model representing the final product and its dimensions. Since all work was accomplished using hand drawings, this model was created in Solidworks after fabrication.

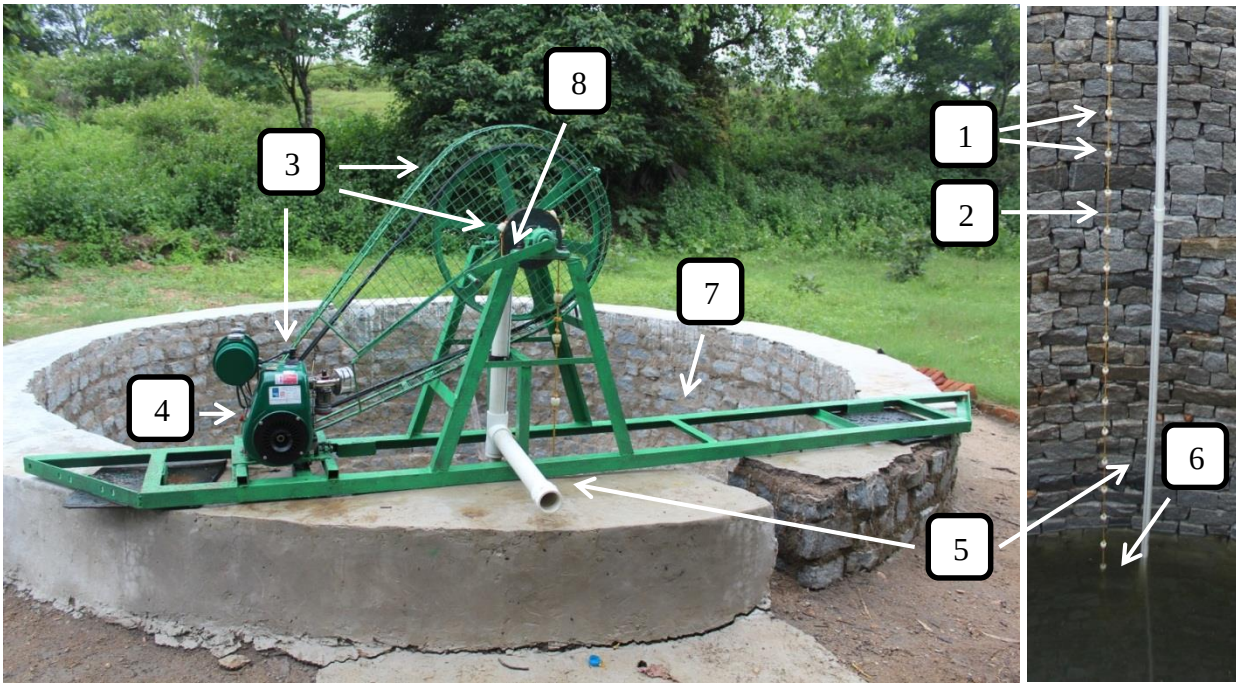

Figure 4.14. Rope pump components. (1) Pistons. (2) Rope. (3) Pulleys. (4) Engine. (5) Piping. (6) Guide. (7) Platform. (8) Hand crank.

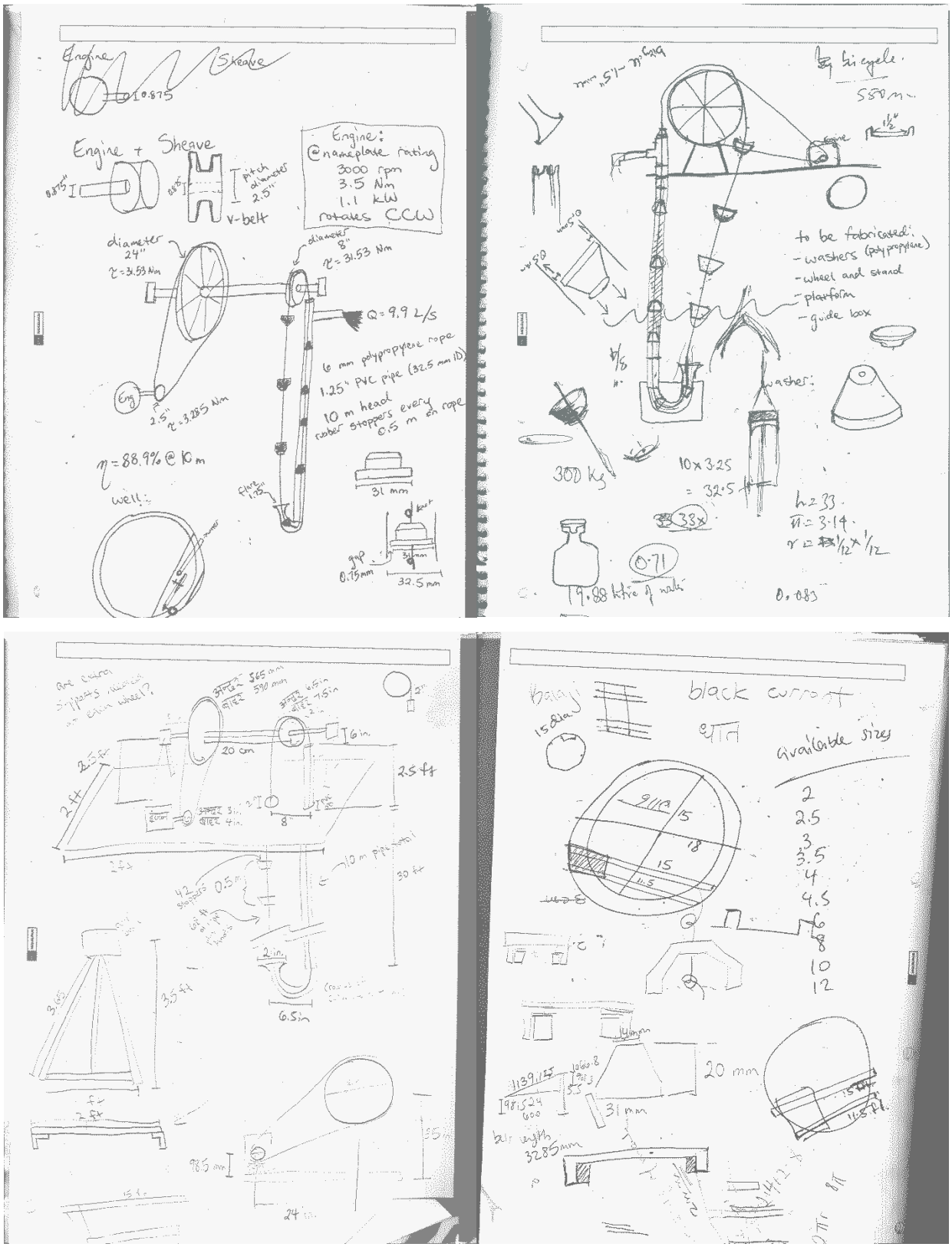

Figure 4.15. Some drawings and notes from the design process with the team at Swastik Engineering Works. Note that none of these drawings represent the final design, because Sharmaji kept the final drawings.

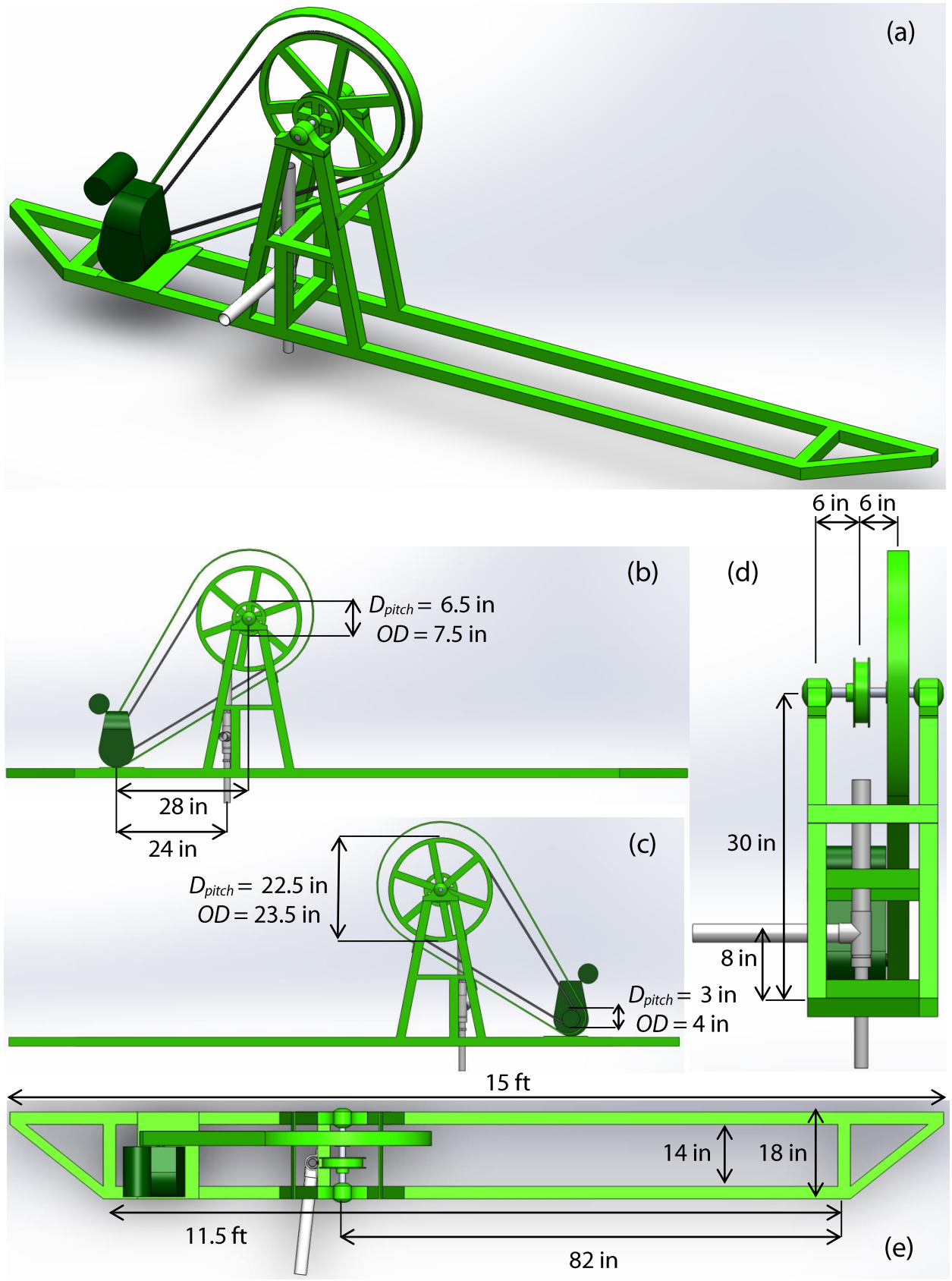

Figure 4.16. 3-D model of the pump system created in Solidworks. (a) Trimetric view. (b) Front view. (c) Back view. (d) Side view. (e) Top view. The metal net of the safety cover was omitted to allow easier viewing of system components such as the large pulley and v-belt. This model was not used for fabrication but was created afterwards.

4.4.1 Pistons

Several options were considered for the pistons. In some countries, the pistons on manual rope pumps are made using injection-molded polypropylene or polyethylene [94]. However, injection molding facilities were not available in Ranchi; one would have to go to Howrah, an industrial zone in the Kolkata metropolitan area, about 390 km away by road. Given the unavailability of such facilities, it may be difficult for farmers or their mechanics to procure replacement parts should they be needed. Therefore, this option was eliminated.

Rubber is widely available in used and new car, motorcycle, and bicycle tire shops. Rubber is even available in remote villages, as people tend to save the worn-out tires of their bicycles. Thus rubber was considered. However, the thin bike wheel rubber can wear down very quickly.

Hospitals and other medical and pharmaceutical facilities have a large supply of thicker rubber in the form of rubber stoppers for saline containers. These rubber stoppers can be acquired directly from the hospital waste management team or from the manufacturers. Some stoppers discarded from a pharmacy were obtained for a trial run. Unfortunately, the knot in the rope tore right through the rubber during the trial.

Ultimately, it was decided to cut pistons out of solid nylon rods, which are easily available in the market. For this prototype, the material was purchased from a shop called Weld Cuts near Lalji Hirji Road in Ranchi. Drawings of the piston dimensions are given in Figure 4.17, and a photograph of the final product in Figure 4.19. They were formed on a lathe, as shown in Figure 4.18.

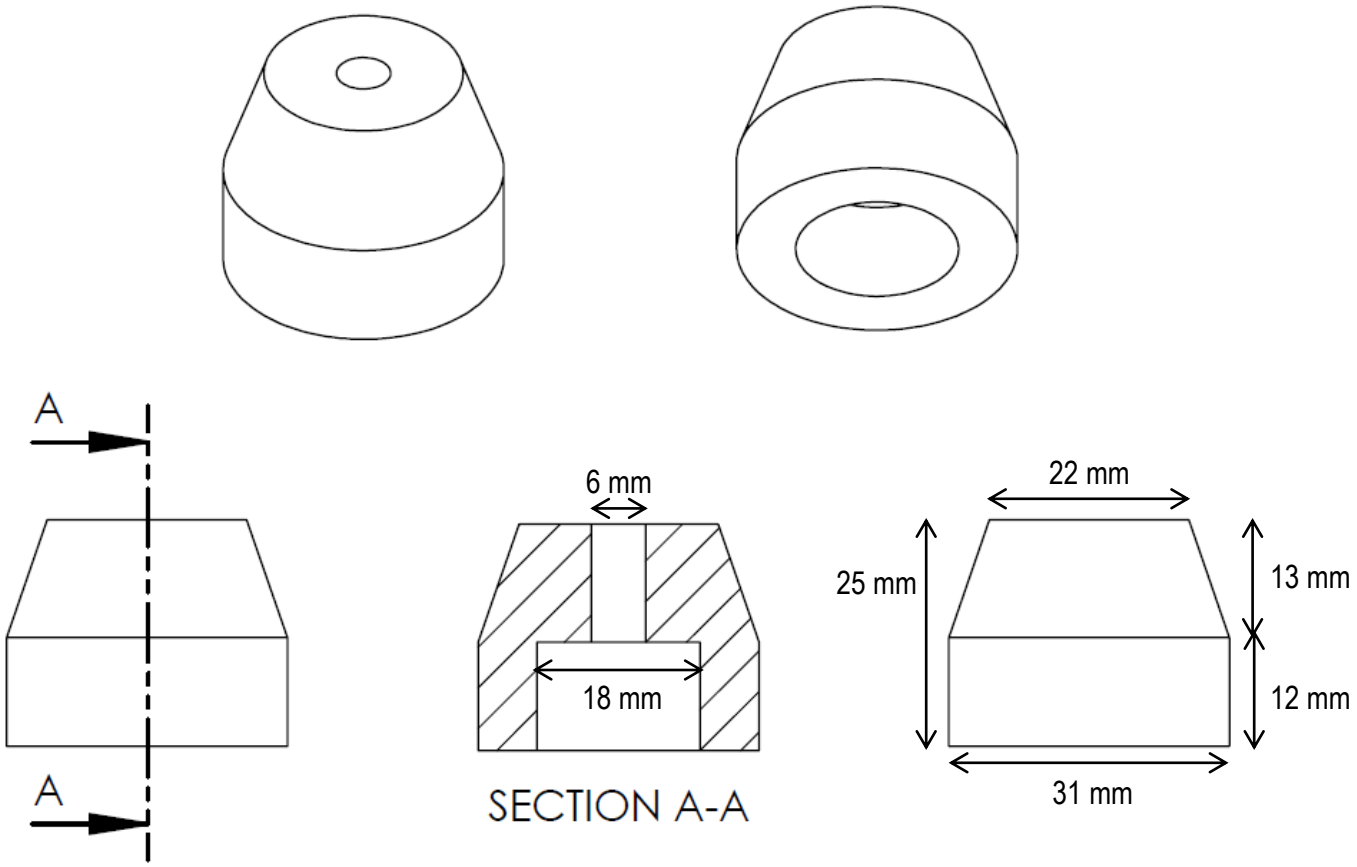

Figure 4.17. Drawings of the pistons made in SolidWorks.

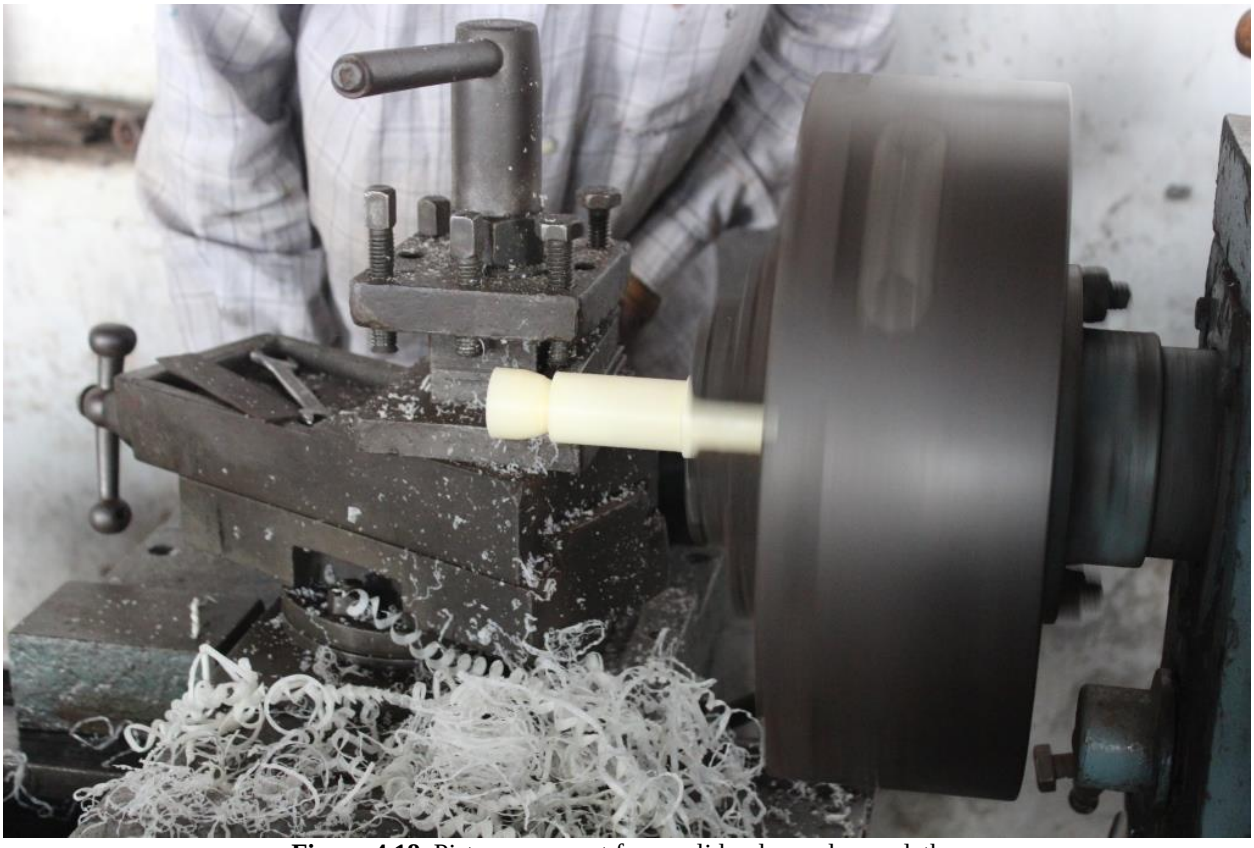

Figure 4.18. Pistons were cut from solid nylon rods on a lathe.

Figure 4.19. Pistons.

4.4.2 Rope

Polypropylene rope, known as "PP rope" in Ranchi's markets, is the standard rope used in manual rope pumps around the world. While other ropes can be used, polypropylene is effective because it is both strong enough to lift water and rough enough to minimize slippage on the pulley. A rope with a thickness of 6 mm was used, because in most rope pump manufacturers' experience this size has been found to work successfully [95].

Originally, the pistons were threaded onto the rope at intervals of 50 cm (2 pistons/m), because the MATLAB model indicated that this would result in the greatest flow rate jump without too much added material cost. However, it turned out that more pistons would be needed in order to reduce slipping, and they were tied at 20 cm intervals (5 pistons/m) (see discussion below in Section 4.6 Troubleshooting). After all the knots were tied, the entire rope was pulled at both ends to ensure the knots were as tight as possible.

Figure 4.20. Polypropylene ("PP") rope with nylon pistons.

4.4.3 Pulleys

The size of each pulley was determined in MATLAB using the equations of a rope pump model described above in Section 4.3 Model. The engine shaft's sheave had a pitch diameter of 3 inches, the larger pulley connecting to the engine had a pitch diameter of 22.5 inches, and the pulley holding the rope had a pitch diameter of 6.5 inches. The larger pulley was connected to the engine sheave with a 122-inch v-belt. Both pulleys were B-type. Initially the rope's pulley was also a B-type v-belt, under the assumption that it would not be a problem for the pistons to sit on the top of the pulley as long as the rope could fit between the walls. However, this proved to be a problem (see below in Section 4.6 Troubleshooting), so a new rope pulley was built. The new rope pulley was made of a double B-type v-belt pulley, with the middle divider removed on a lathe (Figure 4.22) to accommodate the movement of pistons. The pulley was cleaned up with a metal sealant, because the lathe job was a tad uneven and removing the middle divider exposed some holes in the pulley.

The large pulley and rope pulley are connected via a shaft, which is held in place with ball bearings. A bore was drilled in each pulley to match the shaft diameter of one inch.

For safety purposes, a cover was constructed for the v-belt and its pulleys. Thin steel rods were hammered into shape and welded together. A metal net was cut to fit the steel frame and welded to it.

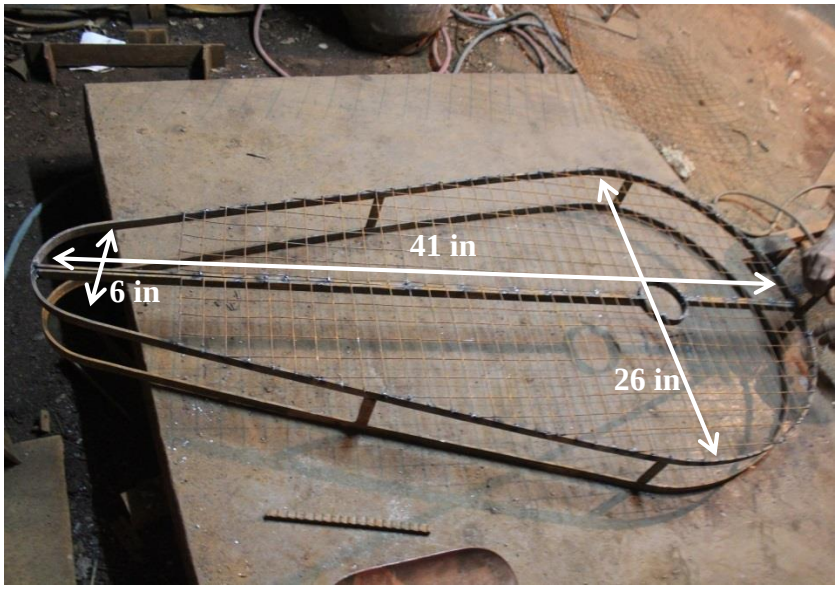

Figure 4.21. The pulley safety cover.

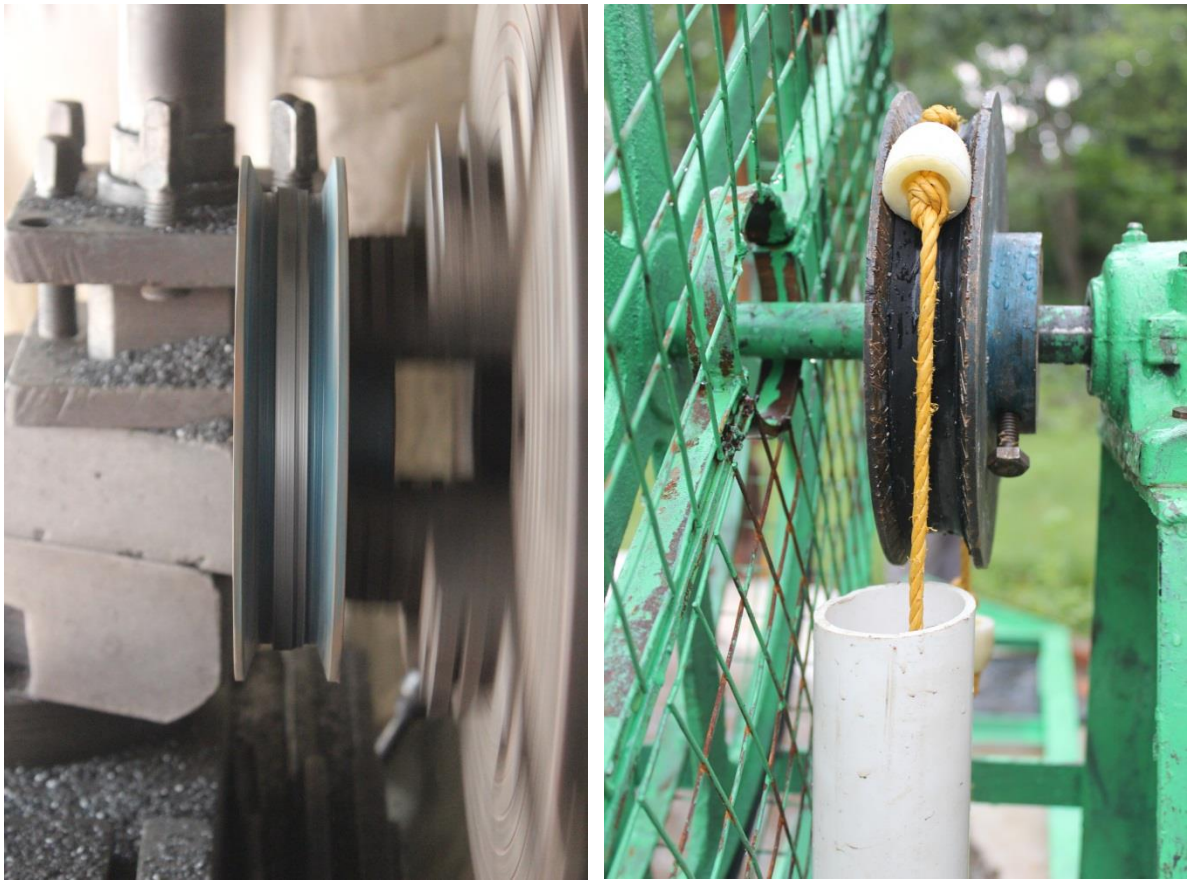

Figure 4.22. Removing the middle divider from a double B-type v-belt pulley to make room for the pistons.

4.4.4 Engine

The smallest fuel-powered engine available on the market in Jharkhand is rated at 1.5 hp. The leading brands include Vijay Villiers, Honda, and Crompton Greaves, and all three engines start on gasoline and run on kerosene. While Honda is the most popular small engine nationwide, in this region the Villiers engine is most common. Because ideally a farmer should be able to use his existing engine in this system, the prototype was built using this most common Vijay Villiers C12 engine. The rated output is 1.5 hp (1.1 kW) at 3000 rpm. Drawings of this engine are shown in Figure 4.23. It was found during interviews with six engine retailers that this engine costs between INR 8200 and 9500 in Ranchi. The engine utilized in this prototype was purchased for INR 8200.

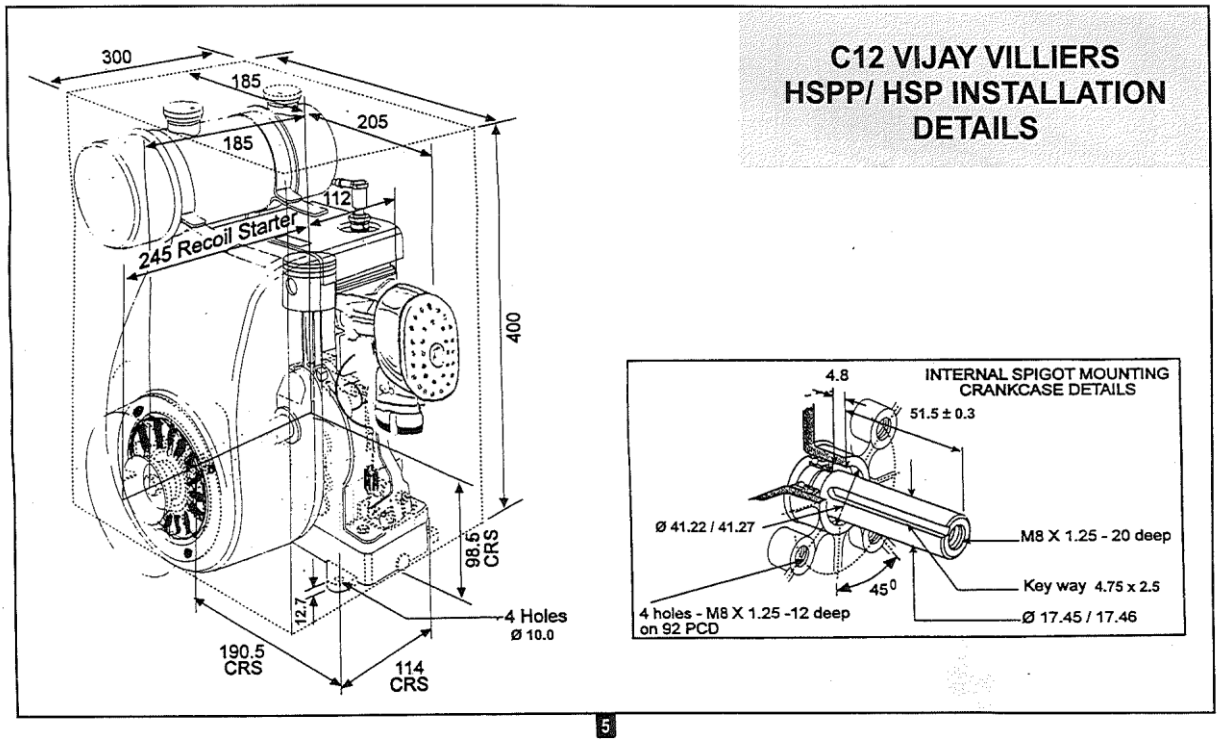

Figure 4.23. Drawing of Vijay Villiers C12 engine used in the prototype. **[96]**

4.4.5 Piping

PVC pipes were employed due to their easy availability, low cost, and long life. The MATLAB model determined that the inner diameter for a ten-meter-deep rope pump employing the pulley sizes and engine specifications described above should be approximately 1.25 inches, so nominal 1 ¼-inch pipes were used for the rising main. The discharge pipe had a nominal two-inch diameter in order to save farmers the money and effort required to purchase new delivery hoses. Farmers already own two inch delivery hoses because the common small centrifugal pumps have a two inch outlet.

4.4.6 Bottom Guide

A guide is necessary to ease the entry of the rope and pistons into the main PVC pipe, maintain tension in the rope, and minimize wear and tear on the rope and pistons. The most-commonly employed design to guide the rope and pistons requires a crafted ceramic piece (Figure 4.24). The usual systems generally involve a very sharp turn into the rising main due to the large rope pulley on the surface, which is often actually a bicycle wheel (Figure 4.1), as it would be

difficult to install a similarly-large pulley or turn at the bottom of the well. The smooth surface of the ceramic piece alleviates this sharp transition and reduces wear on the rope.

Ceramic production facilities, while very likely available in Ranchi among artisans such as potters, were not found for custom work within the time constraints. Instead, a U-shaped guide was constructed using PVC elbows and fittings (Figure 4.25). A nominal two inch to 1 ½ inch reducer served as the entrance, followed by two nominal 1 ½ inch long elbows cut into a 3.25 radius of curvature to match the radius of the rope pulley on the surface and eliminate the sharp transition, and a nominal 1 ½ inch to 1 ¼ inch reducer connected the guide to the rising main, which has a nominal 1 ¼ diameter.

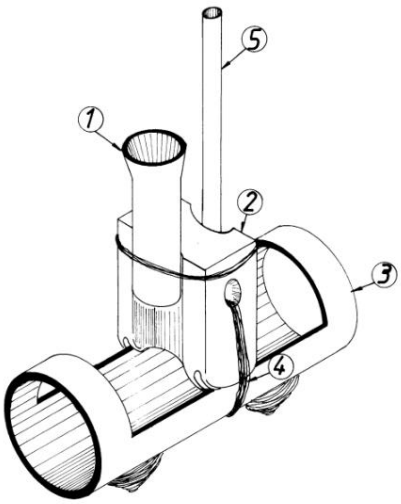

Figure 4.24. Typical rope entry guide used for a manual rope pump.
(1) Entrance pipe. (2) Ceramic guide. (3) Base, which can be made from a glass bottle. (4) Rope tying the ceramic guide to the base. (5) Rising main pipe. **[97]**

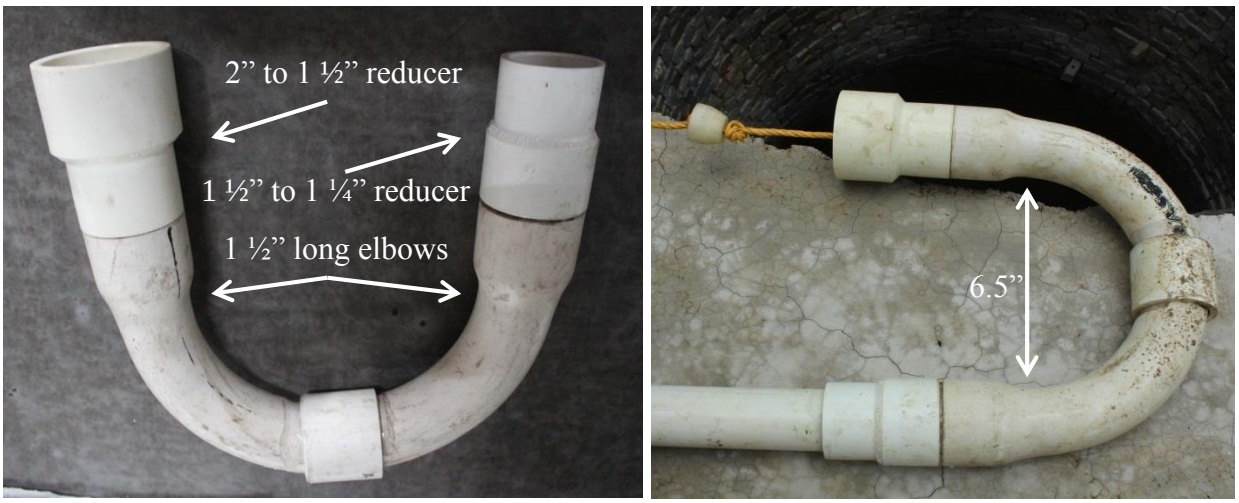

Figure 4.25. U-shaped PVC bottom guide.

4.4.7 Platform

The platform was designed to fit on the rim of a standard upland well, which has an inner diameter of 15 feet and outer parapet diameter of 18 feet, as close to the edge as possible so that even children could reach the hand crank and parts would be easily accessible for maintenance when needed. The platform was 18 inches wide, with the longer side measuring 15 feet across and the shorter side measuring 11.5 feet. The ball bearings were supported by legs and positioned 2.5 feet above the platform. Two-inch angle irons were used to form the primary structure as well as the legs holding up the bearings, shaft, and pulleys. The irons were welded together.

The platform was painted to prevent corrosion from contact with water. The color green was selected because, according to PRADAN, villagers associate green with agricultural productivity. Plus the Villiers engine was already green, so the color matched.

In order to hamper vibration, the platform was placed on 20-mm-thick rubber pads, which were acquired from a shoemaker and had been originally intended for soles of shoes.

A plate for the engine was welded to the platform. The engine had to be made removable, because in some villages families worry about theft. Additionally, if the engine is removable, then multiple wells can share a single engine, or an engine owner can rent out his engine to several different families and their wells, as is currently done with centrifugal pumps. The plate was outfitted with adjusting and lock bolts, as in Figure 4.26, so that the engine could be moved to increase tension in the v-belt when necessary.

4.4.8 Hand Crank

The hand crank was designed to mate with the driveshaft through a press-fit connection. The end of the driveshaft was cut and filed into a male square shape (Figure 4.27), while the interfacing part of the hand crank was formed into a female square shape. For the mating component, a small hollowed-out steel rod was heated and hammered into shape using a squared-off rod as a guide (Figure 4.28). This part was then welded to a piece of steel cut from an angle iron, which in turn was screwed to a handle to complete the hand crank (Figure 4.29).

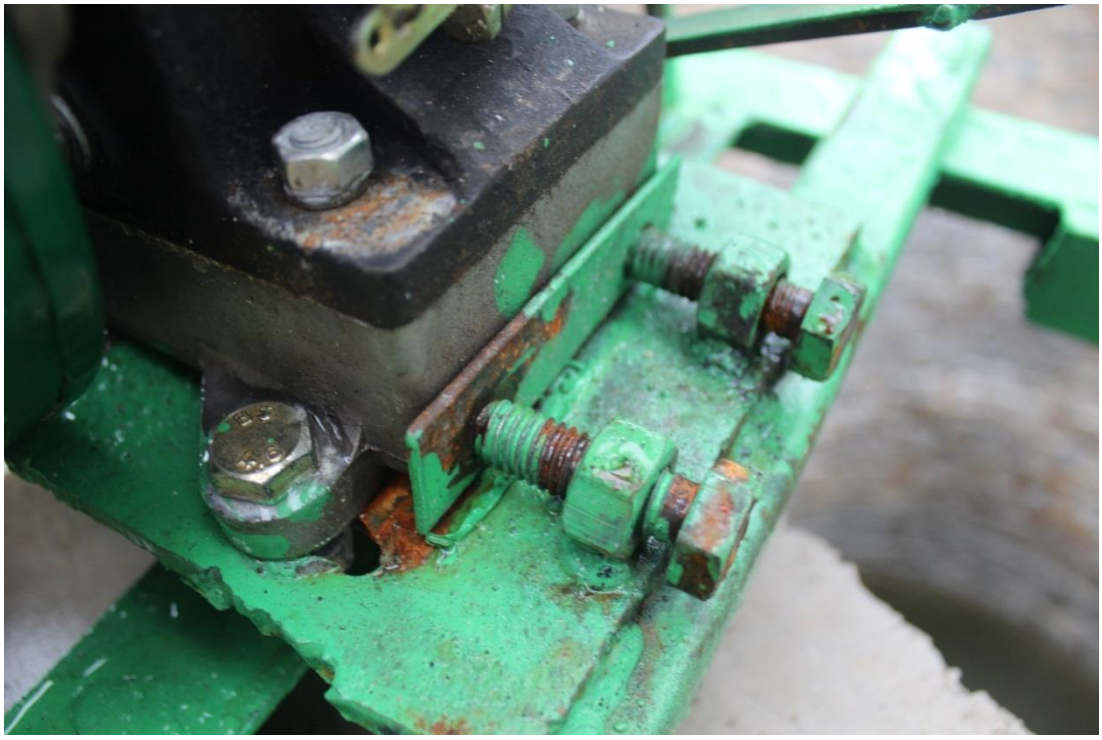

Figure 4.26. Engine plate with adjusting and lock bolts that allows for adjustment of engine placement.

Figure 4.27. Cutting and filing the end of the driveshaft to interface with the handle.

Figure 4.28 Fabricating the part of the hand crank that interfaces with the driveshaft.

Figure 4.29. The completed hand crank.

4.5 Installation of the Prototype on a Well

The rope pump was installed on a hand-dug open well in Ruitola village, Murhu block, Khunti district, Jharkhand. Shahanawaz Alam, PRADAN's field officer for Murhu, identified this well. The well, shown in Figure 4.30, has an inner diameter of 15 feet and the outer diameter of the parapet is 18 feet. The depth is 22 feet, and the water level at the time of installation and testing was 18.5 feet deep. The depth was measured by tying a rock to a long tape measure and lowering

the rock into the well. The well sits near the top of a narrow valley, with fields of rice and vegetables below. The well was installed under a government scheme and is owned by a farming couple named Salim and Turlin.

Although the pump was designed to be used on a 35-foot deep well, which is the standard size well installed under the Mahatma Gandhi National Rural Employment Guarantee Act (MNREGA), this well was selected due to its proximity to a *pukka* (paved) road. The pump was built in the city of Ranchi and brought by truck to the village. A team of six men carried the pump from the truck to the well (Figure 4.31), so it would have been difficult to select a well located further from a road accessible by truck.

Figure 4.30. Well in Ruitola village used for the rope pump trial.

Figure 4.31. Carrying the pump to the well.

First, two 20-mm-thick rubber pads were placed on the well to sit beneath the main structure to absorb the vibrations of the engine. After the main structure was situated on the rubber pads, the rope with pistons was threaded through the pipes. First the rope was put through the U-shaped bottom guide, with the narrower part of the pistons facing inwards, as in Figure 4.32, to reduce hydrodynamic resistance. Interestingly, villagers assumed the piston should be inserted with the wider side inwards, because they believed the pistons, which have a larger indentation on the wide side, acted as miniature buckets carrying water to the surface. The rope was then threaded through each 10-foot PVC pipe and coupling before the parts were glued together using PVC cement.

Figure 4.32. Inserting the piston into a pipe, narrower side inwards.

The pipes and rope were carefully lowered into the well (Figure 4.33), and then the top coupling was cemented to the piece of pipe clamped to the main structure (Figure 4.34). While lowering the pipes and rope, it was important to tie a knot in the rope to ensure that one end did not fall into the well. Once the long set of pipes was securely fastened, the rope knot was untied and then retied over the small pulley wheel with proper tension. The extra rope was then cut off. The complete installation is shown in Figure 4.35.

Figure 4.33. Lowering the pipes and rope into the well.

Figure 4.34. Connecting and gluing the long pipe to the piece of pipe supported by a clamp to the main structure.

Figure 4.35. The complete installation of the rope pump on the well in Ruitola.

4.6 Troubleshooting the Prototype

Several problems were encountered when attempting to run the pump at first. The rope kept slipping on the pulley, so that when the pulley turned, the rope did not move with it. The problem seemed to be that the distance between two pistons was too great. When the piston reached the pulley, the pulley grabbed it and swung the rope over. However, when there was no piston touching the pulley, as in Figure 4.36, the rope did not move with the pulley. The distance between two pistons was 0.5 m, but the half of the circumference—the distance that would have allowed the pulley to always grab a piston—was 0.26 m.

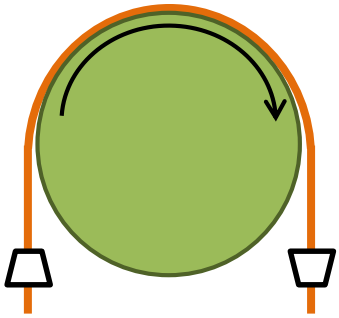

Figure 4.36. The positions of pistons when the rope slipped on the pulley.

It was attempted to resolve the slippage problem with a slice of rubber from the inner tube of a used motorcycle tire (Figure 4.37). This worked temporarily (until the rubber snapped off), which revealed another problem: the water shot straight up the pipe, rather than turning into the discharge pipe at the tee. The issue arose because when a 1 ¼ inch x 2 inch x 1 ¼ inch tee could not be found in Ranchi's market, a 1 ¼ inch x 1 ¼ inch x 1 ¼ inch tee with a 1 ¼ inch x 2 inch reducer was used as a replacement. As a result, the water did not experience the lower flow resistance of the two-inch discharge pipe right at the intersection. In retrospect, this was an absent-minded oversight.

This discharge problem was resolved by replacing the small tee and reducer with a 1 ¼ inch x 2 inch reducer bushing and a 2 inch x 2 inch x 2 inch tee and inserting a 2 inch-diameter pipe into the top of the tee. The larger gap between the piston and the 2 inch-diameter pipe wall would cause water to fall. The pistons would not be able to further push the water upwards and the water would be directed through the discharge pipe. A reducer bushing rather than a regular reducer was selected in order to induce rapid expansion rather than gradual expansion, which may

have led to more water falling before the discharge tee. The original installation and resolved setup are illustrated in Figure 4.38.

Figure 4.37. A slice of used motorcycle tire was wrapped around the pulley wheel in an attempt to eliminate slipping.

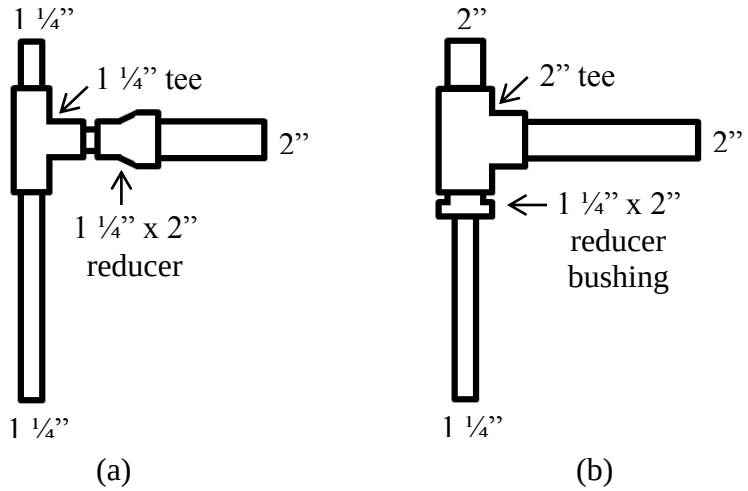

Figure 4.38. Piping at the outlet. (a) Original setup that caused water to shoot out the top. (b) The corrected setup that allowed water to exit via the discharge pipe.

After changing the discharge set-up, motorcycle inner tube rubber was more permanently affixed to the pulley using Fevikwik, an Indian brand of cyanoacrylate adhesive, as the rubber seemed to have addressed the slippage problem previously. However, on the second try the rubber did not prevent the rope from slipping. Instead, as the rope slipped on the pulley rapidly spinning beneath it, friction heated up the rope-rubber interface and melted rubber onto the rope (Figure 4.39). At one point, the friction-induced heat burned through the rope, breaking it in half.

Additionally, though the pistons could be pulled up using the narrow pulley, the sides of the pulley tore through the edges of the pistons, leaving indented streak marks.

Figure 4.39. Friction on the pulley melted rubber onto the rope and burned it to the point of breaking.

A new pulley was built in order to accommodate the full width of the pistons (the fabrication of this new pulley is discussed above in Section 4.4.3 Pulleys), and a strip of rubber from a motorcycle tire inner tube was again affixed to the pulley using Fevikwik. More pistons were added to the rope at shorter intervals in order to ensure that the pulley could always grab a piston in an attempt to achieve less slipping of the rope, and to reduce the contact between the rope and the rubber to eliminate breakage due to friction. Despite these modifications, slipping remained a problem. Using a chisel, the sides of the pulley were roughened, as shown in Figure 4.40, to improve the pulley's ability to grab the pistons.

All these changes together seemed to help; a few seconds went by before slipping started. When the engine was turned off, it was noticed that the rope had become significantly looser. Thus the rope was retied with more tension, and the excess rope was cut off. Again, the pulley ran for a few seconds before slipping began—and, again, the rope had become loose. We realized that all the knots holding the pistons on the rope must have been tightening as they turned around the pulley, thereby lengthening the rope and effectively releasing tension. The process of running the engine until slipping started then retying the rope tighter was repeated until the rope stopped loosening and slipping was eliminated.

Figure 4.40. Roughening the sides of the pulley with a chisel.

Now that slipping was no longer a problem, the pump could be run continuously. At the engine's unadjusted maximum rpm, much more water shot out the top pipe rather than exiting through the discharge pipe, despite the changes made. A small lever was found on the engine that could regulate rpm—even though the salesmen in all the engine shops insisted the Villiers engines could not vary speeds—and reducing the rpm resulted in water exiting only through the discharge pipe. However, reducing the rpm also reduces the flow rate. Future prototypes should be redesigned to take advantage of the full potential flow rate, as discussed below in Section 4.8 Future Modifications. Unfortunately, the lever is not labeled, so it is unknown at which rpm the water fully exited through the intended pipe.

4.7 Testing the Prototype in Two Modes

Once the pump was working properly, it was tested for performance as well as usability in both engine and manual modes.

4.7.1 Performance

Performance data was acquired for only a single head, because the water level in the well could not be varied nor the pump installation raised or lowered. A digital flow meter was attached to the discharge pipe of the pump in order to test for flow rate. The flow meter works by counting the number of times a mini turbine, which the farmers called a *pankha* ("fan" in Hindi), turns within a certain amount of time. However, the flow reading regularly fell to zero as debris or silt in the water clogged the meter and prevented the mini turbine from spinning. Often clogging occurred before the flow reached its maximum rate, so obtaining accurate readings was difficult.

The results acquired for engine mode are given in Table 4.1. The average flow rate of 155.4 L/min performs far below the theoretical flow rate of 654 L/min for a depth of 18.5 ft (5.6 m). It is important to note that this data does not represent the total flow rate moving up through the rising main; more of the water was actually lost through the top of the pipe than passed through the horizontal discharge pipe, which the flow meter was reading (Figure 4.41). Meanwhile, the theoretical flow rate includes all the water ascending through the main pipe. Additionally, the rpm of the engine was significantly reduced in order to limit the water shooting out the top, while the theoretical flow rate assumed the maximum engine rpm.

Table 4.1. Flow rate results in engine mode. Instrumentation error was ±0.04 L/min, and results were rounded.

	Flow Rate (L/min)
Trial 1	150.2
Trial 2	149.6
Trial 3	162.4
Trial 4	156.3
Trial 5	158.5
Average	155.4

Table 4.2. Flow rate results in manual mode. Error is estimated to be ±10% due to uncertainties in exact volume and human response with the stopwatch.

Male Users	**Flow Rate (L/min)**	**Female Users**	**Flow Rate (L/min)**
Man 1	15.6	Woman 1	13.8
Man 2	19.2	Woman 2	12.6
Man 3	16.8	Woman 3	12.9
Average Man	17.2	Average Woman	13.3

(a) (b)

Figure 4.41. Testing the rope pump in engine mode at (a) a higher rpm and (b) a lower rpm. A lot of water is lost through the top of the rising main.

In manual mode, the flow was lower than could be detected by the flow meter, so instead a stopwatch was used to time how long it took for the user to fill up a one-liter bottle. Shortsightedly, the removable handle was not made to be screwed in (the connection was press-fit, as in Figure 4.43), so the handle frequently fell out. This made it difficult for the user to maintain a speed, so the flow rate was less than it otherwise could have been. A photo of a woman using the pump is given in Figure 4.42, and Table 4.2 shows the results of testing the pump in manual mode with various users. The error is estimated to be ±10% as a result of uncertainties in the exact volume of the bottle and the human response time in using the stopwatch. Existing manual rope pumps get flow rates between 10 and 40 liters per minute [98], so at an average of 13.3 L/min for women and 17.2 L/min for men, this pump is at the lower end of the spectrum. This flow rate would be improved with a screwed-in, more ergonomically-designed handle.

Figure 4.42. A woman testing the rope pump in manual mode.

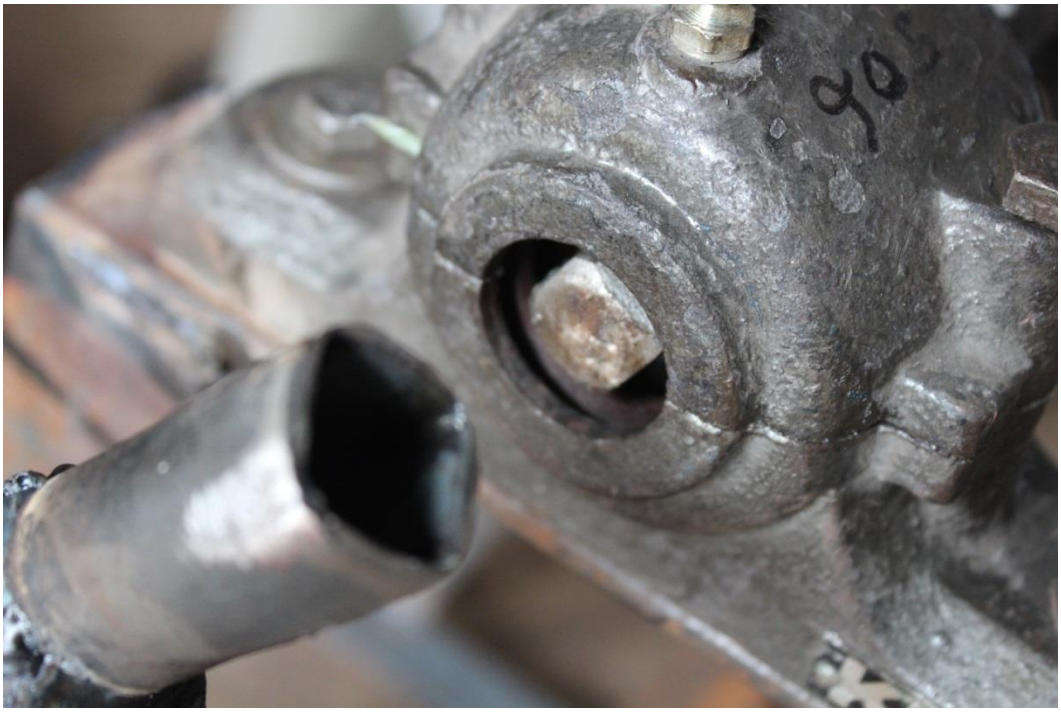

Figure 4.43. The end of the handle was cut into the same shape as the shaft in order to allow for press-fit coupling.

Fuel consumption was difficult to assess. We would put 10 mL into the engine and run it until it was dry, measuring how much time it took to consume all the fuel with a stopwatch. However, the time varied widely, as it did during the testing of the Honda pumps described in Chapter 3. It seems that the performance of Indian engines is quite inconsistent. Before we could get enough fuel consumption readings, a farmer poured all the kerosene we had into the engine, not realizing that we intended to measure exactly how much was consumed. We tried to remove the kerosene from the engine but could not get all of it out.

Due to the shortage of kerosene in the area, we could not purchase additional kerosene to try a different method of running the engine for a fixed amount of time and measuring how much fuel was required to top off the tank. Villagers acquire their first four liters of kerosene each month from the Public Distribution System—if they are able to access it—and then buy the rest from the black market. It was decided not to support the black market, because much of that fuel is in fact stolen from the Public Distribution System, which is intended to help the poor.

Although accurate fuel consumption measurements could not be obtained, it can be assumed that the efficiency was quite low. At a head as low as 18.5 feet, the torque load on the engine shaft was only 1.87 Nm. At the engine's rated speed of 3000 rpm, the engine could handle a torque load of 3.5 Nm. Supposedly, this rating signifies an operation point near the best efficiency point (BEP). Operating away from this point, such as decreasing the load, reduces efficiency. The system was operating so far from the BEP because it had been designed for the BEP to occur at a 10-meter (33-foot) head. Fuel efficiency could be improved by increasing the load on the engine, as discussed below in Section 4.8 Future Modifications.

4.7.2 Usability and User Feedback

For usability, three women and three men were asked to operate the pump and give their feedback. The women currently fetch water by lowering and raising a bucket. They found the pump much easier to use than a heavy bucket. They also expressed excitement that this pump could be operated by children and the elderly (though the pump was not tested with these demographics). Usually, when a child or elderly person requires water, they ask a woman to get the water for them. The woman must then stop what she is doing in order to help. The women explained that if children and the elderly could fetch their own water, they would be able to work more productively with fewer interruptions.

Currently, centrifugal pumps and all accompanying system parts such as suction pipes and foot valves are stored inside farmers' homes and carried to the well every time they are used. The men liked that with an installed rope pump, they would not have to haul the entire pump system, suction pipe and all, to the well every time they wanted to irrigate. Additionally, they noted that priming the centrifugal pump can sometimes be frustrating and time-consuming (as the author too experienced when trying to test the pumps in the US!), so they appreciated that the rope pump does not require priming.

The most common complaint about the pump was the discomfort of the hand crank. Everyone suggested that the handle be made larger and more ergonomic. A larger handle is being fabricated by Birendra at Swastik Engineering Works and will be given to the villagers for further testing. Villagers also disliked being splashed by the water exiting the top of the rising main and explained that they would want to capture and use that water rather than allowing it to fall back into the well.

4.8 Future Modifications

The positive feedback for this prototype proves that this technology is worth taking forward and could potentially greatly benefit farmers and their families. However, a number of modifications to the design are required to improve efficiency and usability before this pump can be disseminated.

The most important problem to be fixed is the direction of the flow exiting the system. Too much water is lost through the rising main, as in Figure 4.41. A few different options could be tried out to address this issue. For example, a funnel could be added to the existing prototype. Rather than using a tee and hoping the water exits through the correct discharge pipe, the tee could be removed and the water allowed to exit through the top, with a funnel beneath the rope pulley to catch the falling water, as in Figure 4.44. Figure 4.45 provides the dimensions for this funnel. If not enough water is captured using only a funnel, a shroud could be placed over the rope pulley to prevent most water from escaping. To attach this closed component to the existing prototype, the funnel and shroud would have to be elliptical (Figure 4.45), as there is not enough space for a circular shroud between the two pulleys (in the version with only a funnel, there is plenty of space below the driveshaft and its components). A future prototype, however, could be designed to allow

for a circular shroud (Figure 4.47), which would be easier to manufacture. These funnels and shrouds would be fashioned from sheet metal, which would likely be steel.

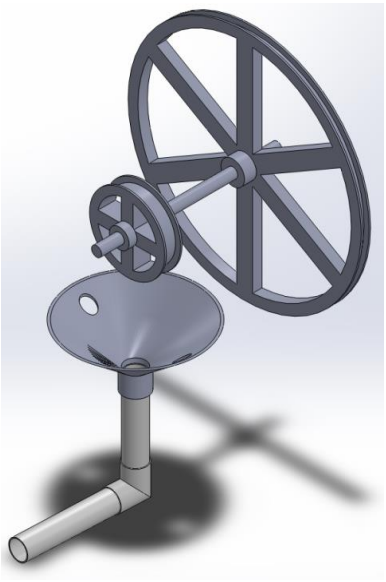

Figure 4.44. An open funnel with a discharge pipe to catch the water falling from the rope pulley wheel. The holes in the funnel accommodate the passage of the rope and pistons. The pipe and funnel can be supported with a clamp attached to the main platform.

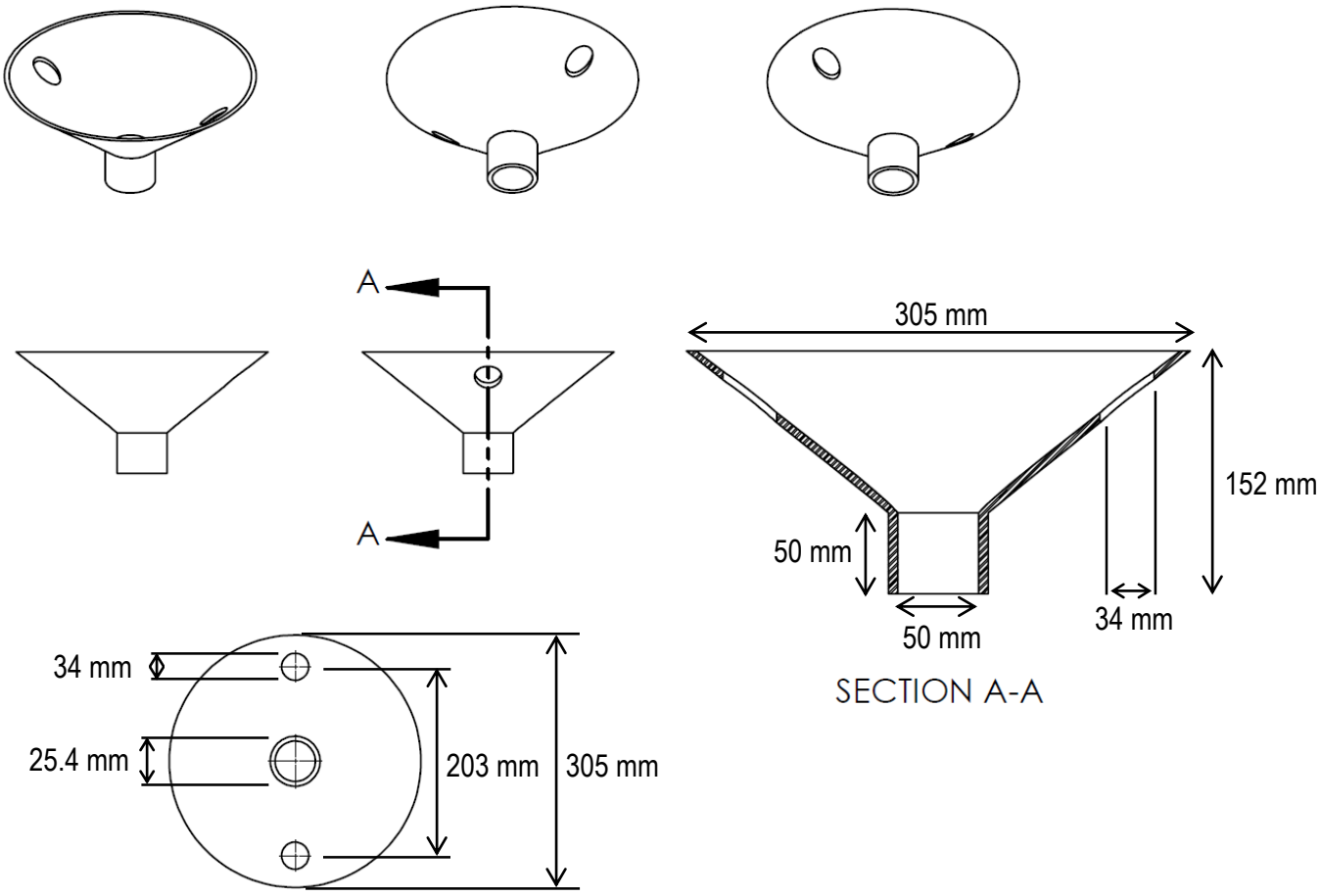

Figure 4.45. Drawings and dimensions of the funnel. The thickness is that of sheet metal.

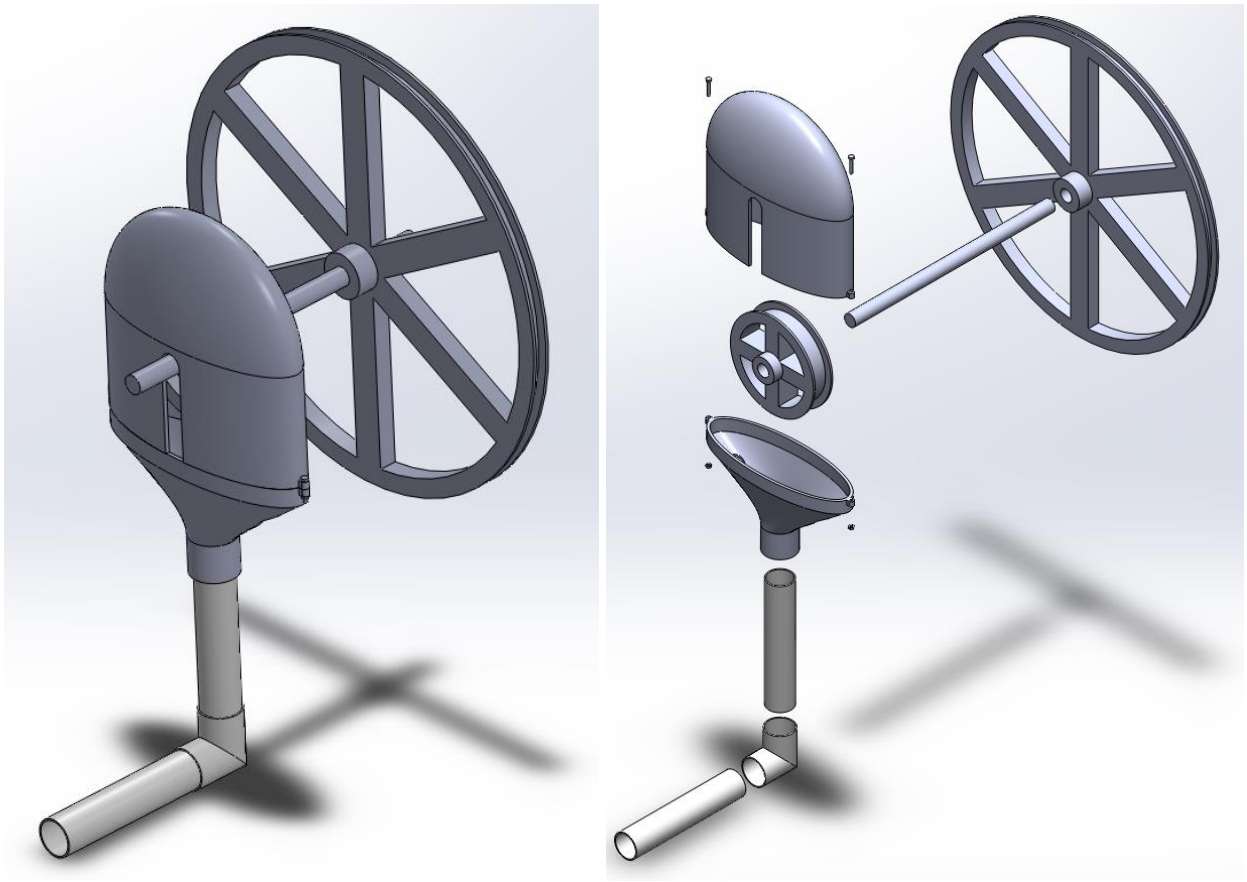

(a) (b)

Figure 4.46. If the open funnel does not successfully capture water, a shroud could be screwed to the funnel in order to cover the pulley and prevent water from escaping. The current prototype has space only for an elliptical shroud. (a) Assembled view. (b) Exploded view.

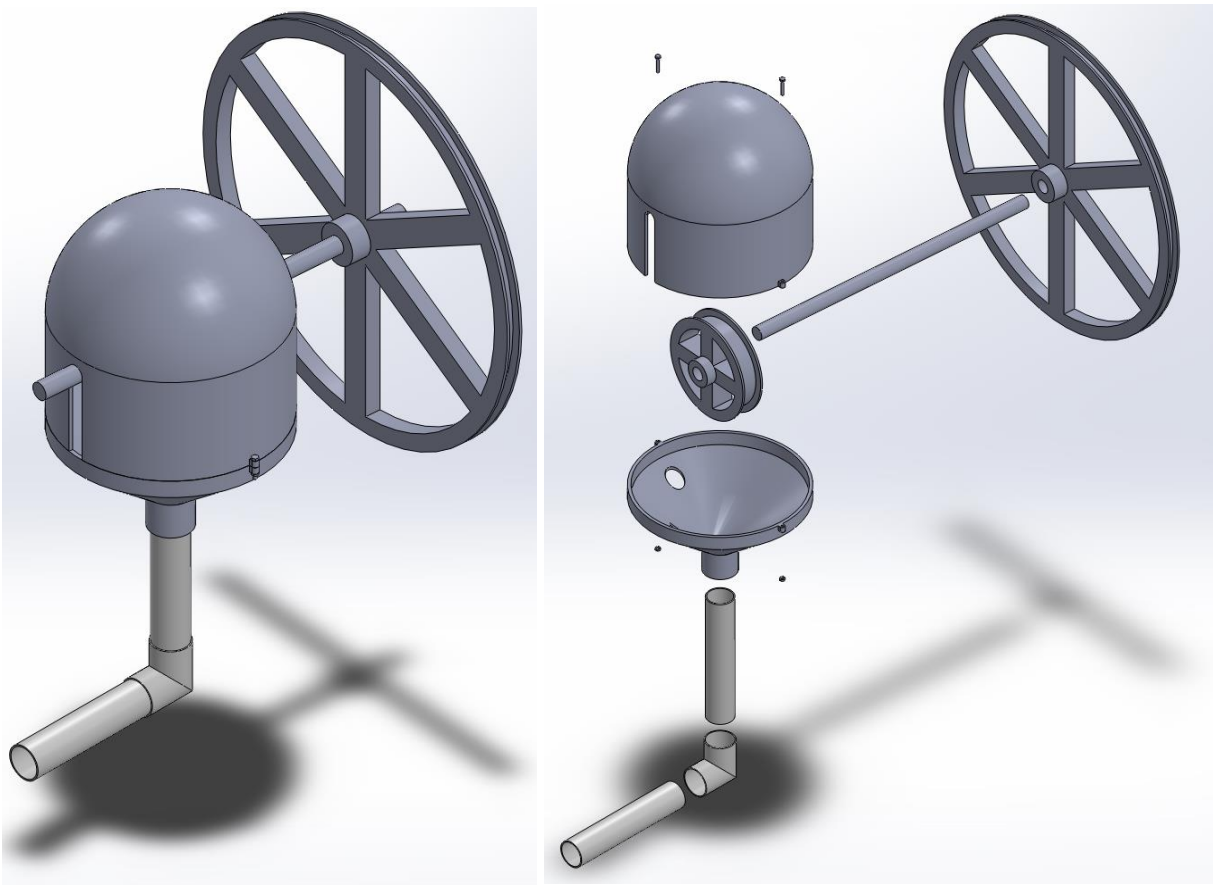

(a) (b)

Figure 4.47. A circular version of the funnel and shroud water capturing solution that could be employed in later prototypes. (a) Assembled view. (b) Exploded view.

For a future prototype, water loss through the rising main pipe could also be eliminated by enlarging the pipe diameter and running the engine at a significantly reduced rpm. Rather than drawing a narrow column of water at high speeds, the pump should draw a wide column of water at low speeds. This would maintain a high flow rate while directing all of the water through the discharge pipe. Increasing the pipe diameter would also increase the torque load on the engine, as the water would be heavier, so that it can operate closer to its best efficiency point.

A higher torque load would make the pump difficult to operate in manual mode. Therefore, the hand crank could not be attached to the main shaft, like it is in the current prototype. Instead, another set of pulleys would have to be added to reduce the load for the user, as in Figure 4.48. The sizes of the various pulley wheels would have to be modified accordingly.

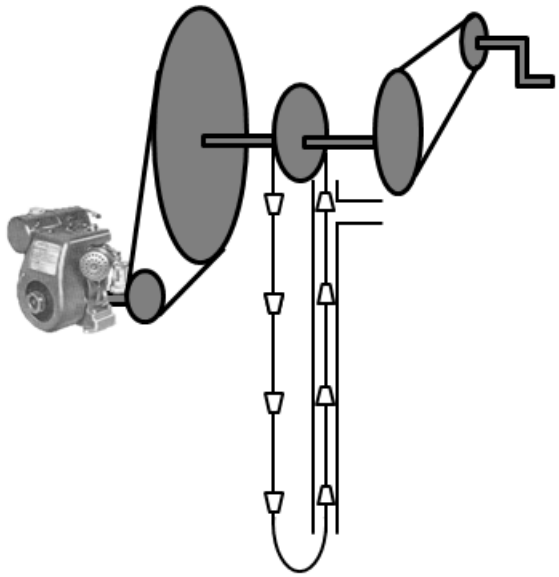

Figure 4.48. Modified concept of the rope pump, with an extra set of pulleys for the hand crank, that allows a user to manually draw a heavier load of water from the well.

The removability of the engine and handle should be improved. When Salim, the farmer who owns the well, removed the engine and then put it back, he did not place it in exactly the same location. Therefore, the v-belt was a bit loose, and when the engine was run, the v-belt fell off the pulleys. Salim did not realize that the adjusting and lock bolts would allow him to adjust the position of the engine to increase the tension. A sticker with clear graphical instructions (the instructions should be text-free because many farmers are illiterate) should be affixed to the engine plate.

On this first prototype, the v-belt must be removed from the large pulley in order to switch into manual mode. Keeping the v-belt on the pulleys requires the user to apply much more force, so it is difficult and exhausting for the user to turn the shaft. Plus, if the user is not careful and forgets to move the engine operation dial to "stop" rather than "start" or "run," the engine could actually turn on—and if the engine unexpectedly turns on, the hand crank could seriously injure the user. However, repeatedly removing and replacing the v-belt could lead to decreased tension in the belt over time and accelerate wear and tear on the belt, thereby decreasing the lifetime of the belt. The need to remove the v-belt could be eliminated by splitting the driveshaft into two between the large pulley wheel attached to the engine and the rope pulley wheel and using a clamp-on shaft coupling that the user can clamp for engine mode and unscrew for manual mode.

As discussed in Section 4.7.2 Usability and User Feedback, the handle for manual mode needs to be more securely fastened to the pump with a set screw. The screws for the handle and

the shaft coupling should be the same size so that the same screwdriver can be used. A better option would be to use screws that could be tightened by hand, such as with wing nuts, so that a screwdriver is not needed. Additionally, the handle needs to be enlarged and more ergonomically designed to improve usability. A small storage pocket for the handle should be welded onto one of the legs of the platform, so that the handle is always available at the pump for manual use without being stored far away in someone's house. Again, easy-to-understand graphical instructions for manual mode would need to be attached to the pump.

During the testing of the rope pump, the Vijay Villiers C12 engine proved capable of operating at points other than the single rating provided by the manufacturer and retailers. Future prototypes should take advantage of the full range of engine performance. The angular velocity and torque of the engine should be tested, perhaps using a tachometer and Prony brake, in order to gain an understanding of the engine's capacities. The next rope pump prototype should be designed such that the torque load at the deepest head is equal to the engine's maximum torque output, rather than the torque at the rated operation point (as in the current prototype).

Redesigning the pistons could improve efficiency. The gap between the piston and the pipe wall as well as the shape of the piston should be optimized. If the piston fits too tightly inside the pipe, friction between the piston and the pipe reduces efficiency; if the gap between the piston and pipe wall is too large, leakage reduces efficiency. Also, the shape of the piston should be investigated. Streamlining the shape to reduce hydrodynamic resistance may or may not make a difference in efficiency, because the knot that keeps the piston in place will change the flow around the piston.

The cost of the pump needs to be brought down to compete on the pump market. For both materials and labor, the first prototype cost INR 30,000 (USD 500), which is approximately twice as much as small centrifugal pumps (INR 10,000 to 18,000, or USD 170 to 300). The families interviewed indicated that they might be willing to invest a little bit more in this pump because it can serve multiple functions. They claimed an appropriate price for the system would be INR 15,000 to 20,000 (USD 250 to 335) and suggested that we investigate available government subsidies to drive down the price for farmers. It is hoped that, eventually, with mass-manufacturing the cost could decline significantly. Alternate materials could also be explored.

4.9 Chapter Conclusion

The hybrid motorized-manual rope pump has great potential to improve off-grid villagers' access to groundwater for irrigation and domestic uses. The first prototype, built with the assistance of Swastik Engineering Works, elicited positive feedback from both male and female users and could be easily repaired with locally-available parts and materials. Although the pump underperformed compared to the theoretical model, with some modifications this design could provide enhanced flow rates and efficiencies and affordability could be achieved. The next generation prototype of the pump should include the following modifications:

- The flow rates should be increased by capturing the flow that escapes through the top of the rising main, whether through a funnel-and-shroud system or by increasing the rising main pipe diameter.
- Mode-switching should be made simpler. The driveshaft could be split into two between the large pulley attached to the engine and the rope pulley so that the v-belt does not need to be removed for manual mode. A clamp could allow the user to connect or disconnect the engine-connected pulley.
- The hand crank should be more securely attached to the driveshaft in manual mode.
- The hand crank should be designed more ergonomically.
- A storage pocket for the hand crank should be welded to the frame.
- The pulleys should be resized to allow the pump to operate within the full range of the engine's capabilities. The next prototype should be designed such that the engine's maximum torque output equals the torque load at the highest head.
- The shape of the pistons should be optimized to maximize efficiency and flow rates.
- Easy-to-understand graphical instructions should be affixed to the pump.

The production costs of the first prototype included materials, mechanical parts, and labor. The fabricator, Swastik Engineering Works, was paid INR 30,000 (USD 500) in total to cover these costs. Once the design was completed, acquiring most of the materials took one day and fabrication took five days (though some materials were purchased after fabrication began). Troubleshooting at the well took another three days. One man (with the author) procured the materials and parts and two men helped with the fabrication process, especially with lathing and welding. One man from Swastik accompanied the author to the village to assist with

troubleshooting. Sharmaji, the owner of Swastik, estimated that the next pump could be built more quickly, likely in only two days, now that they have experience with this particular design. The reduced time required would, in turn, lower the labor costs and total production cost.

Chapter 5: Strategies to Reduce Evaporation from Tanks

5.1 Introduction

Manmade ponds, more commonly called "tanks" in India, are a common form of water storage for irrigation throughout India. According to the Government of India's Ministry of Agriculture, 1.985 million hectares of land, or 3% of all irrigated land, are irrigated with tanks as of 2009. In 2001, the Minor Irrigation Census divided these hectares into farmer classes, as defined by operational land holdings, shown in Table 5.1. Tank usage is skewed towards marginal and small farmers, whose holdings comprise 38% and 26% of all land irrigated by tanks, respectively [99], because in many cases they cannot afford more cost-intensive irrigation systems [100]. Farmers who use tanks have identified that evaporation losses greatly reduce their water supply.

Table 5.1. Distribution of irrigated area according to water source by classes of land holdings, 2001 **[99]**

Holdings Class	Canals [kHa]	Tanks [kHa]	Wells [kHa]	Tubewells [kHa]	Others [kHa]	Total [kHa]
Marginal (< 1 ha)	3405	855	1296	5419	1409	12384
Small (1 – 2 ha)	2929	587	1971	4335	1069	10891
Semi-medium (2 – 4 ha)	3219	463	2500	4740	1010	11932
Medium (4 – 10 ha)	3447	276	2511	4502	811	11547
Large (> 10 ha)	1578	77	952	1715	550	4872
Total	14578	2258	9231	20711	4849	51627

Two solutions are proposed to address this challenge. Used beverage bottles could be utilized to cover the surface of a tank in areas that have access to a large, affordable, and easily-acquired supply of these waste bottles. This bottles approach is akin to plastic balls on reservoirs. Very little preparation or maintenance is involved in simply throwing the bottles onto the surface of the water. The bottles should be somewhat filled with dirt in order to give the bottles more mass to prevent being blown around in the wind and to restrict sunlight from entering the water and feeding algal growth, since algae require UV.

In areas without easy, cheap access to a large supply of bottles, floats to cover the water could be constructed using old fabric stretched across a wooden frame with waste bottles as pontoons. The floats significantly reduce the number of bottles required and, depending on the local economy, may cost less than the bottles-only solution.

In order to determine the feasibility of these solutions, an experiment testing the effectiveness of these strategies was run, and environmental and economic factors were analyzed. The experiment was run—and is, in fact, still being run—at Vigyan Ashram in the village of Pabal, Maharashtra, about sixty kilometers by road from Pune. Vigyan Ashram is a vocational school that trains regular school drop-outs in technical skills related to mechanical and electrical engineering as well as agricultural skills such as animal husbandry and aquaponics, and some of its facilities are part of MIT's Fab Lab network. The solutions proposed therefore were evaluated in the area surrounding Pabal. It is hoped that this solution could be universalized and adopted in other regions of India as well as the world, but similar questions about the tank uses and sizes and the economics of acquiring waste bottles would have to be reassessed in each target region. In order to avoid challenging village politics of common water resources, this research focuses only on privately-owned tanks used solely for irrigation.

5.2 Literature Review

5.2.1 Evaporation Reduction Strategies

Water utilities worldwide have devised strategies to mitigate evaporation losses. Australia has been especially interested in water storage research as the climate there becomes increasingly dry. According to the Department of Natural Resources and Mines (2003), Watts (2005), and Craig (2008), the methods investigated and employed include floating covers, shade structures, chemical retardants, biological covers, and floating objects [101, 102, 103]. The advantages and disadvantages of these options (excluding biological cover), as well as commercially-available products for each option, are given in Table 5.2.

Floating covers work by creating an airtight seal above the water body. These covers experience almost 100% effectiveness in blocking evaporation, but the seal does not allow rainfall to permeate. Installation is complicated and expensive.

Shade structures, also called shade cloths, reduce the amount of solar radiation that reaches the water body and lower the wind speed above the water. Some types of shade cloths allow for rainfall to permeate, thereby increasing the water supply and eliminating pooling on the cloth. Since the structure is not airtight, oxygen can still infiltrate the water. However, maintaining suspension remains difficult, and the cost of installation is often high.

Chemical retardants, also called monolayers because they consist of a single-molecule layer, are usually made of a type of biodegradable fatty alcohol that must be replaced very frequently, sometimes every few days. Monolayers do not impact the wind; they work simply by limiting the transfer of H_2O molecules at the air-water boundary layer. The monolayers are cheaper than most other options, but they must be re-applied (and thus re-purchased) regularly. The long-term environmental effects of the alcohols can also be called into question.

Biological covers such as lily pads, duckweed, or other floating or deep-rooted vegetation have proven ineffective. Depending on the vegetation, transpiration occurs, the albedo could be lower than that of the water, and the surface roughness can raise water vapor transfer rates.

Floating objects, sometimes referred to as modular floating covers, comprise either attached or free-floating individual floating modules, as the name suggests. By trimming the surface area of the water exposed to the air, the floating objects reduce the effective wind speed over the entire water body and, depending on the albedo of the material, and thus can lower the energy input. The modularity allows for flexibility in use, but available products have high costs.

The proposed water bottle and/or floats solutions fall within the floating object category. The advantages of the floating object approach include approximately 70% evaporation reduction, easy installation, and low maintenance requirements, and reduced growth of algae [101]. However, as the Department of Natural Resources and Mines (2003) and Yao et al. (2010) point out, using floating objects can result in several negative impacts on water quality and the environment. These disadvantages include a reduction in dissolved oxygen leading to the growth of anaerobic microbes (which, among other issues, emit methane), trapping of various gases, loss of habitat for aquatic flora and fauna, and disruption of ecosystems (for example, if an aquatic animal in the pond sitting at the bottom of the food chain for the local ecosystem dies out, animals up the chain will suffer from a food shortage) [101, 104]. However, some of these impacts should be less severe using the water bottles, because the space in between bottles allows air to come into contact with the water. Some water quality impacts will be monitored during the experiment.

Table 5.2. Summary of evaporation reduction strategies. **[101, 102, 103]**

Evaporation Reduction Strategy	Effectiveness	Potential Water Quality Impacts	Potential Environmental Impacts	Installation and Maintenance	Products	Range of Costs
Floating Covers	Close to 100%	Anaerobic conditions lead to increased iron, manganese, ammonia. Reduced growth of algae.	Loss of habitat, disruption of ecosystems.	Complex installation, low maintenance requirements.	E-VapCap, FabTech, Fabric Solutions International, Quit Evap, Evap-Mat, CURV, REVOC, Defined Sump	$3.40 (Evap-Mat) – $28.85 (REVOC, Defined Sump) per m^2
Floating Objects	Approx. 70%	Similar impacts as floating covers, but less severe.	Similar impacts as floating covers, but less severe.	Easy installation, low maintenance requirements.	Aquacap, Euro-matic Bird Balls, AgFloats, AquaGuard, Raftex, Layfield Modular Cover, LemTec Modular Cover System, HexDome, MOD-E-VAP	$3.85 (Raftex) – $21.90 (Bird Balls) per m^2
Shade Structures	Up to 75%	Reduced growth of algae.	Loss of habitat, disruption of ecosystems.	Complex installation, low maintenance requirements.	AquaSpan, NetPro, MuzCov, POLYNET	$6.00 (NetPro) – $31.75 (AquaSpan) per m^2
Chemical Evaporation Retardants (monolayers)	Varies, 20 – 40%	None.	Reduced oxygen levels, increased bacterial activity.	Easy installation, no maintenance.	Water$avr, Hydrotect, CIBA Polyacrylamide (PAM), Aquatain	$7.20 (Hydrotect) – $17.30 (Water$avr) per ha

5.2.2 Chemical Leaching from PET Bottles

The disposable beverage bottles to be used in the proposed evaporation reduction strategy are made of polyethylene terephthalate (PET). Toxic chemicals such as phthalates, antimony, and aldehydes can leach out of the PET plastic into the water when the bottles are exposed to the sun for an extended period of time. These chemicals can act as endocrine disruptors and are especially harmful to child development and pregnant women [105, 106]. Floats currently used for evaporation reduction are typically made of high density polyethylene (HDPE), which is not known to leach harmful chemicals [104].

Many studies have proven that these chemicals from PET bottles do not leach at high enough concentrations to pass maximum contaminant levels, as determined by health agencies such as the World Health Organization (WHO), the United States Environmental Protection Agency (US EPA), and the European Food Safety Authority (EFSA) of the European Union (EU). The results of various studies are summarized in Table 5.3. The studies have primarily focused on water within bottles, with volumes between 0.5 and 2 L. Schmid et al. (2008), Leivadara et al. (2008), Casajuana and Lacorte (2003), and Bošnir et al. (2007) find that the phthalates DEHP, DEHA, BBP, and DBP never reach the maximum allowable concentrations [105, 107, 108, 109]. Only one case of antimony leaching surpassed the health limit, but these bottles were subjected to the extreme temperature of 80 °C. That test, conducted by Westerhoff et al. (2008), was attempting to simulate the transportation conditions within a sealed truck in hot climates such as Arizona [110]. As hot as India can get, the bottles on the tanks will not experience such high temperatures in open air. The rest of the antimony studies, by Shotyk (2006), Westerhoff et al. (2008), Keresztes (2009), Bach (2011), and Cheng (2010), do not find any unacceptable concentrations [111]. The limits for formaldehyde and acetaldehyde are also never reached, as proven by Wegelin (2001) and Dabrowska et al. (2003) [111].

Even in the small volumes within water bottles and in the longer-term studies up to six months, the concentrations of phthalates and antimony do not pass limits set by health organizations around the world. In a typical tank, which has a significantly larger volume of water than a bottle, the chemicals will exist in much lower concentrations. It is thus highly unlikely that the chemicals leaching from PET will pose a threat. In addition, the water in the tanks is primarily

used for irrigation, which has lower water quality requirements than drinking water. Therefore, these chemicals will not be monitored during the experiment.

Table 5.3. Summary of study results for various chemicals leaching from PET bottles. Modified from **[111]**.

Chemical	Health Limit	Exposure Conditions	Upper Bound Concentration	Study
DEHP	6 mg/L (US EPA)	17 hours, sunlight, room temperature	0.38 μg/L	Schmid et al. [2008]
		17 hours, sunlight, 60 °C	0.71 μg/L	Schmid et al. [2008]
		3 months, sunlight, up to 30 °C	< 0.02 μg/L	Leivadara et al. [2008]
		30 days, 22 °C	50 μg/L	Bošnir et al. [2007]
		10 weeks, up to 30 °C	0.188 μg/L	Casajuana and Lacorte [2003]
DEHA	80 μg/L (WHO)	17 hours, sunlight, 60 °C	0.046 μg/L	Schmid et al. [2008]
		17 hours, sunlight, ambient temperature	0.025 μg/L	Schmid et al. [2008]
BBP	30 mg/L (EU)	30 days, 22 °C	< 0.005 μg/L	Bošnir et al. [2007]
		10 weeks, up to 30 °C	0.010 μg/L	Casajuana and Lacorte [2003]
DBP	0.3 mg/L (EU)	30 days, 22 °C	50 μg/L	Bošnir et al. [2007]
		10 weeks, up to 30 °C	0.070 μg/L	Casajuana and Lacorte [2003]
Antimony	6 μg/L (US EPA)	24 hours, room temperature	10.51 μg/L	Cheng et al. [2010]
		6 months, room temperature	0.566 μg/L	Shotyk et al. [2006]
		3 months, 22 °C	0.386 μg/L	Westerhoff et al. [2008]
		< 1 year, 22 °C	0.42 μg/L	Keresztes et al. [2009]
		45 days, 40 °C	2.0 μg/L	Bach [2011]
		7 days, sunlight, 80 °C	4.611 μg/L	Cheng et al. [2010]
		7 days, 80 °C	14.4 μg/L	Westerhoff et al. [2008]
Formaldehyde	15 mg/L (EU)	63 days, sunlight	44 μg/L	Wegelin [2001]
		126 days, sunlight	1 μg/L	Wegelin [2001]
		6 days, room temperature	7.8 μg/L	Dabrowska et al. [2003]
Acetaldehyde	6 mg/L (EU)	63 days, sunlight	3 μg/L	Wegelin [2001]
		126 days, sunlight	2 μg/L	Wegelin [2001]
		6 days, room temperature	5.3 μg/L	Dabrowska et al. [2003]

5.2.3 Tanks as Common Property and Government Policy

In addition to health and environmental concerns, societal challenges may impede implementation. Karthikeyan (2010) and Anbumozhi et al. (2001) describe the history and present-day problems of tank management. Historically, tanks were built and maintained by an authoritarian ruler. The Chola kings of present-day Tamil Nadu originally established the tank system. When the British conquered South India, they imposed the *zamindari* system, wherein a single landlord, called a *zamindar*, ruled over a large area. Both the kings and the *zamindar*s had the power to enlist people to maintain the tanks [100]. In the case of Maharashtra specifically, the revenue collector, called a *malguzar*, held this power [112]. In 1947, independence gave birth to democracy, thereby abolishing the *zamindari* system. As a result, these tanks became common property resources under the responsibility of the democratic local governments. Competing uses of the water (irrigation, livestock, domestic uses, etc.) and murky water rights have led to weak water management and water conflicts continue to frequently erupt in villages [100]. The lack of regulation and disagreements over who owes labor to maintain the tanks have resulted in many tanks falling into disrepair and disuse [113].

Despite these challenges, the government and several organizations recognize the potential for tanks to harvest rainwater. Government initiatives heavily subsidize farm tanks for irrigation purposes on individual farms. The Rashtriya Krishi Vikas Yojana (RKVY), or National Agriculture Development Program, funds the installation of farm tanks as well as ponds for fisheries. The Mahatma Gandhi National Rural Employment Guarantee Act (MNREGA), the National Food Security Mission, the National Horticulture Mission, the Rainfed Area Development Programme, the Acceleration Irrigation Benefit Programme, and other government policies also promote and fund the construction of farm tanks. For example, the National Horticulture Mission gives a farmer 50 to 75% of the total cost of tank installation. Deeper subsidies are allocated to Scheduled Tribes and Scheduled Castes [114].

Non-governmental organizations such as PRADAN, NM Sadguru Water and Development Foundation, and Samaj Pragati Sahayog, which tend to focus on smallholder farmers, have incorporated mini-tanks into their watershed development schemes for poorer farmers. These NGOs encourage farmers to set aside approximately 5% of their land to build a tank for rainwater harvesting, among other water management strategies.

5.3 Tank Usage in Maharashtra and Demand of Waste Bottles

Approximately 52% of cultivable land in Maharashtra is prone to drought, so the state government has been encouraging the construction of tanks as a back-up water supply, a form of insurance in case of rain failure called "protective irrigation," as part of the RKVY. The tanks can also provide water for irrigation during the *rabi* and summer crop seasons. Modern-day tanks in Maharashtra fall primarily into two categories: rehabilitated historical community tanks, called Malguzari tanks after the *malguzar*s, or revenue collectors, who were in charge of hiring workers to maintain the tanks [112], and government-subsidized individually-owned farm tanks. This research is focusing on the individual tanks, as the Malguzari tanks, a common property resource, are subject to many competing uses and complicated community politics.

As of December 2011, the RKVY funded the construction of 69,279 farm tanks with approximately INR 4.1 billion (USD 67 million) in Maharashtra. In April 2012, another 100,000 tanks were planned under various programs in the state, including MNREGA, National Horticulture Mission, and the Integrated Development of 60,000 Pulses Villages in Rainfed Areas initiative. The National Food Security Mission provides pump sets for these farm tanks. The sizes of tanks installed under the RKVY vary depending on each farmer's landholdings and the terrain. Average subsidies vary from INR 52,000 to 82,500 (USD 850 to 1330) and the farmers must contribute INR 150,000 to 250,000 (USD 2420 to 4040), depending on the tank size [115]. The most common sizes in Maharashtra are 20 meters long by 20 meters wide by 3 feet deep and 30 meters long by 30 meters wide by 3 meters deep. Between forty and fifty bottles are required to cover a one square meter area (the variation in number stems from the diverse sizes of beverage bottles). Therefore, in order to cover a typical tank's surface area of 900 m^2, approximately 36,000 to 45,000 bottles would be required.

The National Fisheries Development Board and Maharashtra's Department of Fisheries promote aquaculture in these ponds in order to both increase the fertilizing properties of the water and enhance livelihood through the sale of fish for human consumption. Farmers have seen that irrigating with water fertigated with fish dung reduces their expenditures on chemical fertilizers. Fish require 5 ppm of dissolved oxygen to live healthily, but they can survive (albeit stressed) at levels of dissolved oxygen above 2 ppm [116]. The dissolved oxygen levels in the treatment tanks are thus being monitored. If dissolved oxygen levels are found to be too low when the entire surface is covered, it may be better to cover less of the water surface in order to achieve a balance between

aquatic life and irrigation. Another option would be to leave the tank uncovered while fish are raised, and then to cover the water after the fish are harvested.

5.4 Supply of Waste Bottles in Pabal and Pune, Maharashtra

The area around Pabal is served by two scrap dealers, who pay waste pickers to collect trash from the streets. One scrap dealer explained that he hires his own waste pickers who live in the area, while the other scrap dealer said he relies on traveling waste pickers, who roam from village to village collecting and selling waste. One owner of a hotel (in India, a hotel implies an eatery, not necessarily a place of lodging) who was interviewed explained that he encouraged his customers to simply throw their trash out of the hotel and in the street—or if they did not do this, then he did—and waste pickers would come by regularly to collect what had been discarded. However, several local hotels and shopkeepers see the opportunity to earn an additional source of income and sell their garbage directly to the scrap dealers, without waste picker intermediaries. Typically, the scrap dealers in Pabal sell their waste, unprocessed, to wholesalers who come from Pune. The scrap dealers purchase PET bottles from waste pickers for INR 15 to 21 (USD 0.24 to 0.34) per kilogram and sell to the Pune wholesalers at INR 30 to 40 (USD 0.38 to 0.65) per kilogram.

Upon interviewing the scrap dealers, it was discovered that approximately 100,000 bottles are collected over the course of a year, with the majority being collected during the hot summer season from early April to early June. An unknown percentage of these bottles are not usable on a tank; many bottles are crushed or missing caps. The annual distribution of waste bottle collection is summarized in Table 5.4. Not only is summer the time of year when people are thirstiest due to the dry heat, but it also coincides with the marriage season. Weddings bring travelers, and it is actually travelers who purchase the disposable bottles, to take with them on their journeys. Pabal serves as a commercial and transport hub for the surrounding villages, so many travelers pass by the village center on their way to weddings. Perhaps collection points could be set up throughout the area for travelers to deposit their bottles. Awareness campaigns could educate the public on the need for uncrushed bottles with caps.

Table 5.4. Waste PET bottle market in Pabal, Maharashtra. **[117]**

	Amount Collected					
	Summer		Winter		Buys at	Sells at
	kg	bottles	kg	bottles	(INR/kg)	(INR/kg)
Scrap Dealer 1	600	25000	—	—	15 – 21	40
Scrap Dealer 2	1200	50000	600	25000	16	30

Since the Pabal area does not collect enough bottles to cover more than two tanks, bottles could be transported from Pune. A meeting with the Data Manager of Solid Waste Collection and Handling Cooperative (SWaCH), the enterprise founded by Kagad Kach Patra Kashtakari Panchayat (KKPKP), the trade union of waste pickers, revealed that a large supply of bottles is available in Pune. Approximately 200,000 bottles are collected every day by the SWaCH waste pickers, who collect waste from homes, the Pune Municipal Corporation (PMC), which sweeps streets and empties public dumpsters, and large commercial entities such as malls, which run their own waste collection operations. Waste pickers do not have space to store the bottles themselves, so at the end of the day they sell the bottles to scrap dealers at INR 20 to 25 (USD 0.32 to 0.40) per kilogram (there are approximately forty bottles in a kilogram). Typically, each waste picker collects between half a kilogram (20 bottles) and one kilogram (40 bottles) in a day. The scrap dealers then sell the bottles in bulk to larger scrap dealers or wholesalers at INR 30 to 40 (USD 0.38 to 0.65) per kilogram. These wholesalers either process the bottles into pellets to be used in manufacturing or sell the bottles to "super" wholesalers who process the pellets. The municipal solid waste cycle for Pune, excluding electronic waste and informal waste collection such as scavenging from landfills, is illustrated in Figure 5.1. The PET bottles fall into the "recyclables" category.

SWaCH recommended that if farmers choose to cover their tanks with bottles, it would be best to purchase the bottles from the scrap dealers for several reasons: (a) the waste pickers themselves do not have the capacity to store a large amount of bottles, (b) the scrap dealers maintain a sizable supply of bottles in their storehouses, (c) scrap dealers are fairly low in the waste chain and thus would be willing to sell the bottles at a lower price, and (d) the Pune Municipal Corporation (PMC) would not sell the bottles they collect to someone outside their system. According to SWaCH, the cost to transport bottles is INR 40 per kilometer per two thousand bottles. If a typical RKVY tank of 900 m^2 in Pabal requires an average of 40,500 bottles that must be transported sixty kilometers from Pune, the cost of the bottles for a tank would be INR 30,375

to 40,500 (USD 495 to 660) and delivery would cost INR 48,600 (USD 790), for a total of INR 78,975 to 89,100 (USD 1273 to 1440) to cover a tank. The cost per unit area would thus be INR 88 to 99/m^2 (USD 1.42 to 1.61/m^2).

5.5 Value of Water in Maharashtra

In order to determine the value of water to farmers, the author spoke with some farmers to discuss how much additional income they might be able to earn from improved yields due to increased water availability. All the farmers said they did not know and could not provide an answer, but one farmer explained that he paid the government a fee for irrigation water from state projects. This government tariff, then, will be used to assess the cost-effectiveness of the evaporation reduction strategies. Water rates for irrigation in Maharashtra, established by the Maharashtra Water Resources Regulatory Agency (MWRRA), are given in Table 5.5.

Table 5.5. MWRRA tariff for agricultural water. **[118]**

Season	**Water Rate for Rice (Rs/m^3)**	**Water Rate for Other Crops (Rs/m^3)**
Monsoon	0.04	0.03
Winter	0.08	0.06
Summer	0.12	0.09

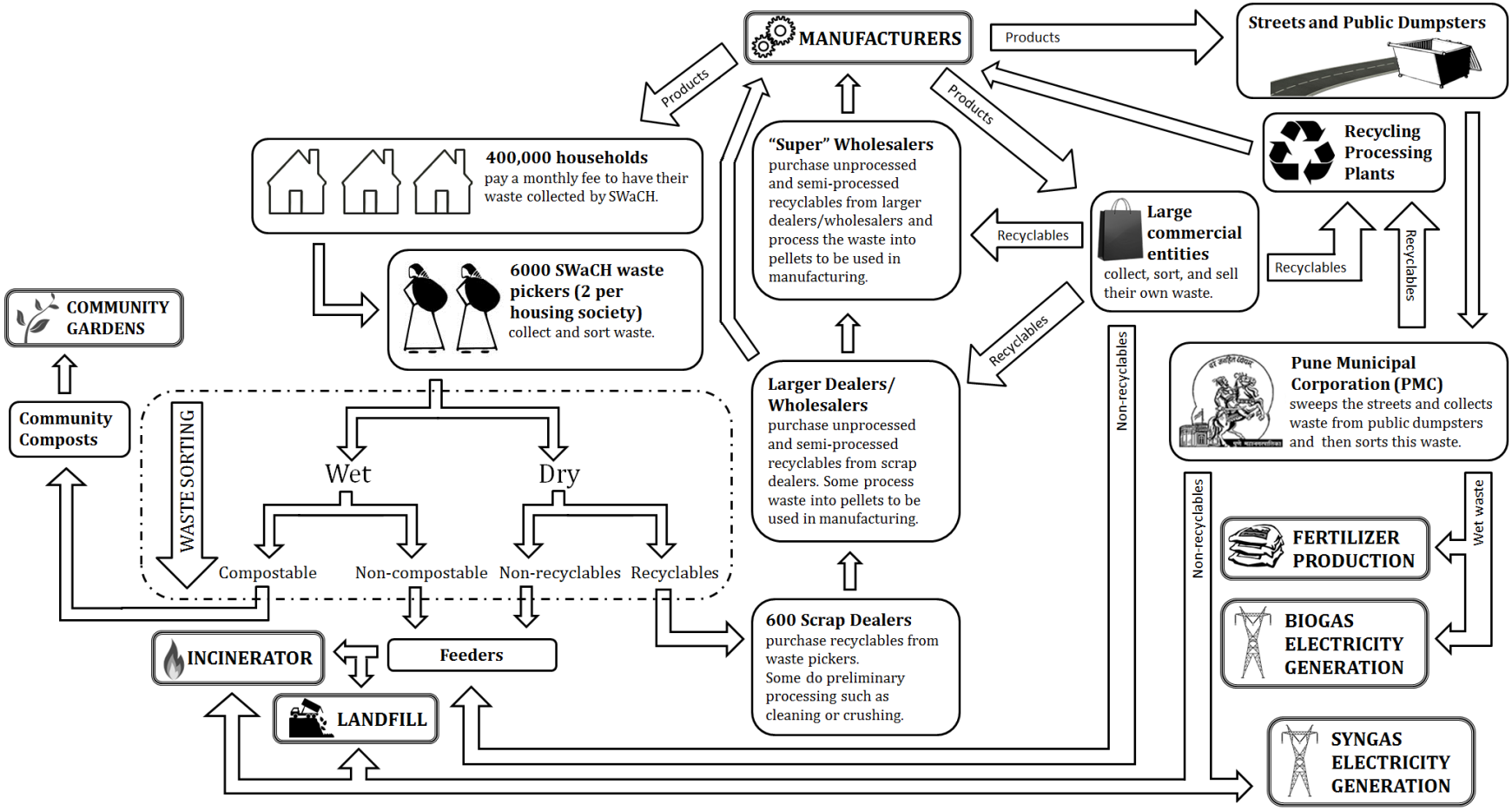

Figure 5.1. Waste cycle in Pune. PET bottles fall into the "recyclables" category. Information for this figure was gathered during interviews with SWaCH. **[119]**

5.6 Evaporation Model

The water level of a tank can be estimated through a water balance analysis. Water inputs include diversion of canals to the tank, runoff, and rainfall while water outputs include evaporation, seepage into the soil, spillage, and both irrigation and non-irrigation uses. The water balance is depicted in Figure 5.2. In order to isolate the water lost to evaporation, the experimental tanks were closed to users and disconnected from incoming sources such as canals and runoff. Only rainfall was allowed to enter the tanks. Although soil seepage was not accounted for in the experiment, it is important to keep in mind that as water levels rise, there is greater pressure at the water-soil interface, thereby increasing the rate of seepage. Thus the real gain in water level will not be as large as in the idealized experiment (unless the tank has an impermeable lining, but this is not very common, nor is it recommended due to the negative effects on groundwater recharge [120]). Li and Gowing (2004) found that water lost to seepage and percolation is equal to 10 ±2% of water lost to evaporation [121].

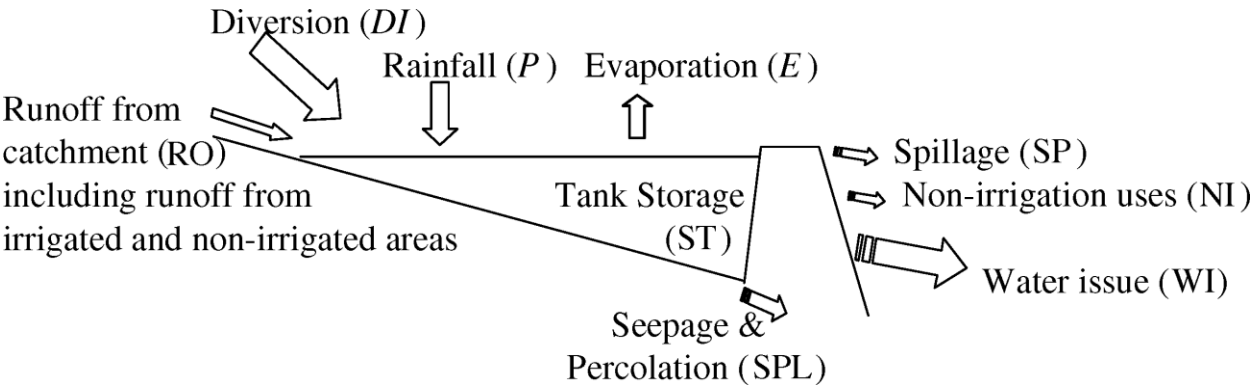

Figure 5.2. Model for water balance analysis of a tank. **[121]**

Various mathematical models for evaporation are described and evaluated by Kashyap and Panda (2001), McJannet et al. (2008), and Craig (2008) [122, 123, 103]. They conclude that the Penman-Monteith method most accurately predicts evaporation water losses. The Penman-Monteith equation for millimeters of water evaporated in a day is

$$E = \frac{1}{\lambda}\left[\left(\frac{\Delta}{\Delta+\gamma}\right)(R_n - G) + \left(\frac{\gamma}{\Delta+\gamma}\right) f(u)(e_s - e_a)\right] \quad \text{(Eq. 5.1)}$$

where

E	=	evaporative flux	[mm/day]
λ	=	latent heat of vaporization	[MJ/kg]
R_n	=	net radiation	[MJ/m^{2}day]
G	=	ground heat flux	[MJ/m^{2}day]
Δ	=	slope of the saturation vapor pressure-temperature (svp-t) curve	[kPa/°C]
γ	=	psychrometric constant	[kPa/°C]
$f(u)$	=	function of wind speed	
e_s	=	saturated vapor pressure	[kPa]
e_a	=	actual vapor pressure	[kPa]

The latent heat of vaporization λ is approximated as 2.45 MJ/kg, and the psychrometric constant, which is the ratio of the specific heat of moist air at constant pressure to the latent heat of vaporization, is approximated as 0.067 kPa/°C. The ground is assumed to be adiabatic, so $G = 0$. The slope of the svp-t curve is

$$\Delta = 0.2(0.00738T_a + 0.8072)^7 - 0.00016 \quad \text{(Eq. 5.2)}$$

where

T_a	=	average dry bulb air temperature	[°C]

The function of wind speed is

$$f(u) = 6.43(1 + 0.0536u) \quad \text{(Eq. 5.3)}$$

where

u	=	average wind speed	[m/s]

The saturated vapor pressure e_s is

$$e_s = 0.6108e^{\frac{17.27T_a}{T_a+237.3}} \quad \text{(Eq. 5.4)}$$

The actual vapor pressure e_a is

$$e_a = \frac{RHe_s}{100} \quad \text{(Eq. 5.5)}$$

where

RH	=	average relative humidity	[%]

The ground in this case is assumed to be adiabatic, so the heat flux G is zero. The daily net radiation R_n is calculated as

$$R_n = \frac{24 \text{ x } 60 \text{ x } 60}{10^6}\{\alpha Q_{sol} - \varepsilon\sigma[(T_w + 273.15)^4 - (T_a + 273.15)^4]\} \quad \text{(Eq. 5.6)}$$

where

α	=	absorptivity	
Q_{sol}	=	global horizontal solar radiation	[W/m^2]
ε	=	emissivity	
σ	=	Stefan-Boltzmann constant	[5.67 x 10^{-8} W/m^{2}K^4]
T_w	=	average water temperature	[°C]

and 24*60*60 represents the number of seconds in a day and 10^6 represents the number of joules in a megajoule to convert the J/m^{2}s to MJ/m^{2}day, as required by the original equation. Treating the water as a gray body and applying Kirchhoff's Law ($\alpha = \varepsilon$), the absorptivity and emissivity of water are assumed to be 0.97. The temperature of water is calculated using the following set of equations:

$$T_w = T_e + \left(T_{w_0} - T_e\right)e^{-\frac{1}{\tau}} \quad \text{(Eq. 5.7)}$$

where

T_e	=	equilibrium temperature	[°C]
T_{w0}	=	initial water temperature	[°C]
τ	=	time constant	[days]

The equilibrium temperature T_e is calculating using

$$T_e = T_{wb} + \frac{R_{wb}}{4\sigma(T_{wb} + 273.15)^3 + f(u)(\Delta_{wb} + \gamma)} \quad \text{(Eq. 5.8)}$$

where

T_{wb}	=	wet bulb temperature	[°C]
R_{wb}	=	net radiation at wet bulb temperature	[°C]
Δ_{wb}	=	svp-t curve at wet bulb temperature	[°C]

The wet bulb temperature is

$$T_{wb} = \frac{0.066T_a + \left(\frac{4098e_a}{(T_d + 237.3)^2}\right)T_d}{0.066 + \left(\frac{4098e_a}{(T_d + 237.3)^2}\right)} \quad \text{(Eq. 5.9)}$$

where

T_d	=	dew point temperature	[°C]

The net radiation at wet bulb temperature is

$$R_{wb} = \frac{24 * 60 * 60}{10^6}\{\alpha Q_{sol} - \varepsilon\sigma[(T_{wb} + 273.15)^4 - (T_a + 273.15)^4]\} \quad \text{(Eq. 5.10)}$$

and the svp-t curve at wet bulb temperature is

$$\Delta_{wb} = \frac{4098\left[0.6108e^{\frac{17.27T_{wb}}{T_{wb}+237.3}}\right]}{(T_{wb} + 237.3)^2} \quad \text{(Eq. 5.11)}$$

The time constant τ is calculated as

$$\tau = \frac{\rho_w C_w Z}{4\sigma(T_{wb} + 273.15)^3 + f(u)(\Delta_{wb} + \gamma)} \quad \text{(Eq. 5.12)}$$

where

ρ_w	=	density of water	[kg/m^3]
C_w	=	specific heat of water	[MJ/kgK]
Z	=	depth of water	[m]

The density of water is assumed to be 1000 kg/m^3 and the specific heat of water is approximated as 4.18 x 10^{-3} MJ/kgK. The depth of water Z is re-calculated each day to account for the previous day's rainfall gains and evaporative losses.

$$Z_i = Z_{i-1} - E_{i-1} + RF_{i-1} \quad \text{(Eq. 5.13)}$$

where

RF	=	daily rainfall	[mm]

To determine the range of possible water levels, the effectiveness of evaporation reduction was varied as follows:

$$Z_i = Z_{i-1} - (1 - \varepsilon)E_{i-1} + RF_{i-1} \quad \text{(Eq. 5.14)}$$

where

ε	=	effectiveness

Effectiveness was varied from 0 to 100%.

In order to estimate the amount of evaporation the experiment site might experience, data from a nearby weather station was input into these equations. The input data for dry bulb temperature, dew point temperature, wind speed, relative humidity, and global horizontal radiation were taken from the typical meteorological year (TMY) file prepared for the US Department of Energy's EnergyPlus building modeling program by the Indian Society of Heating, Refrigerating, and Air-Conditioning Engineers (ISHRAE) [124]. The TMY file stores data recorded from the weather station at the Pune airport in 1990. Pune was selected because it is the closest major weather station to the experiment site in Pabal, which is about 40 km northeast of Pune as the crow

flies. Rainfall data for the same year, 1990, for Pune was taken from Asian Precipitation – Highly Resolved Observational Data Integration Towards Evaluation of Water Resources (APHRODITE), an initiative conducted jointly by the Research Institute for Humanity and Nature (RIHN) and the Meteorological Research Institute of Japan Meteorological Agency (MRI/JMA) [125].

These calculations were completed for every day of a calendar year using MATLAB. The initial water temperature was determined through an iterative process that concluded when T_w of the control tank on January 1 of the first year was within 0.01 °C of T_w of the control tank on December 31 of the first year. Because the experiment was to be conducted starting June 1, the calculations were run for a second year, with the initial water depths and temperatures for control and treatment tanks on January 1 of the second year equal to the water depths and temperatures for each on December 31 of the first year. The results for the daily water depths are given in Figure 5.3**.** Figure 5.4**,** Figure 5.5**,** and Figure 5.6 show the results for water temperature, daily evaporative losses compared to rainfall, and a closer look at daily evaporative losses. These four plots all assume the treatment tanks to be 100% effective in blocking evaporation to show the maximum potential differences.

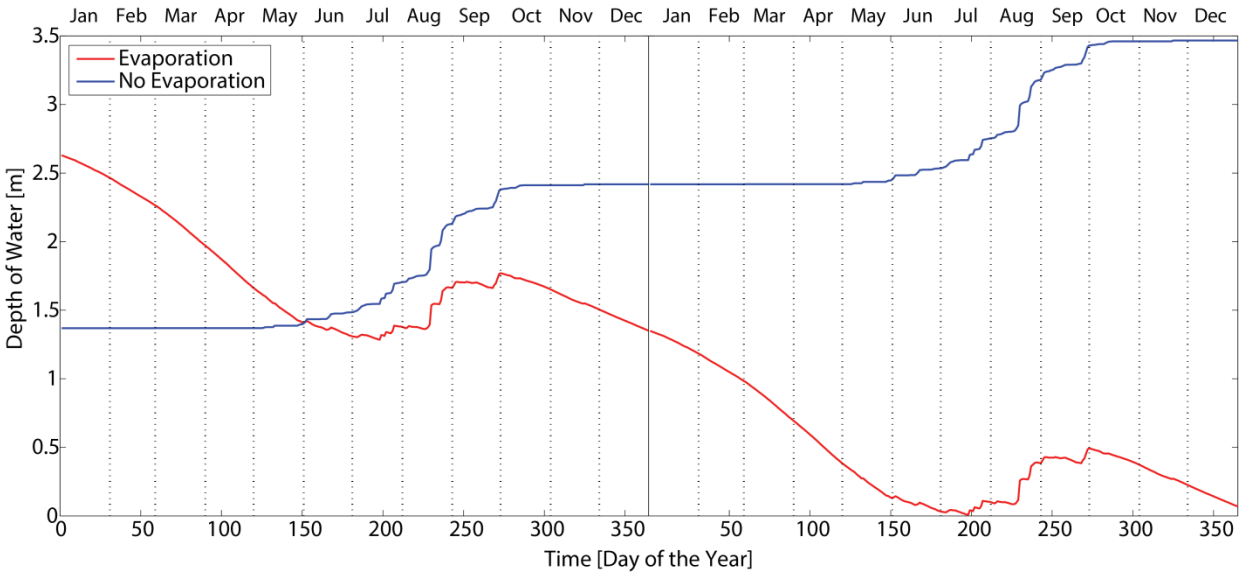

Figure 5.3. Water depth over two years for the control tank and the treatment tank. The treatment tank is assumed to be 100% effective here in order to find the maximum possible water depth. However, in actuality the depth would be expected to be about 70% effective in the treatment tank.

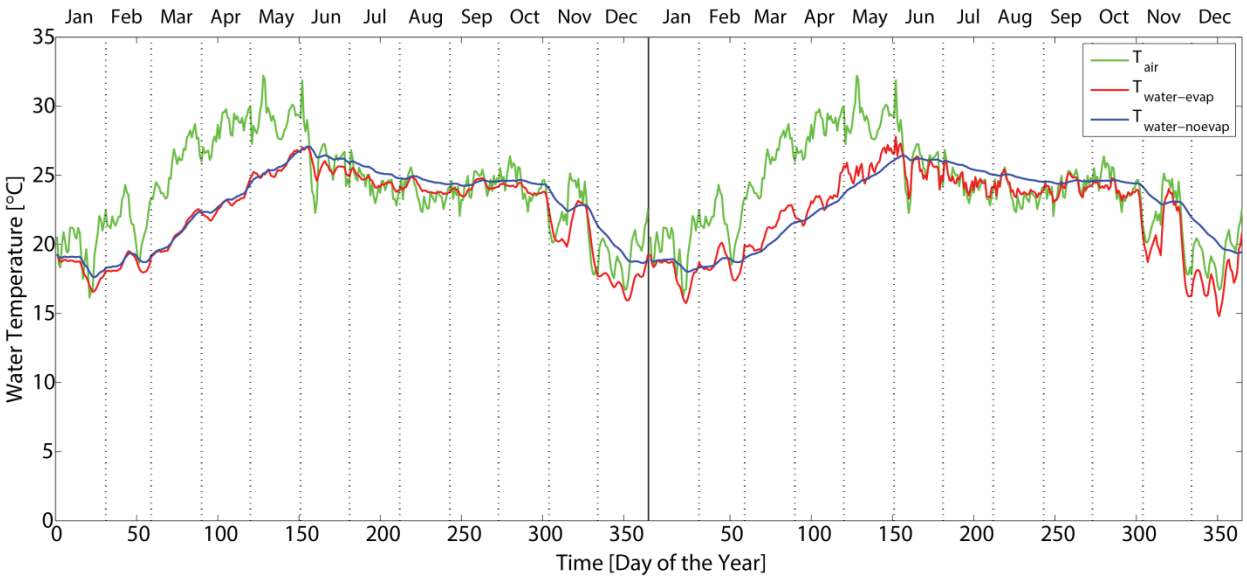

Figure 5.4. Temperatures of the air and water throughout the year. $T_{water\text{-}evap}$ is the temperature of the water in the control tanks, while $T_{water\text{-}noevap}$ is the temperature of the water in the treatment tanks.

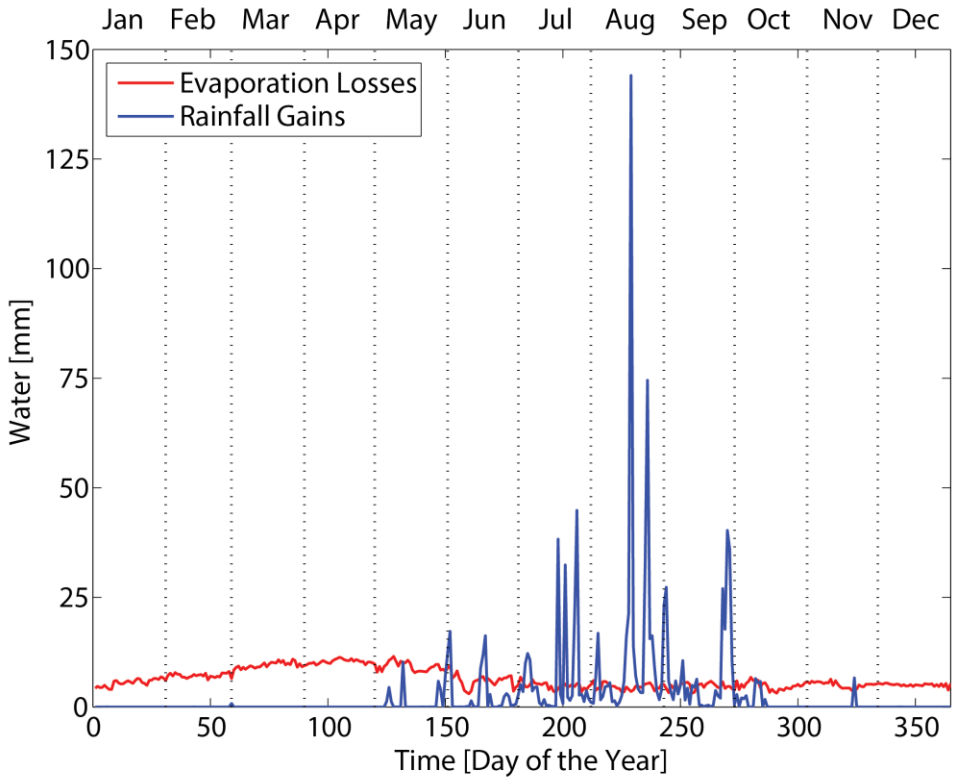

Figure 5.5. Water losses from evaporation and water gains from rainfall throughout a calendar year.

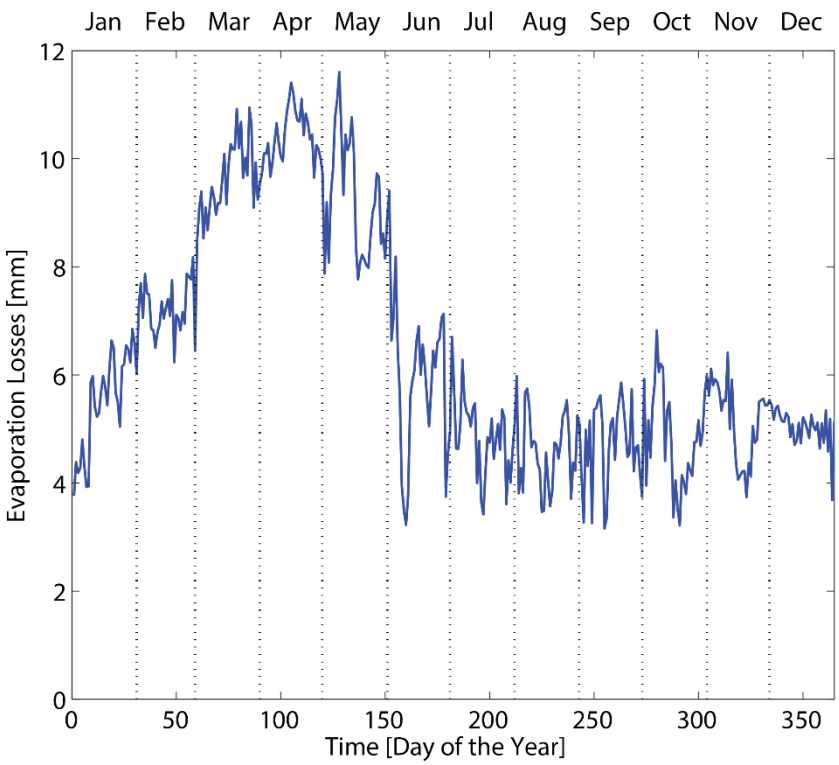

Figure 5.6. A closer look at evaporative losses throughout a calendar year.

5.6.1 Potential Return of Investment

In order to estimate the water gains over a year with the bottles treatment, the model was run again assuming a full tank at the end of monsoon season (October 1) for a typical tank with a depth of 3 m and varying evaporation effectiveness. Figure 5.7 shows the water levels over the course of a year, and Figure 5.8 gives the effectiveness versus total water gain in one year. Assuming an evaporation reduction effectiveness of 70% and typical tank dimensions of 30 m x 30 m, the water gained in one year would be 1476 m^3. The potential return of investment (ROI) was calculated for several crops commonly cultivated in Maharashtra, including pearl millet, soybean, wheat, and gram. The ROI is

$$ROI = \frac{profit}{investment} \quad \text{(Eq. 5.15)}$$

It was assumed that the extra water available would be used to irrigate and cultivate additional land. This additional land would then require all the inputs of cultivation such as fertilizer, pesticides, herbicides, and labor. These costs were included in the investment, so the total

investment was calculated as the sum of the cost of waste bottles (assumed to be INR 78,975, as described above in Section 5.4) and the cultivation costs (excluding irrigation, since that is the benefit of the evaporation reduction scheme). The revenue was assumed to be the farm-gate price of each crop. (The farm-gate price is the price a farmer receives for his crop and is not the same as the retail price on the market.) The profit was the revenue minus the costs. All yield, farm harvest price, and cultivation cost data is for Maharashtra in the year 2009-2010. This data was retrieved from IndiaStat.com and was originally collected by the Government of India's Ministry of Agriculture. The results are shown in Table 5.6. Interestingly, the data reveals that farmers earn very little money from their crops. More investigation is required to understand why profits are so small and why farmers continue to farm despite the minimal profits. The ROI for the waste bottle evaporation reduction strategy for one year varies from -4.2% for pearl millet to +1.8% for wheat.

Table 5.6. Return of investment for the waste bottle evaporation reduction treatment for various crops. **[126, 127]**.

	Farm Harvest Price [INR/kg]	**Yield [kg/ha]**	**Revenue [INR/m^2]**	**Cultivation Cost Excluding Irrigation [INR/m^2]**
Pearl Millet	8.62	741	0.64	1.74
Soybean	21.32	728	1.55	1.32
Wheat	12.08	1610	1.94	1.42
Gram	20.24	863	1.75	1.73
	Water Required [mm]	**Additional Land Cultivated [m^2]**	**Profit from Additional Land [INR]**	**ROI [%]**
Pearl Millet	400	3690	-4064.14	-4.22
Soybean	670	2203	507.43	0.55
Wheat	450	3280	1699.20	1.82
Gram	250	5904	73.19	0.08

*The water gained from the 70% effective treatment is 1476 m^3, based on the evaporation model.

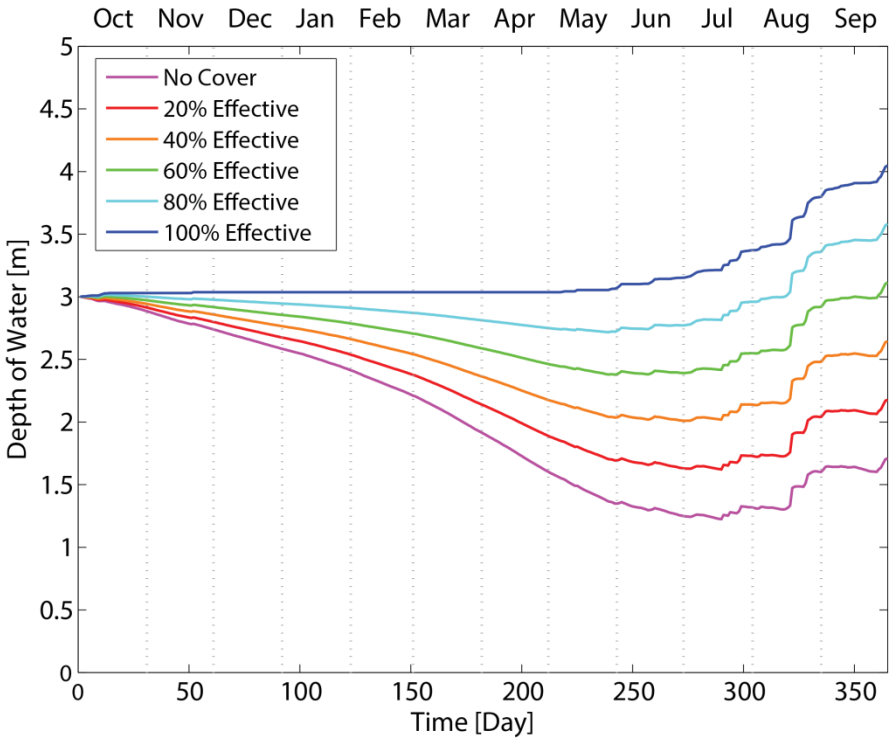

Figure 5.7. Water levels in a typical 3 m deep tank with varying evaporation reduction effectiveness over a year starting at the end of monsoon season.

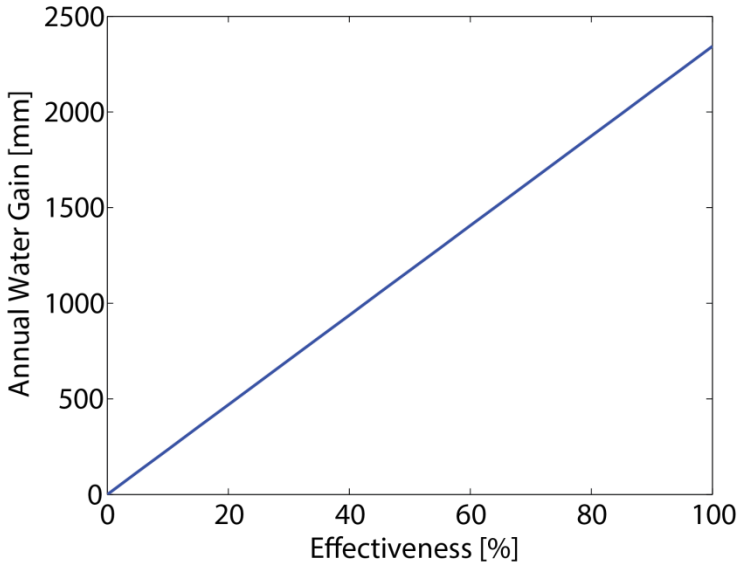

Figure 5.8. Evaporation reduction effectiveness vs. annual water gain for Pune, Maharashtra.

5.7 Experiment

An experiment to test each solution is currently taking place over the course of one year, or until the control tanks dry out. Both water levels and water quality are being monitored in order to ensure that the method of placing waste bottles or a float on the surface of a pond is both effective and safe for human health and the environment.

5.7.1 Trial Run

Before the longer-term experiment was set up, Vigyan Ashram conducted a brief trial run for five days from April 23 to 27, 2013 in Pabal. During this trial run, two 1 m wide x 1 m long x 12 cm deep tanks were placed side-by-side on a rooftop and filled with water. The treatment tank was completely covered in bottles (forty were required), and the control tank was left uncovered. The water level was recorded four times each day, at 9:30 am, 12:30 pm, 4:30 pm, and 6:00 pm. The results of this trial experiment are shown in Figure 5.9. In these five days, evaporative losses were reduced by 47%. Therefore, this treatment proved promising and it was decided to move forward with the larger experiments.

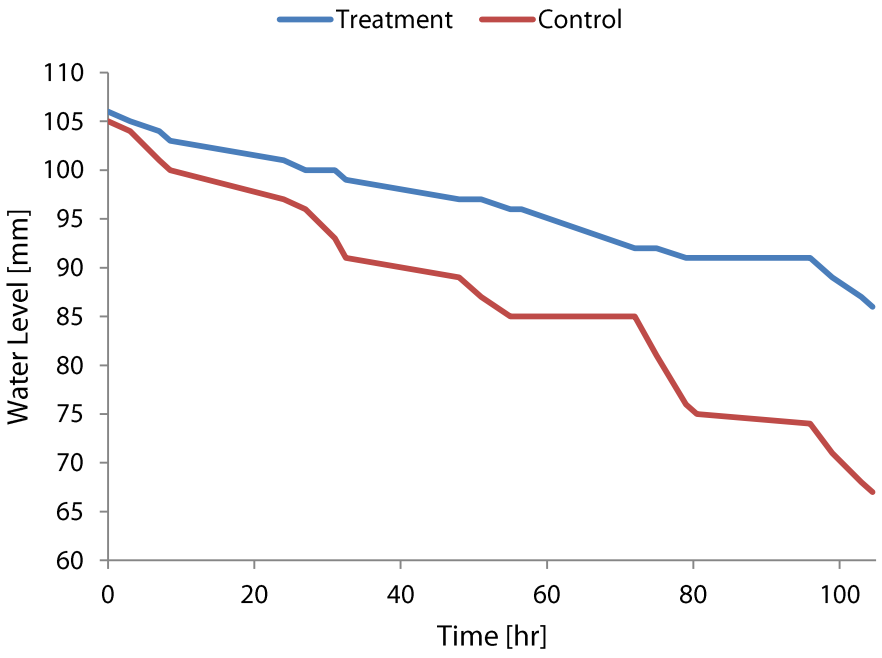

Figure 5.9. Water level results of the trial run from April 23 to 27, 2013 in Pabal, Maharashtra.

5.7.2 Experimental Set-Up

Each experiment, for the waste bottles and the floats, is set up side-by-side perpendicular to the prevailing wind direction, which is from west to east, so that they experience similar wind effects. For each treatment case, four tanks are set up in a two-by-two matrix. The treatment ponds are set up along a diagonal, and the control ponds are along the opposite diagonal. The tanks are set up adjacent to each other so that they experience the same terrain influences. Additionally, they

are not shaded, as this can alter the results. The tanks are fenced off to prevent people or animals from accessing the water, and chicken coop mesh is placed above the tanks to keep birds away. A marking was drawn at the center of the floor of each tank to indicate where the water height should be measured every day. The tanks were filled with water from Pabal so that the changes in water quality of the treatment and control tanks are comparable to what might happen under real conditions. A diagram of this set-up is shown in Figure 5.10 and a photograph in Figure 5.11. The tanks were labeled with numbers to ensure consistent data recording. Tanks 1 and 4 have floats while tanks 5 and 8 have bottles. Tanks 2, 3, 6, and 7 serve as control tanks.

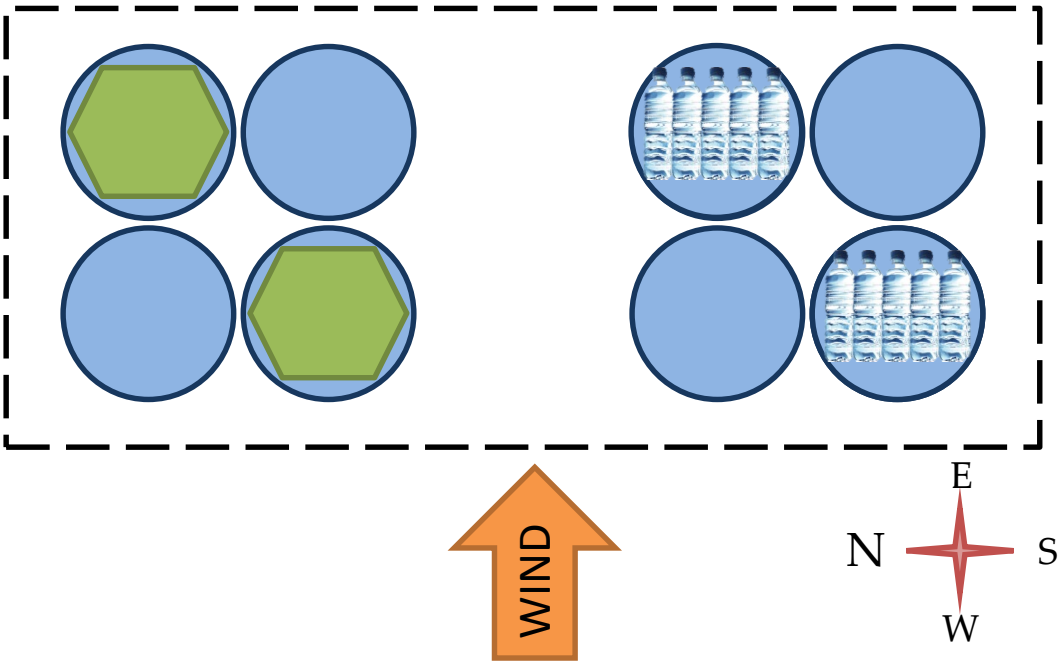

Figure 5.10. Experimental set-up.

Figure 5.11. Photograph of the experimental set-up.

Each tank is constructed using sheet metal, impermeable plastic lining, and plastic tarp. A 15 feet by 3 feet piece of sheet metal was bent and welded into a circle for each tank. The type of impermeable lining farmers use in their irrigation tanks is draped across the ring's rim in order to form a bowl to hold the water. At first, the outer side of the tank was covered in a one-inch thick layer of soil to act as insulation. However, rain very quickly washed away the soil. Several other insulation options were then considered: bricks, fertilizer bags filled with crumbled-up fertilizer bags, and agro-waste. The delivery of the bricks would have been too expensive and time-consuming; the bags-filled-with-bags option would have resulted in inconsistent and unknown conductivity; and agro-waste was unavailable, because farmers were preparing their lands for sowing and use the waste for various purposes during this time. Therefore, instead of insulating the tank, it was decided to attach a white plastic tarpaulin to the rim of the tank and pin it to form a slope to the ground. This sloped tarp would prevent solar radiation from directly reaching the tank and perhaps reduce the effects of convection on the tank. A photograph of this tank is shown in Figure 5.12.

Figure 5.12. Tank set-up.

For the waste bottle test, the wrappers were removed from bottles, and the bottles were filled with a small amount of dirt and placed on the surface to float. The number of waste bottles required to completely fill the surface area of the treatment tanks were 82 and 84. A bottle treatment tank is shown in Figure 5.13.

Figure 5.13. Treatment tank with bottles.

For the float test, the floats were constructed using bamboo, waste bottles, and old saris. Hexagonal floats were used, as they cover more surface area than a square in a circular tank. The pieces of bamboo were nailed together, and the bottles were affixed using nylon string. Two layers of old saris were stretched tight across the frames. In order to maintain consistency, each float was covered with the same two saris and layered in the same order. The underside of the float is shown in Figure 5.14 and a treatment tank with a float in Figure 5.15.

Figure 5.14. Float made of waste PET bottles, bamboo, and old saris.

Figure 5.15. Treatment tank with float.

5.7.3 Procedure

The tanks are monitored on a daily basis at 7:00 am. This time was chosen because dissolved oxygen is the lowest in the morning (so this is the lowest dissolved oxygen level a fish might experience) and the students at Vigyan Ashram are free between morning meditation and breakfast. The following procedure is performed for each tank:

1. Place a measuring stick with 1 mm gradations into the tank, aligned along the marking on the bottom of the tank. Read and record the water level.
2. Take water quality measurements using the dissolved oxygen meter and the multi-parameter water sensor in each tank and record the results. The following parameters should be tested:
    a. Dissolved oxygen (DO)
    b. Total dissolved solids (TDS)
    c. pH
    d. Temperature
    e. Salinity
3. Inspect the condition of the water bottles. Record all observations, and replace bottles as necessary. If bottles have been replaced, record how many.
4. Inspect the condition of the floats. Record all observations.
5. Copy all measurements and notes into an Excel spreadsheet.

5.7.4 Preliminary Results

The water level and water quality data recorded by the students for six weeks from June 17 to July 31 are displayed in Figure 5.16 and Figure 5.17, for the bottles and floats, respectively. The plots reflect the averages of each set of control tanks and each set of treatment tanks for each parameter.

Unexpectedly, leaking occasionally occurred, and the tank had to be repaired with a replacement tarpaulin. These leaks may have been caused by small animals, but sometimes holes could not be detected and it seemed as if the increased pressure due to higher water levels pushed water through the pores of the tarpaulin. The leaks were surprising, as the tarpaulin had been

utilized by Vigyan Ashram to build tanks in the past, and they had previously proven impermeable. Each time the tank is repaired, a different type of tarpaulin is used in order to Figure out which material will work best. In cases where a tank seemed to be leaking, as determined by a large, unexpected decline in the water level compared to the other tank within its category (e.g. the bottle treatment tank compared to the other bottle treatment tank), the data from the tank was excluded. Due to the leakage problems, on the sixteenth day, the teachers at Vigyan Ashram decided to reset the experiment and refilled all the tanks to the same level.

The batteries for the digital multi-parameter sensor died twice, and it was difficult to find new batteries in Pabal village. It took some time to acquire new batteries from Pune. During these periods without batteries, pH, conductivity, salinity, and total dissolved solids were not recorded.

On some days, the rise in water level was recorded as larger than the recorded rainfall. Because rainfall is the only water input, this must have been a result of human error. Therefore, these data points were excluded. If human error was revealed when recorded water rise surpassed precipitation, it is possible other data reflects inaccuracy due to human error as well.

We expected that the treatment tanks would experience lower water losses and maintain higher water levels than the control tanks for both experiments. However, the data did not match these expectations. The treatment tanks with the bottles actually show greater water loss than the control tanks, and the treatment tanks with the floats sometimes lose more and sometimes lose less water than the control tanks. Because some of the tanks were leaking, the total water losses were caused by both evaporation and seepage through the tank lining. Thus conclusions about evaporation reduction effectiveness cannot be made because the evaporative losses could not be isolated from total water losses. However, the water loss after resetting the water levels falls in a similar range (about 0 to 7 mm) to the values predicted by the evaporation model for July and August (approximately 3 to 7 mm) for the bottles experiment, but the losses are much greater (up to 15 mm) for the floats experiment. Additionally, heavy rain during monsoon season reduces evaporation, so the difference in water levels between tanks would not be as large as during drier seasons.

Water quality requirements for both irrigation and freshwater fisheries are met for some parameters but not for others. The water quality requirements are given in Table 5.7. It is expected that the conductivity, salinity, and total dissolved solids would increase as water levels decrease, because the amount of salt and solids should remain the same within the water body as water

evaporates. The data from this experiment does not meet this expectation. Instead, the data reveals the opposite: the tanks with higher water levels also have higher conductivity, salinity, and total dissolved solids. For both experiments, when the control tanks have more water than the treatment tanks, they have more salt and solids than the treatment tanks. The trend largely decreases for all three parameters, except for the control tanks in the bottles experiment the first few days. For the most part, these parameters seem to be higher for the control tanks than the treatment tanks in both experiments.

In the control tanks of the bottles experiment, conductivity and total dissolved solids pose a moderate hazard for irrigation and could not sustain fish life, but salinity levels seem safe. In the bottles treatment tanks, conductivity and total dissolved solids pose zero to moderate threat to irrigation and are safe for fish. Salinity is safe for fish as well. In both the control and treatment tanks for the floats experiment, all the water quality parameters stay at safe levels for irrigation. Conductivity, however, sometimes poses danger to fish in both tanks and total dissolved solids threaten fish in the control tank. In all the tanks, dissolved oxygen remains in the safe ranges for crops and fish.

The pH levels in all tanks reveal that the water is too basic to maintain the health of plants and aquatic animals. These pH levels, though, do not seem to be consistently higher or lower for the treatment tanks; sometimes the treatment tanks are more basic and sometimes the control tanks are more basic. The rising pH might be a result of precipitation. Rain can become basic near factories due to industrial waste, and Maharashtra has set aside a special economic zone not far from Pabal.

Table 5.7. Water quality requirements for irrigation and fisheries. **[128, 129]**

	Irrigation			
	No Hazard	Moderate Hazard	Severe Hazard	**Freshwater Fish Tolerance****
Conductivity [µS/cm]	< 700	700 – 3000	> 3000	150 – 500
TDS [ppm]	< 450	450 – 2000	> 2000	100 – 320
Salinity [ppt]	Not Available*			5 – 15
Dissolved Oxygen [ppm]	Not Available			> 5
pH	Normal range: 6.5 – 8.4			6.5 – 8.0

*Literature about water requirements for irrigation discusses TDS rather than salinity.
**Tolerances indicate the survival limits across a range of fish species, not a range of limits for a single species.

The results do not seem to reveal any specific trends associated with the impact of a treatment to reduce evaporation. In fact, the effectiveness of evaporation is unclear. Human error

seems to play a huge role in data (un)reliability, as does leakage and the heavy precipitation of the monsoon season. Conclusions thus cannot be made from this experiment yet

The students of Vigyan Ashram are continuing to take data, and the teachers have identified an impermeable material to use to repair the tanks to prevent further leakage. Hopefully after monsoon season, when the rain ends and evaporative losses increase, clearer trends describing the impact of evaporation reduction measures on water quantity and quality will emerge.

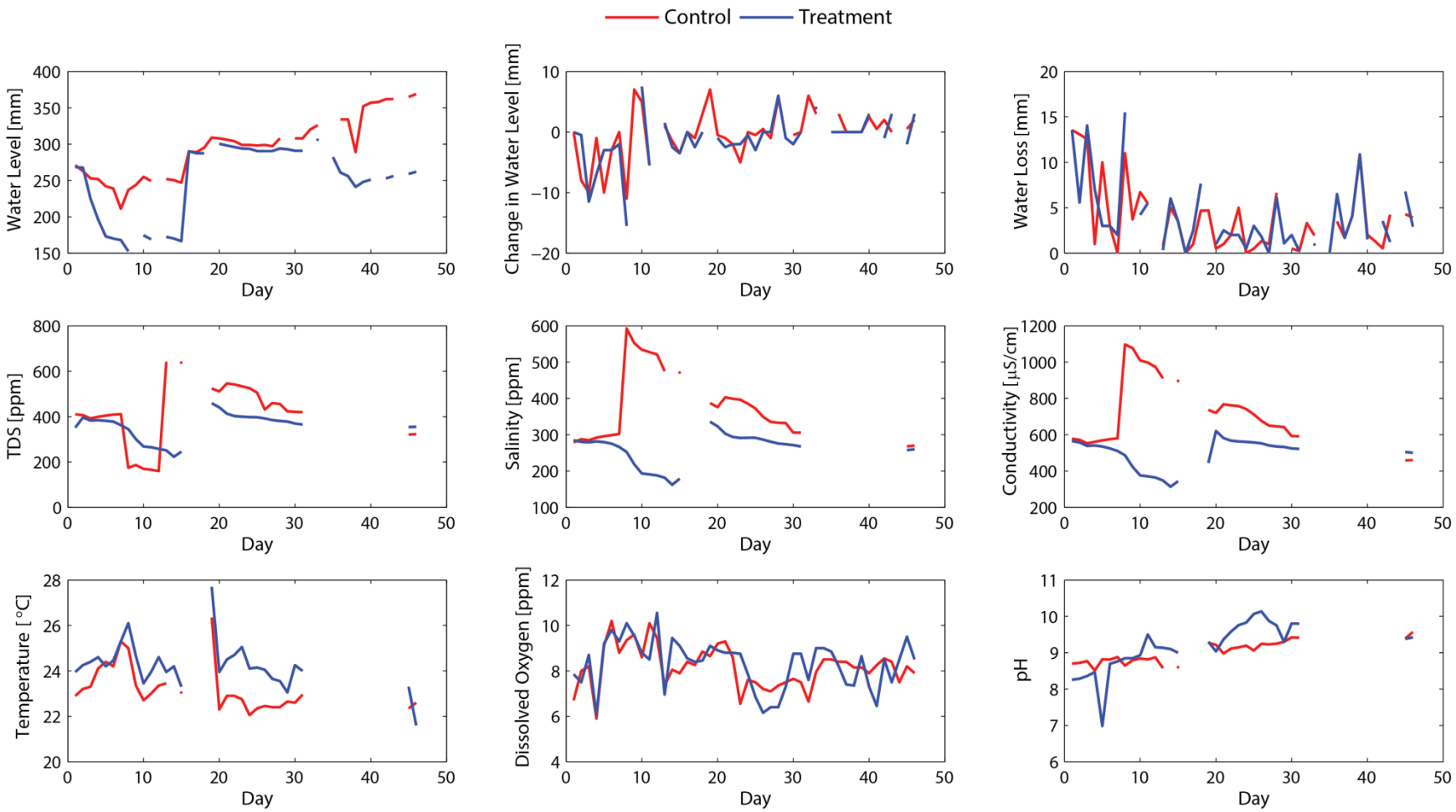

Figure 5.16. Results for the experiment testing the bottles solution. Blank space in the top row represents data excluded because the rise in water level recorded was greater than precipitation, the only water input. Blank space in the last two rows indicates data that was never collected due to battery failure in the multi-parameter sensor.

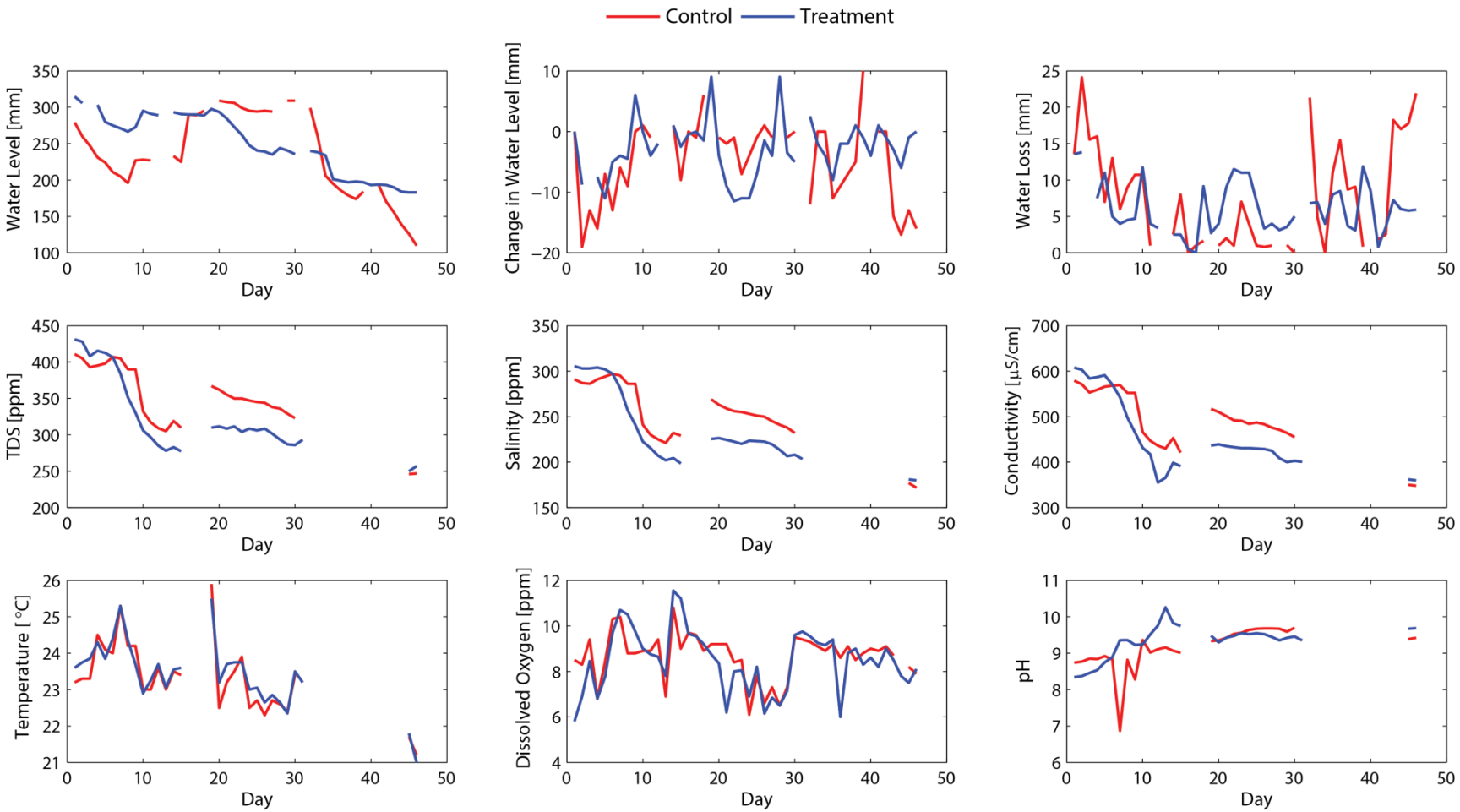

Figure 5.17. Results for the experiment testing the floats solution. Blank space in the top row represents data excluded because the rise in water level recorded was greater than precipitation, the only water input. Blank space in the last two rows indicates data that was never collected due to battery failure in the multi-parameter sensor.

5.8 Chapter Conclusion

Experiments were carried out to test the impact of floating objects made of waste materials, including bottles filled with dirt and floats made of waste bottles and old saris, on evaporation and water quality. Although the initial trial run proved promising with an evaporation reduction of 47%, the results of the larger experiments were inconclusive due to leaking in some tanks, human error in recording data, and monsoon rain. The experiment must be continued using different tanks: either the tarpaulin has to be replaced with an impermeable lining or a hard solid tank of plastic or metal must be used instead. Additionally, the experiments should be carried out during a dry season so that rain and clouds do not limit evaporation. The effectiveness of evaporation reduction strategies will be easier to assess during hotter, drier weather both because evaporative rates are higher and incoming precipitation does not alter water quality. Once experiments under these conditions have been conducted by the Vigyan Ashram students, a cost analysis should be executed for each strategy in order to determine if these solutions are cost-effective.

Chapter 6: Conclusions

6.1 Conclusions

About two-thirds of the Indian population depends on agriculture for their livelihood, and approximately 55% of this agriculture is rain-fed. Irrigation could raise yields and allow for additional crop seasons, thereby providing smallholder farmers with a more stable livelihood and improving quality of life for their families. However, due to high fuel and pump rental costs, irrigation remains a major challenge for small farmers, especially in eastern India where cheap electricity is not widely available. The objectives of this research were two-fold: (1) to design a pumping system with lower operation costs in order to promote irrigation in eastern India and (2) to reduce evaporation from tanks to increase the water resource. For the pumping system, rather than concentrating on developing a new power source, it was decided to focus on increasing efficiency and discharge by eliminating or reducing suction lift while continuing to employ fuel engines. The design requirements for the new pumping system included higher flow rates, lower fuel consumption, portability on a bicycle, maintainability and availability of replacement parts, and affordable capital cost.

6.1.1 Pumping System Conclusions

In order to establish baseline performance and assess the hypothesis that eliminating suction head would improve performance, pumps on the Indian market were tested for efficiency, discharge, and operation costs under suction and simulated submerged conditions. We discovered that rental costs of pumps actually outweigh fuel costs. Rent accounted for 69 to 92% of the total operation costs for a five-year-old 3 hp Honda pump and 67 to 85% for a twelve-year-old 3 hp Honda pump. Therefore, increasing flow rates to obtain more water per hour is more important than reducing fuel consumption. In addition, the proportion of total costs resulting from rent decreased with rising head, so fuel consumption becomes a greater concern at higher heads. Furthermore, it was found that almost eliminating suction lift lowered total operation costs by 17 to 25% for the five-year-old pump and up to 44% for the twelve-year-old pump, thereby verifying the hypothesis. Greater savings were accomplished at higher heads, as expected. These total savings resulted from up to 31% savings in rent and up to 52% savings in fuel for the five-year-

old pump and up to 34% savings in rent and up to 67% savings in fuel for the twelve-year-old pump. Removing suction head thus had a greater impact on energy efficiency than on water discharge.

Several technology alternatives were investigated to develop a pumping system that met all the design requirements described above and in Chapter 1. These options included extended torque transmission in the form of flexible and telescoping shafts, fluid machinery such as semi-open hydraulic systems, jet pumps, compressed air motors, and air lifts, and off-grid electricity generation employing household back-up generators or automotive alternators. However, no technology met all the design requirements. Although some of these alternatives would outperform the current system, they proved to be insufficiently portable, maintainable, and/or affordable for smallholder farmers. Specifically, the flexible shaft required a radius of curvature too large to be stored on a spool transportable on a bicycle, the nested telescoping shaft would be too difficult to repair, and the segmented telescoping shaft would be too heavy. The fluid machinery options were all too inefficient and too expensive. The household back-up generator was too expensive and too heavy for a bicycle, and the automotive alternator system was too expensive and did not receive good feedback from the community partner organization.

Instead of trying to modify the existing pumping system by lowering the centrifugal pump component, it was decided to build an entirely different type of system. A hybrid motorized-manual rope pump was modeled in MATLAB and then fabricated. This system would allow women to extract water from the well using a hand crank for low-flow applications such as drinking water, cleaning, and cooking, as well as allow farmers to extract water at higher flows for irrigation using an engine. The engine was removable so that it could still be protected from theft and stored safely inside a home and rented out from well to well (so not every farmer would need to own his own engine for the pump and pump renters could stay in business using the engine they already have). The hand crank, too, was made removable for safety purposes during operation in motorized mode. The materials and parts for the rope pump were all locally available in the Ranchi market and affordable, so the system should be maintainable. Admittedly, this system does not perfectly meet all the design requirements, as the entire system is not portable. However, due to the extra benefit of providing women with an easier, faster means to extract water for domestic use than the buckets they currently use, this option was deemed worthy of pursuing.

Flow rates in motorized mode achieved an average of 155.4 L/min and in manual mode 17.2 L/min for men and 13.3 L/min for women at a lift of 18.5 ft. These flows are lower than desired but can be improved through a series of modifications described in Chapter 4 and below in Section 6.3. Fuel consumption for this prototype could not be tested due to a farmer pouring out the kerosene brought from the city and a shortage of kerosene in the village (families understandably did not want to sacrifice their limited supply to test a prototype). The prototype cost INR 30,000 (USD 500) to fabricate, which is more expensive than the irrigation pumps currently in use, but the costs could be brought down. Additionally, villagers expressed willingness to pay a bit more for this system because of its dual functionality. The rope pump system received positive feedback from both the villagers as well as the partner organization, PRADAN, so further iterations of the design should be developed.

6.1.2 Evaporation Reduction Strategies Conclusions

In addition to designing a new pumping system to address groundwater irrigation challenges in eastern India, this research explored evaporation reduction strategies employing waste materials to increase water availability in tank irrigation. These methods included using waste PET bottles slightly filled with dirt and floats comprised of waste PET bottles, bamboo, and old saris.

The materials required for the evaporation reduction strategies were found to be widely available in cities and could be transported to villages nearby. In Pune, a mature waste bottle market could supply the farmers with the bottles needed for their tanks. Specifically, scrap dealers purchase bottles from waste pickers and collect, store, and sell these bottles; they could likely serve as the supplier for farmers. Experiments were run to test the effectiveness of the strategies on evaporation reduction and the impacts on water quality. Unfortunately, despite a trial run for the waste bottle solution that reduced evaporative losses by 47%, the results of the longer-term experiments were inconclusive due to tank leaking, unreliability in data due to human error, and heavy monsoon rains.

6.2 Future Work

This research has made progress in understanding irrigation efficiency issues and evaluating pumping system and evaporation reduction options. However, more work is required

to further understand the costs of irrigation using different pumping systems, identify more opportunities for improving efficiency, design a pumping system that will benefit farmers and their families, and evaluating the effectiveness and cost of evaporation reduction methods.

Only two pumps were tested for baseline performance, but other pumps are available on the market. Chinese pumps are rapidly growing in popularity due to their lighter weight and supposed better performance. Thus the efficiency and discharge of the Chinese pumps should be tested to see if they actually do outperform Indian-manufactured pumps. Additionally, changes to the centrifugal pump design, including the shaft seal, distance between the disks of the impeller, and impeller-to-chamber fill ratio, should be explored to improve efficiency and discharge.

The hybrid motorized-manual rope pump received positive feedback from farmers and their families and has potential to make an impact. However, several modifications are required to improve the design. In motorized mode, much flow was lost through the top of the rising main rather than exiting through the intended discharge pipe. Flow rates through the discharge pipe could be increased either by increasing the diameter of the rising main pipe, in which case an extra pulley would be required for manual mode, or by adding a funnel and shroud to catch the water lost through the top. In order to increase flow rates in manual mode, the hand crank should be made more ergonomic and comfortable. Users suggested enlarging the diameter. The hand crank should also be more securely attached. Furthermore, mode-switching should be made easier by splitting the driveshaft into two between the engine pulley wheel and the rope pulley wheel and using a clamp-on shaft coupling that the user can clamp for engine mode and de-clamp for manual mode. Finally, due to a lack of data, the first prototype was designed to run at the engine's rated operation point at the maximum head. Efficiency could be improved if the system is redesigned to operate within the full range of the engine's torque capacities. Given the positive feedback and expressed interest from the villagers who tested the pumps, future prototype iterations should continue until the product is ready to go to market.

Because the experiments to assess evaporation reduction strategies proved inconclusive due to leakage and rain, the experiments must be continued using impermeable tanks during a dry season. Once better data is acquired, a cost analysis must be carried out to determine if these strategies are a cost-effective way to obtain water for irrigation. The cost analysis should incorporate the savings from reducing the need to purchase water from elsewhere as well as the increased profits from greater yields.

6.3 Working in India: Lessons Learned

Interest in India is increasing abroad due to the great opportunities both to do humanitarian work with the impoverished as well as to tap into a new vast market. At the Massachusetts Institute of Technology, for example, a new center focusing on India has emerged. This program, the *Tata Center for Technology and Design*, funded this research and will continue to fund dozens of projects. The author has learned some lessons during this research and previous work in India that may prove valuable to future researchers.

First and foremost, the author recommends that anyone considering working in India learn the local language of his or her target community. Note that India is a diverse country home to hundreds of languages. The author worked with a local fabricator in Jharkhand and had to communicate the design and instructions in Hindi. The author also had to interview farmers in Hindi. Sometimes a translator was available, but there were many times when one was not. Furthermore, translators do not always translate correctly, and being able to understand whether or not the translator is conveying the right information or question is crucial. Knowing at least some of the local language can also help tremendously with navigating the streets.

An outsider cannot simply enter a community alone, for outsiders are not always readily trusted. It is important to establish a relationship with an organization that has deep roots in the target community. Not only can an organization trusted by the community give a researcher access to the community, but the organization can also provide invaluable insight into local conditions, behaviors, needs, and desires. For this research, PRADAN served as the trusted local organization and very generously hosted the author in villages, provided translators, purchased and shipped pumps to the United States, connected the author with a local fabricator, and located a well for the prototype. At PRADAN, Achintya Ghosh, Ashok Kumar, Satyabrata Acharya, Bapi Gorai, and Samir Kumar were particularly helpful. This research could not have been accomplished without a local partner.

When testing technology, it would be preferable to test locally with the users. We spent a huge amount of time troubleshooting the pumps in the United States and ultimately failed to get them to work properly. However, in the field the tests were completed quickly, as the farmers knew exactly how to operate and troubleshoot the pumps, thanks to years of experience using the pumps. Additionally, testing technology in the same manner that users utilize the technology will give results that the users actually experience. Furthermore, if a sample is required and the

researcher is going to India anyway, it makes more sense for the researcher to purchase the equipment in-country and ship it him or herself back to the United States. Relying on a local partner to do this for you can be very time-consuming due to complicated logistics. (In the case of this project, acquiring the pumps from India with the help of a local organization took five months.)

If the researcher is designing a new product, it is important to build the prototype(s) locally. As the author learned, many materials and parts that could be easily acquired in the United States are unavailable locally. The design of the rope pump system, for example, had to be modified several times when the desired parts could not be found. Additionally, navigating local markets can be difficult, so it is crucial to work with a local fabricator. The fabricator knows all the suppliers in the area and can quickly procure materials and parts. The added bonus of constraining the design to local material and part availability is that repairs and replacement parts will be much easier for a local mechanic when the technology breaks down.

Perhaps most importantly, it is best to reserve judgment. India is extremely culturally different from the West, and sometimes these differences can lead to misunderstandings. One should try not to take anything at face value and always investigate issues further from a local perspective.

Appendix

Appendix A: MATLAB Codes

A.1 Flexible Shaft

```
E = 210e9; %modulus of elasticity for steel
a = 1; %index for T (torque)
b = 1; %index for L (length of shaft)
c = 1; %index for d (diameter of wires)
f = 1; %index for s (spacing)
g = 1; %index for p (pitch angle)

V_layer = [];
V_tot = 0;

for T = 0:1:20;
    T
    for L = 0:5:30;
        for d = 0.0001:0.0001:0.01; %diameter of wire in m
            for s = 5e-6:1e-6:1.5e-5;
                r_shaft(a,b,c) = sqrt(T*L/(2*pi^2*(d/2)^2*E))+d/2; %radius of shaft
                V_shaft(a,b,c) = r_shaft(a,b,c)^2*pi*L;
                Rc(a,b,c,f)   =   sqrt(T*L/(2*pi^2*(d/2)^2*E))*((d+s)/s);   %critical   radius   of
curvature
                if (r_shaft(a,b,c)-(d/2))/(d+s) > 0 && (r_shaft(a,b,c)-(d/2))/(d+s) <= 100
                    n_layers(a,b,c,f) = ceil((r_shaft(a,b,c)-(d/2))/(d+s));
                    for p = pi/6:pi/60:pi/3; %pitch angle in radians
                        for i = 1:1:n_layers(a,b,c,f);
                            r_layer = (d/2) + s + d/2 + (i-1)*(d+s);
                            n_wires_per_layer (a,b,c,f,g,i)= ceil(pi*2*r_layer*sin(p)/(d+s));
                            h_s(a,b,c,f,g,i) = n_wires_per_layer(a,b,c,f,g,i)*(d+s)/cos(p);
                            V_layer                                                          =
n_wires_per_layer(a,b,c,f,g,i)*2*(d/2)^2*pi^2*L/h_s(a,b,c,f,g,i)*r_layer;
                            V_tot = V_tot + V_layer;
                        end
                        V_tot2(a,b,c,f,g) = V_tot + pi*(d/2)^2*L;
                        V_tot = 0;
                        g=g+1;
                    end
                end
                g = 1;
                f = f+1;
            end
            c = c + 1;
            f=1;
        end
        c = 1;
        b = b + 1;
    end
    b = 1;
    a = a + 1;
end
```

A.2 Nested Telescoping Shaft

```
P_motor = 3.8; %hp %1 hp = 745.7 W
RPM = 3600;
T_motor = P_motor*745.7/(RPM*2*pi/60);
E_s = 210e9; %modulus of elasticity for steel
tao_allow = 1e8; %allowable steel shear stress
s1 = 1e-5;
```

```
a=1;
b=1;
for T = 0.5:0.5:50; %torque
    M=0;
    r1(a) = (2/(pi*tao_allow)*sqrt(M^2+T^2))^(1/3);
    syms rs positive
    r2(a)=solve(tao_allow == 2*rs/(pi*(rs^4-r1(a)^4))*sqrt(M^2+T^2));
    r3(a)=solve(tao_allow == 2*rs/(pi*(rs^4-r2(a)^4))*sqrt(M^2+T^2));
    r4(a)=solve(tao_allow == 2*rs/(pi*(rs^4-r3(a)^4))*sqrt(M^2+T^2));
    r5(a)=solve(tao_allow == 2*rs/(pi*(rs^4-r4(a)^4))*sqrt(M^2+T^2));
    r6(a)=solve(tao_allow == 2*rs/(pi*(rs^4-r5(a)^4))*sqrt(M^2+T^2));
    r7(a)=solve(tao_allow == 2*rs/(pi*(rs^4-r6(a)^4))*sqrt(M^2+T^2));
    r8(a)=solve(tao_allow == 2*rs/(pi*(rs^4-r7(a)^4))*sqrt(M^2+T^2));
    r9(a)=solve(tao_allow == 2*rs/(pi*(rs^4-r8(a)^4))*sqrt(M^2+T^2));
    r10(a)=solve(tao_allow == 2*rs/(pi*(rs^4-r9(a)^4))*sqrt(M^2+T^2));
    r11(a)=solve(tao_allow == 2*rs/(pi*(rs^4-r10(a)^4))*sqrt(M^2+T^2));
    r12(a)=solve(tao_allow == 2*rs/(pi*(rs^4-r11(a)^4))*sqrt(M^2+T^2));
    r13(a)=solve(tao_allow == 2*rs/(pi*(rs^4-r12(a)^4))*sqrt(M^2+T^2));
    r14(a)=solve(tao_allow == 2*rs/(pi*(rs^4-r13(a)^4))*sqrt(M^2+T^2));
    r15(a)=solve(tao_allow == 2*rs/(pi*(rs^4-r14(a)^4))*sqrt(M^2+T^2));
    for L = 0:1/3:33+1/3;
        V1(a,b) = L*pi*r1(a)^2;
        V2(a,b) = L/2*pi*r2(a)^2;
        V3(a,b) = L/3*pi*r3(a)^2;
        V4(a,b) = L/4*pi*r4(a)^2;
        V5(a,b) = L/5*pi*r5(a)^2;
        V6(a,b) = L/6*pi*r6(a)^2;
        V7(a,b) = L/7*pi*r7(a)^2;
        V8(a,b) = L/8*pi*r8(a)^2;
        V9(a,b) = L/9*pi*r9(a)^2;
        V10(a,b) = L/10*pi*r10(a)^2;
        V11(a,b) = L/11*pi*r11(a)^2;
        V12(a,b) = L/12*pi*r12(a)^2;
        V13(a,b) = L/13*pi*r13(a)^2;
        V14(a,b) = L/14*pi*r14(a)^2;
        V15(a,b) = L/15*pi*r15(a)^2;
        b = b+1;
    end
    b=1;
    a=a+1;
end
```

A.3 Segmented Telescoping Shaft

```
P_motor = 3.8; %hp %1 hp = 745.7 W
RPM = 3600;
T_motor = P_motor*745.7/(RPM*2*pi/60)
E_s = 210e9; %modulus of elasticity for steel
rho_s = 7800; %density of steel in kg/m3
tao_allow = 1e8; %allowable steel shear stress
s1 = 1e-5;
%%
%SOLID
a=1;
b=1;
c=1;
k=3.142;
for P_hp = 0.5:0.25:4;
    P_W = P_hp*746;
    for T = 0.5:0.5:50;
        for L = 1:0.5:20
            RPMmotor(a,b,c) = P_W*60/(T*2*pi);
            M = 0;
            r2(a,b,c) = (2/(pi*tao_allow)*sqrt(M^2+T^2))^(1/3);
            I2(a,b,c) = pi*r2(a,b,c)^4/4;
            V2(a,b,c) = pi*r2(a,b,c)^2*L;
            m2(a,b,c) = V2(a,b,c)*rho_s;
            I2new = I2(a,b,c);
```

```
            m2new = m2(a,b,c);
            RPM2new = RPMmotor(a,b,c);
            error = 1;
            while error ~= 0
                Nc2 = 60/(2*pi)*k^2*sqrt(E_s*I2new/(m2new/L))/(L^2);
                Nc2-RPM2new;
                if Nc2-RPM2new < 0.000000001 && Nc2-RPM2new >= 0
                    r2(a,b,c) = r2new;
                    V2(a,b,c) = V2new;
                    m2(a,b,c) = m2new;
                    Nc2new(a,b,c) = Nc2;
                    RPMmotor(a,b,c) = RPM2new;
                    T2(a,b,c) = T2new;
                    break
                else
                    T2new = P_W*60/(Nc2*2*pi);
                    RPM2new = Nc2;
                    M2new = 0;
                    r2new = (2/(pi*tao_allow)*sqrt(M2new^2+T2new^2))^(1/3);
                    I2new = pi*r2new^4/4;
                    V2new = pi*r2new^2*L;
                    m2new = V2new*rho_s;
                end
            end
            c = c+1;
        end
        c = 1;
        b=b+1;
    end
    b = 1;
    a = a+1;
end

%HOLLOW VARYING INNER DIAMETER
a=1;
b=1;
c=1;
d=1;
k=3.142;
T = 1;
for P_hp = 0.5:0.25:4;
    P_W = P_hp*746
    for L = 1:0.5:20;
        for r_ID = 0.01:0.01:0.02;
            RPMmotor3(a,b,c) = P_W*60/(T*2*pi);
            M = 0;
            syms rs positive
            r3(a,b,c)=vpa(solve(tao_allow == 2*rs/(pi*(rs^4-r_ID^4))*sqrt(M^2+T^2)));
            I3(a,b,c) = pi*(r3(a,b,c)^4-r_ID^4)/4;
            V3(a,b,c) = pi*(r3(a,b,c)^2-r_ID^2)*L;
            m3(a,b,c) = V3(a,b,c)*rho_s;
            I3new = I3(a,b,c);
            m3new = m3(a,b,c);
            RPM3new = RPMmotor3(a,b,c);
            error = 1;
            while error ~= 0
                Nc3 = 60/(2*pi)*k^2*sqrt(E_s*I3new/(m3new/L))/(L^2);
                Nc3-RPM3new;
                if Nc3-RPM3new < 0.000000001 && Nc3-RPM3new >= 0
                    r3(a,b,c) = r3new;
                    V3(a,b,c) = V3new;
                    m3(a,b,c) = m3new;
                    Nc3new(a,b,c) = Nc3;
                    RPMmotor3(a,b,c) = RPM3new;
                    T3(a,b,c) = T3new;
                    break
                else
                    T3new = P_W*60/(Nc3*2*pi);
                    RPM3new = Nc3;
                    M3new = 0;
                    syms rsnew positive
```

```
                    r3new=solve(tao_allow                 ==                 2*rsnew/(pi*(rsnew^4-
r_ID^4))*sqrt(M3new^2+T3new^2));
                    I3new = pi*(r3new^4-r_ID^4)/4;
                    V3new = pi*(r3new^2-r_ID^2)*L;
                    m3new = V3new*rho_s;
                end
            end
            c = c+1;
        end
        c = 1;
        b=b+1;
    end
    b = 1;
    a = a+1;
end
```

A.4 Rope Pump

```
rho = 1000; %density of water 1000 kg/m3
g = 9.8; %gravity 9.8 m/s

%Engine Features
rpm_eng = 3000;
W_eng = 1100; %W
angvel_eng_shaft = rpm_eng*2*pi/60; %rad/s
angvel_eng = angvel_eng_shaft;
torq_eng_shaft = W_eng/angvel_eng_shaft; %Nm
torq_eng = torq_eng_shaft;
d_shaftin = 0.022225; %m
d_shaft = d_shaftin*3/0.875 %m sheave

%Wheel 1 Features
d_wheel3 = 0.564;
angvel_wheel3 = angvel_eng*d_shaft/d_wheel3;
torq_wheel3 = torq_eng*d_wheel3/d_shaft;
Vp3 = angvel_wheel3*d_wheel3/2;

%Wheel 2 Features
d_wheel = 6.5*2.54/100;
angvel_wheel = angvel_wheel3;
torq_wheel = torq_wheel3;
Vp = angvel_wheel*d_wheel/2;

%Pipe Features
gap = 0.00075; %gap between piston and pipe in m
L = 10; %length of pipe in
r1in = 1.25; %inner diameter of pipe in inches
r1 = r1in/39.3701; %inner diameter of pipe in m
A1 = pi*r1^2;
a=1;
for h = 0:0.1:L;
    torq_wheel2(a) = A1/2*rho*g*h*d_wheel;
    torq_shaft2(a) = torq_wheel2(a)/d_wheel3*d_shaft;
    %angvel_shaft2(a) = W_eng/torq_shaft2(a);
    %angvel_wheel2(a) = angvel_shaft2(a)*d_shaft/d_wheel3;
    %rpm2(a) = W_eng/torq_shaft2(a)*60/2/pi;
    rpm2(a) = 3000;
    %angvel_shaft2(a) = 3000/60*2*pi;
    if rpm2(a) >= 2800 && rpm2(a) <= 3200
        rpm_mid(a) = rpm2(a)*d_shaft/d_wheel3;
        rpm_rope(a) = rpm_mid(a);
        angvel_shaft2(a) = rpm2(a)*2*pi/60;
        angvel_wheel2(a) = angvel_shaft2(a)*d_shaft/d_wheel3;
        Vp2(a) = angvel_wheel2(a)*d_wheel/2;
        for n = 1:1:5;
            Vc1(a,n) = 4*gap/(2*r1)*sqrt(2*g*h/(L*n));
            Q1(a,n) = A1*(Vp2(a)-Vc1(a,n));
            W_out1(a,n) = rho*g*h*Q1(a,n);
            eff1(a,n) = W_out1(a,n)/W_eng;
            eff_vol1(a,n) = 1 - Vc(a,n)/Vp;
```

```
        end
    elseif rpm2(a) < 2800
        rpm2(a) = 2800;
        rpm_mid(a) = rpm2(a)*d_shaft/d_wheel3;
        rpm_rope(a) = rpm_mid(a);
        angvel_shaft2(a) = rpm2(a)*2*pi/60;
        angvel_wheel2(a) = angvel_shaft2(a)*d_shaft/d_wheel3;
        Vp2(a) = angvel_wheel2(a)*d_wheel/2;
        torq_shaft2(a) = W_eng/angvel_shaft2(a);
        for n = 1:1:5;
            Vc1(a,n) = 4*gap/(2*r1)*sqrt(2*g*h/(L*n));
            Q1(a,n) = A1*(Vp2(a)-Vc1(a,n));
            W_out1(a,n) = rho*g*h*Q1(a,n);
            eff1(a,n) = W_out1(a,n)/W_eng;
            eff_vol1(a,n) = 1 - Vc(a,n)/Vp;
        end
    else
        rpm2(a) = 3200;
        rpm_mid(a) = rpm2(a)*d_shaft/d_wheel3;
        rpm_rope(a) = rpm_mid(a);
        angvel_shaft2(a) = rpm2(a)*2*pi/60;
        angvel_wheel2(a) = angvel_shaft2(a)*d_shaft/d_wheel3;
        Vp2(a) = angvel_wheel2(a)*d_wheel/2;
        torq_shaft2(a) = W_eng/angvel_shaft2(a);
        for n = 1:1:5;
            Vc1(a,n) = 4*gap/(2*r1)*sqrt(2*g*h/(L*n));
            Q1(a,n) = A1*(Vp2(a)-Vc1(a,n));
            W_out1(a,n) = rho*g*h*Q1(a,n);
            eff1(a,n) = W_out1(a,n)/W_eng;
            eff_vol1(a,n) = 1 - Vc(a,n)/Vp;
        end
    end
    a=a+1;
end
```

A.5 Evaporation Reduction

```
P_a = csvread('Pune.csv',8,9,['J9..J8768']); %atmospheric pressure in Pa
T_dry = csvread('Pune.csv',8,6,['G9..G8768']);%dry bulb temp in C
T_dry_K = T_dry+273.15;
T_dew = csvread('Pune.csv',8,7,['H9..H8768']);%dew point temp in C
T_dew_K = T_dew+273.15;
v = csvread('Pune.csv',8,21,['V9..V8768']); %wind speed in m/s
RH = csvread('Pune.csv',8,8,['I9..I8768']); %relative humidity in %
Qsol_hr = csvread('Pune2.csv',8,1,['A9..A8768']); %global horiz radiation
RH = csvread('Pune3.csv',8,1,['A9..A8768']); %rainfall
alpha = 0.97; %emissivity of water
sigma = 5.67e-8; %Stefan Boltzmann constant W/m2K4
sigma2 = 4.9e-9;
cp_a = 1.013e-3; %MJ/kgC
cp_w = 4.18e-3; %MJ/kgC
rho_w = 1000; %kg/m3
h_fg = 2.45; %latent heat of vaporization MJ/kg
gamma = ones(1,365)*0.067; %psychrometric constant (kPa/C)

T_w0 = 20;
cont=true;
while(cont)
    z0 = 3;
    z_r0 = z0;
    e_s_hr = 0.6108.*exp(17.27.*T_dry./(T_dry+237.3));
    e_a_hr = RH.*e_s_hr/100;
    a = 1;
    for i=1:24:8760
        T_dewavg(a) = mean(T_dew(i:i+23));
        v_avg(a) = mean(v(i:i+23));
        Qsolavg(a) = mean(Qsol_hr(i:i+23));
        T_airavg(a) = mean(T_dry(i:i+23));
```

```
        RH_avg(a) = mean(RH(i:i+23));
        a=a+1;
    end
    delta = 0.2.*(0.00738.*T_airavg + 0.8072).^7 - 0.00016; %slope of svp-t curve (kPa/C)
    f_u = 6.43.*(1+0.0536.*v_avg); %function of wind speed
    e_s = 0.6108.*exp(17.27.*T_airavg./(T_airavg+237.3)); %saturated vapor pressure (kPa)
    e_a = RH_avg.*e_s./100; %actual vapor pressure (kPa)
    T_n                                                                                                    =
(0.00066.*100.*T_airavg+(4098.*e_a./((T_dewavg+237.2).^2)).*T_dewavg)./(0.00066*100+(4098.*e_a./(
(T_dewavg+237.2).^2))); %wet bulb temperature
    Q_rad_wetbulb        =       24*(0.97.*Qsolavg       -       alpha.*sigma.*((T_n+273.15).^4-
(T_airavg+273.15).^4))*60*60/1e6; %net radiation at wet bulb temp
    Q_rad_wetbulb_r       =       24*(0.91.*Qsolavg       -       0.91.*sigma.*((T_n+273.15).^4-
(T_airavg+273.15).^4))*60*60/1e6;
%slope of svp-t curve (kPa/C) at wet bulb temp
    T_e   =   T_n+Q_rad_wetbulb./(4.*sigma.*(T_n+273.15).^3+f_u.*(delta_n+gamma));   %equilibrium
temperature
    T_e_r = T_n+Q_rad_wetbulb_r./(4.*sigma.*(T_n+273.15).^3);
    b = 1;
    for j = 1:1:365
        if b == 1
            T_w(b) = T_w0;
            T_w_r(b) = T_w0;
            z(b) = z0;
            z_r(b) = z_r0;
            tau(b) = rho_w*cp_w*z0/(4*sigma2*(T_n(j)+273.15)^3+f_u(j)*(delta_n(j)+gamma(j)));
            tau_r(b) = rho_w*cp_w*z_r(b)/(4*sigma2*(T_n(j)+273.15)^3);
            Q_radnet(b)      =      24*(0.97*Qsolavg(j)      -      alpha*sigma*((T_w0+273.15)^4-
(T_airavg(j)+273.15)^4))*60*60/1e6;
            Evap(b)                                                                                    =
1/h_fg*((delta(j)/(delta(j)+gamma(j)))*Q_radnet(j)+(gamma(j)/(delta(j)+gamma(j)))*f_u(j)*(e_s(j)-
e_a(j)));
        else
            z(b) = z(j-1)-10^-3*Evap(j-1)+10^-3*RF(j-1);
            z_r(b)= z_r(j-1)+10^-3*RF(j-1);
            tau(b) = rho_w*cp_w*z(b)/(4*sigma2*(T_n(j)+273.15)^3+f_u(j)*(delta_n(j)+gamma(j)));
            tau_r(b) = rho_w*cp_w*z_r(b)/(4*sigma2*(T_n(j)+273.15)^3);
            T_w(b) = T_e(j) + (T_w(j-1)-T_e(j))*exp(-1/tau(j));
            T_w_r(b) = T_e_r(j) + (T_w_r(j-1)-T_e_r(j))*exp(-1/tau_r(j));
            Q_radnet(b)      =      24*(0.97*Qsolavg(j)      -      alpha*sigma*((T_w(b)+273.15)^4-
(T_airavg(j)+273.15)^4))*60*60/1e6;
            Evap(b)                                                                                    =
1/h_fg*((delta(j)/(delta(j)+gamma(j)))*Q_radnet(j)+(gamma(j)/(delta(j)+gamma(j)))*f_u(j)*(e_s(j)-
e_a(j)));
        end
        b = b+1;
    end
    if abs(T_w(365)-T_w0) > 0.01
        T_w0 = (T_w0 + T_w(365))/2;
    else
        cont=false;
    end

end

y = 1;
for eff = 0:0.05:1;
    EvapTot = sum(Evap)
    WaterGainedAnnual(y) = eff*EvapTot;
    y = y + 1;
end
```

Appendix B: Rope Pump Drawings

B.1 Hand Drawings from Design Process

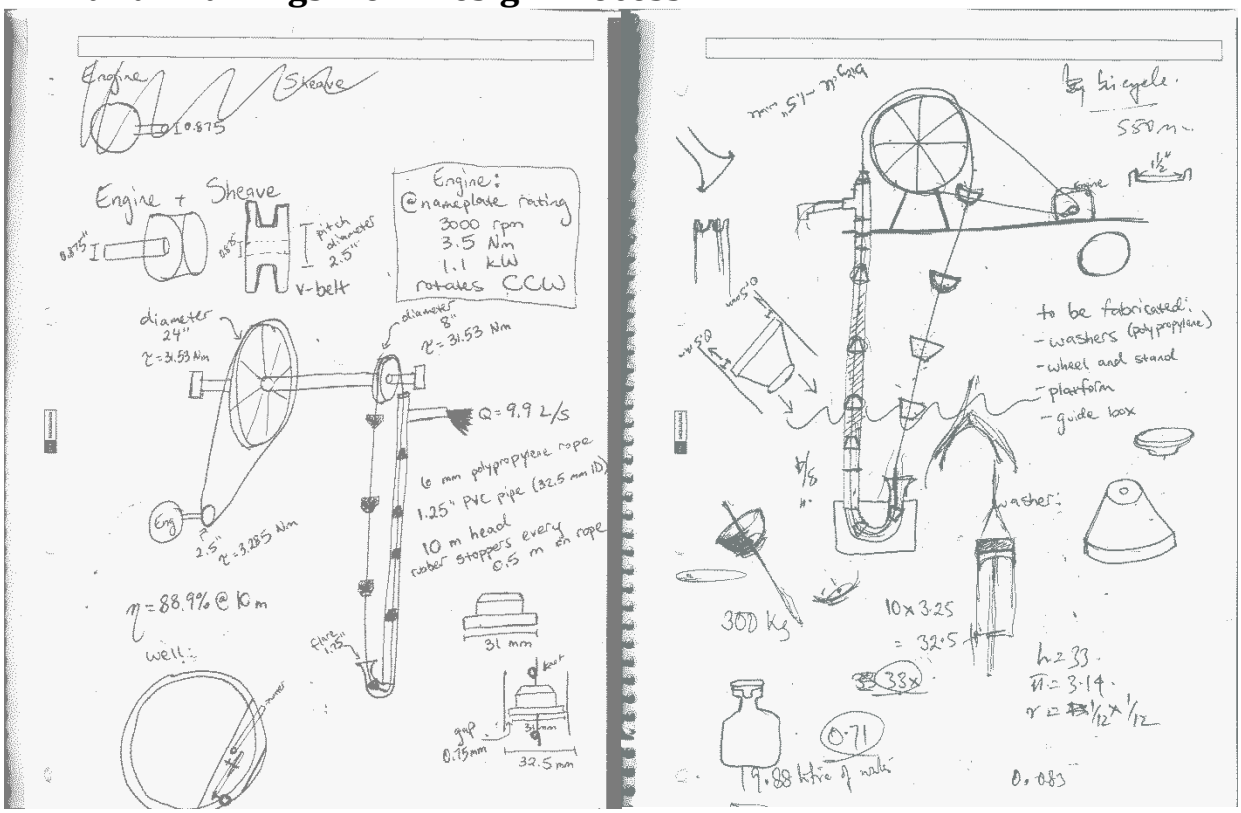

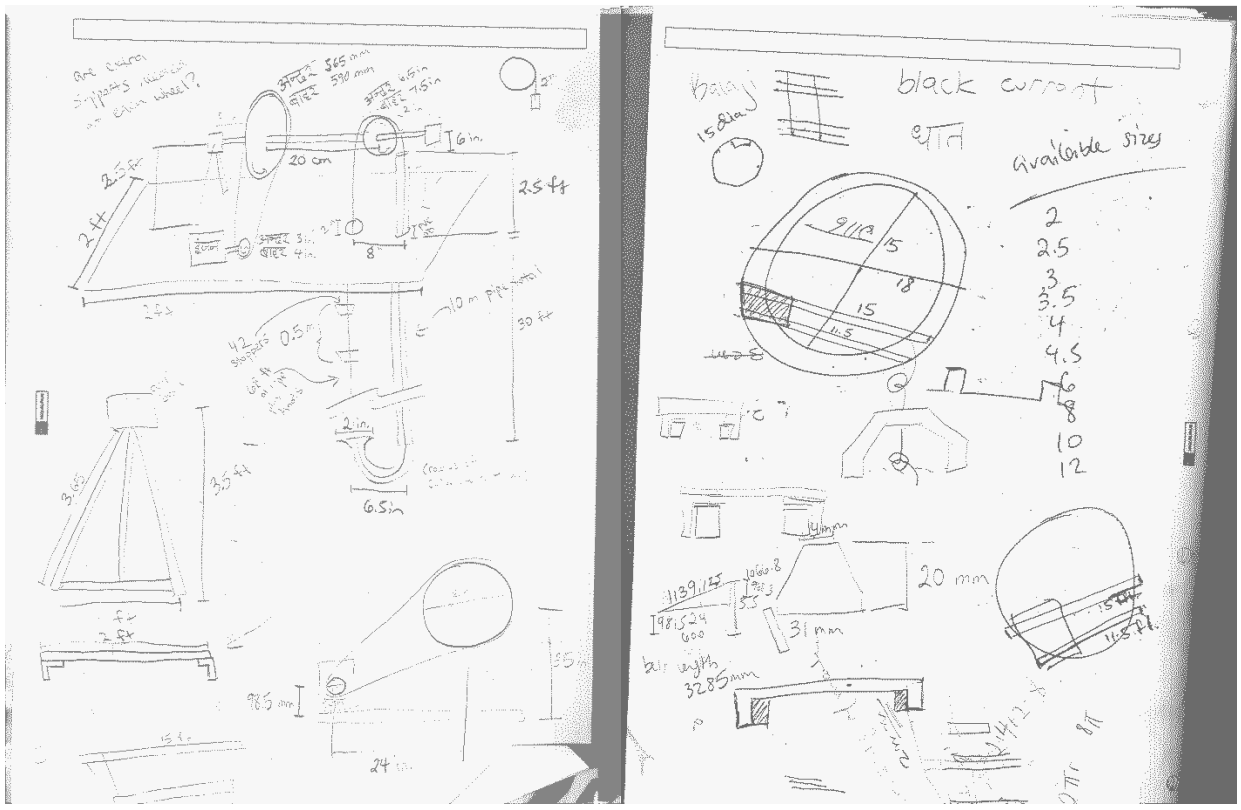

B.2 Solidworks 3-D Models

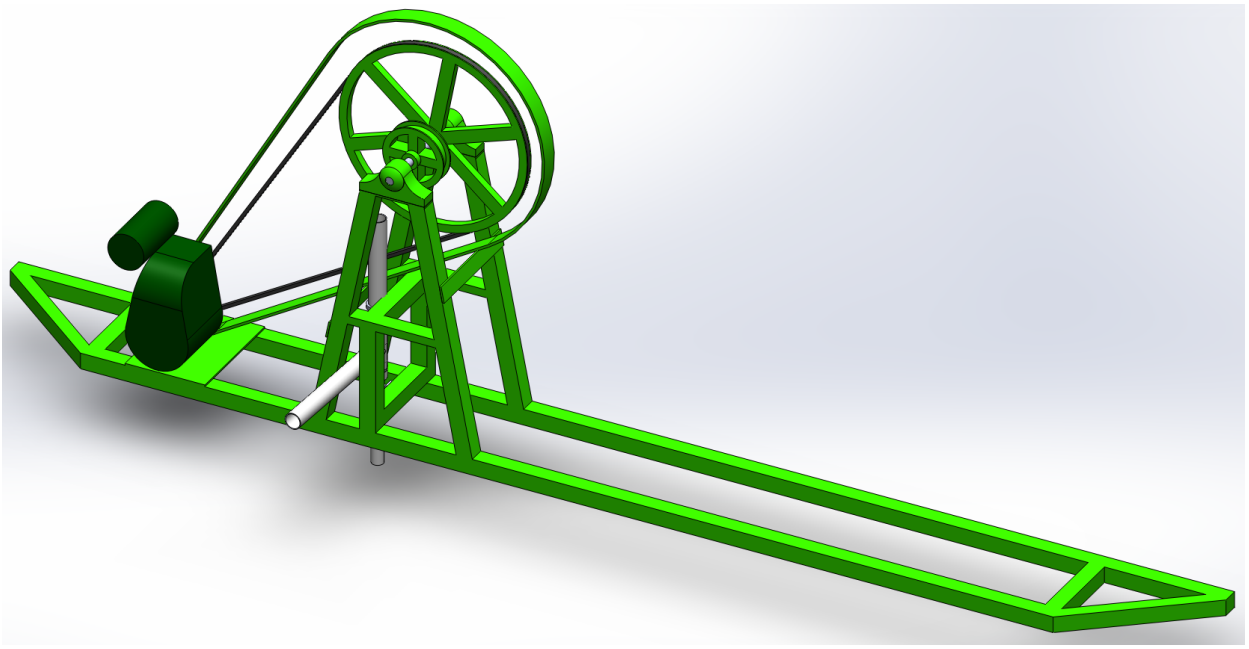

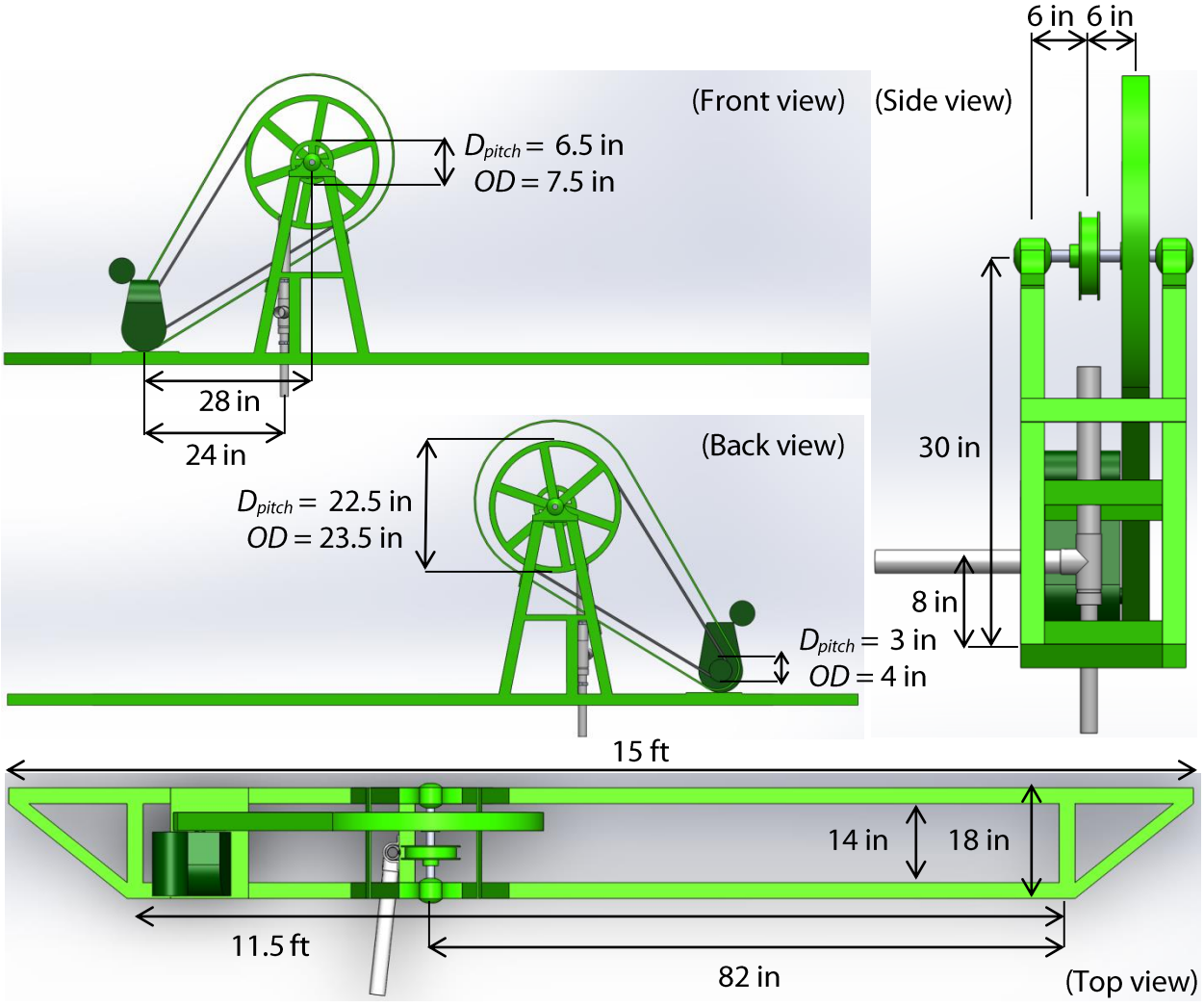

Bibliography

[1] "Census of India, IndiaStat.com," Ministry of Home Affairs, Government of India, 2011.

[2] World Bank, "India: Priorities for Agriculture and Rural Development," [Online]. Available: http://go.worldbank.org/8EFXZBL3Y0. [Accessed 5 March 2013].

[3] "Rajya Sabha Unstarred Question No. 1087, IndiaStat.com," 23 March 2012. [Online]. [Accessed 2013 March 5].

[4] Ministry of Agriculture, Government of India, "IndiaStat.com," 2009. [Online]. [Accessed 5 March 2013].

[5] T. Shah, *Wells and Welfare in the Ganga Basin: Public Policy and Private Initiative in Eastern Uttar Pradesh,* Colombo, Sri Lanka: International Water Management Institute, 2001.

[6] Ministry of Water Resources, "Minor Irrigation Census," 2001.

[7] S. Phansalkar and S. Verma, *Mainstreaming the Margins: Water-centric Livelihood Strategies for Revitalizing Tribal Agriculture in Central India,* New Delhi: Angus & Grapher, 2005.

[8] R. Kumar Sinha and A. Kumar, "Water Markets and Groundwater Economy in Bihar and Jharkhand," Agro-Economic Research Center for Bihar and Jharkhand, Bhagalpur University, Bhagalpur, India.

[9] A. Mukherji, S. Rawat and T. Shah, "Major Insights from India's Minor Irrigation Censuses: 1986-87 to 2006-07," *Economic and Political Weekly,* vol. 48, no. 26 & 27, pp. 115-124, June 2013.

[10] Central Ground Water Board, Ministry of Water Resources, Government of India, *Ground Water Year Book – India 2011-12,* 2012.

[11] "Lok Sabha Unstarred Question No. 2805, IndiaStat.com," 2011 December 21. [Online]. [Accessed 2013 February 15].

[12] "Rajya Sabha Unstarred Question No. 101, IndiaStat.com.," 10 August 2012. [Online]. [Accessed 15 February 2013].

[13] Oxford Poverty and Human Development Initiative (OPHI), Oxford Department of International Development, "Country Briefing: India," University of Oxford, December 2011.

[14] MapsofIndia.com, "Jharkhand District Map," 2009.

[15] Ministry of Tribal Affairs, Government of India, "Districts having more than 50% ST population : Statewise".

[16] A. Samal, *Implementing Integrated Natural Resource Management Projects under the National Rural Employment Guarantee Act 2005: A Resource Book.,* New Delhi: Ministry of Rural Development, Government of India, 2005.

[17] A. Mukherji, "Spatio-temporal analysis of markets for groundwater irrigation services in India: 1976-1977 and 1997-1998," *Hydrogeology Journal,* vol. 16, pp. 1077-1087, 2008.

[18] A. Mukherji, "Groundwater Markets in Ganga-Meghna-Brahmaputra Basin: Theory and Evidence," *Economic and Political Weekly,* pp. 3514-3520, July 2004.

[19] A. Kishore, Interviewee, *Postdoctoral Fellow, International Food Policy Research Institute.* [Interview]. 2013 May 24.

[20] E. Duflo and A. V. Banerjee, *Poor Economics: A Radical Rethinking of the Way to Fight Global Poverty*, Public Affairs, 2011.

[21] "India begins phased diesel price hikes," 18 January 2013. [Online]. Available: http://www.iisd.org/gsi/news/india-begins-phased-diesel-price-hikes. [Accessed 20 January 2013].

[22] T. Shah, "Crop per drop of diesel! Energy-squeeze on India's smallholder irrigation," *Economic and Political Weekly,* vol. 42, no. 39, September 29, 2007.

[23] A. Mukherji, "The energy-irrigation nexus and its impact on groundwater markets in eastern Indo-Gangetic basin: Evidence from West Bengal," *Energy Policy,* vol. 35, no. 12, pp. 6413-6430, December 2007.

[24] M. D. Kumar, O. P. Singh and M. V. K. Sivamohan, "Diesel price hikes and farmer distress: the myth and the reality," in *Managing water in the face of growing scarcity, inequity and declining returns: exploring fresh approaches. Proceedings of the 7th Annual Partners Meet, IWMI TATA Water Policy Research Program,* Hyderabad, India, April 2008.

[25] A. K. Sikka and P. R. Bhatnagar, "Realizing the potential: Using pumps to enhance productivity in the Eastern Indo-Gangetic plains," in *Groundwater Research and Management: Integrating Science into Management Decisions,* 2006.

[26] G. Sant and S. Dixit, "Agricultural pumping efficiency in India: the role of standards," *Energy for Sustainable Development,* vol. 3, no. 1, pp. 29-36, May 1996.

[27] A. Kumar and T. C. Kandpal, "Renewable energy technologies for irrigation water pumping in India: A preliminary attempt towards potential estimation," *Energy,* vol. 32, no. 5, pp. 861-870, May 2007.

[28] P. Purohit, "Financial evaluation of renewable energy technologies for irrigation water pumping in India," *Energy Policy* , vol. 35, no. 6, pp. 3134-3144, June 2007.

[29] I. Karassik and T. McGuire, *Centrifugal Pumps, 2nd Edition,* Norwell, Massachusetts: Chapman & Hall, 1998.

[30] F. M. White, *Fluid Mechanics, Sixth Edition,* Boston: McGraw-Hill Higher Education, 2008.

[31] National Institute of Standards and Technology, U.S. Secretary of Commerce, " "Thermophysical Properties of Fluid Systems." NIST Standard Reference Data.," 2011. [Online]. Available: http://webbook.nist.gov/chemistry/fluid/. [Accessed 5 April 2013].

[32] *Hydraulic Institute Engineering Data Book*, Hydraulic Institute, 1979.

[33] J. Lewis and R. Niedzwiecki, "7.8 Aviation Fuels, Chapter 7: Aircraft Technology and Its Relation to Emissions, Aviation and the Global Atmosphere," in *IPCC Special*

Reports on Climate Change, The Hague, Netherlands, United Nations Environmental Programme, 200.

[34] J. A. Muelhoefer, "Flexible Shaft Drilling for Cased Well Exploration," MS Thesis. Massachusetts Institute of Technology, Cambridge, MA, 1995.

[35] Elliott Manufacturing, *Flexible Rotary Power Transmission Handbook*, 2001.

[36] A. R. Black III, *On the Mechanics of Flexible Shafts,* 1988: Ph.D. Dissertation, Stevens Institute of Technology.

[37] A. R. Black III, "Flexible push/pull/rotary cable". United States Patent 7,089,724, 15 Aug 2006.

[38] N. Stow, "Flexible Shaft". United States Patent 571,869, 24 November 1896.

[39] H. W. Webb, "Flexible shaft". United States Patent 1,952,301, 27 March 1934.

[40] S. Pile, "Flexible power transmission". United States Patent 2,401,100, 28 May 1946.

[41] R. Remi, "Windable flexible shaft capable of withstanding high tractive forces and torsional stresses and process for manufacturing the same". Patent 3,791,898, 1974.

[42] M. Fukuda, "Flexible drive cable". Patent 4,112,708, 12 September 1978.

[43] Y. Ishikawa, "Flexible shaft having element wire groups and lubricant therebetween". United States Patent 5,288,270, 22 February 1994.

[44] R. J. Schwartz, "Wire wound flexible shaft having extended fatigue life and method for manufacturing the same". United States Patent 6,881,150, 19 April 2005.

[45] N. J. Pacelli, A. J. Losier, S. L. Thelen and B. N. Sisk, "Flexible Shaft". United States Patent 2007/0093840, 26 April 2007.

[46] "Material Properties Table," MIT, [Online]. Available: http://web.mit.edu/course/3/3.11/www/modules/props.pdf. [Accessed 11 January 2013].

[47] "Products: Engines," Honda Siel Power Products, [Online]. Available: http://www.hondasielpower.com/products_engines.html. [Accessed 10 January 2013].

[48] R. S. Mamidi, B. Kulkarni and A. Singh, "Secular trends in height in different states of India in relation to socioeconomic characteristics and dietary intakes," *Food & Nutrition Bulletin,* vol. 32, no. 1, pp. 23-34, 2011.

[49] H. Grosse-Entrup, "Telescoping torque transmitting shaft". United States Patent 4,103,514, 1 August 1978.

[50] R. Lightcap, "Variable length double telescoping drive shaft assembly". United States Patent 6,241,616, 5 June 2001.

[51] J. B. Lukac, "Tubular telescoping drive shaft". United States Patent 7,238,113, 22 September 2006.

[52] T. Yaegashi, "Driving shaft having splined male and female portions". United States Patent 5,697,850 , 16 December 1997.

[53] "Allowable Stress and Factor of Safety," University of Maryland, [Online]. Available: http://arch.umd.edu/Tech/Tech_II/Lectures/Allowable%20Stress%20&%20Factor%20of%20Safety.pdf. [Accessed 2013 January 15].

[54] R. Hibbeler, *Mechanics of Materials*, Prentice Hall, 2000.

[55] US Didactic, "Shaft Whip," [Online]. Available: http://www.usdidactic.com/html/i3610_Zeichnung_Einzelheit_2.htm. [Accessed 12 February 2013].

[56] A. Slocum, "Topic 6: Power Transmission Elements II.," in *FUNdaMENTALs of Design*, 2008.

[57] "Diesel Engines," United States Department of Energy, [Online]. Available: http://www1.eere.energy.gov/vehiclesandfuel/pdfs/basics/jtb_diesel_engine.pdf. [Accessed 24 February 2013].

[58] "Hydraulic Pumps and Pumps-to-Motors Adapters.," McMaster-Carr, [Online]. Available: http://www.mcmaster.com/#hydraulic-pumps/=nyv7oz. [Accessed 24 February 2013].

[59] "Hydraulic Motors," M&S Hydraulics, [Online]. Available: http://www.hydrotech-bg.com/common/dimages/src/file/PDF/E1-SPOOLVALVE.pdf. [Accessed 24 February 2013].

[60] Kirloskar, "Domestic Catalogue".

[61] "Nameplate on USHA UNK 2020B pump".

[62] "Nameplate on Mahendra WMK 2020 pump".

[63] "Hydraulic Motors," McMaster-Carr, [Online]. Available: http://www.mcmaster.com/#hydraulic-motors/=nyw50r. [Accessed 24 February 2013].

[64] "Hydraulic Fluid Hoses," McMaster-Carr, [Online]. Available: http://www.mcmaster.com/#hydraulic-fluid-hose/=nyw05y. [Accessed 24 February 2013].

[65] I. J. Karassik, J. P. Messina, P. Cooper and C. C. Heald, *Pump Handbook, Fourth Edition,* New York: McGraw-Hill, 2008.

[66] P. Fraenkel, *Water Lifting Devices,* Food and Agriculture Organization, 1986.

[67] "Air-Powered Motors," McMaster-Carr, [Online]. Available: http://www.mcmaster.com/#air-motors/. [Accessed 14 March 2013].

[68] "30 CFM Air Compressors," Air Compressors Direct, [Online]. Available: ttp://www.aircompressorsdirect.com/tools/30-cfm-air-compressors.html. [Accessed 14 March 2013].

[69] A. Kumar, Interviewee, *PRADAN.* [Interview]. July 2 2013.

[70] "Submersible Solar Pumps," Lorentz , [Online]. Available: http://www.lorentz.de/en/products/submersible-solar-pumps.html. [Accessed 2013 March 15].

[71] "Power Products: Water Pumps," Honda Siel Power Products, [Online]. Available: http://hondasielpower.com/products_waterpumps.html. [Accessed 10 January 2013].

[72] J. Larabee, B. Pellegrino and B. Flick, "Induction Motor Starting Methods and Issues," in *Petroleum and Chemical Industry Conference, IEEE,* 2005.

[73] EPCOS, *Inrush Current Limiters: Application Notes,* August 2012.

[74] "Products: Generators," Honda Siel Power Products, [Online]. Available: http://www.hondasielpower.com/products_generators.html. [Accessed 15 March 2013].

[75] Delco Remy, *Electrical Specifications and Selection Guide: Starters and Alternators,* 2008.

[76] Robert Bosch GmbH, *Automotive Electrics Automotive Electronics, Fifth Edition,* Sussex: Jon Wiley & Sons Ltd, 2007.

[77] B. Hollembeak, *Automotive Electricity and Electronics: Classroom Manual, Third Edition,* New York: Thomson Learning, 2003.

[78] D. Ton and W. Bower, *Summary Report on the DOE High-tech Inverter Workshop,* United States Department of Energy, 2005.

[79] Cobra Electronics Corporation, "Power Inverters," [Online]. Available: https://cobra.com/category/power-inverters.cfm. [Accessed 10 April 2013].

[80] Whistler Group, "Catalog: Power Inverters," [Online]. Available: http://www.whistlergroup.com/power-inverters-catalog/group.aspx?id=7. [Accessed 10 April 2013].

[81] Bestek Ltd, "Products: Power Inverter," [Online]. Available: http://www.bestekltd.com/product_c8_p1.html. [Accessed 10 April 2013].

[82] W. Dankoff, "How to Choose an Inverter for an Independent Energy System," *Home Power,* no. 82, 2001.

[83] G. W. McLean, G. F. Nix and S. R. Alwash, "Performance and design of induction motors with square-wave excitation," *Proceedings of the IEEE,* pp. 1405-1411, 1969.

[84] Bombas de Mecate SA, "Rope Pump: The Technology," [Online]. Available: http://www.ropepump.com/tec/tec.htm. [Accessed 5 July 2013].

[85] S.K. Industries, "India Mark II Hand Pump," [Online]. Available: http://www.skipumps.com/mark2_details.htm. [Accessed 5 July 2013].

[86] J. Needham, *Science and Civilization in China: Volume 4, Physics and Physical Technology,* Cambridge: Cambridge University Press, 1971.

[87] P. Smulders and R. Rijs, "A Hydrodynamic Model of the Rope Pump," Arrakis, Veldhoven, Netherlands, 2006.

[88] Demotech, "Rope Pump," [Online]. Available: http://www.demotech.org/d-design/designA.php?d=43. [Accessed 9 July 2013].

[89] M. Tiele Westra, "The rope pump," Akvopedia, 5 February 2010. [Online]. Available: http://www.akvo.org/blog/?p=1073. [Accessed 9 July 2013].

[90] "Motor rope pumps," RopePumps.org, [Online]. Available: http://ropepumps.org/English/motor.php. [Accessed 9 July 2013].

[91] Practica Foundation, "Motorized rope pump," [Online]. Available: http://www.practica.org/products/pumps/motorized-rope-pump/. [Accessed 9 July 2013].

[92] C. Marroquin and H. Godfrey, "Pedal Powered Water Pump," Maya Pedal, San Andrés Itzapa, Guatemala, 2010.

[93] H. Holtslag, "Smart Tech Against Poverty: Rope Pump in Mozambique," [Online]. Available: http://henkholtslag.nl/2011/12/30/a-rope-pump-in-mozambique/rope-pump-mozambique-before/. [Accessed 9 July 2013].

[94] Bombas de Mecate S.A., *Experiences and Tolerances in Rope Pump Production,* Managua, Nicaragua, 1998.

[95] H. Holtslag and J. de Wolf, "Rope Pump: A Model," Foundation Connect International, 2009.

[96] Vijay Villiers, *C-12 & V-12 User Manual.*

[97] S. Bombas de Mecate, *Extra Strong Rope Pump: Manual of Technical Drawings,* Managua, Nicaragua, 1998.

[98] Groupe Urgence Réhabilitation Développement, "Rope Pump Experience in Chad," 2009.

[99] Ministry of Agriculture, Government of India, "IndiaStat.com," 2001. [Online].

[100] C. Karthikeyan, "Competition and conflict among multiple users of tank irrigation systems," in *Fourteenth International Water Technology Conference,* Cairo, Egypt, 2010.

[101] Department of Natural Resources and Mines, "Methods for Reducing Evaporation from Storages used for Urban Water Supplies: Final Report," GHD Pty Ltd, Brisbane, Australia, March 2003.

[102] P. J. Watts, "Scoping Study: Reduction of evaporation from farm dams. Final report to National Program for Sustainable Irrigation," Feedlot Services Australia Pty Ltd, Toowoomba, Australia, 2005.

[103] I. P. Craig, "Loss of storage water through evaporation with particular reference to arid and semi-arid zone pastoralism in Australia," DKCRC Working Paper 19, The WaterSmart Literature Reviews, Desert Knowledge CRC, Alice Springs, Australia, 2008.

[104] X. Yao, H. Zhang, C. Lemckert, A. Brook and P. Schouten, "Evaporation Reduction by Suspended and Floating Covers: Overview, Modelling, and Efficiency. Urban Water Security Research Alliance Technical Report No. 28.," Griffith University, Queensland, Australia, August 2010.

[105] P. Schmid, M. Kohler, R. Meierhofer, S. Luzi and M. Wegelin, "Does the reuse of PET bottles during solar water disinfection pose a health risk due to the migration of plasticisers and other chemicals into the water?," *Water Research,* vol. 42, pp. 5054-5060, 2008.

[106] L. Sax, "Polyethylene Terephthalate May Yield Endocrine Disruptors," *Environmental Health Perspectives,* vol. 118, no. 4, pp. 445-448, April 2010.

[107] V. S. Leivadara, A. D. Nikolaou and T. D. Lekkas, "Determination of organic compounds in bottled waters," *Food Chemistry,* vol. 108, pp. 277-286, 2008.

[108] N. Casajuana and S. Lacorte, "Presence and release of phthalic esters and other endocrine disrupting compounds in drinking water," *Chromatographia,* vol. 57, pp. 649-655, 2003.

[109] J. Bošnir, D. Puntarić, A. Galić, I. D. T. Škes, M. Klarić, M. Grgić, M. Čurkovic and Z. Šmit, "Migration of Phthalates from Plastic Containers into Soft Drinks and Mineral Water," *Food Technology and Biotechnology,* vol. 45, no. 1, pp. 91-95, 2007.

[110] P. Westerhoff, P. Prapaipong, E. Shock and A. Hillairaeu, "Antimony leaching from polyethylene terephthalate (PET) plastic used for bottled drinking water," *Water Research,* vol. 42, pp. 551-556, 2008.

[111] C. Bach, X. Dauchy, M.-C. Chagnon, Etienne and Serge, "Chemical compounds and toxicological assessments of drinking water stored in polyethylene terephthalate (PET) bottles: A source of controversy reviewed," *Water Research,* vol. 46, 2012.

[112] R. A. Velankar, *Village Tanks and Community Based Management in Gondia District, Maharashtra State, India.,* The Hague, Netherlands: Master's thesis, Institute of Social Studies, 2011.

[113] V. Anbumozhi, K. Matsumoto and E. Yamaji, "Towards improved performance of irrigation tanks in semi-arid regions of India: modernization opportunities and challenges.," *Irrigation and Drainage Systems,* vol. 15, pp. 293-309, 2001.

[114] A. Phule ed., *A Farmer Friendly Handbook for Government Schemes and Programs,* Pune: Department of Agriculture, Government of Maharashtra, August 2012.

[115] V. Venkatachalam, S. C. Garg, A. Purkayastha, S. Chopra, R. Saha, J. Singh and S. Sen, *Incentivizing Agriculture: RKVY Initiatives,* New Delhi: Department of Agriculture and Cooperation, Ministry of Agriculture, Government of India, April 2012.

[116] J. V. Morrow and C. Fischenich, "Habitat Requirements for Freshwater Fishes," EMRRP Technical Notes Collection, U.S. Army Engineer Research and Development Center, Vicksburg, MS, May 2000.

[117] Scrap Dealers in Pabal, Interviewee, [Interview]. 29 May 2013.

[118] Maharashtra Water Resources Regulatory Agency, "Public Notice on the Determination of Bulk Water Tariff in the State of Maharashtra for 2010-2013," Water Resources Department, Government of Maharashtra, Mumbai, 2010.

[119] A. Susarla, Interviewee, *Data Manager, Solid Waste Collection and Handling (SWaCH) Cooperative.*. [Interview]. 15 June 2013.

[120] T. Shah and K. V. Raju, "Rethinking Rehabilitation: Socio-ecology of tanks and Water Harvesting in Rajasthan, North-West India," CGIAR Systemwide Program on Collective Action and Property Rights (CAPRi), September 2001.

[121] Q. Li and G. John, " A Daily Water Balance Modelling Approach for Simulating Performance of Tank-Based Irrigation Systems," *Water Resources Management,* vol. 19, pp. 211-231, 2004.

[122] P. Kashyap and R. Panda, "Evaluation of evapotranspiration estimation methods and development of crop-coefficients for potato crop in a sub-humid region," *Agricultural Water Management,* vol. 50, pp. 9-25, 2001.

[123] D. McJannet, I. Webster, M. Stenson and B. Sherman, "Estimating open water evaporation for the Murray-Darling Basin. A report to the Australian Government from the CSIRO Murray-Darling Basin Sustainable Yields Project," CSIRO, 2008.

[124] US Department of Energy, "Weather Data : All Regions : Asia WMO Region 2 : India," [Online]. Available: http://apps1.eere.energy.gov/buildings/energyplus/cfm/weather_data3.cfm/region=2_asia_wmo_region_2/country=IND/cname=India. [Accessed 10 May 2013].

[125] RIHN and MRI/JMA, "APHRODITE's Water Resources," [Online]. Available: http://www.chikyu.ac.jp/precip/. [Accessed 10 May 2013].

[126] Ministry of Agriculture, Government of India, "IndiaStat.com," 2009-2010. [Online]. [Accessed 17 August 2013].

[127] Tamil Nadu Agricultural University, "Irrigation Management: Water Requirements of Agricultural Crops," [Online]. Available: http://www.agritech.tnau.ac.in/agriculture/agri_irrigationmgt_waterrequirements.html. [Accessed 17 August 2013].

[128] R. Ayers and D. Westcot, *Water Quality for Agriculture. FAO Irrigation and Drainage Paper.*, Rome, Italy: FAO Irrigation and Drainage Paper. United Nations Food and Agriculture Organization, 1994.

[129] S. Behar, *Testing the Waters: Chemical and Physical Vital Signs of a River*, Montpelier, VT: River Watch Network, 1997.